A universal approach to phenomenological compartment models of unit operations

Kieran Paul Jervis

Submitted in accordance with the requirements for the degree of Doctor of Philosophy

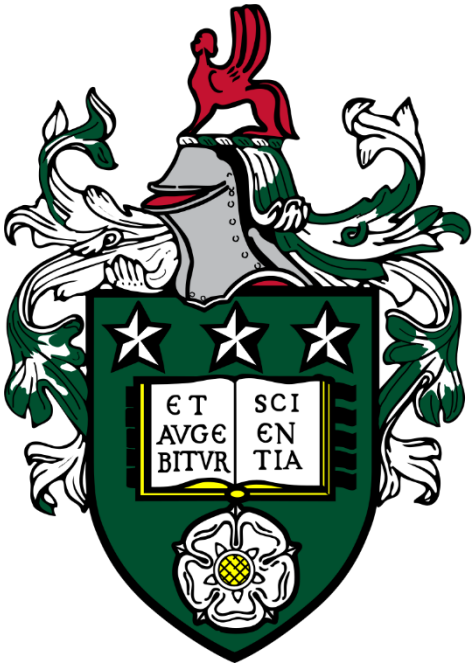

The University of Leeds
School of Chemical and Process Engineering

May 2022

The candidate confirms that the work submitted is his own and that appropriate credit has been given where reference has been made to the work of others.

Acknowledgements

I want to give my most profound appreciation and gratitude to my supervisor Professor Frans Muller; he has had the most significant influence upon my academic development over my eight years at the UoL, and I am thankful to have had the privilege of his mentorship throughout.

I would also like to sincerely thank my other supervisor, Dr Jitse Niesen, for his commitment to my project and Professor Daniel Ruprecht's initial contributions.

And a great thank you to Harsh Kumar of ITT Delhi for his assistance in identifying defective code within CompArt’s early development phase, and my peer, Alex Fells, for the swift proofreading of my final chapter when the deadline was dawning.

Getting through this stage of life required more than academic support. My grandparents, to both of you, Margaret Weightman and John Weightman; without you, I would not be the person I am today, and I thank you for everything you have done for me. I pursued this work on your advice, Grandad, and now you see me at the end; without your encouragement, I would not be at this point. Thank you both for the immeasurable amount of support and love you have given me.

And to my friends, thank you all for the considerable influence you have had upon my journey.

Abstract

A compartment model describes the transmission of materials and/or energies through a unit operation, as a network of flow connected sub-volumes. Each sub volume is a well-mixed compartment, formed based on the identification of negligible gradients in the system properties of interest. Ordinary differential equations describe the temporal phenomenological and flow effects imposed on the variables (species mass and compartment enthalpy) of the system. Along with the associated initial values of the system, the variable ODE's are numerically solved over time. Compartment modelling is widely used in chemical engineering as it provides a balance between flow and phenomena resolution, and solution times.

From the profusion of compartment models in literature, the model development and thus solutions for this approach are both bespoke. Models are either hard coded ODE's or built through the improvised use of available non-domain-specific tools; the former is especially error prone, and the latter restricts the model development to the capability of the tool used. For full modelling flexibility, modellers are required to have knowledge of software design for implementing and solving ODE's with many variables.

CompArt - A universal compartment modelling tool for unit operations has been developed in this work, this is formed of (i) a universal input language used to describe unit operation compartment models, (ii) complemented by an interpretation algorithm for the conversion of the model description into ODE's for solving (utilising a universal compartment modelling equation set developed in this work) and, (iii) the wrapping of choice numerical solvers targeting stiff non-linear problems. This addition to the field circumvents the need for modelers to have specialised skills to utilise this modelling approach allows focus upon their domain of model development to take priority.

The universal compartment modelling system, CompArt is validated against a benchmark set of 20 models ranging in structural make-up and applied phenomena.

Table of Contents

List of Tables

List of Figures

Nomenclature

$\widehat{P}_k$	Maximum compartment pressure	Pa
$\overline{Mw_j}$	Average molecular weight of phase j	$\frac{kg}{mol}$
$\dot{Q}_k$	Rate of change in compartment k sensible enthalpy	$\frac{J}{s}$
$\vec{\dot{V}}$	Directional volumetric flowrate	$\frac{m^3}{s}$
$\check{V}_k$	Minimum volume of compressible phases of compartment k	m^3
$\dot{m}_{j,k}$	Mass flowrate of phase j from compartment k	$\frac{kg}{s}$
$\dot{n}$	Molar rate of transport	$\frac{mol}{s}$
$\dot{n}_i$	Molar flowrate of species i	$\frac{mol}{s}$
$\emptyset_{t_0}$	Timed activation at time $t = t_0$	$-$
$\emptyset_{t_i}$	Timed activation at time $t = t_i$	$-$
$\dot{\mathrm{Q}}$	Conductive heat rate	$\frac{J}{s}$
$\boldsymbol{A}$	surface area between compartments	m^2
$A_{j,k}$	Interfacial area of contact between the continuous phase and dispersed phase j of compartment k	m^2
C	Chemical species concentration	$\frac{mol}{m^3}$
$C_{A_{phase}}$	Concentration of A in phase “phase”	$\frac{mol}{m^3}$
C_{eq}	Equilibrium concentration	$\frac{mol}{m^3}$

$C_{i,So}$	Source phase concentration of species i	$\frac{mol}{m^3}$
$C^*_{i,So}$	Source phase interfacial equilibrium concentration	$\frac{mol}{m^3}$
$C_{i,T}$	Termination phase concentration of species i	$\frac{mol}{m^3}$
$C^*_{i,T}$	Target phase interfacial equilibrium concentration	$\frac{mol}{m^3}$
$C_{i,j,k}$	Concentration of species I in phase j of compartment k	$\frac{mol}{m^3}$
C_i	Species i molar compartment concentration	$\frac{mol}{m^3}$
$\boldsymbol{Cp}$	Heat capacity	$\frac{J}{kg.K}$
Cp_j	Heat capacity of phase j	$\frac{J}{kg.K}$
$\boldsymbol{Cp}_{k\rightarrow}$	Heat capacity of material leaving compartment k	$\frac{J}{kg.K}$
$\boldsymbol{Cp}_{k\rightarrow}$	Heat capacity of material entering compartment k	$\frac{J}{kg.K}$
D	Impeller diameter	m
$D_{p,j}$	Characteristic diameter of phase j	m
$D_{p,j+1}$	Characteristic diameter of phase j+1	m
Da	Damköhler number	$-$
E	enhancement factor	$-$
$E(t)$	Exit age	$-$
$\boldsymbol{Ea}$	Activation energy	$\frac{J}{mol}$
F	The rate of liquid flow	$\frac{m^3}{s}$

$F_{\rightarrow k}$	Material transport entering compartment k	$\frac{m^3}{s}$
$F_{k\rightarrow}$	Material transport leaving compartment k	$\frac{m^3}{s}$
H	Henrys constant	$\frac{mol}{m^3.Pa}$
K_C	Coefficient of circulated flow due to impeller action	$\frac{m^2}{rev}$
K_L	Liquid side mass transfer coefficient	$\frac{m}{s}$
$K_L a$	Volumetric mass transfer coefficient	$\frac{m^3}{s}$
Mw_i	species i molecular weight	$\frac{kg}{mol}$
Mw_p	Molecular weight of phantom species	$\frac{kg}{mol}$
$\bar{N}o_{PT}$	number of phase transport phenomena per compartment	$-$
N	Stirrer speed	$\frac{rev}{s}$
N	Number of tanks in series	$-$
No_Q	Number of material transport phenomena	$-$
No_k	Number of compartments	$-$
No_n	Number of networks	$-$
No_p	Number of phenomenon types	$-$
$P_{\mathbb{C},k,max}$	Maximum compressible material pressure in compartment k	Pa
$P_{\mathbb{C},k,min}$	minimum compressible material pressure in compartment k	Pa
$P_{\mathbb{C},k}$	Compressible material pressure of compartment k	Pa

P_{in}	Pressure of inlet feed	Pa
P_k	Pressure of compartment k	Pa
P_{k+1}	Pressure of compartment k+1	Pa
P_l	Container pressure	Pa
Q_k	Sensible enthalpy of compartment k	J
R	Universal gas constant	$\frac{J}{mol.K}$
S	Partition coefficient	$-$
T	Temperature	K
$T^{\emptyset}$	Standard formation temperature	K
$T_{\rightarrow k}$	Temperature of material entering compartment k	K
$T_{k,0}$	Initial compartment temperature at $t = t_0$	K
T_k	Temperature of compartment k	K
$T_{k\rightarrow}$	Temperature of material leaving compartment k	K
T_{ref}	Reference temperature	K
U	Heat transfer coefficient	$\frac{J}{K.m^2.s}$
V	Activation volume	m^3
V_{k+1_0}	Initial volume of compartment k + 1	m^3
V_{k_0}	Initial volume of compartment k	m^3
$\dot{V}$	volumetric flow	$\frac{m^3}{s}$
$V_{\mathbb{C},l}$	Total compressible volume in a container	m^3
$V_{\mathbb{C}}$	Compartment volume free to compressible phase occupation	m^3
$V_{i\mathbb{C},k}$	Total volume of incompressible material in compartment k	m^3

$V_{j,k}$	Volume of phase j in compartment k	m^3
V_j	Volume of phase j	m^3
V_k	Volume of compartment k	m^3
V_{k+1}	Volume of compartment k + 1	m^3
$V_{l,0}$	Initial Container volume at $t = t_0$	m^3
V_l	Container volume	m^3
Z	Basis of reaction rate	$-$
$f_{i\mathbb{C},k}$	Compartment k factor incompressible phase relaxation factor	$-$
$f_{j,k}$	Volume fraction of phase j in compartment k	$-$
$k_{(\mathrm{a}),}k_{(b)}$	Gradient of sigmoid response	$-$
$k_{T_{ref}}$	Specific reaction rate at reference temperature	$= f(rate)$
k_0	Pre-exponential factor/ frequency factor	$= f(rate)$
k_{So}	Source side mass transfer coefficient	$\frac{m}{s}$
k_T	Termination side mass transfer coefficient	$\frac{m}{s}$
$m_{i,j,k}$	Mass of species i in phase j of compartment k	kg
m_i	Mass of species i	$\frac{kg}{s}$
$m_{j,k}$	Total mass in phase j of compartment k	Kg
$\mathrm{m}_{\mathrm{k},\mathbb{C}}$	Total mass of compressible material in compartment k	kg
m_k	Mass of material in compartment k	
$n_{\mathbb{C},k}$	Total compressible moles, not including phantom species, in compartment k	mol
n_A	Moles of species A	mol
$n_{i,So}$	Moles of species i in the source phase	mol

$n_{i,T}$	Moles of species i in the termination phase	mol
$n_{i,j,k}$	Moles of species i in phase j of compartment k	mol
$n_{j,k}$	Total moles in phase j of compartment k	mol
$n_{k,\mathbb{C}}$	Total moles of compressible material in compartment k	mol
n_{min}	Minimum reactant moles required for reaction activation	mol
$n_{p,j,k}$	Moles of phantom species in phase j of compartment k	mol
$n_{p,k}$	Total phantom species moles in compartment k	mol
$n_{reactants}$	List of moles of each reactant of a reaction phenomenon	mol
p_1, p_2	Activation parameters of sigmoid response	$-$
r_{rxn}	Reaction rate	$\frac{mol}{s.Z}$
t	Instantaneous time of simulation	s
tol	Tolerance value below which a y value of the numerical solution is rejected	$-$
t_0	Initial time of simulation	s
$t_{max,[B]}$	Time at which maximum concentration of B occurs	s
t_{pulse}	Time of pulse injection into system	s
$x_{i,j,k}$	mole fractions of chemical species i in phase j of compartment k	$-$
y	Calculated value of variable value array	$-$
$y(t)$	y values returned from the numerical solver solution at time $t = t$	mol, J

y^*	Next best Calculated value of variable value array	–
y_0	Initial y values fed to numerical solver for solution	mol, J
y_i	Number of species moles variables	–
y_{ii}	Number of compartment enthalpy variables	–
y_{iii}	Number of compartment volume variables	–
y_{iv}	variables for tracking system and surroundings - mass and enthalpy	–
y'_t	Combined array of all differential values, for each variable, at time $t = t$	–
y_{total}	Total number of variables fed to a numerical solver	–
$\Theta_{I/O}$	Sigmoid response	–
$\Theta_{k+1 \to k}$	Activation of phenomena in direction from compartment k+1to compartment k	–
θ_t	Timed sigmoid response	–
Φ	Molar flux	$\frac{mol}{s.m^2}$
$\Phi_{So \to T}$	Molar flux from source to termination phase	$\frac{mol}{s.m^2}$
α_k	Minimum compressible phase volume factor of compartment k	–
β	Exchange flow factor of bulk flow	–
γ	Variable volume stiffness constant	m^3
ε	Stiffness constant which determines the impact of density deviation from ideal upon the compartment pressure	–
κ	Material velocity	$\frac{m}{s}$

$\rho_{j,i\mathbb{C}}$	Density of incompressible phase j	$\frac{kg}{m^3}$
$\rho_{j,k}$	Density of phase j in compartment k	$\frac{kg}{m^3}$
$\rho_{j,k}^{0}$	Ideal density of incompressible phase j in compartment k	$\frac{kg}{m^3}$
ρ_k	Density of material in compartment k	$\frac{kg}{m^3}$
σ^2	Variance of $E(t)$ plot	–
τ	Convective transport stiffness constant	s
τ_{res}	Residence time	s
τ_{flow}	Convective transport time constant	$\frac{m.s}{Pa}$
τ_j	Phase transport stiffness constant	s
τ_l	Container stiffness constant	s
τ_{rxn}	Reaction stiffness constant	mol
υ_a	Stoichiometric coefficient of species a	–
υ_b	Stoichiometric coefficient of species b	–
υ_c	Stoichiometric coefficient of species c	–
υ_d	Stoichiometric coefficient of species d	–
υ_i	Stoichiometric coefficient of species i	–
φ	Stiffness constant for the timed activation of phenomena	–
$[A]_{Aqueous,k}$	Concentration of species A in the aqueous phase of compartment k	$\frac{mol}{m^3}$
$[A]_{Gaseous,k}$	Concentration of species A in the gashouse phase of compartment k	$\frac{mol}{m^3}$
$[C]_{p,j,k}$	Concentration of phantom species in phase j of compartment volume V_k	$\frac{mol}{m^3}$

∞	Infinity	–
$\Delta[A]$	Concentration difference of species A between two volumes	$\frac{mol}{m^3}$
ΔC	Species concentration gradient	$\frac{mol}{m^3}$
$\Delta H_{j,k}^{\emptyset}$	Enthalpy of formation of the phase j in compartment k	$\frac{J}{kg}$
$\Delta H_{f,i}^{\circ}$	Enthalpy of formation of species i	$\frac{J}{mol}$
ΔH_{rxn}	Molar enthalpy of reaction	$\frac{J}{mol}$
ΔH_{trp}	Molar enthalpy of transport	$\frac{J}{mol}$
ΔP_{pump}	Pump differential pressure	Pa
ΔQ_k	Change in enthalpy of compartment k	J
ΔT	Temperature difference	K
ΔV_k	overflown volume of compartment k	m^3
ΔX	Generic driving force for phenomenon	–

List of Abbreviations

CFD	Computational Fluid Dynamics
CM	Compartment Modelling
CPU	Central processing Unit
CSTR	Continually Stirred Tank Reactor
DAE	Differential Algebraic Equation
DiV!0	Division by Zero error
EOS	Equation Of State
GPU	Graphics Processing Unit
IDE	Integrated Development Environment
IVP	Initial Value Problem
LHS	Left Hand Side
MTR	Mass Transfer
NoZ	Network of Zones
ODE	Ordinary Differential Equation
PBM	Population Balance Model
PFR	Plug Flow Reactor
RAM	Random Access Memory
RHS	Right Hand Side
RTD	Residence Time Distribution
S. T. P	Standard Temperature and Pressure
UoL	University of Leeds

Chapter 1 Introduction

The study of chemical process unit operations is of high interest in chemical engineering. Experimental rigs and computer simulations alike are developed and built to investigate the parameters affecting such systems and to understand and predict the observed phenomenological behaviour. Experimental rigs produce information on the process relationship between parameters and system performance. However, experimentation can be expensive, and intrusive noise of real-world set-ups result in the distortion of crucial detail.

Numerical simulation of large complex dynamic systems of equations, that mimic the system behaviours, is the current alternative offered to overcome the expenses of such set-ups. Along with the lower capital expense, once set up, numerical experiments can be investigated in parallel, facilitating optimisation. However, for fully 3D resolved computational modelling, such as computational fluid dynamics (CFD), solutions can take weeks to months of solution time to simulate a few seconds of simulation time solving due to the large number of equations associated with the Navier-Stokes equations on a detailed grid.

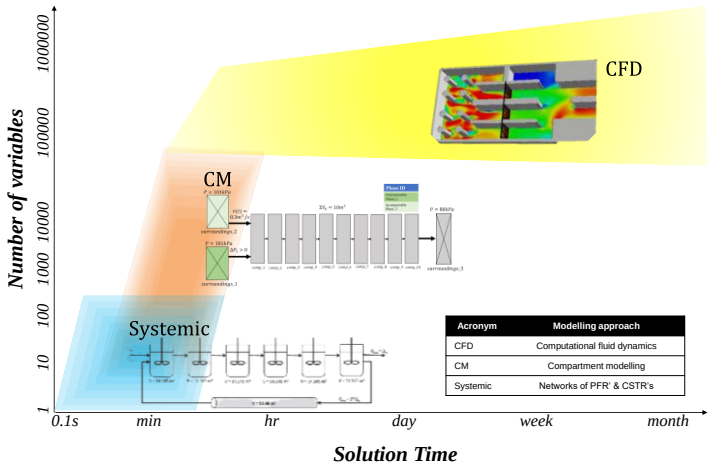

Figure 1 - Chemical unit operation modelling techniques, rated by number of variables and solution time.

A coarser approach to modelling unit operations is compartmental modelling (Introduced in detail in Chapter 2); this approach is compared to other process modelling techniques common in chemical engineering, in Figure 1. The solution time is the time investment required to solve a given model in real-world time. Number of variables represents the numeric detail, length scale, that can typically be resolved by the modelling approach. A positive correlation between an increase in solution complexity and output resolution is observed, CFD has the largest solution time and greatest resolution and single unit models (e.g., CSTR, PFR) have the lowest solution times and output resolution. Compartment modelling ranks central between that of systemic modelling, a complex network of CSTR/PFR's, and computational fluid dynamics. This intermediate approach, compartment modelling, describes the system and its processes at a cheaper computational cost than CFD and thus resolves a solution in a shorter time, whilst still holding the intricate complexity of the process geometry.

Compartments of a chemical process compartment model represent sub-volumes of the process/unit. Each is regarded as a well-mixed volume of which the constituent phasic and chemical species material is intimately mixed. Multiple phenomenological models are applied in compartment modelling to describe the semi-empirical inter-relationship of system variables; phenomenological models are not derived from first principles but are consistent with fundamental theory; they are designed for application rather than understanding the fundamental theory of the process modelled, focused upon describing the relationship of variables instead of why they interact in the manner they do. Phenomena can either occur between the compartments, such as in the transport of material or transformation of material. Or phenomena can occur within the compartments, e.g., the Chemical kinetic rate equation is a function of component concentrations and a rate constant computed from an expanded version of the Arrhenius equation; a prevalent phenomenon issued to compartment modelling applications.

In the development of a compartment model, the compartmentalisation of the system is like CFD, dissecting the larger process geometry into an interconnected collection of sub-volumes (compartments). The compartmental network is coarser, formed of fewer compartments and flows were compared to the converged mesh of CFD. The specification of fixed flow rates between compartments, instead of calculating them with each time step in CFD; the coarser grid; and the non-solution of the Navier-stokes momentum equation, all invoke a comparatively reduced solution time when comparing compartment modelling to the modelling approach of CFD.

Mathematically, compartmental models are extensive first-order differential equation sets (ODE's) which describe the system variables' time dependence, functional of rates of change induced by phenomenological models. The value of a differential at any given time within the simulation is the sum of the instantaneous phenomenological rates (e.g., reaction, mass transfer, phase transport, heat transfer) effect upon each variable of the system. Because of the interconnected complexity of the equation systems of a compartmental model, analytical methods cannot be used; instead, numerical solvers are employed.

The application of compartment modelling is broad, with the four most-prevalent topics (*excepting chemical process unit operations*) being in the field of **combustion** (Komninos, Hountalas and Kouremenos, 2004; Bohbot *et al.*, 2009; Kozarac, Lulic and Sagi, 2010; Komninos and Rakopoulos, 2016), **Pharmacokinetics** (Leaning and Boroujerdi, 1991; Barrett *et al.*, 1998; Golberg and Rubinsky, 2013; Laínez-Aguirre, Blau and Reklaitis, 2014; Moxon and Bakalis, 2016; Uno *et al.*, 2019; Rico-Ramirez *et al.*, 2020; Kim, Kim and Chung, 2021), **physiology** (Huang, Niokal and Chance, 2002; Piemonte *et al.*, 2017) and **ecology** (Eriksson, 1971; Schramski, Kazanci and Tollner, 2011).

The difference in these models of each topic is the nature in phenomena applied and the conceptualisation of the model structure.

With physiology compartment models, the compartments represent a store of a species (e.g., plasma insulin, plasma glucose; see (Piemonte et al., 2017))

with rates of exchange between compartments. Material transport from one compartment to another is modelled as a transport term but once arrived at the target compartment the species is conceptualised as to have undergone a chemical transformation. Thus, transport between compartments is representative of a reaction pathway. Physiology modelling differs to Pharmacokinetics by the representation of the compartment. In physiology, the compartment can represent the blood system, an organ, bones, or another part of the body. In pharmacokinetics the compartment is a store of species of no real location.

Pharmacokinetic models metabolic effects upon drugs within the body through one-sided conversion "flows" and high-detail reaction schemes. Compartments represent stories of drug states and the flows between them, the reactive conversion of states, e.g., (Laínez-Aguirre, Blau and Reklaitis, 2014). The compartment volumes are abstract and adjusted to fit experimentally obtained data to the constructed model.

Ecology compartment models predict the change in populations of an ecosystem, formally referred to as "*Reservoir theory*". The systems model the plant foliage, sea and atmosphere as separate compartments and the exchange of carbon, living species, nutrients between these compartments as either of transport or transformative (synonymous with reaction probability theory) phenomena.

Combustion models are used to understand the distribution of temperature within a cylinder during piston movement. The systems modelled operate at high pressure and temperature, with only a single gaseous phase ever considered. Semi-empirical models for evaluation of spray penetration into a chamber, heat transfer and ignition/combustion are common to the compartment models of combustion.

Construction of these models of differing topics to unit operations is relatively matured, reflected in the more significant number of papers published. This is due to domain-specific tools being readily available to the modellers of these topics, Pharmacokinetics, e.g., NONMEM (Kim, Kim and Chung, 2021), ecology, e.g., Econet, (Schramski, Kazanci and Tollner, 2011), combustion,

e.g., AVL Boost (Kozarac, Lulic and Sagi, 2010). Domain specific tools assist the modeller, removing the need for domain knowledge in implementation/solution of a model, and instead permitting focus of the modeller upon model development.

Such domain specific tools are **not** available for the application to compartment models of chemical process unit operations.

1.1 Project Motivation

Fluid flows coupled with chemical or physical transformations are ubiquitous in engineering, examples being combustion, crystallisation, and reactor design. Compartment models are a critical established tool since spatially fully resolved simulations (e.g., CFD) are often too expensive (with impractical solution times of days or weeks).

Compartment models decompose the geometry into compartments, e.g., a pipe section or the agitator zone in a batch reactor. For each zone, fixed flowrate flows, and multiple phenomena are solved in combination with the transport of materials across interfaces between compartments.

The phenomena are often complex, and may have vastly different time scales, the resulting systems are mathematically stiff, difficult to solve, and existing standard ODE solvers are often inefficient, making near real-time simulations very difficult; either not converging, or requiring small time steps to reach solution, invoking even longer times to solution.

The preconceived simplicity of compartment modelling motivates modellers to approach their models with bespoke model development. Those without the skills required to design, develop, implement, and solve compartment models – *those without domain knowledge in the modelling approach, programming, domain expertise of the physical system and implementation of the model and numerical solvers* – face a hurdle when the model goes beyond a simplistic size; of more than a few phenomenon/compartments. This gap in the knowledge is the lack of a universal compartment modelling framework for chemical process unit operations. The modelling of complex unit operations

requires a solid understanding of the physio-chemical systems, the domain expertise. In other areas domain experts access compartment modelling software infrastructure, whereas in engineering the domain experts also require the skills to implement programmatically solve these models, this has resulted in an underutilisation of this approach in chemical engineering.

1.2 Project Objectives & Thesis Structure

Although compartment modelling is an established modelling approach, the models of unit operations created are bespoke to the problem being modelled, even though derived from the same building blocks, phenomena, and structure.

Objectives:

(i) Develop a universal compartment modelling theory of unit operations in chemical engineering (Chapter 3),

(ii) implement said theory into a prototype tool framework (Chapter 4) that can take a domain expert description (requiring development of a universal input language) of a model and automatically generate the equations for a corresponding network of compartments and associated phenomena in the digital space and,

(iii) to validate the correct implementation of the theory (Chapter 5) through a subset of models representing the scope of the framework's capability, solved within the tool with numerical solvers to produce model solution in faster than real-time.

The thesis structure is given below.

Chapter 2: Literature is surveyed for data relating to the construction, implementation, and solution of chemical process unit operation compartment models. A particular focus is drawn to compartment modelling structure and integration of phenomenological models. Analysis of the literature reveals the

prevalence of themes, such as (i) the number of compartments, (ii) the complexity of models, measured as the number of ODE's is discussed and, (iii) the nature of phenomena. The requirements of a universal compartment modelling framework are synthesised, giving a universal definition of compartment modelling based upon the state of the application in literature.

Chapter 3: A universal chemical process compartment modelling framework is conceptualised to cover the scope of observed practical applications of compartment modelling to unit operations in literature. The framework mathematically describes the temporal state and evolution of species, phase, and compartments within a chemical process compartment model due to common phenomena of literature.

Chapter 4: The implementation of the universal equation set, developed in Chapter 3, is formulated into a tool named CompArt, with an associated universal compartment modelling language. In this chapter, explanation of CompArt’s interpretation of the model description and generation of the associated differential system is detailed. The system is solved over the time interval with the specific solver settings passed to the tool for the solution of the compartment model.

Chapter 5: The final stage of this project is the validation of the tool CompArt, within this chapter simulation results are analysed verifying the phenomenological models behave as expected with analytical results.

Chapter 6: A summary of the work and conclusions drawn with a suggested future works list, including but not limited to the performance evaluation of CompArt and future integration of design space optimisation.

Chapter 2 Literature Review

2.1 An Introduction to compartment modelling

Compartment modelling is a non-linear approach to the modelling of process unit operations in a computably less intensive manner than full resolution CFD but more spatially accurate approach than ideal reactor modelling (e.g., single CSTR or PFR, see (Stoller, Bravi and Chianese, 2005; Du *et al.*, 2015)). The decrease in computational requirement compared to CFD lies in (i) the decoupling of the unit hydrodynamics from the phenomena, (ii) the removal of momentum balance when compared to CFD, and (iii) increased coarseness of the model compared to the number of cells in a CFD mesh. Compartment modelling provides the means to investigate the effects of phenomena upon the mass and energy quantities of the system where it would be otherwise too computationally intensive to run full resolution CFD hydrodynamics with the phenomena, and the resolution of ideal reactor modelling is not great enough for the study of the local effects of the phenomena.

Compartment modelling, initially coined in applications to chemical processes by Wiley, Hepburn and Levenspiel (1999) was introduced as an approach to construct "*systemic models"* of more extensive systems as a network of flow connected compartments, to study the effects of phenomena (including flow) upon the systems composition over time. These systems were composed of spatially non-representative ideal CSTR's and PFR's (each referred to as a compartment) connected by a network of material flows. A small amount of non-interactive tracer, inert material, is input into the system via the inlet for the model and experimental rig. The evolution of tracer concentration at the outlet of the system is evaluated to give a residence time distribution (RTD) of tracer through the system – giving indication to the internal hydrodynamics of the system. A *"systemic model*" was said to be representative of the unit hydrodynamics if the experimental tracer results of the model and experiment (RTD) were a match.

However, due to the non-spatially representative nature of the compartments in the systemic modelling approach, multiple compartment network arrangements result in the same RTD profile. As a result, the application of system phenomena to each of the differing models, with an identical RTD, result in differing global mass and energy values over time. Although the hydrodynamics of a systemic model can be validated through RTD comparison, the modelling approach is unreliable and difficult to validate where phenomena is applied. Compartment modelling, as coined at this early stage, was seen as a simple modelling approach inherent in high inaccuracies due to the multiplicity of RTD from varying model networks. And due to the non-spatial compartment's this approach cannot account for the geometry of phenomena within a system (Jourdan *et al.*, 2019), making investigation of spatially accurate local compositions an difficulty.

Prior to this, Knysh and Mann (1984) developed a Computational 10 x 10 "*zonal"* model, where the zones – each a well-mixed compartment – are spatially representative of a sub-volume within the process operation. This was the first paper to develop a large enough model, measured by number of compartments, to reasonably predict the distribution of tracer due to bulk and turbulent material flow. And, although named zonal modelling, this is the paper to which current applications of what we refer to as "compartment modelling" are built upon.

In this project it is important to note we refer to compartments as Knysh and Mann (1984) presented them in the earlier *"zonal"* model, as spatially representative sub-volumes (compartment) – e.g., see Figure 2; as opposed to the older nomenclature of Levenspiels spatially non-representative compartments which are still abundantly referred to as compartment models and present in literature. We maintain the naming "compartment modelling" for the spatially representative modelling approach going forward and "systemic modelling" for non-spatially representative compartment modelling in line with the definitions of Haag *et al.* (2018).

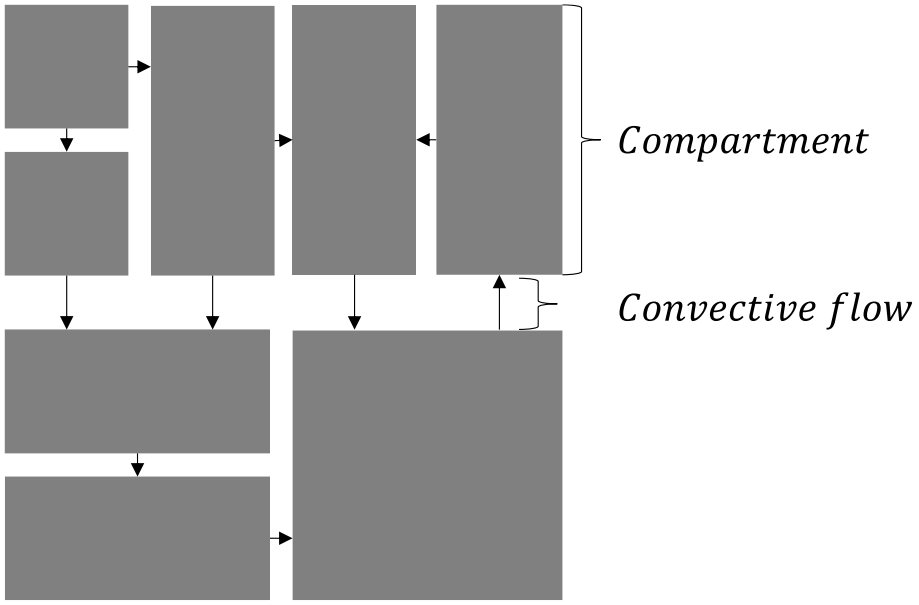

Figure 2 - Abstracted compartment model formed of 8 compartments (of total volume equal to system volume), of which are connected through a network of 10 convective transports (representing the hydrodynamics of the modelled system).

In this chapter, further to the well-mixed nature of compartments, the network of compartments and flows are discussed in section 2.3 Elements of Compartment Models and section 2.4 Material Flow; most compartment models of literature are built (compartmentalisation of the unit) based on the agglomeration of CFD mesh results. Advancements in access to computational fluid dynamics through general model developments which eventually found their way into commercial tools, provided opportunity for better-discretised compartment models based on the accurate hydrodynamic results of CFD; the hydrodynamics of which are tightly bound to a particular piece of equipment (Rigopoulos and Jones, 2003).

A compartment is a well-mixed, fixed volume. In special cases compartments with dynamic compartment volumes e.g., the timed volume change of compartments in (Öner *et al.*, 2019) have been observed; see section 2.3.3 . The well mixed nature of a compartment lends to the value of each variable of a compartment (e.g., Temperature, moles of species A, moles of species B) represented each as a single value. The change in variable values within the spatially discretised model is due to phenomenological mechanisms (see section 2.5 Applied phenomena), which is mainly flow between

compartments; represented as a differential value e.g., the change in concentration of species A, $d[A]/dt$. Mechanisms produce rates of change, mathematically ordinary differential equations, which describe the instantaneous change in variable values per time; solved over a time domain with an appropriate numerical solver. The modelling approach is scalable as the underlying physics of the system and mechanisms are scale-independent (Nauha *et al.*, 2018).

Flow between compartments is typically of set volumetric or mass rate as to maintain the balance about each compartment to net zero change. The compartments, and fixed flows of a compartment model together represent the steady state hydrodynamics of the process. With the compartment modelling approach, it is assumed the phenomena of the model do not influence the hydrodynamics. However, there are a minority of examples of compartment modelling where phenomena influence has been accounted for such as the bubble slip velocity of (Laakkonen et al., 2006), further discussion is given in section 2.5.1 Phase Transport.

A compartment model is visualised, further discussed in section 2.3.1 Compartmentalisation, as rectangles representing compartments and arrows that symbolise flow through the network of compartments (Krychowska *et al.*, 2020). The shape of a compartment and boundaries are inconsequential; the importance lies in the interconnectivity of compartments (Rigopoulos and Jones, 2003).

The initial variable values and differential equations form the mathematical equations of a compartment model. An investigation into the approach to describing and implementing compartment models, section 2.6 Compartment model Implementation & Solution, points towards the use of bespoke modelling techniques which are neither repeatable nor reliable with the injunction of human error severe.

Appendix A contains the surveyed data from 48 papers of literature, this is the basis data set for the review. Table 1 shows the papers of this survey categorised into process operations headers. From this table we see the unit

operations of primary focus in literature are **bioreactors** and **crystallisers**, which are complex multi-phase systems, and **reactors** which involve both hydrodynamics and species reactions – a complex combination of phenomena.

Bioreactors are most prominent in the literature at 36% of the papers cited, followed by **reactors**, of a non-biological nature, at 24% and **crystallizers** at 11%. **Specialty units** include the walking beam furnace of (Švantner, Študent and Veselý, 2020), powder mixing process of (Portillo, Muzzio and Ierapetritou, 2006) and chronographic bubble trap of (Beck et al., 2020) equal a 9% portion of the survey. **Stirred tanks** have the same portion of the papers as the **specialty units**. With the units of the least proportion of the literature in descending order, the **water treatment** units (7%) such as the stabilization pond of (Alvarado et al., 2012) followed by **separators** (4%) such as the high-purity air separator of (Bian et al., 2005).

Table 1- Relative composition of process unit compartment models observed in literature

Unit operations	Percentage of examples
Bioreactor	36%
Reactor	24%
Crystalliser	11%
Stirred tank	9%
Speciality unit	9%
Water treatment	7%
Separator	4%

2.2 Focus of the literature review & surveyed data

Compartment models of chemical engineering unit operations, formed of a system of ODE's is the focus of the review and work. Although, compartment models can be described as a system of differential algebraic equation set (DAE) / as a boundary problem, this involves an entirely separate approach

to solution and description of the model and so is not involved in this review. However, it must be noted, DAE models which can be translated to an ODE by embedding the algebraic equations in the ODE's are considered in this review (Bermingham, Kramer and Van Rosmalen, 1998; Bezzo, Macchietto and Pantelides, 2003; Wells and Ray, 2005a; Zheng, Smith and Theodoropoulos, 2005; Le Moullec *et al.*, 2010; Kim *et al.*, 2020).

Compartment models with an analytical solution have also been removed from consideration; those with analytical solutions are inherently simple and derive little information on the complex models of this works focus.

Finally, stochastic solutions of compartment models are not included, as the focus is upon the opposing system type - deterministic modelling.

For the following reasoning pre year 2000 models have been mostly retracted from review, they consist of either.

(a) **Ideal reactor networks** (networks of CSTR's and PFR's) which are solved analytically, which are **out of scope** due to the nature of the solution.

(b) Or **analytically solved RTD models**, a network of flow connected compartments, which are excluded for the following three reasons. (1) Unlike current models, the model compartment volumes do not summate to the process unit volume (spatially non-representative) ~ *Systemic modelling*. A product of systemic modelling is the model developed does not produce a unique RTD pattern; (other compartment network arrangements can produce the same RTD). (2) As a result of the above point, any added phenomena could have significant variance in results in two models of the same RTD. (3) The solution method is typically analytical; the review focus is upon numerically solved ODE compartment models.

A common implementation of compartment modelling is in symbiote with population balance models, a method to observe the change in multi-phase system droplet size and number of dispersed phase entities over time. Those compartment models which hold a greater focus on population balance modelling and defected from the review as PBM is a separate complex entity

of modelling, not a phenomenological model applied to compartment modelling e.g., (Dompazis, Kanellopoulos and Kiparissides, 2006; Dueñas Díez *et al.*, 2006; Chaudhury, Armenante and Ramachandran, 2015).

The prevalence of compartment model papers published per year from 1991-2021, subject to the constraints of the reviews scope, is given in Figure 3; there is a consistent positive trend in published material over this period; an average of 3 papers a year – the number of which is hypothesised to be low due to the current non-tool assisted approach a modeller is required to take in model implementation, and the bespoke nature of models resulting in a low reusability - this is discussed further in section 2.6.1 Implementation of a compartment model.

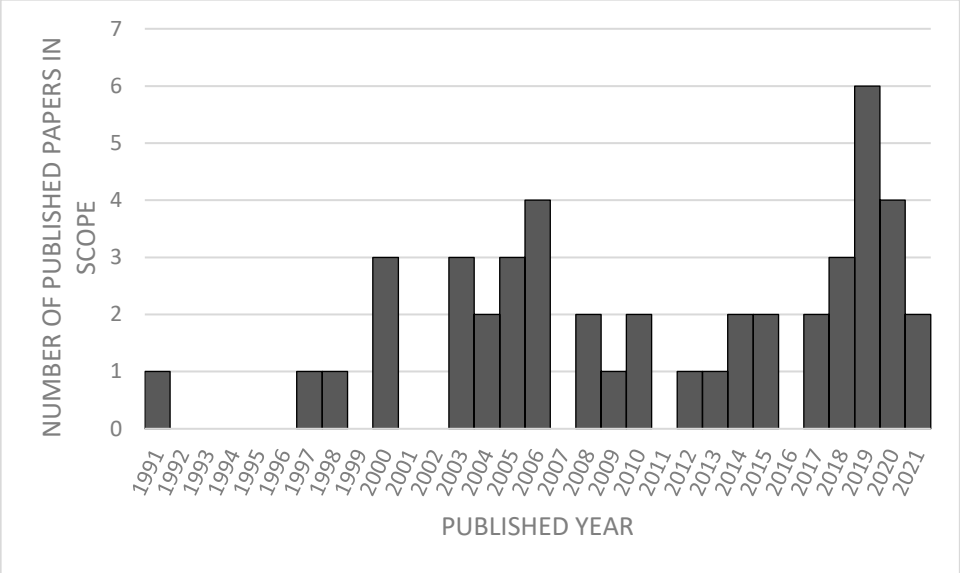

Figure 3 - Quantity of published review-focus compartment modelling papers per year between 1991-2021 with positive correlation in time.

Of the compartment modelling literature investigated, 18% is excluded due to a prevalence for population balance modelling (PBM), 7% are DAE models. 75% of the papers were composed of ODE models, 20% of the total were either analytically solved systemic or RTD models and 20% of stochastic solution. The total percentage of compartment modelling papers in literature within scope is 35%, totalling 48 papers – summarised in Figure 4.

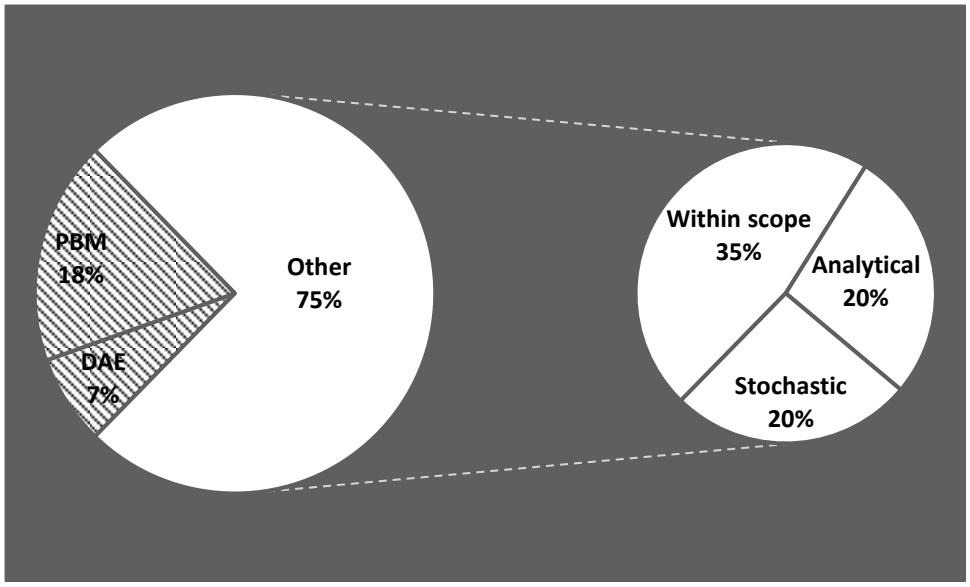

Figure 4 - Compartment modelling scope and context.

The hypothesis of this work is that compartment models are both bespoke in implementation and solution. Model construction is an activity in exclusive to domain experts who can program compartment models or develop bespoke tools for the simulation of models. A detailed literature review, consisting of models which fit the scope of investigation, is completed, and is reported in Chapter 2 to determine the extent to which this is correct, and to collate the elements of compartment modelling at each stage, construction, implementation, and solution. Table 2 is a key, describing the column data captured in Appendix A.

Table 2 - The relation of literature data collected to the state-of-the-art investigation of compartment modelling.

Column data of Appendix A	Capture statement
Reference	The author and the published year.
Unit Operation	The process/unit operation modelled, previously discussed in section 2.1 An Introduction to compartment modelling.
Differential variables per compartment	A measure of the complexity, by number of differential variables in the system.
Number of compartments	Represents the structure of the system, the size of which is intimately linked to the compartmentalisation approach.
Phenomena Number per compartment	Highlights the most utilized sub-models within the scope papers, each bracketed number representing the average number of phenomena per compartment of the model.
Compartmentalisation	The *flow-volume* topology development method - compartmentalisation.
Tool	Highlights the bespoke nature of practical model implementation – due to lack of domain specific tools.
Solver	The numerical integration solver utilized in the model variable value's progression over the time domain investigated.

2.3 Elements of Compartment Models

2.3.1 Compartmentalisation

The compartmentalisation of a unit operation is the first step in the development of a compartment model, it is the partitioning of the unit volume into several compartments which are subsequently connected by convective flow rates; together this represents the fixed hydrodynamics of the system. The summed volume of the compartments equates to the volume of the unit and the flows are typically of fixed flow values, the compartment is discussed further in section 3 and flowrates are discussed further in section 2.4 Material Flow.

From the data of Appendix A, column “Compartmentalisation” we see to compartmentalise a unit, the hydrodynamic data required is either (i) predicted using a higher resolution model (*computational fluid dynamics, CFD*) without phenomenological complexity e.g., (Wells and Ray, 2005a) or, (ii) assumed based on *process knowledge* such as in the case of the compartmentalisation of a gas-liquid flash separator (Pladis *et al.*, 2011).

In the process of model development, the collected hydrodynamic data is processed to produce the topology of the subsequent compartment model via one of the following routes.

(1) Compartment topology, discretisation, developed from *process knowledge* is typically **heuristic** in nature, which can be based upon chamber sizes in the unit, the detailed process knowledge beheld by the modeller, observation of the unit in operation. A **heuristic** approach can be taken where a unit is discretised without the need for a CFD map of the flow by simply discretising the unit int an increasing number of compartments (based on process knowledge) until grid independence is reached. A compartment topology is accepted as independent when a tracer run through the system produces no differing RTD upon further discretisation, and the Damköhler number (the ratio of convective transport time and reaction time of the reactants in that location)

is sufficiently small $Da < 1$. See; (Rahimi and Mann, 2001; Zheng, Smith and Theodoropoulos, 2005; Stanley *et al.*, 2008)

(2) **NoZ** - Network of zones (NoZ) compartmentalisation is a special case where the compartments are a product of progressive dissection of a unit operation axially, laterally, and horizontally into slices, this results in compartments of equal size. The benefit of the NoZ approach is the removal of user decision in the compartmentalisation approach. Instead, the number of slices in each of the planes is increased until a tracer run through the system produces a RTD consistent with the previous coarser model; synonymous with grid independence of CFD, the solution is “independent of the grid” where any further discretisation shows no change in output RTD result. This approach to compartmentalisation factors in grid independence testing. Using a further term, the Damköhler number, the ratio of convection time scale to reaction time scale (Guha *et al.*, 2006; Yang *et al.*, 2019), is evaluated to justify the well-mixed assumption of compartments; if not satisfied the unit is further sliced into a larger number of compartments.

(3) With **Tolerance based CFD** compartmentalisation, a low value is set, the tolerance, to which key intrinsic properties of the system (e.g., temperature, concentrations, pressure, k-e) are evaluated in the CFD result. Compartments are formed of agglomerated volumes in the system where these properties vary within the tolerance set. An example, for the concentration of a reagent extracted from a CFD result (assuming this to be one of/the intrinsic property chosen for compartmentalisation), if a connected sub volume in the unit operation spans part of the system with a variance in this quantity within the tolerance set $(+/-0.1 mol/m^3)$, this sub volume is then considered as a single compartment. This results in several compartments of typically varying size of summed volume equal to the volume of the unit modelled. The development of algorithms for the automatic conversion of **CFD** data into a compartment model has been of peak interest in the past two decades, examples include; (Bezzo and Macchietto, 2004; Delafosse *et al.*, 2010; Öner *et al.*, 2018; Tajsoleiman *et al.*, 2019).

(4) NoZ is also utilised in conjunction with a **CFD** result, formally referred to as **CFD + NoZ** compartmentalisation. e.g., (Guha *et al.*, 2006; Delafosse *et al.*, 2014), with momentum balance eliminated and flows set based on the CFD run (see section 2.4 Material Flow for further information on compartment flow determination). A CFD output of the unit operation is progressively dissected using the NoZ approach until the intrinsic properties of each compartment abide by the tolerance value set.; resulting in a NoZ model topology structure.

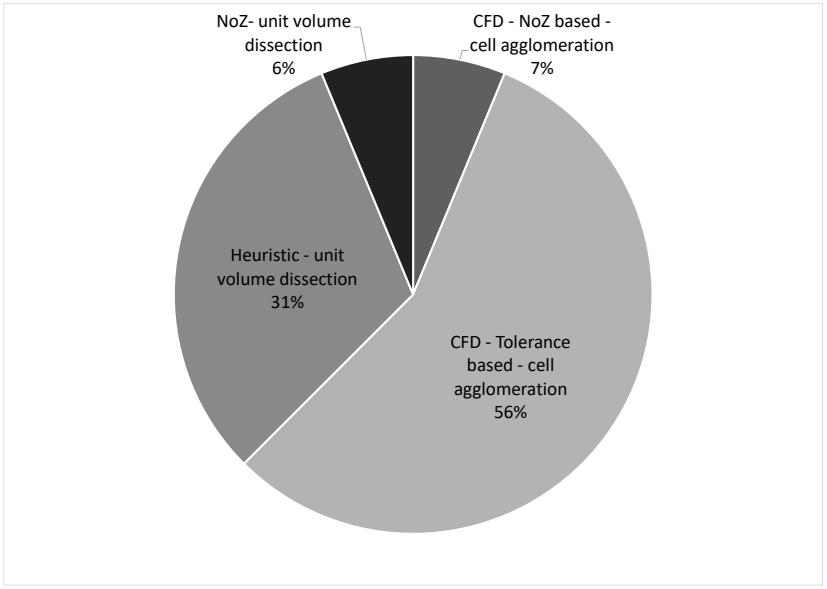

Figure 5 - Compartmentalisation approach of reviewed papers.

The proportion of the approaches to compartmentalisation of a unit operation, based on the database of compartment modelling papers in Appendix A, is given in Figure 5. The most utilised approach is the conversion of CFD hydrodynamic map into a compartment model, through the aggregation of cells of similar intrinsic properties value (56% of citations) with a set tolerance, e.g., the agglomeration of cells based on the pressure and turbulent dissipation (Nauha and Alopaeus, 2015). Through this approach the critical resolution of unit hydrodynamics produced through CFD are captured within the compartment model post compartmentalisation.

The heuristic approach to compartmentalisation, dissection of process volume based on process knowledge covers 31% of citations. Process knowledge refers to modeller's perception of well mixed zones in the unit or to the observation of well-mixed zones during the unit operation. Such as in (Le Moullec *et al.*, 2010), the compartmentalisation of a wastewater treatment unit based upon the gas fraction observation, resulting in sliced sections of the channelled unit based on volumes with and without bubbles of gas.

Network of zones modelling has had a lesser implementation in the topic of compartment modelling of chemical processes, combining papers with and without the assistance of CFD, the proportion of cited papers in Appendix A is only 13% of the total. The reality of this low number likely comes from the resultant model size of NoZ compartmentalised compartment models; being of 10^3 orders of magnitude greater than models from the other approaches to compartmentalisation e.g., Number of compartments for NoZ compartment models, 2160 (Guha *et al.*, 2006), 8000 (Zheng, Smith and Theodoropoulos, 2005), 12000 (Stanley *et al.*, 2008), 12960 (Delafosse *et al.*, 2014) and 32768 (Rahimi and Mann, 2001).

Building NoZ compartment models of this size inhibits the application of complex phenomena such as mass transfer and the modelling of multi-phase systems; the result, rigid plane-symmetric models which are synonymous with coarser CFD, without a momentum balance applied. Although the number of compartments is immense, it cannot be ignored that in the case of (i) CFD not being applicable for compartmentalisation (potentially difficulties include, unattainable convergence of CFD due to incapacity for multiphase modelling and insufficient computation for coupled phenomena) and (ii) a heuristic approach based on process knowledge not applicable (where the unit operation is novel and not self-evident in operation), the NoZ approach combined with Damköhler number requirement for compartment size offers an instrumental early stage understanding of process hydrodynamics.

As per the "number of compartments" column of Appendix A, a majority, 77%, of the cited models are composed of 100 or less compartments, of which 57% are constructed through agglomeration of CFD cells and the remaining 43%

are formed through a heuristic unit volume discretisation. With 8% of models are formed of $100 < \text{model size} \leq 1000$, these models are formed with the agglomeration of CFD cells with the exception of one case (Gresch *et al.*, 2009) which uses the CFD + NoZ approach to compartmentalisation. The remaining 15% having equal to or more than 1000 compartments; composed of near equivalent number of CFD, CFD + NoZ and NoZ cases.

2.3.2 Compartment Composition

The typical compartment, a well-mixed CSTR, is composed of a single phase, where in a multiphase model (42% of the cases cited in Appendix A) each phase is encapsulated within an individual compartment. Compartments, although not of a distinct shape, are typically illustrated as a four-sided 2D box with nomenclature indicating the phase type within (e.g., gas, liquid, solid). Species are homogenously distributed within a compartment phase volume; the resultant concentration of each species is the molar value per fixed compartment volume.

Accurate phase volume modelling is key to accurate phenomena modelling e.g., Reaction, Mass-Transfer. The phase of a compartment is assumed to fill the compartment volume, this assumption is independent of the species composition within the phase. This approach to phase modelling, named *"Assumed-solvent",* is typical and invokes the assumption of a non-disclosed solvent as always present in the system; filling the compartment volume where the species are not present.

The *"Assumed-solvent"* assumption is fine for use with single phase dilute systems of constant unit volume, tracking species of interest in low concentration. However, this approach does not account for changing phase volumes, an important consideration with non-dilute systems where species contribute a significant proportion of the volume to the phase. As the species molar quantity is reduced, the compartment volume is unchanged where it should otherwise reduce; the result is an underestimated concentration – a property of the species key to many phenomenological mechanisms including flow of material.

In the more advanced exception of (Laakkonen *et al.*, 2006), the phases (sub-regions) within the compartment are permitted to change in volume. The volume of each phase calculated based on the molar volume, synonymous with density; where for liquid the molar volume is a fixed value, and for gaseous phases an equation of state revealed the molar volume based on constant temperature and pressure values. Where the summed volume of phases is greater than the compartment capacity, and overflow of material is used to drive the sum of phase volumes towards that of the compartment, discussed further in section 2.5.1 Phase Transport.

Continuum-dispersion modelling, where one phase encapsulates the others present, has only been observed within compartment modelling where a population balance model (PBM) is implemented, of which 6 citations Appendix A utilise. With PBM, the dispersed phase is split into dispersion categories, each representing the number of dispersed phase bubbles/droplets of a particular spherical size range e.g., 1-2mm, 3-4mm in size. As PBM is excluded from the review due to its empirical nature, see scope reasoning in section 2.2 Focus of the literature review & surveyed data, the only means to multiphase modelling is (i) the presented phase-specific compartments as described prior (individual compartments representing individual phases), (ii) the work of Laakkonen *et al.* (2006) where multiple phases can exist in a compartment represented a separate sub-volumes, or (iii) other phase species are not existing within their own phase but enmeshed within the liquor of the compartment, only identified as a differing phase component by the naming of the species (e.g., $CO2(l), CO2(g)$ in (Kim et al., 2020)). Treating gaseous, liquid, and solid phase volumes as phases of the same nature, both the pressure-volume relationship and incompressible/compressible nature of the phase, is inaccurate especially where gaseous phases are present, and pressure is a variable in the process. There is a clear lack of continuum-dispersion modelling, to be addressed in the development of a universal framework.

2.3.3 Dynamic phase volume modelling

Fixed volume compartments (the *"Assumed-solvent"* method as described in section 2.3.2 Compartment Composition) is the standard approach in compartment modelling. This assumption is recognised as an inhibiting feature due to the inability to model the filling and emptying stages of units. Subsequently adaptations to the modelling of phase volumes have been made to address this missing feature of the approach, see cases (1-4), where the phase volumes within the compartment are dynamic – each case takes a unique approach.

Case 1 - *Phenomena induced volume change:* To account for volume change due to reaction, Zheng, Smith and Theodoropoulos (2005) introduced a volume differential for each compartment which determines the change in phase volume, and subsequently reaction volume, as a function of change in species molar quantity within a compartment and the constant property of the species "molar volume" synonymous with density of the phase it inhabits.

Case 2 - *System level control:* To maintain a constant reactor liquor level Arizmendi-Sánchez and Sharratt (2008) introduced a differential to model the change in phase volume of the reaction space in a jacketed reactor. The change in volume is a function of reactor liquor height and target height, emptying the volume species proportionally to the concentration in the liquor where the height exceeds the target.

Case 3 - *Accounting for addition of material:* To model the volume change of a semi-batch crystallisation unit, due to the addition of a second liquid into the vessel, Öner *et al.* (2019) took a differing approach whereby the volumes of compartments change as a function of simulation time; where during the filling of the vessel, the phase volumes are equally increased in volume from empty $(Volume = 0m^3, at\ time = 0\ Seconds)$ to the final volume. Here the sum of phase volumes is less than the unit volume until the end time in the simulation where the compartments are all filled.

Case 4 – *Fed-batch evolution of model topology:* Volume change, a key feature of fed batch fermentation is considered by Nadal-Rey *et al.* (2021).

The involved approach captures snapshots of the process at varying fill levels. Each snapshot, 8 in this study, is a compartmentalisation of the fermenter at a particular fill level; as increasing fill level exposes more of liquor to the impellers and thus modifies the hydrodynamics; and thus, increasing inhomogeneities in key cultivation variables (e.g., metabolic species concentrations. The model representing the least-filled stage of the fermenter is ran up until the time point at which the fermenter reaches the next model volume (which is greater by a set step size amount between increasing compartment model sizes). The final variable values of the first compartment model are fed into the next until the chain of models have each ran for their allotted time with passed on information.

The dynamic phase volume cases are not interchangeable, in case 1 Zheng, Smith and Theodoropoulos (2005) changed the volume as a function of contents requiring the molar volume definition for each species which is not given in the other cases, In case 2 (Arizmendi-Sánchez and Sharratt, 2008) the control scheme utilises a function which is inherently discontinuous, use of such sub-models results in numerical instability in model solution. The timed phase volumes of (Öner *et al.*, 2019) does not account for the hydrodynamic change due to increasing volume of the liquor. The fault of (Öner *et al.*, 2019) is accounted for in (Nadal-Rey *et al.*, 2021) model as the hydrodynamics at each time-discretised model is re-evaluated to build the compartment model, however the model is in essence a collection of separate models with information passed through them in series; an accurate but brutalist approach to modelling the volume change which is not easily scalable.

Many of the authors approaches to phase volume change is a function of the phasic volume change, conflating the two volume terms (compartment and phase) is confusing where the compartment represents a fixed vessel volume. The vessel does not change in size, the phase volumes do. Changing phasic volumes are typically accounted for based upon the molar influx to outflux out of compartment. The benefits of such feature are clear with regards to fed-batch behaviour and modelling of systems of non-constant volume.

2.4 Material Flow

The route to flow derivation, like with compartmentalisation, is based upon the hydrodynamic data collected (CFD/Experimental/Heuristic). The flow rate of the bulk material flow phenomena between compartments is set at fixed values, the magnitude and connected compartments are determined prior to the simulation.

The flowrates between compartments are intimately linked with the compartmentalisation of the unit operation, with the number of material transport phenomena (No_Q) related to the number of compartments (No_k) via the power relationship of Equation 1, rounded values from the plot of Figure 6. The number of flows spans $2 \leq No_Q \leq 196608$, with the greater number of flows attributed to larger compartment networks built typically through NoZ, CFD + NoZ compartmentalisation. Most models have a flow number, $No_Q \leq 361$ of which are either Heuristic or CFD compartmentalisation derived.

$$No_Q = 1.25 No_k^{1.6} \qquad \text{Equation 1}$$

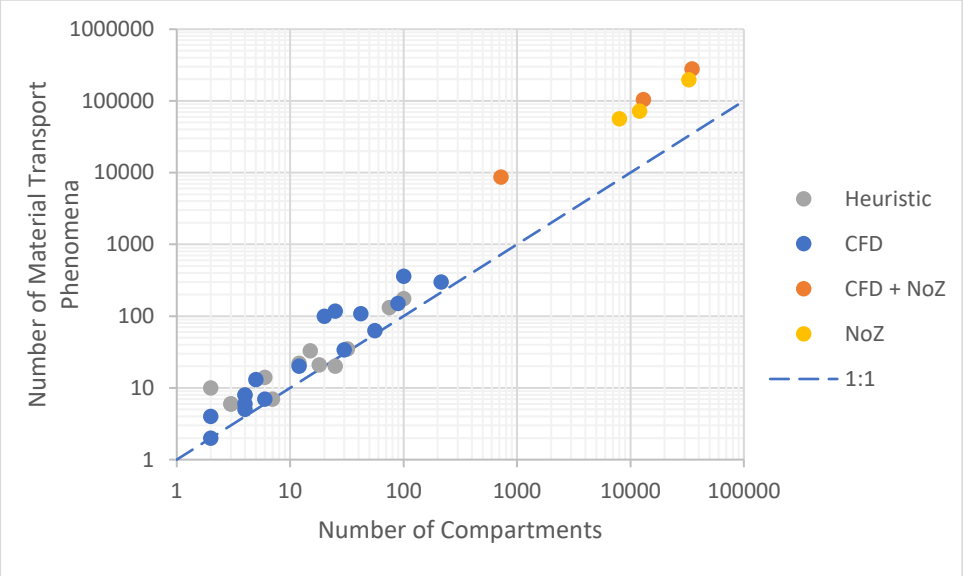

Figure 6 – Log_{10} plot of; The number of compartments vs number of material transport phenomena for 35/ 48 cases in Appendix A, deducting those without material flow and insufficient data on flow number (indicated by (-) next to flow phenomena in column 6 of Appendix A).

As indicated by the 1:1 line plotted on Figure 6, for 47 of the 48 cases the number of material flows is greater than or equal to the number of compartments, $No_Q \geq No_k$.

For a model to be considered a network, all compartments must be connected by a pathway of material transports (not necessarily capable of flow in both directions), for this to be true the number of flows must follow the equality of Equation 2.

$$No_Q \geq No_k - 1 \qquad \text{Equation 2}$$

The model of (Bisgaard *et al.*, 2021) is an outlier case as the only non-networked compartment model in the review. The model is formed of four non-connected chains of compartments, essentially four separate compartment model networks. The number of compartments is greater than the number of materials transports due to this, giving rise to the number of networks term (No_n) in Equation 3. The resultant modification to Equation 2, thus relates the minimum flow number to achieve a desired number of networked clusters (No_n) in a model is then given by Equation 3.

$$No_Q \geq No_k - No_n \qquad \text{Equation 3}$$

Setting $No_n = 1$, as in the case of the 47/48 cited papers, the equation reduces back to the single-network form of Equation 2.

2.4.1 Material flow

In conjunction with determining the flowrate of a flow from the collected hydrodynamic data, the net value of all flows in and out of a compartment must be considered, and balanced so that either the total (i) volume , (ii) mass, or (iii) moles have a net zero change over the time of the simulation for each of the compartments; with the exception of dynamic compartment volumes discussed in section 2.3.3 .

Table 3 shows the collated occurrences of each flow type from the review data of Appendix A.

Table 3 - The number of uses of each material flow type *(definitions to follow)* from the literature of Appendix A, (M) refers to multi-phase systems and (S) to single-phase systems.

Material Flow Type	Number of papers of occurrence
Volumetric flow **(S)**	14
Volumetric flow **(M)**	12
Exchange volumetric flow **(S)**	9
Exchange volumetric flow **(M)**	2
Mass flow **(S)**	9
Mass flow **(M)**	5
Molar flow **(M)**	1

With **Volumetric flows,** the molar flowrate of species i ($\dot{n}_i$) leaving the compartment is a product of the volumetric flow ($\dot{V}$), the species i molar concentration in the compartment (C_i) and the volume of a compartment (V_k). The use of a **molar flow** balance is a singular case presented in (Bian *et al.*, 2005)

$$\dot{n}_i = \dot{V} C_i \; where; C_i = \frac{n_i}{V_k} \qquad \text{Equation 4}$$

Most papers utilise the volumetric flow between compartments to illustrate bulk movement of material, this phenomenon occurs in 26 of the 48 cited cases, 54% single-, 46% multi-phase; see Table 3. Of which the prevalence of use is seen in CFD compartmentalised units (52%) followed by heuristic models (32%), CFD + NoZ (12%) and NoZ (8%).

An **exchange volumetric flow** is the exchange of material between two compartments simultaneously in both directions in equal and opposite magnitude and direction respectively between two compartments: of net zero flow. Each of the two flows of an exchange are equivalent in construction to that of a volumetric flow described above. Exchange flow rates are used to

model the dispersion due to turbulence (Guha *et al.*, 2006) or micro-scale mixing between volumes (Fenila and Shastri, 2018).

Mass flow of species i $\left(\dot{m}, \frac{kg}{s}\right)$is equivalent to volumetric flow via Equation 5, functional of species i molecular weight (Mw_i).

$$\dot{m}_\iota = Mw_i \dot{V} C_i \qquad \text{Equation 5}$$

Models constructed through the CFD compartmentalisation route composed 80% of the cases identified with occurrences of mass flow (single and multi-phase). The number of CFD compartmentalised models was near equivalent in use of volume or mass flows 12:13. The flow of heuristically compartmentalised models are by majority volumetric flows to mass flows 8:3.

2.4.1.1 Bulk Flow Magnitude

To determine the magnitude of a flow (whether volumetric, mas or molar), the modeller looks to the hydrodynamic data collected, in the case of **Heuristic** approach the flowrates are estimated from observations of the unit operation of from process knowledge as in the case of compartment volume construction detailed in section 2.3.1 Compartmentalisation.

For **CFD and CFD + NoZ** compartmentalised models, once compartments have been formed, the velocity fields can be used to determine a main flowrate value as in (Delafosse *et al.*, 2010). Automatic zoning methods have been developed to directly extract the flowrates post compartmentalisation (Tajsoleiman *et al.*, 2019). The benefit of CFD simulations is the extraction of not only the velocity field, but the area between the compartments in contact; a product of the two values gives a volumetric flowrate for use in the compartment model (Gresch *et al.*, 2009). Alternatively, the mass flowrates can be extracted post-CFD simulation, as shown in section 2.4.1 to be equivalent to using volumetric flow between compartments. Other examples of velocity field conversion can be seen throughout literature, such as the distribution of flow based upon number of contact points between compartments seen in (Guha *et al.*, 2006).

A distinctive approach by Laakkonen *et al.* (2006) involved the modelling of displacement liquid flow through a multi-phase system (gas-liquid), whereby the influx of gaseous bubbles into a compartment induces a greater flow of liquid out of the compartment. The system is of unique composition, allowing phase volume change– discussed in section 2.3.3 . The rate of liquid flow (F) out of a compartment is given in Equation 6 as the difference in overflows between the two flow connected compartments and $\tau\,(seconds)$ which represents the residence time of the extra volume in the compartment. This *"overflow"* term accompanies set flow rates between compartments determined from a single-phase CFD map.

$$F = f\left\{\left(\frac{V_k}{V_{k_0}} - \frac{V_{k+1}}{V_{k+1_0}}\right)\frac{1}{\tau}\right\} \qquad \text{Equation 6}$$

In the case of **NoZ** (Delafosse *et al.*, 2014) and some Heuristically derived models, which are typically applied to stirred vessels (Fenila and Shastri, 2019), the flowrate between compartments has been parameterised to relate the flowrate in and out of compartments to the compartments position in the unit and the impeller diameter (D) and stirrer speed (N), exemplar Equation 7. Vrábel *et al.* (2000) utilised a similar equation based on impeller speed and diameter for a multi-Rushton mixed fermenter, where K_C is the coefficient of circulated flow due to impeller action.

$$F_c = K_c N D^3 \qquad \text{Equation 7}$$

As observed from the plot of number of material flows vs number of compartments, Figure 6, we see both CFD + NoZ & NoZ models are skewed towards a larger ratio of $\frac{No_Q}{No_k} > 1$ compared to heuristic and CFD compartmentalisation approaches e.g., For the CFD + NoZ model of (Delafosse *et al.*, 2015) $\frac{No_Q}{No_k} = 8$ and the CFD compartmentalisation approach of (Lee *et al.*, 2019) $\frac{No_Q}{No_k} = 1.4$, with heuristic models between $0.25 \leq \frac{No_Q}{No_k} \leq 5$. This is due to the design of the network of zone model, every compartment, aside from those at the walls of the unit, are surrounded by six other compartments: one for each face of the compartment. For each face, the

compartment has two bulk flows and an exchange volumetric flow with its neighbour compartment (Delafosse *et al.*, 2015), see Figure 7.

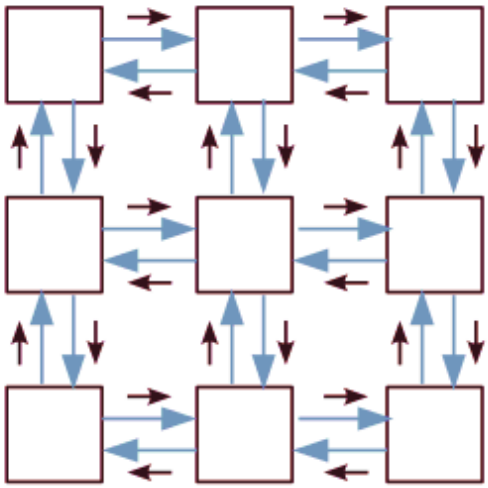

Figure 7 – NoZ compartmentalisation motif, blue arrows indicate bulk material transport, maroon the exchange volumetric flows of lesser magnitude.

2.4.1.2 Exchange volumetric flow Magnitude

Turbulence is modelled as a set of volumetric flow rates (**exchange volumetric flow**), the magnitude is a factor of the bulk flow (Delafosse *et al.*, 2014). A similar use of exchange flows is applied in (Guha *et al.*, 2006) to model the macromixing between compartments. And again by Rahimi and Mann (2001), multiplying the bulk flow by a β value, giving the magnitude of the flow as a function of bulk flow.

Calculation of the exchange rate from the turbulent kinetic energy values, as collected from the CFD run, for a stirred tank bioreactor by Delafosse *et al.* (2015) has also been an approach to estimating the turbulence in a model.

In (Fenila and Shastri, 2018), the bulk flow is calculated as a function of impeller speed and diameter, similarly, the axial flow is modelled as an exchange volumetric flow functional of the same parameters. Similarly, Vrábel *et al.* (2000) modelled the exchange flow as a function of impeller speed and diameter. Both resultant exchange flows were lesser in magnitude than the bulk circulation flow determined from the impeller properties.

2.4.2 Further comments

The fixed flowrates of compartment modelling are not enough to accurately represent the hydrodynamics of the system, beyond the steady state data the model is built upon. Pressure gradients are a major driving force of material flow in many unit operations, the fixed flows of compartment modelling assume a fixed gradient throughout the process but fail to appreciate the pressure gradients induced through phenomenological models. An instance where pressure change is resultant is through a multiphase reaction, this may proceed within a compartment in which a high-density liquid is converted to a low-density gas. Without accounting for change in density of phases due to species composition and type (incompressible, compressible) the movement of material is solely based on the concentration per volume inhabited. Flow induced by pressure resultant from phenomena, such as the case of phase change reaction given above, is ignored and in effect results in incorrectly estimated flowrates. A crucial parameter absent from flow modelling is the pressure of materials and such the effect on flowrates, to be addressed within this work.

2.5 Applied phenomena

A phenomenon, in the context of compartment modelling, is a sub-model which describes the relational interaction of system variables. A phenomenological model is not derived from first principles but is consistent with fundamental theory. To reiterate from section 2.1 An Introduction to compartment modelling, the decoupled material transport of a compartment model is assumed unaffected by the phenomena of a system, within the literature of compartment modelling; e.g., Reactions have no effect on the hydrodynamics (Rigopoulos and Jones, 2003).

The number of phenomena is a measure of how many separate phenomenological sub-models are applied in a single compartment model, not how many differential terms result as it was not possible to extract this more accurate measure from most papers due to insufficient information.

The number of phenomenological sub-models of each case, excluding material transport phenomena, is plotted in Figure 8 against the number of compartments. Not all models of the review detailed the number of phenomena explicitly or in a manner which could be extracted, as a result the figure is plotted with 60% of the cited models from Appendix A. The plot is a measure of model complexity; topological complexity in the positive x-direction and phenomenological complexity in the positive y-direction; with the greatest complexity, a product of the two axes, in the upper right quadrant of the plot (note the absence of cases) indicated by the red shaded box.

Comparing transport phenomena number per compartment of Figure 6 to non-transport phenomena per compartment in Figure 8, material transport are the primary phenomena implemented in the compartment modelling approach; with this fact exaggerated for NoZ compartmentalised models. This is because they are intrinsically linked to the compartment volumes and structure, combined representing the detailed hydrodynamics of the system.

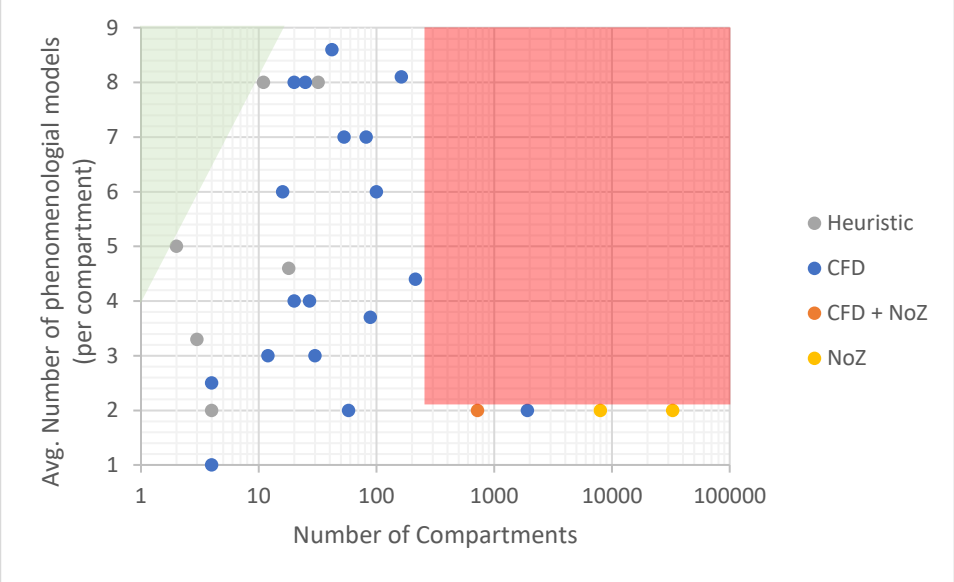

Figure 8 – Complexity plot 1: The number of compartments vs the number of non-material transport phenomena per compartment; the green and red shaded areas highlight an absence of models.

The plotted cases of Figure 8 are segregated into two bands (i) a diagonal band contacting both coloured areas (red and green) with an average phenomena number per compartment ranging the full observed span $1 \leq$

$No_p \leq 8.6$ with compartment number $No_k \leq 214$ and, (ii) a band contacted by the red area and x-axis, formed of models of $No_k \geq 720$, all with a phenomena number of $No_p = 2$. N.B. Fractional values for number of phenomena per compartment result where phenomena are not applied to every compartment within a model.

Band (i) is comprised of models developed through both CFD and the Heuristic compartmentalisation approaches. Because of the low compartment number, when compared to band (ii), the complexity of the models' phenomena can be extended without overburdening the modeller. The unexplored model space of the green and red bands indicates a power law relationship between compartment number and phenomena number with models developed through Heuristic or CFD means, due to the breadth of the band a single representative power relationship cannot be given to describe the relationship.

Whereas band (ii) is comprised of a mix of CFD, CFD + NoZ and NoZ models. Consisting of larger models, in terms of number of compartments, then band (i). In descending number of compartments, the four models of this section are formed through NoZ, then CFD, CFD + NoZ. For compartmentalised models involving a form of NoZ discretisation, and in turn the greatest number of compartments, the number of phenomena is equal to 2 for all cases (Rahimi and Mann, 2001; Zheng, Smith and Theodoropoulos, 2005; Guha *et al.*, 2006); in four models the phenomena applied is chemical reaction. The Red area of Figure 8 illustrates a gap in the compartment modelling applications where large compartment number inhibits the application of phenomena, whether through difficulty in construction, implementation, solution, or a combination of the former is unknown from the present data. The green area is typical of pharmacokinetic compartment models, those with low number of compartments representing zones of the body and a high number of physiological reactions which represent the movement of material between compartments, e.g., (Laínez-Aguirre, Blau and Reklaitis, 2014).

By a measure of number of papers with occurrence of each phenomenon as shown in Figure 9; reactions (24 Papers) are most prevalent in literature,

followed by mass transfer (8 Papers), phase transport (6 Papers) and other phenomena (6 Papers), convective heat transfer (5 Papers) and finally conductive heat transfer (4 Papers).

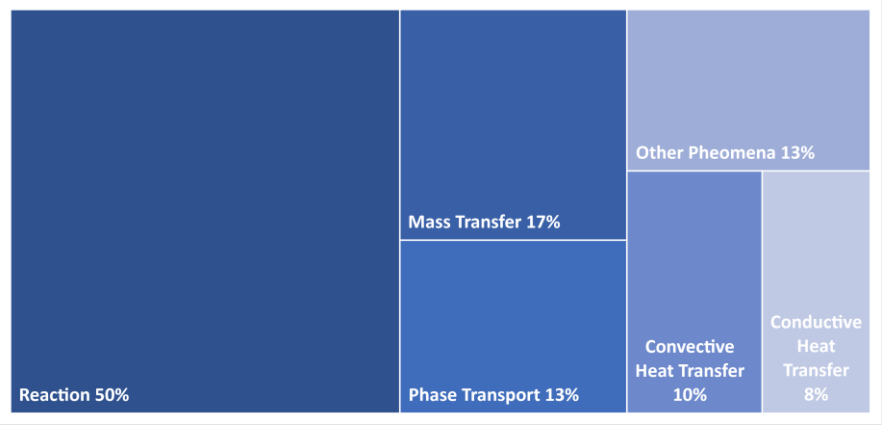

Figure 9 - Map area corresponding to the percentage of papers which included the specific phenomena with or without sufficient detail to determine the specifics of the phenomena.

A further revelation of the phenomena per paper is given in Figure 10 as a plot of number of different phenomenon types [excluding material transport], as listed $a) \rightarrow f)$ for each paper against the number of compartments. Alike Figure 8 the points are coloured to represent the compartmentalisation method.

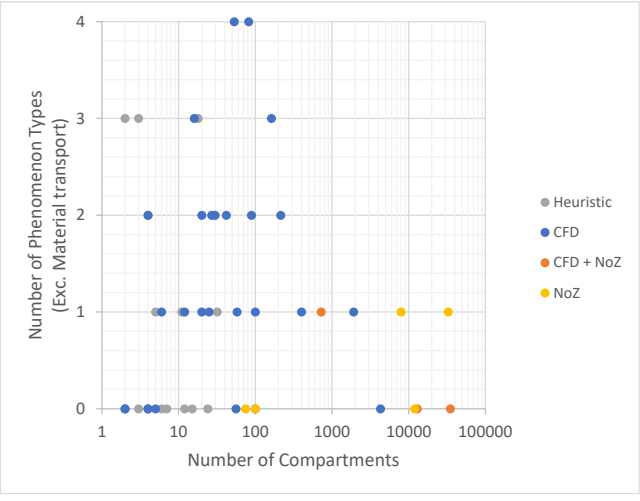

Figure 10 – The number of phenomenon types indicates how many phenomena variations as per the given categories $a) \rightarrow f)$

For a given number of phenomenon types, No_p, the y-axis of Figure 10;

$\boldsymbol{No_p = 0}$**;** No phenomena, the model is either strictly hydrodynamic behaviour (Material Transport) or both Material Transport and population balance modelling (not accounted for in the illustration as it is not a phenomenon of interest in this review); 35% and 2% (Bezzo, Macchietto and Pantelides, 2004) of the literature respectively. Most of the material transport only models are built via CFD compartmentalisation and heuristically; a near equal split between compartmentalised model approaches if CFD+ NoZ and NoZ models are considered together.

$\boldsymbol{No_p = 1}$**;** A single phenomenon is applied to the model, all CFD + NoZ and NoZ models are intwined with one or less phenomenon. The remaining models are mostly CFD built, with few Heuristic models.

$\boldsymbol{No_p > 1}$**;** this area of the plot is primarily formed of CFD and Heuristic models. CFD built compartments of greater than two unique phenomena are of a greater compartment number than their heuristic counterparts of the same unique phenomena number; with the maximum number of unique phenomena $N0_p = 4$ in both CFD built models.

The average phenomena number per compartment for each paper of Figure 8 are separated into the following six categories Phase transport, reaction, mass transfer, other phenomena, convective heat transfer and conductive heat transfer; plotted in respective order in Figure 11$(a) \rightarrow (f)$. The “other phenomena” category contains bespoke phenomena of scare use in compartment modelling of unit operations (e.g., scalar modelling of particulate transport (Portillo, Muzzio and Ierapetritou, 2006)), each of which would form their own category.

Each of the six phenomena categories are discussed in the following sub-sections of section 2.5 Applied phenomena, with regular reference to the data of Figure 11; which is the decomposition of Figure 8 into the individual phenomenon categories.

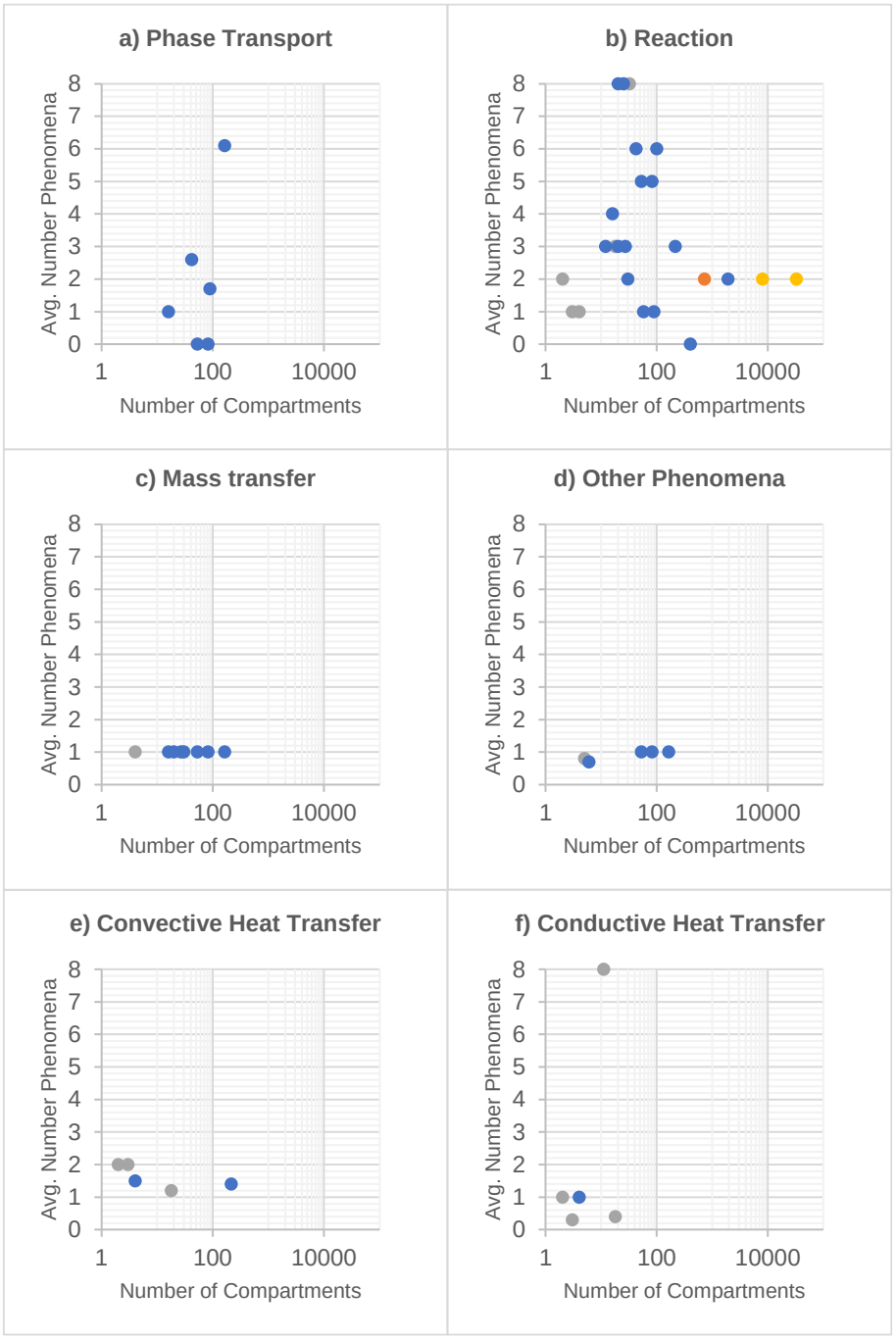

Figure 11 – Compartment averaged number of phenomena for each paper of Appendix A, where sufficient quantitative information is present. Point colour indicates compartmentalisation approach.

<u>Legend:</u> • Heuristic, • CFD, • CFD + NoZ, • NoZ

2.5.1 Phase Transport

The disengagement of dispersed phase material (Phase Transport) from the bulk flow in a multi-phase system is induced by an imbalance in gravitational and buoyant forces acting upon the phase, as in the modelling of biomass sedimentation by Farzan and Ierapetritou (2018), where the rate of sedimentation is a function of the biomass radii. The bulk flow pathway can also influence the direction of the disengaged phase, this is demonstrated in the work of (Laakkonen, 2006; Nauha and Alopaeus, 2013, 2015; Nauha *et al.*, 2018) where a set bubble slip velocity, named so as the bubbles slips out of the bulk flow pathway, multiplied by an area term for the contact between the compartments gives the rate at which the disengagement of gaseous bubbles occurs; the flow of bubble is assumed to follow the liquid flow field with the addition of a slip velocity term determined each step by a force balance upon the bubble. Slip velocity is typically used in conjunction with a population balance model to track the evolution of the dispersed phase volume over the simulation time, however not discussed in this review, as PBM out of the current scope. An increase in dispersed phase volume can also increase the flowrate to which the phase disengages, (Kim et al., 2020), the mass flow of $CO2(g)$ is a multiple of CO2 content relative to the CFD model content at equilibrium.

Each of the above approaches to phase transport are applied separately but do not combine into a unified model. As illustrated in Figure 11(a), the phase transport phenomena are only applied to systems compartmentalised via CFD, of which the number of phase transport phenomena per compartment range between $0 \leq \bar{N}o_{PT} \leq 6$. Phase transport is not applied in models with greater than 163 compartments.

In summary, the disengagement of a phase is unidirectional, in mixed systems the direction may be distorted in direction by bulk flow deviating the phase transport off the lateral plane. Phase transport is also a function of the dispersed phase characteristic size (e.g., average bubble diameter) and the quantity of dispersed phase material within the given compartment volume.

2.5.2 Reaction

Figure 11(b) shows a tendency for a larger number of reaction phenomena, per compartment number, for models of lower compartment number. Comparing the points of this figure against Figure 8 we see that 11 of the cases exclusively modelled Reaction phenomena, aside from material transport. The prevalence of reaction in compartment modelling has already been presented in Figure 9, 50% of papers cited model an evolution in species due to reaction. The data of interest is that in the higher compartment number. Those with more than hundreds of compartments are built for the investigation of distributed reaction kinetics; with smaller compartment number models (65% of literature), $No_k \leq 100$, are typically multi-phenomena models.

Reactions vary in number, order, and stoichiometry. The associated rate equations of a reaction phenomenon are either elementary or non-elementary in nature and calculated as a function of chemical species amounts (concentrations, weights, yield), system parameters and reaction kinetic constants. Common reaction schemes drawn from the literature are, in order of prevalence, the modelling of **biomass kinetics** (Laakkonen *et al.*, 2007; Le Moullec *et al.*, 2010; Alvarado *et al.*, 2012; Nauha and Alopaeus, 2013, 2015; Farzan and Ierapetritou, 2018; Nauha *et al.*, 2018; Fenila and Shastri, 2019; Nadal-Rey *et al.*, 2021), **polymerisation reactions** (Wells and Ray, 2005b; Pladis *et al.*, 2011; Lee *et al.*, 2019), **CO2 capture** (Rigopoulos and Jones, 2003; Zhao *et al.*, 2017; Kim *et al.*, 2020) **Maleic Anhydride production** (Roy, Duduković and Mills, 2000)**, Base type reaction schemes** ($\boldsymbol{e.g., A \rightarrow B}$) (Rahimi and Mann, 2001; Zheng, Smith and Theodoropoulos, 2005; Guha *et al.*, 2006; Arizmendi-Sánchez and Sharratt, 2008; Gresch *et al.*, 2009; Skupin *et al.*, 2017; Yang *et al.*, 2019)**, and pyrolysis/gasification of biomass** (Egedy *et al.*, 2018)**.**

Reactions take place within each compartment per the compartment volume in which the species are situated. Schemes involving multiple phases, the consumption of gaseous oxygen by solids biomass (Le Moullec *et al.*, 2010)**,** capture of CO2 into mineral carbonate (Kim *et al.*, 2020) and the oxygen uptake rate by aerobically growing biomass (Nauha *et al.*, 2018) invoke an

assumed mass transfer step of material absorption into the reacting phase or model the transfer into the reacting phase. An issue with these approaches is that the volume of reaction is not taken as the phase but the volume of the compartment, and thus the rate is typically underestimated due to underestimated concentrations of reactants.

The kinetic constants of a reaction are typically of set numeric value; in a limited number of the papers (2 of 48) the kinetic constant is given as a function of the Arrhenius equation which is the kinetic constant as a function of temperature (T), activation energy (Ea), pre-exponential factor (k_0), and universal gas constant (R). Wells and Ray (2005b) use the Arrhenius equation with both temperature and pressure dependencies, hence the inclusion of absolute pressure (P) and activation volume (V); see Table 4.

Table 4 - Arrhenius equation use in compartment modelling literature and their respective reaction scheme category.

(Skupin *et al.*, 2017)	Base type reaction scheme	$\boldsymbol{k = k_0 e^{-\frac{Ea}{RT}}}$
(Wells and Ray, 2005b)	Polymerisation reaction scheme	$k = k_0 e^{-\frac{Ea+\frac{V}{P}}{RT}}$

The enthalpic effect of reactions are not commonly modelled is only considered in only 12.5% of models with reaction phenomenon. Both Skupin *et al.* (2017) and Wells and Ray (2005b), whom modelled the temperature dependence and temperature-pressure dependence of the kinetic constants also model the enthalpic effects of the reaction schemes. Skupin *et al.* (2017) change enthalpy equivalent to the product of molar enthalpy of reaction (ΔH_{rxn}) and molar reaction rate. Wells and Ray (2005b), ignore the molar composition change due to ethylene decomposition but instead track the effect of the decompositions change upon the enthalpy of the system. Kim *et al.* (2020) modelled the change in reactor temperature as a function of evaporation, reaction, and convective enthalpy transfer.

Reaction modelling is the key phenomena of compartment modelling, after material transport which is intrinsic to the compartmentalisation of the unit operation and representation of the system hydrodynamics. Many schemes have been applied, with **biomass kinetics** and **base type reaction schemes** of most prevalence. These schemes are formed of varying degree of complexity with reference to order, stoichiometry and relation between stoichiometry and rate (non/- elementary). Detailed kinetic constant modelling is only observed in a small number of papers, with the same papers modelling the change in enthalpy of the system as required in symbiote with the temperature dependence of the constants through the Arrhenius equation.

2.5.3 Mass Transfer

The concentration gradient driven mass transfer of species between a gas and liquid phase is near exclusively implemented in CFD constructed compartment models (Bezzo, Macchietto and Pantelides, 2003; Rigopoulos and Jones, 2003; Nauha and Alopaeus, 2013, 2015; Farzan and Ierapetritou, 2018; Kim *et al.*, 2020; Nadal-Rey *et al.*, 2021), with one instance of Heuristic model mass transfer (Pladis *et al.*, 2011); as shown in Figure 11(c).

The (molar, mass – here molar) quantity rate of transfer of species i (dn_i/dt) is a product of concentration gradient (ΔC) and a volumetric mass transfer coefficient $(K_L a)$. All mass transfer rates of literature are based upon the liquid side concentration driving force.

$$dn_i/dt = K_L a \cdot \Delta C \qquad \text{Equation 8}$$

All but one case of mass transfer (Kim *et al.*, 2020) assume a “simplified” mass transfer model, whereby the concentration gradient is composed of a fixed equilibrium concentration $\left(C_{eq}\right)$ and a transient, functional of the moles in the phase - compartment volume, concentration $\left(C_{i,j,k}\right)$. This involves a part of the model which acts as an infinite source or sink to the phenomena of the system.

$$\Delta \mathrm{C} = C_{eq} - C_{i,jk} \qquad \text{Equation 9}$$

The Henry’s constant (H) relates the partial pressure of species to its dissolved concentration in a liquor, where others used the “simplified” method

for mass transfer, Kim *et al.* (2020) modelled a transient liquid interface concentration as a function of Henrys concentration and gaseous concentration. This added level of complexity is surprising to see only implemented in one paper as through the simplified approach the author essentially assumes an infinite supply of gaseous material which is not true in many of the cases; the gas supply is in fact limiting.

The volumetric mass transfer coefficient is a measure of the system's ability to transfer the species of concern from one phase to the other and is a function of either (i) system parameters (Bezzo, Macchietto and Pantelides, 2003; Farzan and Ierapetritou, 2018), (ii) physical and experimental correlations (Kim *et al.*, 2020), (iii) calculated from CFD time-averaged values (Nadal-Rey *et al.*, 2021). In (Nauha and Alopaeus, 2013, 2015) this term is separated into its two components, the liquid side mass transfer coefficient (K_L) and interfacial area between phases available for mass transfer (A); $K_L a = K_L \cdot A$; the liquid side mass transfer coefficient is a function of diffusion coefficient, liquid density and turbulence dispersion extracted from the CFD simulation, the surface area between compartments (A) is taken from the CFD geometry post-compartmentalisation. The evolution of the dispersed phase area (characteristic size) is expected to be captured within the $K_L a$ equation, parameters of these models show no link to dispersed phase volume, size or other attribute which could be related to area of interface.

Unless the time scale of Mass Transfer and reaction are orders of great difference in, they are coupled into a lumped model. The larger concentration of material at the interface of reaction (interfacial concentration), induces a greater rate of reaction and thus increases the gradient of concentration – this effect is accounted for via an enhancement factor (E) which is multiplied by the mass transfer rate in the mass transfer approaches (Rigopoulos and Jones, 2003; Kim *et al.*, 2020).

With improper dispersed interfacial area modelling, the mass transfer mechanism relies on global parameters to derive an area of transfer – the mass transfer models developed without an area in mind are non-scalable, only accurate in the specific unit developed under the same regime conditions.

(Kim *et al.*, 2020) is the best approach to mass transfer modelling, considering both sides of the transfer concentration values with time, transience, a $K_L a$ based upon system correlations (and bubble diameter; accounting for interfacial area) and modifying the mass transfer rate based on the enhancement due to reaction; the only issue with this approach is the lack of evolving phase area considered.

2.5.4 Other phenomena

The lesser occurring phenomena (see Figure 11(d)) are mostly applied to systems constructed through the CFD approach with one, particle flux applied phenomena of Portillo, Muzzio and Ierapetritou (2006), a Heuristically compartmentalisation model.

The timed flow modelling of Öner *et al.* (2019) is required for the timed filling of compartments (see section 2.3.3). Timed flows are key to the filling of fed batch processes, a phenomenon not prevalent in literature, but likely so because of the absence of dynamic compartment modelling (or limited attempts of such compartment behaviour).

The light incidence model of Nauha and Alopaeus (2013, 2015) relates the reaction rate to the amount of light reaching individual compartments. A phenomenological sub model specifically designed for this unit operation. The light incidence is a value used in defining the active reactions and rates of reactions of biomass within the vessel. A similar implementation could be achieved through lumping of a light incidence model within a reaction scheme.

The system wide temperature monitoring of Kim *et al.* (2020), where the global information obtained is a sum of local information per compartment is another uniquely applied phenomenological model. This is discussed in the prevailing phenomena sections where enthalpy is taken into consideration, e.g., reaction, conductive and convective flow.

And the particle flux of Portillo, Muzzio and Ierapetritou (2006) a scalar transfer of particulates between sub volumes of a particle mixing unit. In essence a material flow, but specific to particulate transfer; isolated from the material transport section to demonstrate the use of compartment modelling

to simulate the transfer of scalar units. The unit of measure for material flow will be consistent with most of the literature; either molar or mass – the scalar quantity is not considered in this work.

In summary, timed flow is an important concept to be embedded into the theory. The light incidence model is specific and with only one application, and potentially can be lumped into the reaction schema, so will be dismissed from addition in the universal model development. System wide temperature modelling is essentially a sum of individual compartment enthalpy models which are prevalent as discussed in the following sections on conductive and convective heat transfer. And scalar particle transport is of a quantity were not considering in this work due to singular application in the reviewed literature being synonymous with reduced order dynamic element modelling.

2.5.5 Convective Heat Transfer

Convection of heat is the transport of enthalpy, associated with the physically transported material between compartments. The removal $(subscript: k \rightarrow)$ of enthalpy and addition $(subscript: \rightarrow k)$ is a fraction of the heat capacity of material in question (Cp) and its rate of material transfer (F) and temperature (T); the change in temperature is then given as this change in enthalpy ((RHS) Equation 10) divided by the mass $(m_k = \rho_k V_k)$ and heat capacity (Cp_k) of the compartment k.

$$\frac{dQ_k}{dt} = \rho_k V_k Cp_k \frac{dT_k}{dt} = \sum Cp_{\rightarrow k} T_{\rightarrow k} \rho_{\rightarrow k} F_{\rightarrow k} - \sum Cp_{k\rightarrow} T_{k\rightarrow} \rho_{k\rightarrow} F_{k\rightarrow} \quad \text{Equation 10}$$

Equation 10 is transformed in (Arizmendi-Sánchez and Sharratt, 2008) to instead track the differential change in enthalpy as opposed to temperature of the compartment by combining the terms of the LHS of Equation 10 to form Equation 11.

$$\frac{dQ_k}{dt} = \sum Cp_{\rightarrow k} T_{\rightarrow k} \rho_{\rightarrow k} F_{\rightarrow k} - \sum Cp_{k\rightarrow} T_{k\rightarrow} \rho_{k\rightarrow} F_{k\rightarrow} \quad \text{Equation 11}$$

In (Kougoulos, Jones and Wood-Kaczmar, 2006; Lee *et al.*, 2019) the change in temperature as a function of the convective transports as given in Equation

10. The form of Equation 10 is reduced in (Skupin *et al.*, 2017; Fenila and Shastri, 2019) to Equation 12 by assuming all compartments connected via material transport, and in effect convective heat transfer, are of equal density and specific heats.

$$\frac{dT_k}{dt} = \frac{\sum T_{\rightarrow k} F_{\rightarrow k}}{V_k} - \frac{\sum T_{k\rightarrow} F_{k\rightarrow}}{V_k} \qquad \text{Equation 12}$$

All approaches to convective transport either follow the detailed, or reduced form, respectively Equation 10 and Equation 12. The use of convective heat transfer is almost exclusively used with Heuristic models, see Figure 11(e), with a single case of CFD-compartment modelling. As CFD, CFD + NoZ and NoZ models are highest in average number of Material Transports, modelling convective heat transfer would have a greater effect on performance, and potentially attainment of solution with such models and tedium to construct.

2.5.6 Conductive Heat Transfer

The conduction of heat, $\dot{Q}\left(\frac{J}{s}\right)$, is the enthalpy transfer due to a temperature gradient between two contacting compartments. The transfer is synonymous with mass transfer, with the component of transfer enthalpy as opposed to mass. The equation of Equation 13 is used in all papers with conductive heat transfer phenomena applied; U is the heat transfer coefficient, ΔT the difference in temperature of the two compartments and A is the surface area of heat transfer.

$$\dot{Q} = U \cdot A \cdot \Delta T \qquad \text{Equation 13}$$

60% of these are **stirred tank reactors**; 20% **speciality units and** 20% **crystallisers**. Figure 11(f) shows all conductive heat transfer phenomena are implemented in models built through the heuristic approach in compartment models of between 2 & 18 compartments.

As demonstrated in (Skupin *et al.*, 2017; Fenila and Shastri, 2019) the respective temperature change of compartment k $\left(\frac{dT_k}{dt}\right)$ is then given as the enthalpy transfer rate divided by the specific heat (Cp_k), density (ρ_k) and volume (V_k) of compartment k; Equation 14.

$$\frac{dT_k}{dt} = \frac{U \cdot A \cdot \Delta T}{Cp_k \rho_k V_k} \qquad \text{Equation 14}$$

As with mass transfer, the area and coefficient of transfer here for heat transfer are defined in several ways. Švantner, Študent and Veselý (2020) model heat transfer from gas burners to a series of smelted beams within a walking beam furnace uses a fixed surface area per transfer based upon the fixed geometry of the beams in contact with the burners. The work in (Skupin *et al.*, 2017; Fenila and Shastri, 2019) give a combined UA value, specific to the system modelled. Kougoulos, Jones and Wood- Kaczmar (2006) uses a heat transfer coefficient which is a function of time for timed activation of heat removal from the crystalliser, the area is fixed. And Arizmendi-Sánchez and Sharratt (2008) gives a constant value for $U = 2000 KJ/m^2 hK$ and a dynamic area based, a function of the reactor fill level; see section 2.3.3 .

An observation from the literature, where a model implements conductive heat transfer, convective heat transfer is also present (Kougoulos, Jones and Wood-Kaczmar, 2006; Arizmendi-Sánchez and Sharratt, 2008; Skupin *et al.*, 2017; Fenila and Shastri, 2019; Švantner, Študent and Veselý, 2020). This is because the two phenomena are coupled, designed in the model to receive, distribute, and expel heat from the system in tandem.

2.6 Compartment model Implementation & Solution

2.6.1 Implementation of a compartment model

The differentials of a compartment model, which describe the spatial-temporal change in system quantities over time, are given in column 3 of Appendix A - for each case, the number of differentials per compartment are given within the brackets following the differential type. The differential types are classified into four categories in Table 5, (i) compartment energy, (ii) species quantity, (iii) dynamic volume and (iv) population modelling. Reporting of differential data in literature is better than phenomena reporting, only 6 of the 48 papers presented an issue with differential data collection; of these 6 papers with

insufficient differential information, the authors focused upon the results as opposed to the methodology of the modelling.

Table 5 - Classifying the multitude of compartment modelling differentials in literature.

Differential Category (prevalence in literature)	Differentials extracted from literature Appendix A	Differential Inter-Relationship
Compartment Energy **(19%)**	Temperature Enthalpy	Related through $Q = mCp\Delta T$
Species Quantity **(95%)**	Mass concentration Weight, Mass Weight-, Mass-Fraction Molar Concentration Moles	Related through Mw_i and V_k.
Dynamic Volume **(7%)**	Phase Volume	–
Population Modelling **(16%)**	Number of crystals Crystal/bubbles within specific size ranges	$not\ within\ the\ scope\ of\ research$

The change in mass within a system is prevalent in 95% of papers, with two cases not tracking a change in mass (Bermingham, Kramer and Van Rosmalen, 1998; Švantner, Študent and Veselý, 2020); due to a focus on heat transfer and PBM throughout the systems respectively. Modelling the evolution of enthalpy is only prevalent in 19% of papers; where otherwise systems assume a constant temperature, if considered at all. Dynamic volume monitoring is modelled in 7% of papers, low in prevalence, with the out-of-

scope *population modelling* more prevalent at 16%. Compartment models are historically used for modelling systems where the hydrodynamics and well-mixed volumes, are fixed value, based upon the compartmentalisation hydrodynamic data, hence the low application of dynamic compartment volumes in literature.

Collating the differentials observed in literature, a compartment model can be described mathematically as a set of ODE's where each ODE represents a change in either; a (i) Dynamic Volume $\frac{dV_k}{dt}$, (ii) Compartment's Energy $\frac{dQ}{dt}$, or (iii) A Species quantity $\frac{dn}{dt}$. Population Modelling differentials are part of 16% of papers reviewed, but since stated outside of the current scope – it will not be considered in the definition of the compartment model within his work.

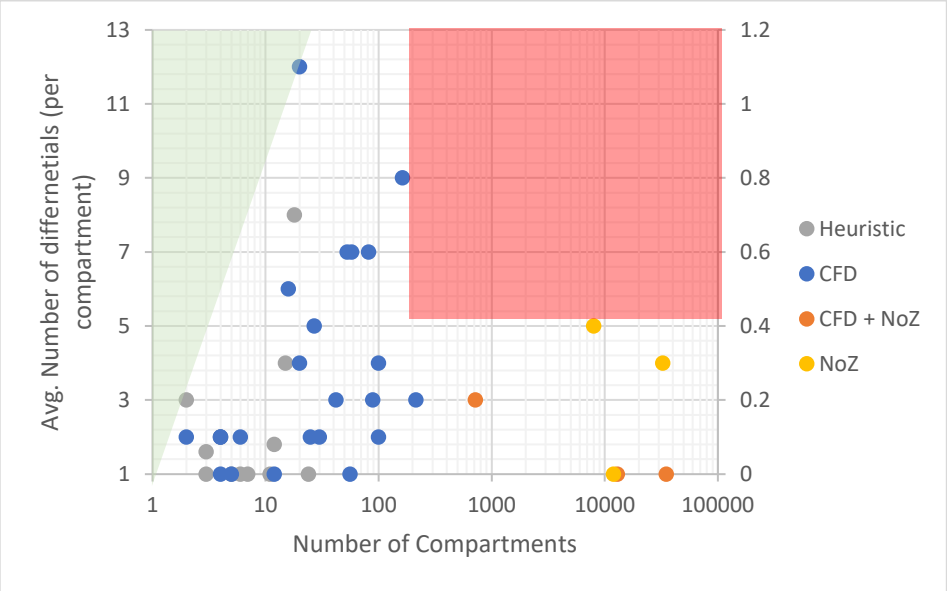

Figure 12 - Complexity plot 2: The number of compartments vs the average number of differentials per compartment; the green and red shaded areas highlight an absence of models

As another measure of the complexity, the average number of differential terms per compartment vs number of compartments are plotted in Figure 12. Phenomenological models link to the differentials of a compartment model system as the rates associated with the models are summed on the RHS of the differential to give the instantaneous rate of change for each differential

variable. Due to the differential data being more readily available than phenomenological data, 85% vs 60% (Figure 8) the plot of Figure 12 is more illustrative of the complexity of compartment models in literature. As seen in Figure 12, the layout of cases does not change; the density of points however does increase due to the added cases, but the trends remain the same as in Figure 8 – indicated by the similar green and red areas of the plot. CFD and Heuristic models have the most expansive number of differentials, with NoZ and CFD + NoZ models having greater compartment number but lesser complexity as a measure of differential per compartment.

The three approaches based upon column 8 Appendix A, to implementing compartment models are presented in Table 6 in descending prevalence. 60% of the papers did not declare the tool utilised or the implementation of solution, beyond definition of the system ordinary differential equation set.

Table 6 - Compartment model implementation approaches derived from literature.

Implementation approach	**Examples from *Appendix A***	***Prevalence* in literature**
Use of a general-purpose language	MATLAB, Python, Fortran	25%
A slightly elevated approach: an equation solver, where the algebraic and ODE equations are given to the tool and the variables are automatically identified. This removes some complexity in implementing the model.	CADET, gProms	10%
Modelling software focusing upon Bespoke implementation and solution.	In-House Software	5%

Every approach to implementation found in the literature review is of a **bespoke** nature. Models written into *general purpose languages* and *in House software* are so that the code is specific to the model and the parameters of the model; and especially within general purpose programming the coding is particularly personal and thus regularly indecipherable. Use of *equation editor software* alleviates some difficulty in programming, but the nature is still present in that the model implemented is specific and immutable without the domain knowledge of programming.

No **universal** implementation tool has been developed to build chemical process compartment models.

2.6.2 Numerical solution of compartment models

From Table 7 we can see that 27% of models are solved with an edition of a general-purpose ordinary differential equation ODE equation set solver, with a minority of 12.5% solved with a differential algebraic equation DAE solver. Where the models solved through DAE solvers are easily modified to form the respective ODEs of the systems. The disconcerting percentage is that of unknown solvers, 60.5% of papers. Declaring the numerical solver is akin to declaring the methodology of measurement in an experimental procedure; without such knowledge one cannot evaluate the error associated or potential faults in the results obtained.

Table 7 - Numerical solvers used in the solution of compartment models, see Appendix A.

***Solver type* (prevalence)**	**Numerical m*ethod***
ODE (27%)	Fortran 77 – ODE pack:
	LSODA
	LSODE
	Sundials (ODE)
	Runge-Kutta:
	RK45
	Gills Modification
	Mersus Modification
	MATLAB:
	ode15s
	ode23tb
DAE (12.5%)	Sundials (IDAS)
	DASSL
	DASPK
	DAE Solver speed-up
Unknown (60.5%)	29 papers without declared solver information
	"step-size 10^{-9}, stiff solver"

Of the ODE solvers row, the Runge-Kutta methods are more appropriate for non-stiff systems, those with slower changes in system variables per time. Whereas the methods of Fortran ODE pack, MATLAB and sundials are targeted towards stiff problems where step size of a problem is modified not for increased accuracy but for attainment of solution. Both stiff and non-stiff numerical solvers need to be embedded into the tool for the solution of these two types of models. DAE solvers are only implemented where the model author has not substituted algebraic equations into the differentials and instead solved the compartment model system as a DAE, for this reason DAE solvers will be omitted from consideration and the focus will remain upon ODE solver implementation.

2.7 Chapter Summary

A compartment model is the discretisation of a unit operation, (Bioreactor, Reactor, Crystalliser, stirred tank, Specialty unit, Water treatment, separation unit), of which compartments representing well-mixed zones of the unit are interconnected by material transports of varying direction and number per compartment ($No_Q = 1.25No_k^{1.6}$) to which the resultant network represents the flow of material about the system; typically tracked as a residence time distribution (RTD).

A compartment is typically formed of one phase of uniformly distributed species. Approaches to the filling and emptying of phase material from compartment volumes has been made, a.k.a. dynamic volume. Species, uniformly distributed about each phase are transported between compartments at a proportion equivalent to their concentration within the well mixed compartment volume although inaccuracies can occur where models follow the *assumed solvent* approach. The multi-phase compartment with pressure and continuum-dispersion modelling is a requirement for accurate modelling, especially when modelling the evolution of phase area as quantities of phase material change within a system; important when considering the transfer of material between phases (mass transfer).

Flowrates between compartments based upon steady state hydrodynamics do not account for pressure variations in the system which in turn have considerable effect upon hydrodynamic flow. The associated convection of enthalpy with flow is typically ignored but in systems where temperature is a key parameter of phenomena must be considered.

Source and sink compartments are commonplace where flows are added and removed from the system and mass transfer assumes an equilibrium constant species source or sink.

The phenomena: reaction, mass transfer, heat transfer and phase transport are key behavioural models of chemical process operations. With Reaction the priority applied phenomena, with greatest prevalence in the literature

(50%). And their timed activation, such as in the timed modelling of filling by Öner *et al.* (2019).

The variables of the system are species quantities, compartment energies and dynamic volume of the compartment phase mixture. The mathematical description of the system is the set of temporal differentials describing the change in each of these variables as a function of phenomenological model terms which directly cause effect to the variable. And an array of initial variable values; an ODE IVP.

The implementation and solution of the ODE initial value problem (IVP) requires a novel tool, one which can be used to describe, build, and solve the compartment models described above in a time to solution much lower than CFD (<<1hr). There is an absence of complex chemical process compartment models of greater than 163 compartments with any of higher number of compartments exclusively reaction based or flow-based investigation. Tools exist in the broader topics of compartment modelling application but not in chemical process compartment modelling, due to the variation in phenomenological and differential complexity, and the lack of a universal framework for compartment modelling of chemical process unit operation compartment models.

Chapter 3 Universal Compartment modelling Theory

3.1 Introduction

Fundamental to process modelling is the understanding of process phenomena and their spatiotemporal scale-interrelationships. This modelling framework is built of two modules, structure and phenomenological models, the structure is tightly interrelated with the phenomena.

In this chapter, the common aspects of compartment modelling in chemical engineering, extracted from and summarised in the literature chapter, are combined to form a unifying theory. This motivation is to create a universal compartment model capable of describing the dynamic behaviour of the wide range of chemical engineering units and processes in the chemical engineering field, which has not yet been realised.

The complexity of the subject necessitates simplification, this requires us to apply a technique that historians apply frequently - named *ideal type* which is based on the works of the German sociologist Max Weber (1949) in castle siege design. We will not look at every individual compartment model, we take recurring elements from different compartment models to construct a typical and ideal compartment model that we then use to explain the most important and most common behaviours (phenomena) and structure of compartment modelling.

The chapter begins with the structure definition of a multiphase (M incompressible & N compressible) continuum-dispersion compartment, formed of three levels: the compartment itself, the phase(s) within and the chemical species of each phase. Whereas in most of the literature, models ignore the volumetric contribution of phases to the compartment volume (*assumed solvent approach)*, assuming a constant set phase volume equal to the compartment volume, here the individual phase volumes are considered separate to the compartment volume.

Two *closure models* developed as part of this work are presented to describe the compartment pressure to phase volume relationship of contents,

the *'variable volume'* and ‘*relaxed density'* models. Dynamic modelling of pressure is here a novel development in compartment modelling of chemical engineering problems, even though pressure is a recognised crucial component in the modelling of chemical engineering phenomenon. Further explained in section 3.3 Compartment closure models.

Due to varying pressure inlets and outlets, the maldistribution of compartment pressures can be used to drive the convective flow of material through a compartment system – removing the tedium of setting flowrates in a compartment system and addressing the fixed-flow issue identified in systems of fixed flow of the literature.

A second novelty is the concept named *'container';* a container is a boundary volume that constrains multiple compartments to one summed volume. The multiple compartment volumes are not rigid within a container; instead, they self-alter their volumetric size to reach an equilibrium pressure between compartments. This higher level of encapsulation enables the dynamic volume change of compartments, permitting vessel fill state modelling.

The phenomenological models, single-phase and inter-phase reaction, inter- and intra-compartmental mass transfer, and convective flow of material, from literature, are generalised with application to the compartment structure herein.

A stiffness coefficient is a value of the system which can be adjusted to relieve or induce stiffness. Increased stiffness results in increased strain on the numerical solver and difficulty in reaching a numerical solution; an increased time to solution of the model. In developing the theory, an effort has been made to avoid discontinuity in place of stiffness - a more readily solvable feature of ODE initial value problems (IVP’s). As a result, stiffness constants have been introduced, highlighted throughout the text, to smooth discontinuities with stiffness.

3.2 Compartment composition

An overview definition of the compartment: Phases values exist within a compartment, a sub volume of space in a unit or processing volume. A phase is a region of space of either incompressible or compressible nature, composed of a perfectly mixed collection of chemical species, throughout which all physical properties are uniform (e.g., Density, molar fraction of species). Within the compartment one phase is the continuum of which the others are dispersed within of a specific characteristic interphasic area. Compartments can then be contained within a container; this level of structure is equivalent to a processing unit where contained compartments can change in volume to achieve a uniform pressure between one another within the compartments of the container; section 3.4 The Container Theory.

3.2.1 Chemical species

At the smallest scale of a compartment model are the chemical species. A chemical species is identified by the subscript denotation i. The molar quantity of chemical species is quantified as a single value $n_{i,j,k}(moles)$, where subscripts j and k refer to the phase and compartment location respectively. The molar quantity of a species is one of the ODE variables of the compartment system.

The physical property molecular weight, $Mw_i\left(\frac{kg}{mole}\right)$ is a constant value related to the elemental make-up of the chemical species. This property is utilised in the calculation of the chemical species mass from its molar amount, m_i.

$$m_{i,j,k} = Mw_i n_{i,j,k} \qquad \text{Equation 15}$$

The temporal change in moles of chemical species i of phase j in compartment k is given by the differential $\frac{dn_{i,j,k}}{dt}(mole/s)$. This is the summed molar effect of phenomenon acting upon chemical species i of the location j,k, describing the change in molar amount of each species at each step of a simulation time domain.

3.2.1.1 Phantom Chemical species

A phantom chemical species, of which a minimal amount is always present in every phase. Phantom chemical species serves to ensure that, when all other species amounts in a phase go to zero, a phase still has a small number of moles and thus a small volume to allow calculation results to remain finite; for example in the case of nucleation, a minute starting volume to build the phase upon – the empty phase requires a molar concentration, with this amendment the concentration will result in nought, as opposed to throwing a division by zero (Div!0) error.

The first stiffness coefficient of the theory is introduced here, the concentration of phantom chemical species in each phase of compartment k; $[C]_{p,j,k}$. The moles of compressible phase phantom species is determined at the initiation of the simulation, $t = t_0$, and fixed throughout; with the exception of phantom species of contained compartments, see 3.4.4 Universal container model (Pressure and volume control).

The molar amount of phantom species concentration in each phase $j \in [0, N]$ of a compartment k, $n_{p,j,k}$, is scaled to the volumetric size of the compartments minimum compressible volume, $V_k \alpha_k$, as given in Equation 16 for **incompressible** phase species; and a total concentration parameter $[C]_{p,j,k}$. Determining the values for each parameter is dependent on the closure model chosen for the compartment – see 3.3 Compartment closure models.

$$n_{p,j,k} = V_k \alpha_k [C]_{p,j,k} \qquad \text{Equation 16}$$

The minimum compressible volume is the volume of the compartment reserved for compressible (e.g., gaseous) phases in the event the compartment is filled with otherwise incompressible phases (e.g., liquid, solids). This compressible volume is key to the calculation of a pressure in the compartment in the event of this complete filling with incompressible phase material.

The calculation of phantom species of each **compressible** phase varies slightly compared to incompressible calculation, with consideration of the

number of compressible phases in a compartment. This is to eliminate the number of compressible phases as a factor in compartment pressure calculation.

$$n_{p,j,k} = \frac{V_k \alpha_k [C]_{p,j,k}}{\sum_{j=0}^{j,k,compressible} 1} \qquad \text{Equation 17}$$

The Molecular weight of the phantom species, $Mw_p \left(\frac{kg}{mole}\right)$; the molecular weight is required to be greater than zero, so the phantom chemical species molar amounts can be converted to a mass quantity as per Equation 15, required for calculating phase volume defined in section 3.2.2 Phase.

Unlike standard chemical species, there is no ODE associated with a phantom chemical species due to no phenomenon interaction with the phantom material; Equation 18.

$$\frac{dn_{p,j,k}}{dt} = 0 \qquad \text{Equation 18}$$

3.2.2 Phase

A phase is a homogeneously mixed collection of one or more chemical species. Each chemical species in a phase is unique e.g., two chemical species of *Nitrogen* cannot be defined in the same phase as they are descriptive of the same species of the same location (same phase).

A phase is either of incompressible $(\mathrm{i}\mathbb{C})$ (e.g., solid or liquid) or compressible$(\mathbb{C})$ (e.g., gaseous) nature. The nature of a phase affects its volumetric behaviour.

A compartment can be formed of multiple phases, of either nature $(\mathbb{C}, \mathrm{i}\mathbb{C})$. Phases, like chemical species, are identified by a unique name in a compartment and no two phases of the same compartment can have the same name. The same named phase can exist in different compartments of a compartment model, (e.g., modelling the discretised continuum of liquor in a mixed vessel). Those phases of the same name have consistent physical properties (sensible heat, density, characteristic diameter).

The sensible heat capacity is the energy in joules added/removed to increase/decrease $1Kg$ of phase material by $1K$. The heat capacities, $Cp_j\left(\frac{J}{KgK}\right)$, of phases within a compartment are used to calculate the evolution of the compartment temperature T_k and sensible enthalpy $Q_k(J)$. Typically, an incompressible phase adopts a greater heat capacity value than a compressible phase.

The characteristic diameter of a phase $D_{p,j}$ is the determined dispersion size of a phase within a compartment, relating the dispersed phase volume to the total phase surface area in the compartment, an important variable in the phenomenon intra-compartmental mass transfer (section 3.5.1.3 Mass transfer).

The total moles of chemical species in phase j, includes the moles of the phantom chemical species, as given in *Equation 19*.

$$n_{j,k} = n_{p,j,k} + \sum_i n_{i,j,k} \qquad \text{Equation 19}$$

The total mass of a phase is calculated from the sum of chemical species mass of the phase, including the phantom chemical species, as shown in *Equation 20*.

$$m_{j,k} = n_{p,j,k} Mw_p + \sum_i n_{i,j,k} Mw_i \qquad \text{Equation 20}$$

The volume of a phase is then the mass of the phase divided by the phase density, $\rho_{j,k}(kg/m^3)$. By modelling the volume as a function of species mass and phase density we remove the *assumed solvent* concept of compartment modelling so regularly applied in literature and so readily abundant in under-estimation of species concentrations.

$$V_{j,k} = \frac{m_{j,k}}{\rho_{j,k}} \qquad \text{Equation 21}$$

3.2.2.1 Phase density

The derivation of phase density is dependent on the type of phase, a similar approach is followed as applied by Laakkonen (2006) based upon the differing

approaches to molar volume (density) based on phase type; in compressible vs compressible.

The state of a **compressible phase** follows the ideal gas law: $'PV = nRT'$, with the ideal gas constant $R = 8.314(J/molK)$, this is used to derive the density of the compressible phase. The state equation is multiplied by the average molecular weight of the phase $\overline{Mw_j}$ to convert the molar quantity to mass $(n \rightarrow m)$. The average molecular weight of phase j is the sum of the mole fractions of each gaseous chemical species in the phase, $x_{i,j,k}$, multiplied by the molecular weight of that substance; Equation 22 & Equation 23.

$$\overline{Mw}_{j,k} = \sum_{i \cap \mathbb{C}} x_{i,j,k} Mw_i \qquad \text{Equation 22}$$

$$x_{i,j,k} = \frac{n_{i,j,k}}{\sum_{i \cap \mathbb{C}} n_{i,j,k}} \qquad \text{Equation 23}$$

The density of a compressible phase is given by Equation 24, the density is calculated as the mass of compressible material (given by the sum of compressible chemical species moles in compartment k $(\sum_{i \cap \mathbb{C}} n_{i,j,k})$ divided by the molar fraction of free compressible volume $(V_{\mathbb{C}})$ for occupation by the compressible material within the compartment (not occupied by incompressible phase material).

$$\rho_{j,k} = \frac{\mathrm{m_{k,\mathbb{C}}}}{V_{\mathbb{C}}} = \frac{\overline{Mw}_{j,k} P_k}{RT_k} = \frac{\overline{Mw}_{j,k} \sum_{i \cap \mathbb{C}} n_{i,j,k}}{\left(V_k - \sum_{i\mathbb{C}} V_j\right) \frac{n_{j,k}}{n_{k,\mathbb{C}}}} \qquad \text{Equation 24}$$

The relation of compressible phase density to the compartment pressure is shown as this is how we derive compartment pressure later in this chapter (section 3.2.3 The Compartment), where $P_k(Pa)$ is the pressure of the compartment and T_k is the compartment temperature.

Incompressible phases exhibit a constant density / negligible change in density (very low compressibility). The definition of incompressible density is dependent on the compartment closure model; see 3.3 Compartment closure models. For both closure models, the term ideal density is given as the set density of the phase, $\rho^0_{j,k} = 900kg/m^3\ (default)$.

Overfilled material from a compartment exits via pressure induced flow (section 3.5.1 Material Transport). The density of an incompressible phase slightly deviates from this ideal within the relaxed density closure model (section 3.3.2 Relaxed density) where the compartment is overfilled with material which in turn induces a sharp pressure increase in the compartment; providing the increased pressure required to propagate material out of the compartment.

3.2.2.2 Phantom phase

A phantom phase is an inert compressible phase present in each compartment, where a compartment has a deficiency of phase material to fill its volume, the phantom phase of compressible nature expands to fill this volume with the resultant pressure of the compartment dropping. Phantom phase is a key component of the compartment pressure modelling, given in detail in section 3.3 Compartment closure models.

The phantom phase, formed solely of phantom chemical species, defined in Equation 4, has no phenomenological interaction within the system, requiring no definition of $D_{p,j}$ or Cp_j.

3.2.3 The Compartment

The compartment represents a sub-volume of a unit operation or processing system. A compartment boundary represents an adjoining continuum volume, physical boundary (e.g., vessel wall) or a phase boundary between two differing or same continuous phases. Typically, compartments are discretised to represent a system sub-volume with consistent turbulence levels (mixing intensity), a near-uniform temperature, pressure, and composition (See section 2.3.1 Compartmentalisation).

Figure 13 illustrates the structure of a compartment as a cube. The compartment is formed of a white continuous phase with the dispersed phased represented as smaller coloured cubes; of which one is the phantom phase. The phases, nor the compartments truly have shape – cubes have been chosen for a simple representation and are not illustrative of the phase shape or area of contact with the continuum.

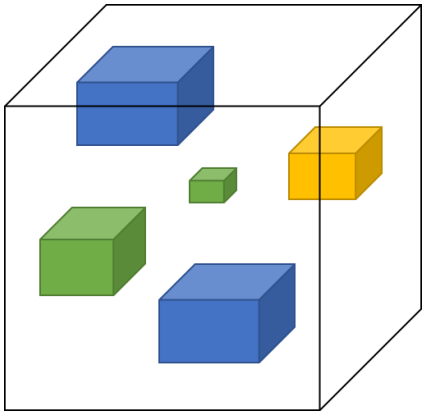

Figure 13- 3D representation of a compartment with multiple dispersed phases (coloured cubes) dispersed within continuous phase (white volume of cube.

A compartment is characterised by the following properties.

A defined volume of space V_k, is composed of a single phantom phase and one or more other phases. The volume is organised as one continuous phase (not the phantom phase), with the remainder uniformly dispersed. The compartment volume is always equal to its defined volume due to the presence of the phantom phase expanding to fill the space.

An initial compartment temperature $T_{k,0}$ which is used to calculate the sensible enthalpy of the compartment Q_k. The evolution of compartment sensible enthalpy is a variable of the ODE system defining compartment modelling.

And an absolute $(P_k > 0)$ compartment pressure, functionally determined through the contents of the compartment; see 3.3 Compartment closure models for definition.

3.2.3.1 Continuum-dispersion composition of a compartment

A compartment is composed of a continuous phase, or a dispersion of one or more phases bubbles/droplets/particles in a continuous phase. With the latter, a compressible-compressible continuum cannot occur as compressible phases cannot form surfaces with one another, instead meshing into a single phase.

Important process phenomena, inter-compartmental mass transfer and interfacial reaction occur between the dispersed phase(s) and the continuous phase through an interfacial area of contact, $A_{j,k}(m^2)$. The area is a function of the dispersed phase volume V_j and its characteristic dispersion diameter $D_{p,j}$. The characteristic phase diameter can be considered as the maximum stable size of a phase single bubble/droplet/particle suspended/dispersed in the continuous phase.

A spherical phase dispersion is assumed for dispersed phase material within the continuous. The interfacial area of a phase j is from Equation 25.

$$A_j = \frac{6}{D_{p,j}} V_j \qquad \text{Equation 25}$$

e.g., for a phase of volume $V_j = 1m^3$ and $D_{p,j} = 0.001m$, the area of the phase is, $A_j = \frac{6}{0.001} 1 = 6000m^2$.

Two dispersion structures exist within a compartment.

An *incompressible* continuous phase with any number of incompressible and compressible phases dispersed within it, an example given in Figure 14.

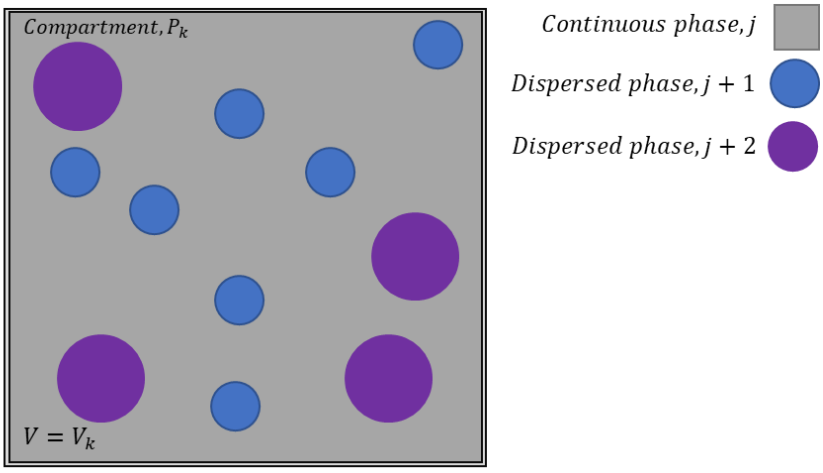

Figure 14 – incompressible continuous phase j, with dispersed incompressible phase $j+1$ and dispersed compressible phase $j+2$ with $D_{p,j+1} < D_{p,j+2}$. The phantom phase of the compartment is also dispersed. In such a small quantity, it is negated from the illustration.

The second dispersion type is a *continuous compressible* phase with any number of incompressible phases dispersed. Phase immiscibility is due to

surface tension at the boundary interface of one phase with another. A mixture of compressible phases (e.g., gases) do not form interfacial surfaces at standard conditions S.T.P – instead phases merge with the continuous.

3.2.3.2 Enthalpy and temperature

The **sensible enthalpy** of a compartment, $Q_k(J)$, is the energy required to heat or cool the compartment from a reference temperature (for convenience we use $T_{ref} = 0\ K$) to the compartment temperature, T_k. The derivation of the formula for sensible energy of the compartment, from T_{ref} to $T_k(K)$, is given below, where $\Delta H^{\emptyset}_{j,k}(J/kg)$ is the enthalpy of formation of the phase j in compartment k at standard temperature and pressure $T^{\emptyset} > 0K$.

$$
\begin{aligned}
Q_k = \sum_j m_{j,k} \Big(& \Delta H^{\emptyset}_{j,k} + Cp_j\left(T_k - T^{\emptyset}\right) \\
& - \left(\Delta H^{\emptyset}_{j,k} + Cp_j\left(T_{ref} - T^{\emptyset}\right)\right)\Big) \\
& = \left(T_k - T_{ref}\right) \sum_j m_{j,k} C_p \\
& = T_k \sum_j m_{j,k} C_{p,j}
\end{aligned}
$$

Equation 26

For clarity, the derivation is illustrated in Figure 15.

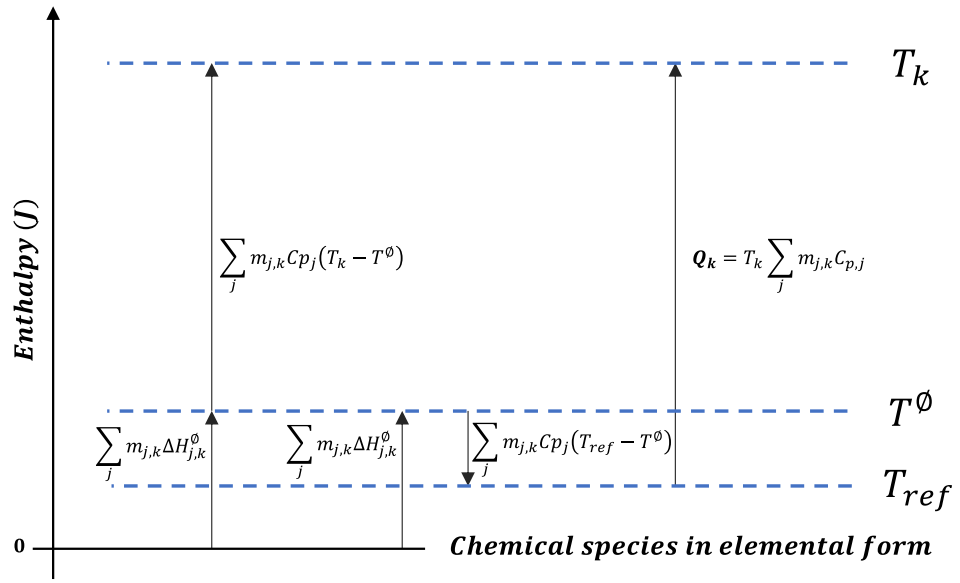

Figure 15 - Sensible energy, Q_k, derivation. $(T^{\emptyset} > T_{ref} = 0K)$

Upon model initialisation, from the initial temperature given to the respective compartment $T_{k,0}$ and the collective sum of each phase j specific heat Cp_j and mass $m_{j,k}$ of compartment k, we find the sensible enthalpy of each compartment to be given as in Equation 27.

$$Q_k = T_{k,0} \sum_j m_{j,k} Cp_j \qquad \text{Equation 27}$$

The differential change in enthalpy of compartment k, $\frac{dQ_k}{dt}$, is the sum of enthalpic changes due to following acting phenomenon; (i) the transport of material to/from the compartment; convective flow transport, phase transport and mass transfer, (ii) enthalpy change associated with heat transfer between compartments; heat transfer and (iii) reactive exothermic or endothermic consumption/production of material accompanied by a change in compartment sensible enthalpy. See section 3.5 **Transport and Transformation phenomena** for the phenomena associated terms affecting a change in compartment sensible enthalpy. This differential is the third variable of the ODE system which describes the compartment model mentioned thus far.

For each compartment k the temperature is calculated at each solution point from Equation 27 rearranged, where an updated value of Q_k is returned from the solver with the effect of $\frac{dQ_k}{dt}$ applied:

$$T_k = \frac{Q_k}{\sum_j M_{j,k} Cp_j} \qquad \text{Equation 28}$$

The compartment sensible enthalpic differentials are solved in parallel with chemical species molar quantity differentials across the model period.

3.2.4 Surrounding

A special compartment exists named the 'surrounding'. It represents a source or sink of material and energy to a modelled system, of set pressure, temperature, and composition. The surrounding addresses the need for the infinite source of material commonly seen in the filling of a continuous unit operations in literature. The surrounding also addresses the need for a source

of phase material of constant concentration, as in the set equilibrium concentrations examples in literature.

A surrounding behaves and interacts precisely like a compartment regarding the construction, definition of composition, and phenomenological interaction. The enthalpic quantities of connected compartments and their respective chemical species molar quantities exhibit change due to interacting phenomenon with a surrounding. However, the surrounding variables of enthalpy and species moles exhibit no change in enthalpic or chemical species molar quantities throughout the simulation.

$$\frac{dn_{i,j,k}}{dt} = 0 \qquad \text{Equation 29}$$

$$\frac{dQ_k}{dt} = 0 \qquad \text{Equation 30}$$

Surroundings are fixed volumes of fixed enthalpic and molar quantities. The phantom phase of a surroundings is insignificant in its quantity except in filling the remaining volume of a surrounding not filled by material added through user specification. The phantom phase is therefore free for manipulation, here to serve the purpose of artificially setting a surroundings pressure. Setting the pressure of a surrounding through a single value streamlines the ability of the modeller to set up their process – adding a new attribute to the surroundings "pressure".

The pressure is calculated, following molar addition of user defined chemical species, by adjusting the number of phantom moles in the isolated phantom phase of the surrounding. The formula considers the possibility of relaxed incompressible material within the surrounding; adjusting the phantom phase mass appropriately to achieve the desired pressure; formula given below.

$$n_{p,k} = \left(\frac{P_k V_{\mathbb{C}}}{f^{i\mathbb{C}} R T_k} - \sum_{j \cap \mathbb{C}} \sum_{i \neq p} n_{i,j,k} \right) \qquad \text{Equation 31}$$

Where the pressure set by the user is not possible; requiring non positive phantom moles $n_{p,k} \leq 0$, the user will have to specify a new pressure or reconsider the volume and or moles within the surrounding.

3.3 Compartment closure models

To address the gap in the literature, the absence of pressure modelling in compartment modelling applications, a novel approach to the pressure modelling within the compartment modelling approach is presented. A compartment closure model defines a compartments pressure-to-volume relationship when the phase content is described as; empty, partially filled, full and filled beyond the compartment's volumetric capacity (total incompressible phase volume in a compartment > compartment volume).

Here both the '*variable volume*' and '*relaxed density'* compartment closure models are described to describe the change in pressure of a compartment at the point overfilling and further addition of material – where incompressible material is added beyond the capacity of the compartment volume. Without such closure model, overfilling a compartment would lead to numerical errors/instability in the model due to a negative volume for compressible material to exit within.

Typically, compartment models do not assess the contribution of the phasic contents to the volumetric size of a compartment, instead for dilute systems the volume is assumed filled with an imaginary solvent with the volumetric flowrates in and out of each compartment balanced to assume maintenance of compartment volume. In the new approach presented here, the volume of a compartment is a function of its the contents. Incompressible and compressible phase material contribute to the compartment volume in different manners, because of this we can also model the pressure of a compartment dynamically as a function of its contents. The pressure in each compartment is a natural driving force for the propagation of material through a compartment system through pneumatically driven convective flow; removing the tedium of manually mass balancing each compartment and inaccuracy of assuming an imaginary solvent without repercussion, discussed further in section 3.5.1.5 Convective Transport.

The closure models are presented in order of development throughout the project. The variable volume approached was the first of the two approaches

developed, with the improved relaxed density model developed afterwards, the relaxed density closure model is favoured as it can be used in conjunction with the container, another novel development of this work (see section 3.4 The Container Theory).

3.3.1 Variable volume

In the '*variable volume*' closure model, a new compartment property is defined; the maximum compartment pressure $\widehat{P}_k(kPa)$. The maximum pressure is a limit of the compartment pressure P_k. The compartments pressure is maintained at or below the maximum pressure $P_k \leq \hat{P}_k$. If incompressible material is added to the compartment of a volume beyond the compartment's capacity, the phase volumes within the compartment expand beyond the capacity of the compartment volume V_k. The total phase volume grows beyond that of the compartment capacity, the compartment is overfilled. The sum of phase volumes is either equal to or greater than the capacity, compartment volume, of the compartment; (Equation 32).

$$\sum_k V_{j,k} \geq V_k \qquad \text{Equation 32}$$

A compartment in an overfilled state, under the variable volume closure model, are of a constant set pressure equal to $\widehat{P}_k$ and thus, assuming no further addition of compressible phase, do not change in volume.

In this simpler closure model, the minimum compressible volume, α_k, and total concentration of phantom material in a compartment – parameters used to determine phantom moles in each phase of the compartment (section 3.2.1.1 Phantom Chemical species) - are not linked to the pressure of the compartment but set to reasonable values to ensure solution is achieved.

3.3.1.1 Incompressible density

In this closure model, each incompressible phase of a system is given an ideal density value $\rho^0_{j,k}\left(\frac{kg}{m^3}\right)$. This is either a set value, or a function of the constituent chemical species properties, describing the constant mass per unit

volume of the phase assuming ideal incompressibility. Under the variable volume closure model, the density of incompressible phases does not change from this value for the simulation's duration, Equation 33.

$$\rho_{j,k} = \rho_{j,k}^{0} \qquad \text{Equation 33}$$

3.3.1.2 Compartment pressure

A compartments pressure $P_k(Pa)$ is calculated from the compressible material within the compartment using the ideal gas equation of state, as introduced in Equation 24. As there is always a phantom phase in each compartment, there is always compressible material to consider in the compartment pressure calculation, Equation 34. The minimum of the two values, calculated pressure and $\hat{P}_k$ is taken as the compartment pressure as the basis of the closure model is the limitation of the maximum compartment pressure – the maximum pressure is a boundary value at which point the phases are permitted to grow beyond the capacity of the compartment volume at the constant maximum pressure, $\hat{P}_k$.

$$P_k = \min\left(\frac{RT_k \sum_{j \cap \mathbb{C}} n_{j,k}}{V_{\mathbb{C}}}, \hat{P}_k\right) \qquad \text{Equation 34}$$

The volume of the compartment not occupied by incompressible phase material, $V_{\mathbb{C}}$, is calculated as the maximum of either (i) the difference in compartment volume and incompressible phase material, and (ii) the arbitrary set value γ to ensure $V_{\mathbb{C}} > 0$; Equation 35. This calculation requires the definition of the incompressible phase density, as given in the prior subsection, $V_{j,k} = f(\rho_{j,k})$, Equation 21.

$$V_{\mathbb{C}} = \max\left(\left(V_k - \sum_{j \cap i\mathbb{C}} V_{j,k}\right), \gamma\right) \qquad \text{Equation 35}$$

The default value for $\gamma = 10^{-300}$, this is to ensure positive values from the pressure calculation. This parameter is another of the stiffness coefficients in the model.

Figure 16 illustrates the 2D compartment volumetric behaviour as more incompressible material is added to the compartment. The compressible phase density in a compartment filled to critical pressure becomes constant, exhibiting incompressible density behaviour. As a result, additional material added beyond this point causes an increase in phase volume beyond the set compartment volume, V_k. In this scenario, for simplicity, the dispersion of phases in the compartment is not illustrated. Instead, the incompressible phases are grouped into the green area and compressible phase (phantom only) into the blue area of the illustration.

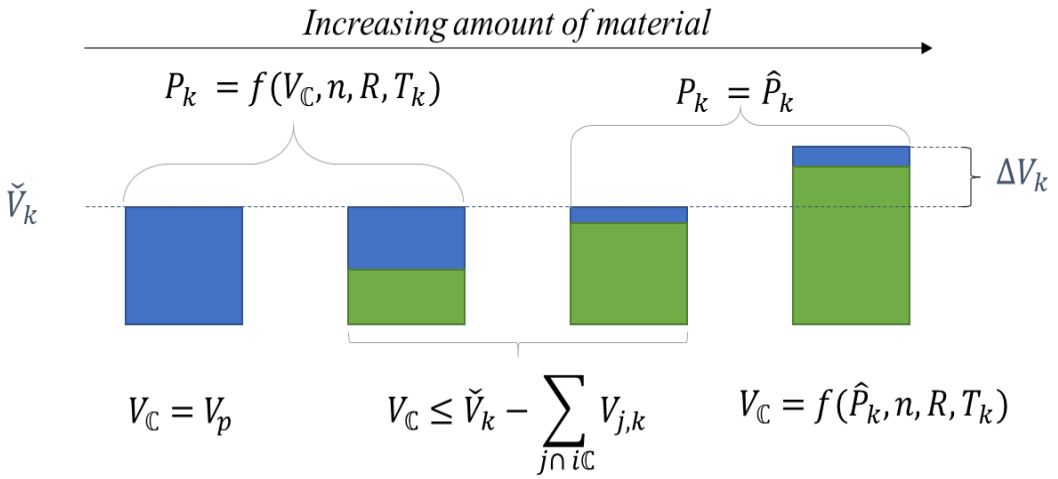

Figure 16 – The compartment pressure increases until the maximum, where the phase material no longer compresses within the compartment volume but expands beyond it at the fixed maximum pressure; V_p is the volume of phantom material.

The overflown volume is the volume of material exceeding the capacity of the compartment, Equation 36, ΔV_k.

$$\Delta V_k = \sum_k V_{j,k} - V_k \qquad \text{Equation 36}$$

The overflown volume can be used to determine velocity and activation of convective flow leaving an overfilled compartment, introduced, and discussed further in section 3.5 **Transport and Transformation phenomen**. From preliminary validation it has been observed that if a compartment does not have a pathway for removal of overflown material, the compartment will grow indefinitely – an issue addressed with the "*relaxed density*" closure model, to follow.

3.3.2 Relaxed density

With the relaxed density closure model, the phase volumes do not grow larger than the compartment volume. Instead, where the sum of incompressible phase volumes in a compartment approaches the compartment volume, the incompressible phase densities begin relaxing (increasing in value) to maintain the total phase volume in the compartment at V_k.

A minimum volume is set for the sum of compressible phases in compartment k, $\check{V}_k$, at which the density relaxation begins and incompressible phase growth stops. This is required as to always have a small volume allocated to compressible phase pressure calculation, Equation 37.

$$\sum_{j \cap \mathbb{C}} m_{j,k}\rho_{j,k} \geq \check{V}_k = \alpha_k V_k \qquad \text{Equation 37}$$

$$where: \alpha_k \ll \sum_j [C]_{p,j,k}$$

Limiting the maximum volume of incompressible material in the compartment to $(1-\alpha_k)V_k$. The solution sensitivity to the minimum compressible volume constant α_k is detailed in the validation chapter, section 4.6.3 Balancing model stiffness with attainment of solution.

By limiting the maximum volume of incompressible material in the compartment to below the volume of a compartment, V_k, any material fed to a compartment beyond its capacity does not overfill the compartment. Instead, the additional material beyond capacity causes an increase in incompressible

phase densities and in turn dramatically increases the compartment pressure; illustrated in Figure 17.

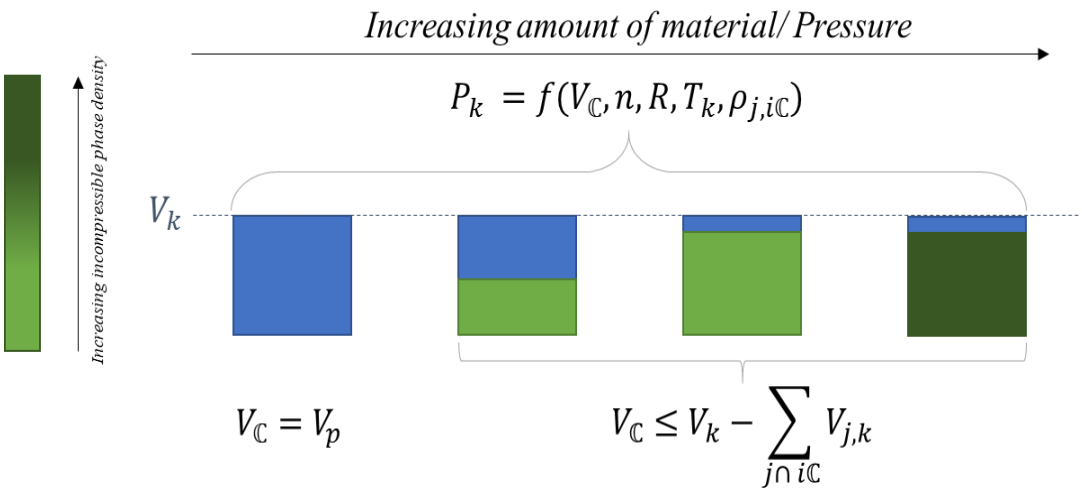

Figure 17 - Compartment relaxed density closure model concept.

Unlike the variable volume model, the more universal relaxed density compartment model can be used in conjunction with container modelling (3.4 The Container Theory).

3.3.2.1 Incompressible density

The ideal fluid density, $\rho_{j,k}^{0}\left(\frac{kg}{m^3}\right)$ introduced in the variable volume closure model is again utilised here. The density of an incompressible phase, $\rho_{j,k}$, is equal to the ideal fluid density value up until the compartment is 'overfilled' with material.

$$\rho_{j,k} = \rho_{j,k}^{0} \qquad \text{Equation 38}$$

$$when: \sum_{j \cap i\mathbb{C}} m_{j,k}\rho_{j,k}^{0} \leq \hat{V}_k$$

$$\hat{V}_k = V_k - \check{V}_k = (1 - \alpha_k)V_k \qquad \text{Equation 39}$$

When the compartment is 'overfilled', we relax the ideal fluid density of each incompressible phase proportional to the phase volume fraction within the compartment based on the ideal phase density, for each incompressible phase j,

$$\rho_{j,k} = \frac{m_{j,k}}{f_{j,k}\hat{V}_k} \quad \text{Equation 40}$$

$$when: \sum_{j \cap i\mathbb{C}} m_{j,k}\rho_{j,k}^{0} > \hat{V}_k$$

$$f_{j,k} = \frac{m_{j,k}\rho_{j,k}^{0}}{\sum_{j \cap i\mathbb{C}} m_{j,k}\rho_{j,k}^{0}} \quad \text{Equation 41}$$

$$V_{j,k} = \hat{V}_k f_{j,k} \quad \text{Equation 42}$$

Maintaining the sum of phase volumes to that of the compartment at V_k throughout the simulation.

3.3.2.2 Compartment pressure

The pressure of a compartment is determined from two components, Equation 43, (i) the pressure of the compressible material, $P_{\mathbb{C},k}$, and (ii) a multiplying factor due to incompressible phase relaxation, $f_{i\mathbb{C},k}$.

$$P_k = f_{i\mathbb{C},k} P_{\mathbb{C},k} \quad \text{Equation 43}$$

(i) A compartment compressible pressure $P_{\mathbb{C},k}$ has a set maximum $(P_{\mathbb{C},k,max})$ and minimum $(P_{\mathbb{C},k,min})$ value for the compartment in the absence of compressible phase material – bar phantom species, which in turn determine the minimum compressible volume factor, α_k, and total concentration of phantom species in the compartment $[C]_{p,j,k}$.

The minimum compressible volume factor α_k where the minimum compressible volume $\breve{V}_k = \alpha_k V_k$, and thus the moles of compressible material cannot be compressed further is determined through Equation 44.

$$\alpha_k = \frac{P_{\mathbb{C},k,min}}{P_{\mathbb{C},k,max}} \quad \text{Equation 44}$$

The concentration of total phantom moles each of all compressible phases combined, $[C]_{p,j,k}$, is given by Equation 46. This is a rearrangement of the ideal gas law, calculating the required concentration of compressible phantom

moles to achieve a max compressible volume of $P_{\mathbb{C},k,max}$ if only phantom species are present; R is the ideal gas constant.

$$[C]_{p,j,k} = \frac{P_{\mathbb{C},k,max}}{RT_k} \qquad \text{Equation 45}$$

For a compartment devoid of compressible phase chemical species, aside from the mandatory phantom species of each phase, the pressure range of the compartment at a temperature of T_k is given in Equation 46.

$$P_{\mathbb{C},k,min} = R[C]_{p,j,k}\alpha_k T_k \leq P_{\mathbb{C},k} \leq R[C]_{p,j,k}T_k = P_{\mathbb{C},k,max} \qquad \text{Equation 46}$$

More universally, for a compartment with the phantom and non-phantom species moles ($n_{\mathbb{C},k}$), Equation 47.

$$\left(\frac{n_{\mathbb{C},k}}{V_k} + \alpha_k[C]_{p,j,k}\right)RT_k \leq P_{\mathbb{C},k} \leq \left(\frac{n_{\mathbb{C},k}}{\alpha_k V_k} + [C]_{p,j,k}\right)RT_k \qquad \text{Equation 47}$$

Consider a compartment with $P_{k,max} = 101{,}325Pa$, $P_{\mathbb{C},k,min} = 1Pa$ at a temperature of $T_k = 298°K$ – an adequately small enough pressure to represent an empty medium-vacuumed compartment. The value of the minimum compressible volume factor is $\alpha_k = 10^{-5}$ per Equation 44; and from Equation 45, the total concentration of compressible phantom species in the compartment can be calculated $[C]_{p,j,k} \cong \frac{40mol}{m^3}$. These values are then used to determine the moles of phantom species in each phase of a compartment, see section 3.2.1.1 Phantom Chemical species, and the point at which the relaxation of density occurs.

(ii) The incompressible pressure factor translates the relaxed density difference to ideal density of incompressible phases into a pressure factor, calculated through Equation 48. The factor has a value equal to or greater than unity, $f_{i\mathbb{C}}(\rho_0, \rho) \geq 1$, dependent on the difference in average ideal and relaxed density of the compartment incompressible phases; respectively ρ & ρ_0. Where ε is the stiffness coefficient which determines the impact of density deviation from ideal upon the compartment pressure, P_k.

$$f_{i\mathbb{C}} = (1 + \rho - \rho_0)^{\varepsilon} \qquad \text{Equation 48}$$

The resultant pressure of a compartment can be of any value greater than or equal to the minimum compartment pressure $P_{\mathbb{C},k,min} \leq P_k$.

3.3.3 Summary

A compartment with phase volume functionally related to the composition of material has been developed. The *assumed volume* modelling, which results in under-estimated concentration values, is addressed by this advancement.

Pressure modelling of a compartment was introduced as a novel concept applied to compartment modelling. Phases of incompressible and compressible nature permitted the use of an EOS to relate the known compressible phase volume, compressible species moles and compartment temperature to the pressure of the compartment.

Two closure models, named so as they deal with the extremes of the pressure model – when more phase material is present within a compartment than the compartment can contain – were developed. Although similar results, allowing compartment overfilling and driving force-based evacuation of material, the *relaxed density* model ranked higher as keeping the volume of phase material equal to the compartment volume allows for the use of the container theory, presented next.

3.4 The Container Theory

Process and unit operations rarely contain a single continuum (continuous-dispersion mix), e.g., one of the simplest units in a process - the stirred tank (Figure 18) is composed of at least two continuums: the liquor and headspace gas. Accurately defining the volumes of continuums in a process is important for many phenomenological models which depend upon volume-based rates and molar concentrations. However, modelling this variation in continuum volume during filling, emptying and over the course of a process is not typically considered in compartment modelling found in literature – instead,

continuums are typically assumed a constant volume throughout the time domain of solution (steady state).

Attempts to address this issue have been observed, section 2.3.3 , non-universal approaches specifically addressing the system at hand.

Built upon the compartment theory, where the phasic contents of a compartment determine the pressure within the compartment, the container theory introduced here provides a solution to modelling the change in compartment volumes over time in a unit/process operation. The management of compartment volume change is completely automated, driven by the need of each compartment to reach pressure equilibria and the sum of compartment volumes to equal that of the unit/process operation. This development can be applied to models where the change in compartment volumes cannot be ignored, e.g., fed batch units.

A **Container** is the furthermost outward structural layer of the compartment model, representing a unit operation or process' boundary volume. A container encapsulates, with no ordering, one or more compartments - sub-volumes of a process - to the container volume $V_{l,0}(m^3)$. The sum of the contained compartment volumes varies with time, V_l, dependent on initial compartment volumes and acting phenomena.

The compartment volumes are changed towards reaching an equilibrium at which the following two objectives of the container are met: (i) the sum of compartment volumes to that of the container volume, $V_l \rightarrow V_{l,0}$ and (ii) towards equilibrating the contained compartment pressures, $P_k = P_{k+1} = \cdots P_{k-1}$.

3.4.1 Ideal container operation example

The change in contained compartment volumes is demonstrated over time due to a fixed pressure feed to a closed compartment, in Figure 18. This is an example of a closed vessel being filled with liquor – separated into a compressible phase headspace compartment (grey) and incompressible phase liquor compartment (blue). A feed of incompressible phase material to the liquor compartment is initiated. This increases the pressure of the liquor

compartment from low pressure (LP) to medium pressure (MP) until the pressure within the vessel is equal to the feed, disabling the feed. The yellow box indicates the container volume boundary within, the inner boxes represent the two separate compartments.

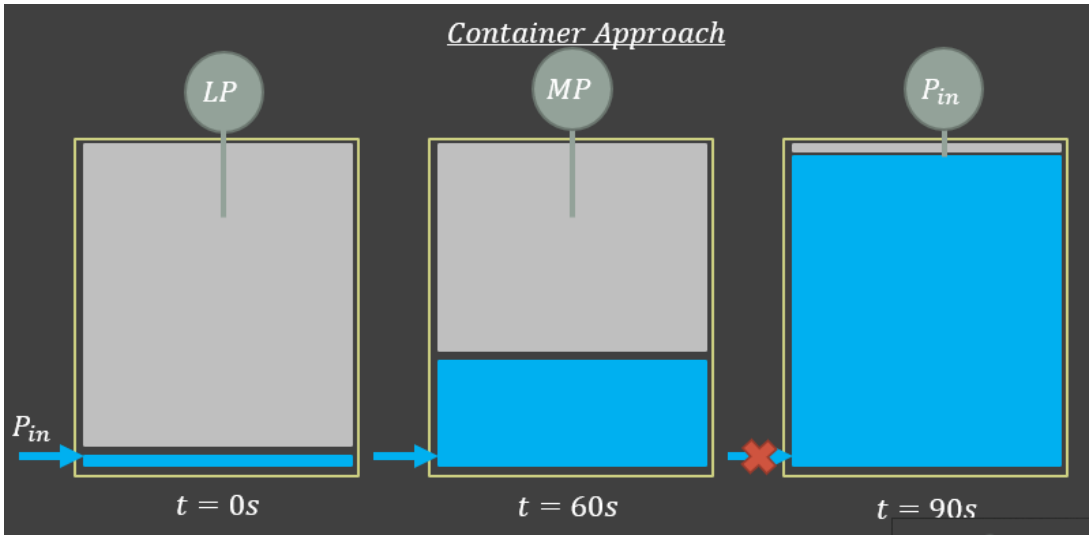

Figure 18 – Container incompressible compartment expanding and compressible compartment contracting over time to (i) sum to equal the container volume, and (ii) equilibrate pressure between compartments. $(\boldsymbol{LP < MP < P_{in}})$

The ideal behaviour of the container is to either reduce or increase each contained compartment volume to reach the objective equality at equilibrium where the sum of compartment volumes is equal to the container volume, $V_{l,0}$, which may not be initially true, objective (i) Equation 49.

$$V_l \rightarrow V_{l,0} \qquad \text{Equation 49}$$

And objective (ii) to drive the compartment pressures in the set k to $k+n$ towards equilibration, Equation 50.

$$P_k = P_{k+1} = \cdots P_{k+n} \qquad \text{Equation 50}$$

In the example of Figure 18 the two objectives are achieved simultaneously by increasing the liquor compartment volume and reducing the headspace compartment volume as liquor is added to the incompressible compartment. Throughout the filling procedure the pressure of both compartments increases, until the pressure of the fed compartment equals that of the feed

flow. Without a driving force to propagate filling, the flow shuts off. Both compartment pressures are equilibrated by the action of the container. And the summed volumes of the compartments total to equal the volume of the container at the final time, 90 seconds.

3.4.2 Container Volume control

The ideal container model assumes that the volume V_l is at fixed value $V_{l,0}$. In practice, there are times that the sum of compartment volume in fact deviates from the container volume $V_l(t) \neq V_{l,0}$; during change in compartment volumes. To ensure the contained compartment volumes converge to $\Sigma V_k = V_{l,0}$, the container modifies compartment volumes using the differential, Equation 51. A multiplier V_k sets the rate of volume change to be relative to the compartment volume size; smaller compartments exhibit slower changes in volume in comparison to larger compartments. The multiplier ensures smaller volumes do not fall below zero in aid of reaching container equilibrium.

$$\frac{dV_k}{dt} = \frac{V_k}{\tau_l}\left[\frac{V_{l,0} - \sum_k V_k}{V_l}\right] \qquad \text{Equation 51}$$

The time constant τ_l determines the rate at which equilibrium is reached, another stiffness constant of the theory.

3.4.2.1 Example of container volume control

An example of the container compartment volume control differential is given in Figure 19. The compartment volumes of the container initially sum to a value less than that of the container, Figure 19(a). The driving force for the differential is to increase the volume of the compartments to the equilibrium point at which $V_l = V_{l,0}$, the equilbrum point shown in Figure 19(b). The volume of each compartment grows at the same rate. In this example the incompressible phases were initially in a relaxed state, having an artificially increased density, hence the growth in compartment volume (represented as area of yellow shading) without addition of material.

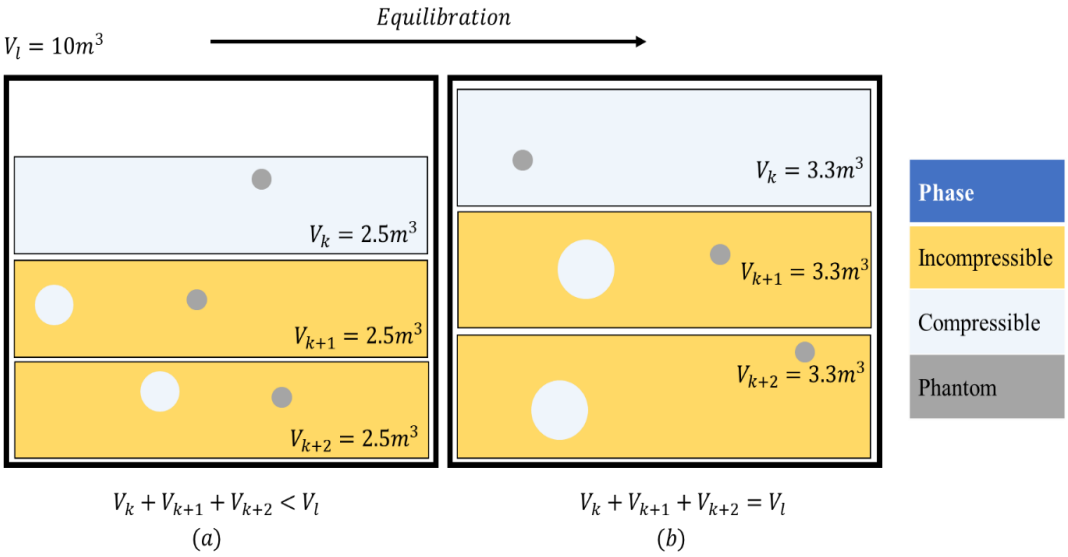

Figure 19 – The sum of compartment volumes increases at equal rates until the sum of compartment volumes equals that of the container.

3.4.3 Container Pressure control

As the compartment volumes are modified to converge to $V_l = V_{l,0}$ over the simulation time; the relative pressures of contained compartments potentially diverge from equality, the following compartment volume differential (Equation 52) is applied to all compartments of a container to drive the compartment pressures towards equilibration. The pressure of each compartment is driven towards an equilibrium pressure – the pressure of the container, P_l.

$$\frac{dV_k}{dt} = \frac{V_k}{\tau_l}\left[\frac{P_k - P_l}{P_l}\right] \qquad \text{Equation 52}$$

And τ_l is the time constant from the previously introduced volume differential.

Where through the ideal gas law, Equation 53, the container pressure is calculated as the sum of all compressible moles in all compartments of the container; multiplied by the temperature of each respective compartment T_k; and the ideal gas constant R; divided through by the compressible volume of the container, $V_{\mathbb{C},l}$.

$$P_l = \frac{R \sum_k T_k \sum_{j \cap \mathbb{C}} \sum_i n_{i,j,k}}{V_{\mathbb{C},l}} \quad \text{Equation 53}$$

And the container compressible volume is the sum of the contained compartments equivalent compressible phase volumes; this is the volume of the compressible phase required to obtain a compartment pressure of P_k (through the relaxed density closure model) without the induction of the incompressible pressure factor, $f_{i\mathbb{C}}$. This equivalent volume for each compartment is obtained through the rearrangement of the compartment pressure equation, Equation 54. Moving the incompressible factor to the denominator of the equation we see the true volume required to observe the same compartment pressure P_k without the multiplication of $f_{i\mathbb{C}}$ is given as $\frac{V_k - V_{i\mathbb{C}}}{f_{i\mathbb{C}}}$.

$$P_k = f_{i\mathbb{C}} P_{\mathbb{C},\boldsymbol{k}} = f_{i\mathbb{C}} \frac{R\left(\sum_k \alpha_k \sum_j [C]_{p,j,k} + n_{\mathbb{C},k}\right) T_k}{V_k - V_{i\mathbb{C},\mathbf{k}}} \quad \text{Equation 54}$$

$$= \frac{1}{\frac{\boldsymbol{V_k - V_{i\mathbb{C},k}}}{\boldsymbol{f_{i\mathbb{C}}}}} R\left([C]_{p,j,k} + n_{\mathbb{C},k}\right) T_k$$

The container compressible volume is then the sum of the equivalent compressible volumes of all contained compartments, Equation 55.

$$V_{\mathbb{C},l} = \sum_k \left(\frac{V_{\mathbb{C},k}}{f_{i\mathbb{C},k}}\right) = \sum_k \left(\frac{V_k - V_{i\mathbb{C},k}}{f_{i\mathbb{C},k}}\right) \quad \text{Equation 55}$$

To maintain the compartments $P_{\mathbb{C},k,max}$ and $P_{\mathbb{C},k,min}$ values, each of the phantom components (subscript p) of the compartment are altered proportional to the change in compartment volume and phantom component concentration within the compartment volume, Equation 56. This includes the phantom species of the phantom phase, and any other phases present in the compartment.

$$\frac{dn_{p,j,k}}{dt} = [C]_{p,j,k} \frac{dV_k}{dt} \quad \text{Equation 56}$$

In conjunction with phantom mole differential, the enthalpy of the compartment is equivalently modified, Equation 57. Without such modification, the removal or addition of mass would cause a direct affect to the temperature as the enthalpy of the system is distributed over a lesser/greater amount of mass. The affect is especially prominent in an empty compartment, where phantom moles are the only mass of the compartment which the enthalpy is distributed throughout. The change in phantom moles is a differential of the ODE system.

$$\frac{dQ_k}{dt} = Q_k \sum_j \frac{1}{\sum_j m_{j,k}} \sum_p Mw_p \frac{dn_{p,j,k}}{dt} \qquad \text{Equation 57}$$

$m_{j,k}$ is the mass of phase j of compartment k.

Due to the nature of compartment pressure, an empty compartment can only present a minimum pressure of $P_k = P_{k,min}$. The modification of the phantom moles poses a problem in the calculation of P_l, as compartments within the container are likely to exist at pressures greater than $P_{k,min}$ when containing phasic contents other than phantom. The inequality of compartment pressures results in an overestimation of container pressure.

To overcome this issue, where the compartment volume is less than a small volume, $\alpha_k V_l$– relative to the container volume – the phantom moles are no longer modified. This permits empty compartments of low volume to reach pressures greater than P_{min}, and resolve the issue of overestimation of compartment volumes from an incorrect P_l; see Equation 58.

$$\frac{dn_{p,j,k}}{dt} = \begin{matrix} \boldsymbol{if\ V_k < \alpha_k V_l}: & 0 \\ \boldsymbol{if\ V_k \geq \alpha_k V_l}: & [C]_{p,j,k} \frac{dV_k}{dt} \end{matrix} \qquad \text{Equation 58}$$

3.4.3.1 Example of container pressure control

In this system example, the compressible compartment within the container is of a magnitude greater in pressure than the incompressible compartments, as seen in Figure 20(a). The pressure driven change in compartment volumes drives the compressible compartment to increase in volume, reducing P_k to P_l and to decrease the volumes of the incompressible compartments to

increase their pressures towards $P_l(t)$; in doing so relaxing the density of the incompressible phases $\rho_{j,i\mathbb{C}} \geq \rho_{j,0}$. The incompressible phases are compressed, and thus enter a state of relaxed density, as the maximum pressure of the compressible phase is $P_{\mathbb{C},\mathbf{max}} = 1bar$ - and the equilibrium target pressure of the compartment is greater than this between $1 \,\&\, 10\ Bar$. The resultant pressures of the compartment are equal at equilibrium; however, the volume of compartments explode beyond the capacity of the container. Note the compressible phases of the incompressible continuous phase compartments do not shrink as they're at the maximum compression, hence the initiation of incompressible phase relaxation to achieve greater pressures in the compartment.

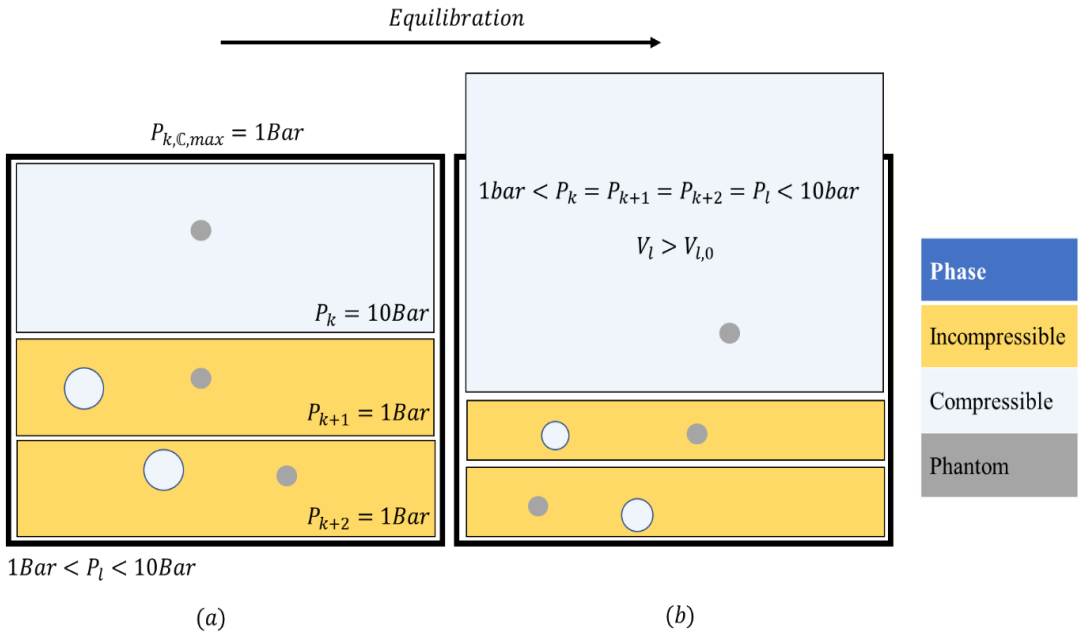

Figure 20 – Initially underpressurised incompressible compartments shrink in volume to reach the equilibrium pressure, whilst the initially over-pressurised compressible compartment expands; the result, the breach of container objective (i).

Considering pressure control alone does not constrain compartment volumes to the container volume. The two schemes of control are combined to form the universal container model next.

3.4.4 Universal container model (Pressure and volume control)

The universal formula developed for equilibration of the containers volume and pressure objectives is given below, Equation 59, combining the above two differentials for container objective management.

$$\frac{dV_k}{dt} = \frac{V_k}{\tau_l}\left[\frac{V_{l,0} - V_l}{V_{l,0}} + \frac{P_k - P_l}{P_l}\right] \qquad \text{Equation 59}$$

The container model is complete with the formula of Equation 58 using the universal $\frac{dV_k}{dt}$ formula of Equation 59. This is a differential of the ODE system. With the addition of container theory, the change in compartment volume can be modelled automatically within the system as a function of maintain equilibrated pressure and summed compartment volume to that of the container.

In summary, the formula for the rate of compartment volume change for contained compartments is formed of three components; defined in ascending order:

$\frac{V_k}{\tau_l}$

The volume of the compartment V_k divided by a time constant $\tau_l(seconds)$. The volume ensures larger compartments undergo larger changes relative to smaller volume compartments. The time constant determines the stiffness of the rate of change.

$\frac{V_{l_o} - V_l}{V_{l_o}}$

Objective one; $V_{l,0} - V_l = 0$ is directly substituted into the equation. Any deviation from this equality, produces a change in volume of the compartments – increasing/decreasing volume towards $V_l = V_{l,0}$.

$\frac{P_k - P_l}{P_l}$

Objective two; $P_k = P_{k+1}$ ... is managed through the third component. The container pressure, P_l, which represents a distributed pressure of all the compartment compressible phases is compared to each compartment pressure, P_k. This

deviation produces a change in compartment volumes in the direction of increase/decrease towards equilibrating the compartment pressures.

Both the second and third component are divided by their equilibrium values $V_{l,0}$ and P_l to maintain influence of both the pressure difference and volume difference on the rate of volume change at the same magnitude – and thus same scale. This also eliminates the units of the components, maintaining the correct unit balance of the volume rate differential to m^3/s.

3.4.4.1 Local equilibrium Container Failure hypothesis

Concerns with a local equilibrium forming where all compartments exhibit zero change in volume when neither objective are met is formulated as follows:

$$all\ \frac{dV_k}{dt} = 0$$

$$where; \frac{P_k - P_l}{P_l} = -\frac{V_{l,0} - V_l}{V_{l,0}}$$

This however is not possible as, although the volume component has the same value for all compartments, being it is a construction of all compartments and the container volume; the pressure component differs for each compartment unless the pressures are equal $P_k = P_{k+1}$ … at which point they're equal to the container pressure and thus the pressure component is null.

It is to be noted, one compartment may be subject to no volume change due to the above conditional occurrence; but not all compartments can be subject to the same local equilibrium without the container objectives achieved. Thus, a local equilibrium where the objectives are not met, and the compartments differentials are all equal to nought cannot exist and is not a failure point of the theorem.

3.4.4.2 Universal container scenarios

In the scenarios below, a container of volume V_l contains three compartments. Two compartments are filled with incompressible material and one with compressible material, like the examples prior.

In **scenario one**, Figure 21, the incompressible compartments are at a lower pressure than the compressible phase; the container pressure lies somewhere between the incompressible and compressible compartment pressures. All compartment volumes summate to the volume of the container. In the procedure of equilibrating the compartment pressures, the container reduces the incompressible compartment volumes which induces density relaxation and as a result compartment pressure increase. The result is the summed compartment volume decreasing below V_l. Simultaneously, the compressible compartment is in turn increased in volume to reduce the compressible pressure and meet objective one of the containers. The result at equilibrium is the summed compartment volumes equal that of the container, the reduction of incompressible phase compartments and increase in compressible phase compartment; and the pressures of all contained compartments are at the container pressure, $1Bar < P_l < 10Bar$.

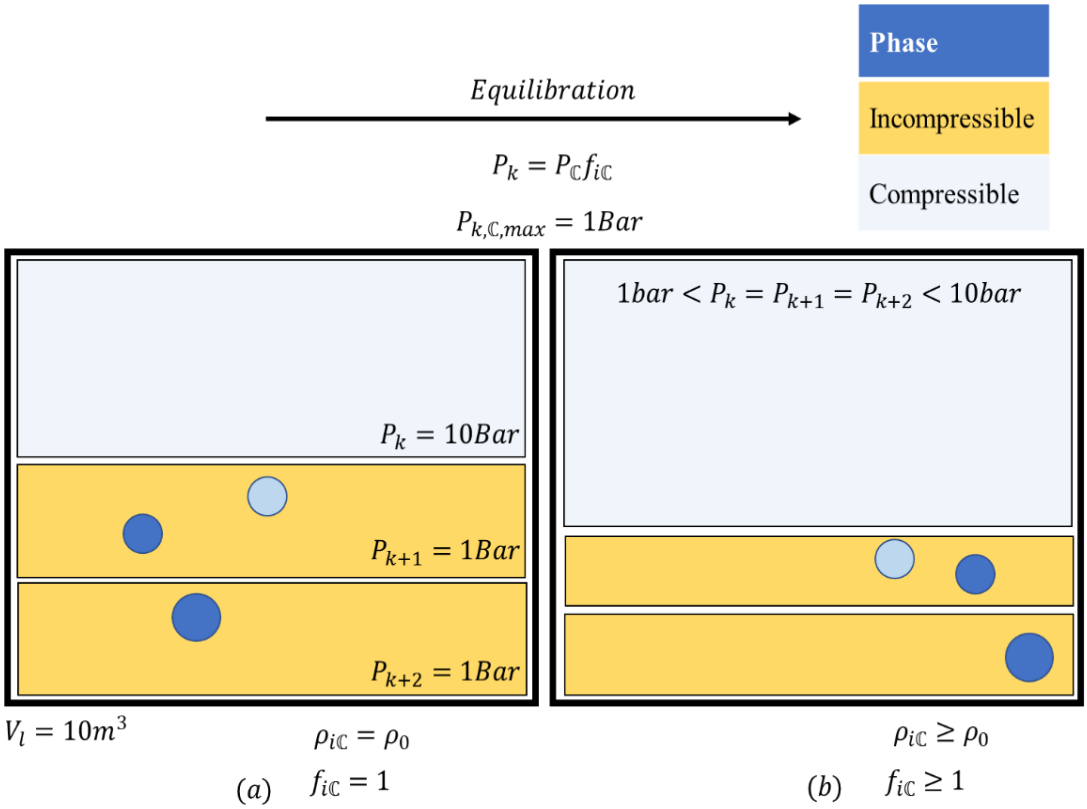

Figure 21 - Overfilled container, non-relaxed compartments (a) Before equilibrium, (b) at equilibrium

Note in this example, as mentioned above, density relaxation is required as the maximum compressible pressure, prior to incompressible density relaxation, is below equilibrium pressure of the compartments which lies between $1 < P_k < 10Bar$. As the pressure of the compartment is initially at maximum compressible pressure ($P_k = P_{\mathbb{C},\mathbf{max}}$), the compressible phases are at the minimum compressible volume, therefore the phantom phase and compressible phase dispersed in the incompressible continuum do not change in volume.

Scenario two, Figure 22,depicts the compartments of the same initial volume as scenario one; except in this case the incompressible phases are at 10Bar, under a relaxed state, and the compressible phase begins at 0.1Bar. The result is the un-relaxing of the incompressible phases which results in an incompressible compartment pressure of 1Bar – in turn increasing the incompressible compartments volumes and decreasing the compressible compartment volume. Further increase in the incompressible compartment volume accommodates the expanding compressible material which in affect reduces the incompressible compartment pressures below 1Bar. The end, at equilibrium, there are two incompressible compartments of greater volume than initially - part due to de-relaxation of incompressible material and part due to increase in compressible phase volume (see dispersed phantom phase volume increase). The compressible compartment volume is decreased, this results in an increase in its pressure.

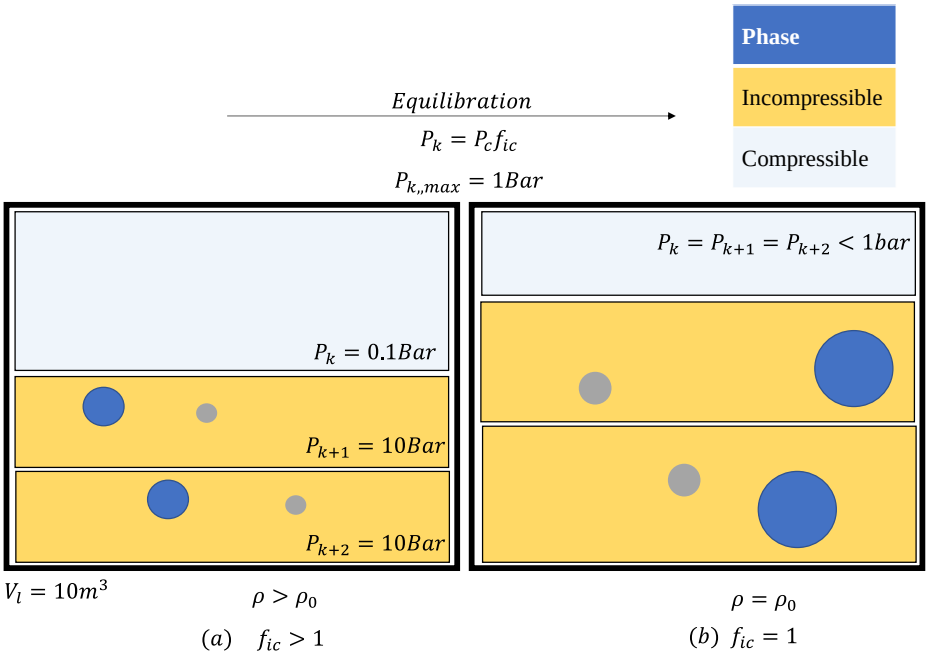

Figure 22 - Overfilled container, relaxed compartments (a) Before equilibrium, (b) at equilibrium.

Both cases exhibit, universally, the behaviour of the universal container model in modifying contained compartment volumes and the underlying compartment pressure to phase volume relationship.

3.4.5 Application to a filling vessel

An application of the container is shown in Figure 23, which demonstrates the filling procedure possible with a container. A container representing the hard boundary of a closed vessel contains two compartments; one represents the gaseous headspace – the other the liquor of the vessel. The vessel is closed, filled only with inert headspace gas at an initial atmospheric pressure of 1Bar. The liquor compartment is empty, a feed begins adding incompressible material from a source tank at a pressure of 2Bar.

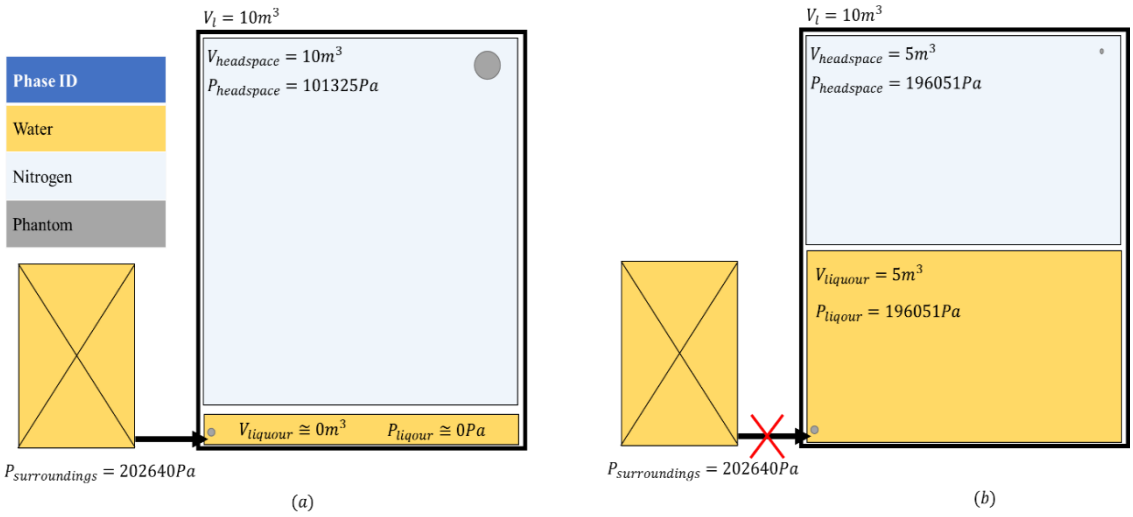

Figure 23 - Closed vessel filling compartment model (a) pre-filling, (b) at equilibrium.

The model input file is as follows, language terms are in bold – model object properties in italics and property values are in standard font; see section 4.3 CompArt High-level input language for language clarity.

```
Solver Radau
    t_start : 0
    t_final : 100
    atol : 10**-8
    rtol : 10**-8

Defaults
    conc_p : 40.4
    tau l : 0.0000001
    alpha_k : 10**-5

DefineComponents
    Nitrogen : 0.028
    Water : 0.018
Surroundings surroundings_1 of continuous phase incompressible
    volume : 10
    pressure : 202650
    IncompressiblePhase incompressible to surroundings_1
        Water : 500000
Compartment gas of continuous phase compressible
    volume : 10
    CompressiblePhase compressible to gas
        Nitrogen : 404
Compartment liq of continuous phase incompressible
    volume : 0.001
    IncompressiblePhase incompressible to liq
ConvectiveTransport transport from surroundings_1 to liq
   velocity : 0.1
Container l encapsulating compartments gas liq
   volume : 10
end
```

The results of Figure 24 show the equilibrium is obtained at approximately $50s$, at which time the volume of both compartment's reach $5m^3$ and the pressures are equal at $199702Pa$. The equality of volumes at equilibrium is expected as reducing the headspace compartment by 50% should induce an increase in pressure of 100% of the original value – as per the ideal gas law, $P_k \propto \frac{1}{V_k}$. At which point the liquor compartment is filled and a pressure gradient does not exist for propagation of material from the surroundings to the liquor compartment. The pressure values of the compartments fall short of the surroundings pressure as the sigmoid, the mechanism controlling flow activation only active when a driving force is present, is subject to an error (case dependent, 1.36% here) to ensure no backflow of material.

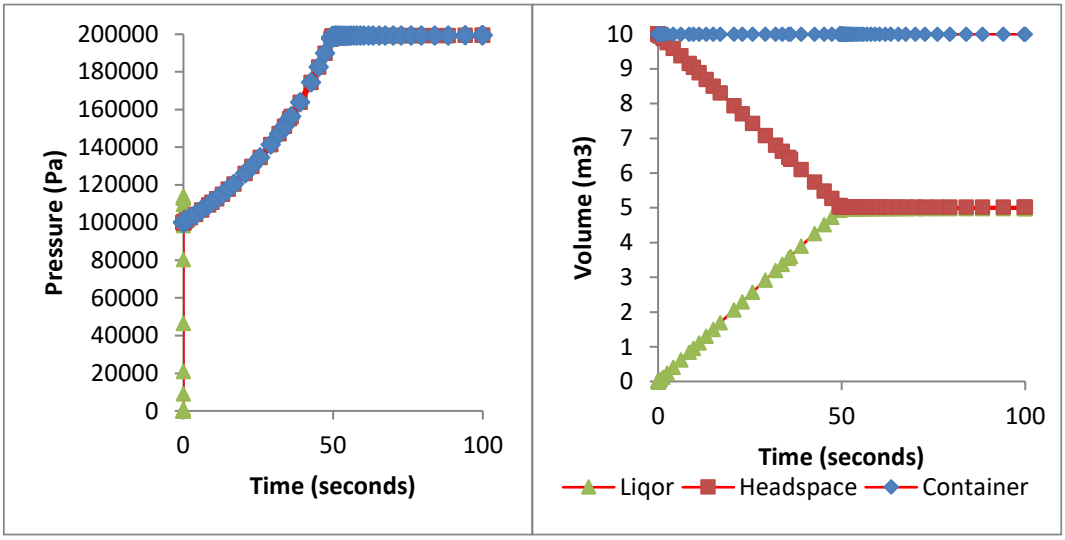

Figure 24 - Compartment Pressure and Volume development over course of case study; filling a closed vessel with liquor.

3.4.6 Limitations of the Container

Convective transport, introduced in more detail in section 3.5.1.5 Convective Transport, is a mechanism by which all phasic material of one compartment is transported to another compartment at a volumetric rate. The molar rate of species transported from the source compartment is given as the product of the molar concentration of species in the source compartment and said volumetric flowrate.

An advancement upon the state of the art is the introduction of automatically calculated volumetric flow rates based upon the difference in pressure between compartments. However, due to the nature of the container and its behaviour in equilibrating the compartment pressures it contains, no such pressure gradient between compartments can exist between compartments of the same container. Thus, no automated convective transport of propagated material between two compartments contained within the same container.

Instead, volumetric flowrates must be defined as set constant flow rates throughout simulation for convective transport mechanism internal to a container. Convective transport connecting two compartments not of the same container is possible as a pressure gradient is plausible in such model.

3.5 Transport and Transformation phenomena

A phenomenon is a directly observed event exhibiting either, or a combination of; (i) a rate of change in the molar quantities of one or more chemical species, (ii) a rate of change in the sensible enthalpies of one or more compartments. The rate of change in quantities due to phenomenon m is represented as a temporal differential $\left(e.g., \frac{dn_{i,j,k}^{m}}{dt}, \frac{dQ_{k}^{m}}{dt}\right)$; the mass and energy change due to phenomena is conserved. The total change of chemical species i of location j,k moles is the sum of the phenomenological differentials associated with a change in the quantity at the instance in time, Equation 60.

$$\frac{dn_{i,j,k}}{dt} = \sum \frac{dn_{i,j,k}^{m}}{dt} \qquad \text{Equation 60}$$

Similarly, the total change in the sensible enthalpy of compartment k is the sum of the phenomenological differentials associated with a change in the quantity at that instance in time, Equation 61.

$$\frac{dQ_{k}}{dt} = \sum \frac{dQ_{k}^{m}}{dt} \qquad \text{Equation 61}$$

In this section the fundamental phenomenon of chemical process compartment modelling synthesised from the literature, material transport,

reaction, and heat transfer are introduced. Their implementation into the universal compartment model structure is described, along with the developed generalised equations.

3.5.1 Material Transport

Material transport is a group of phenomena involved in the movement of one or more chemical species, and the associated sensible enthalpy, between two volumes.

Within the universal compartment model, chemicals species are transported either (a) between two phases of the same compartment - Intra-compartmental material transport (mass transfer between the continuous and dispersed phase of the same compartment), or (b) between the phases of two adjacent compartments - Inter-compartmental material transport (convective bulk transport, phase transport or mass transfer).

The four components of a material transport are discussed in this section: (i) The mode of transport, (ii) The nature of the transport, (iii) The molar transport rates and (vi) The heat of transport.

3.5.1.1 The mode of transport

A material flow connects two volumes together with the movement of chemical species permitted in a single direction from the source volume (V_S) to termination volume (V_T); material cannot flow backwards along a flow channel – they are strictly one directional. The volumes connected by a flow can be (a) two adjacent phases, or (b) two adjacent compartments.

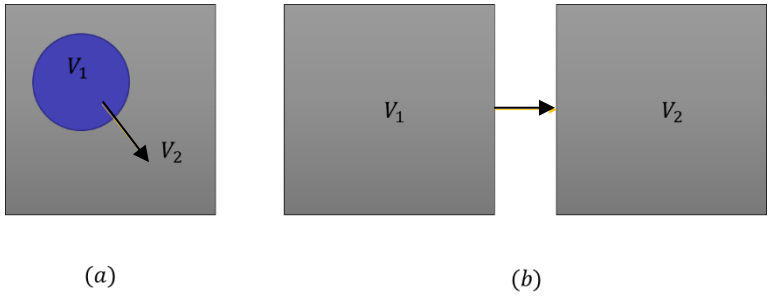

Figure 25 – (a) Intra-compartmental material transport (b) or Inter-compartmental material transport

Chemical species are transported by a flow from a source to a termination volume. Each chemical species removed from the source volume chemical species quantity is added to quantity of the same chemical species in the termination volume – where the termination volume differs in either compartment, phase, or both.

As part of the theory development, the automatic propagation of material transport was developed – removing the tedium of setting system flowrates in the compartment model and balancing material about each compartment – the typical pre-simulation procedure of compartment model construction. This is achieved by using the sigmoid function (Θ) to activate the transport of material flow only when a transport driving force is present in the direction of flow. The driving force is determined by comparing activation variables of the two connected volumes, $\Delta \mathrm{X} = f(X_1, X_2, p_1, p_2)$. The variable compared, when activating/deactivating a transport, differs based on the nature of transport (mass transfer, convective transport, phase transport); e.g., pressure difference driven transport of phases and chemical species material associated through the convective transport phenomena – discussed further in sections 3.5.1.2 The nature of the transport and 3.5.1.6 The molar transport .

The activation of a flow is modelled using a sigmoid function (Θ) as given in Equation 62.

$$0 < \Theta_{\mathrm{I/O}}(\Delta \mathrm{X}) = \frac{1}{1 + e^{-k\Delta \mathrm{X}}} < 1 \qquad \text{Equation 62}$$

An alternative to the sigmoid activation function was tested, the $tanh$ function - Equation 63.

$$\Theta_{\mathrm{I/O}} = \mathrm{Tanh}(k\Delta \mathrm{X}) \qquad \text{Equation 63}$$

The $tanh$ function scaled and translated is equipollent to the sigmoid function. The relation is given below.

Tanh Sigmoid

$$\mathrm{Tanh}\left(\frac{\mathbf{1}}{\mathbf{2}}k\Delta\mathrm{X}\right) \equiv \mathbf{2}\left(\frac{1}{1+e^{-\mathbf{2}k\Delta\mathrm{X}}}-\frac{\mathbf{1}}{\mathbf{2}}\right)$$

The $tanh$ function was rejected as, although the response does reach one instead of being asymptomatic with 1, its values range from $-1 \leq \Theta_{\mathrm{I/O}} \leq 1$. The response's negative region would create a reversed flow, mismatching the simplified unidirectional definition of a flow in this theory.

Sigmoid functions are used more commonly in the hidden layer on/off switches of neural networks (Muthuramalingam, Himavathi and Srinivasan, 2008), it is here applied to model the gradual on/off ($\Theta_{\mathrm{I/O}} \cong 1$, $\Theta_{\mathrm{I/O}} \cong 0\ \mathrm{respectively}$) behaviour of a material transport flow to (i) ensure transport only occurs in a single direction of which is predetermined in the model specification, and (ii) the transition of flow activation is smoothed compared to a Dirac function, and in turn, the discontinuity of the model is reduced.

(i) To ensure no flow occurs where a driving force is not present, where $\Delta X \leq 0$, we accept a small error before the phenomena is activated whilst a driving force is present. This error, p_1, is the fraction value of the termination variable which the source variable must be greater by for the full activation of the transport $\Theta_{\mathrm{I/O}} \approx 1$.

$$\Delta X = \frac{X_1 - X_2(1+\frac{p_1}{2})}{X_2(1+\frac{p_1}{2})+p_2} \qquad \text{Equation 64}$$

Of Equation 64, the parameter p_1 ensures that the transport activation is equal to approximately zero $\Theta_{\mathrm{I/O}} \approx 0$ when the variables are equal $X_1 = X_2$. The transport activates partially, $\Theta_{\mathrm{I/O}} = 0.5$, when the source volume activation variable (X_1) is $1+\frac{p_1}{2}$ times greater than the termination volume, $\mathrm{X}_1 = X_2\left(1+\frac{p_1}{2}\right)$. And the response is fully active $\Theta_{\mathrm{I/O}} \approx 1$ when the source variable is $1+p_1$ times larger than the termination volume; $\mathrm{X}_1 = X_2(1+p_1)$.

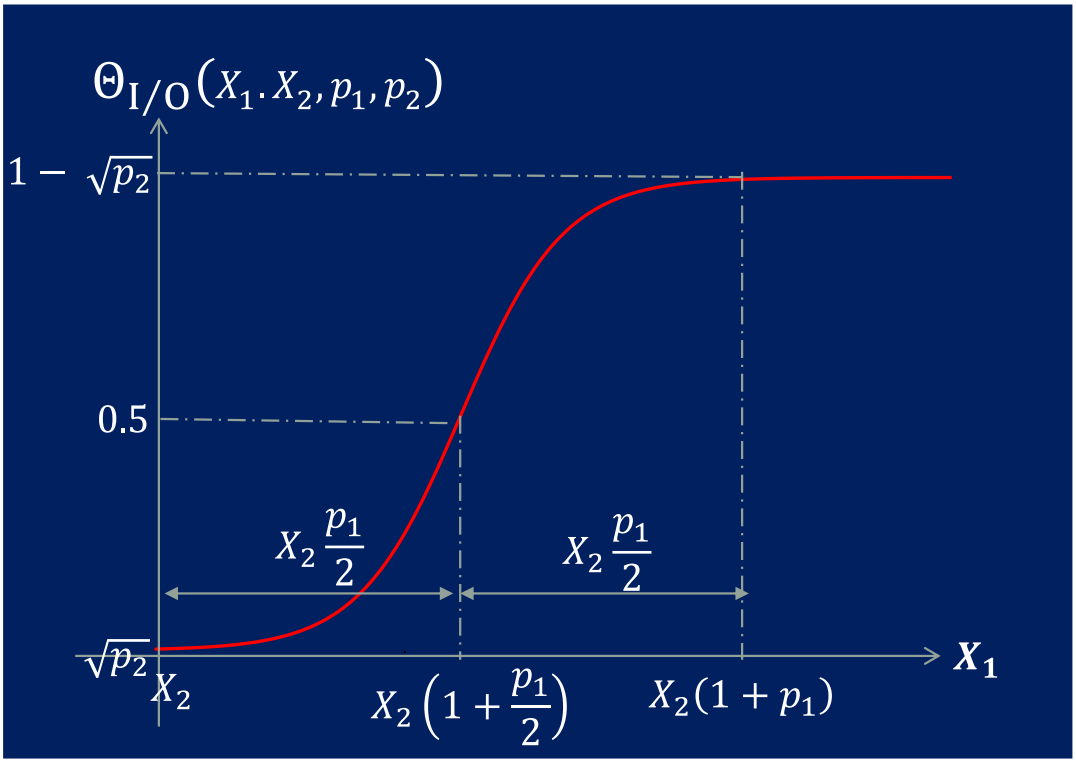

Figure 26 – The relation of sigmoid parameters to the response curve.

The denominator of the activation variable difference removes the dependence of the response upon the magnitude of the variables compared – resulting in a consistent response between transports of differing magnitudes. A small value of $p_2 = 10^{-21}$ is summed to the denominator to ensure no errors associated with a zero value X_2 arise.

(ii) The sigmoid function offers a smoothing parameter k for alteration of the on/off transition. The value of k is used to tighten the response range between deactivation and activation to satisfy the following; (a) the response, as it is asymptotic with zero, must approximate 0 when there is no driving force $X_1 = X_2$, and (b) the response, as it is asymptotic with one, must approximate 1 when the source variable is $1 + p_1$ times greater than the termination variable, $\mathrm{X}_1 = X_2(1 + p_1)$.

The result, in the reversed direction from activated phenomena to deactivated, is a response curve that switches the phenomena on when there's a greater than or equal to $1 + p_1$ times difference in source and termination variables; with decreasing response below this fraction until the point where the source

and termination variables are equal and thus have no driving force – where the response is near zero (deactivating the transport).

Setting the smoothing parameter to be extremely large, $k \gg$, will ensure the two above conditions *(a)* $\Theta_{I/O} \approx 0$ *when* $X_1 = X_2$ *and (b)* $\Theta_{I/O} \approx 1$ *when* $X_1 = X_2(1 + p_1)$ within the difference of p_1 but would also remove the smoothing transition the sigmoid provides – essentially returning to the Dirac function we aim to avoid. Alternatively, an estimation can be made, based on trial and error, requiring further work from the modeller, or we can optimise the value of k for each transport analytically – the latter process is shown below.

First, we select numbers for the approximate responses, for convenience we use the already defined parameter p_2; $\Theta_{I/O} \approx 0 = \sqrt{p_2}$ & $\Theta_{I/O} \approx 1 = 1 - \sqrt{p_2}$.

Then rearranging Equation 62 to make k the objective parameter.

$$k_{(a)} = -\frac{ln\left(\frac{1}{\Theta_{I/O}} - 1\right)}{\Delta X} \qquad \text{Equation 65}$$

For deactivation scenario (a), $\Theta_{I/O} \approx 0 = \sqrt{p}_2$ when $X_1 = X_2$; substituting the latter into Equation 64, with the div!0 error parameter p_2 approximated to be equal to zero in the equation to make the analytical solution derivation possible, and rearranging we find the driving force value to be;$\Delta X = -\frac{p_1}{2+p_1}$

Then, substituting Equation 64 and $\Theta_{I/O} \approx 0 = \sqrt{p}_2$ into Equation 65, we find analytically the k value required is given as.

$$k_{(a)} = \frac{ln\left(\frac{1}{\sqrt{p}_2} - 1\right)}{\frac{p_1}{2 + p_1}} \qquad \text{Equation 66}$$

Following the same procedure for scenario (b), activation of the transport where, $\Theta_{I/O} \approx 1 - \sqrt{p}_2$ when $X_1 = X_2(1 + p_1)$.

$$\Delta X = \frac{p_1}{2 + p_1} \qquad \text{Equation 67}$$

Then, substituting Equation 67 and $\Theta_{I/O} \approx 1 = 1 - \sqrt{p}_2$ into Equation 65, we find analytically the k value required is given as.

$$k_{(b)} = \frac{-ln\left(\frac{1}{1-\sqrt{p}_2} - 1\right)}{\frac{p_1}{2+p_1}}$$ Equation 68

The result is two k parameters of the same value, $k_{(a)} = k_{(b)}$; due to the symmetry of the sigmoid curve, the same would be found if solving for the k value at the midpoint of activation $\Theta_{I/O} = 0.5$ *when* $X_1 = X_2\left(1 + \frac{p_1}{2}\right)$.

3.5.1.2 The nature of the transport

Mass transfer, phase transport and convective transport all transport material unidirectionally from one volume to another over an interfacial area $A(m^2)$, the difference between the three transports is the scale at which the chemical species are transported.

3.5.1.3 Mass transfer

Mass transfer occurs in many processes such as absorption, evaporation, drying, precipitation, membrane filtration, and distillation. A single chemical species is transported between two contacting phases, over an interfacial area A. The phases can be in contact either at (a) inter-compartmental level: transport of a chemical species across the interfacial area between two adjacent compartment continuum phases in a single direction, or (b) intra-compartmental level: in a single direction over the interfacial area between a dispersed phase and continuous phase of the same compartment - Figure 27. If the mass transfer occurs at the inter-compartmental level between two continuums of the same phase, this transfer is commonly referred to as diffusion. The interfacial area of intra-compartmental mass transfer is a function of the dispersed phase characteristic diameter, as given in 3.2.3.1 Continuum-dispersion composition. Inter-compartmental interfacial area, the mass transfer between two adjacent compartment continuous phases, is determined by the modeller prior to simulation.

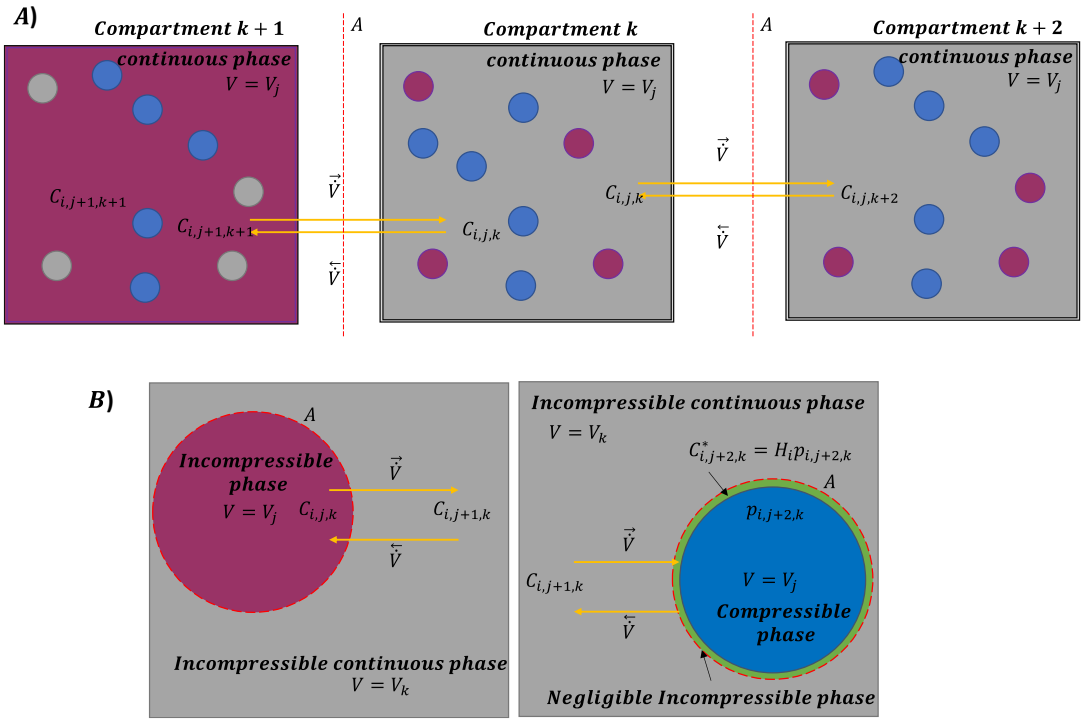

Figure 27 – A) Inter compartmental & B) Intra-compartmental, mass transfer. The subscription i, j, k refers to species, phase, and compartment respectively.

The steady state two-film theory (Wang and Langemann, 1994) is adopted here to model mass transfer between the two phases as the most prevalent observed in literature; the alternatives to two-film theory, penetration and surface renewal theories, can be implemented through differing specification of the mass transfer constants of the phenomenon (Morsi and Basha, 2015). On either side of the adjoining phase boundary, a hypothetical stagnant film of phase material exists. Phase mediums are referred to as source and termination phases (subscript So & T respectively) with the net movement of chemical species from the source to the termination phase. The net transfer from a source phase to a termination phase is the lumped transport of; (i) chemical species diffusion from the bulk of the source phase $C_{i,So}$ to the film of concentration $C^*_{i,So}$ (ii) the stagnant equilibrium of phase interface equilibrium at the interfacial surface, linearly related through a partition coefficient value, $S = 1(default)$; $C^*_{i,So} = SC^*_{i,T}$, (iii) and the chemical species transport from the stagnant film of the termination phase, $C^*_{i,T}$, to the bulk of concentration $C_{i,T}$.

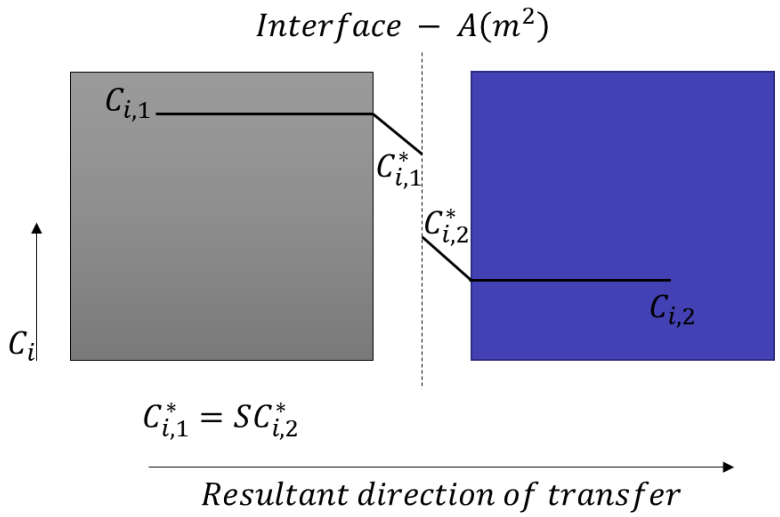

Figure 28 - Inter-compartmental mass transfer of a single chemical species.

3.5.1.4 Phase transport

Phase transport is a derivative of convective transport, the transport of all chemical species of a single-phase j, k at a volumetric rate disengaged from the bulk convective flow, if present, to the same phase in an adjacent compartment, the location $j, k + 1$; Figure 29. The individual species are transported at a rate equivalent to their concentration in the source phase volume and at a total velocity rate a function of the transported dispersed phase volume in the compartment, V_j.

Caveat If the transported phase cannot exist in the receiving compartment, due to the transported phase being compressible and continuum being a differing compressible phase, the source phase is instead transported into the receiving continuum. In this circumstance, the phase transport can only be one-directional; flow of the same phase in the opposite direction is not possible in such scenario as it does not exist.

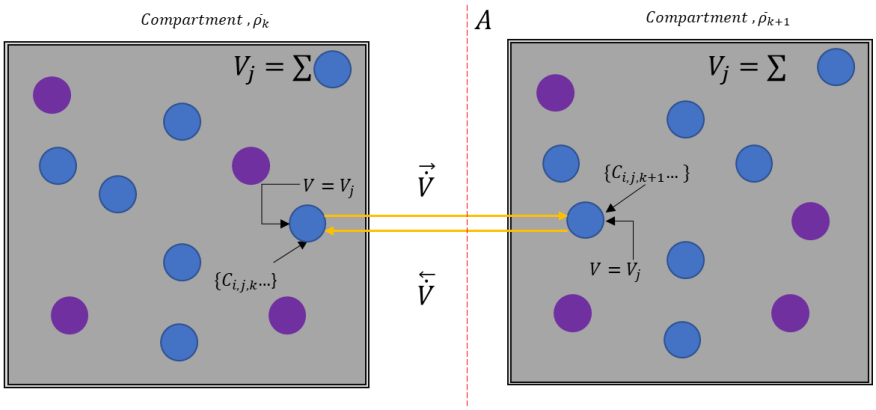

Figure 29 – Phase transport of dispersed phase (blue) between two compartments.

Phase transport is any phase disengaged movement of a phase from the bulk between adjacent compartments driven by the balance of buoyant, gravitational and drag forces acting upon the transported phase, e.g., settling of bio-particulates in a wastewater treatment settler-mixer, the rising bubbles in a bubble column (Figure 30), the phenomenon of rising bubbles resulting in a fluidised bed. It is typically disguised as convective flow in literature, or for the case of bubble transport a slip velocity embedded into a population balance model. As PBM is outside of this works scope, here, a mean residence time model is utilised to permit the modelling of the settlement of particulates, rising of bubbles or mechanical separation of a phase(s) within a system.

The volume of the phase in the source location drives the movement of phase in the direction of phase transport; alternatively, a set rate for phase transport can be set, see section 3.5.1.6 The molar transport . It is important to note, both the approach in literature and approach to phase transport presented here are rudimentary; hydrostatic pressure, phase density and surrounding phase densities, shape, and area of moving phases are not accounted for.

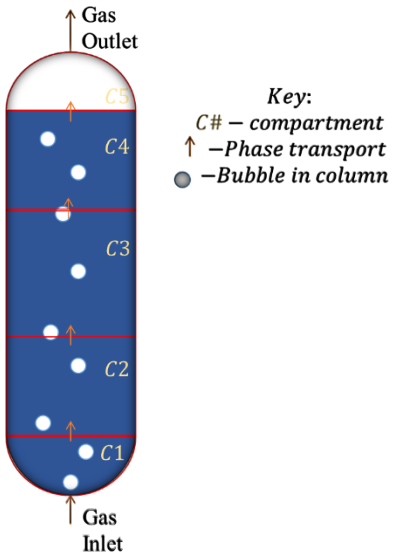

Figure 30 - Bubble column reactor model depicting bubble phase disengagement up column.

3.5.1.5 Convective Transport

Convective transport is the macroscale mechanically stirred (stirring) or pressure driven inviscid transport of all chemical species of all phases in a compartment to the respective phases in an adjacent compartment; $j, k \rightarrow j, k + 1$. The convective transport is modelled as inviscid as viscosity is the ability of a fluid to transfer momentum, the compartment modelling approach ignores momentum instead assuming fixed flow conditions – decoupling hydrodynamics, permits the intensive modelling of phenomena in a system.

The flowrate of a material transport is of either a set value or function of the pressure difference between the compartments, manual compartment mass or volumetric balancing as seen typically in literature is in this framework automated where the pressure driven flow is utilised, addressing the tedium of setting high-flow number compartment models observed in literature (section 2.4 Material Flow). The pressure driven flow of material is a feature not considered in literature due to the current absence of dynamic pressure modelling capability within compartment models, addressed in this framework (section 3.3 Compartment closure models). The individual chemical species

are transported at a molar rate equivalent to their molar concentration within the source compartment volume V_k.

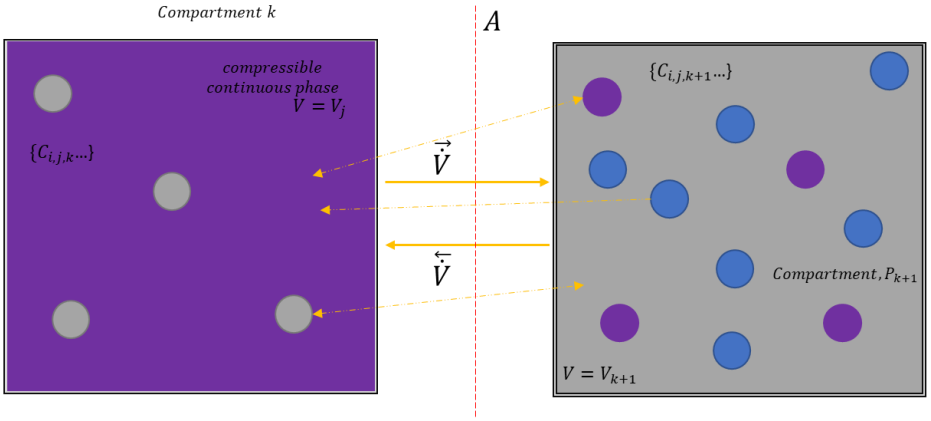

Figure 31 – convective transport of phase material and the species at a rate equivalent to the species molar fraction within the source compartment; convective transport as illustrated here through he changes in purple phase from continuum to dispersed phase and vice versa, accounts for change in continuum.

Caveat If a compressible phase is transported to a compartment of a different compressible phase continuum, it cannot form a surface and thus addition would result in merging of the compressible phases – see Figure 32.- as introduced in section 3.2.3.1 Continuum-dispersion composition. Unlike phase transport, where flow in the reverse direction is not possible in such a scenario, the continuous compressible phase can be transported to its own dispersed phase within the connected compartment. If both compartments are compressible phase continuous then both continuums exchange chemical species with one another.

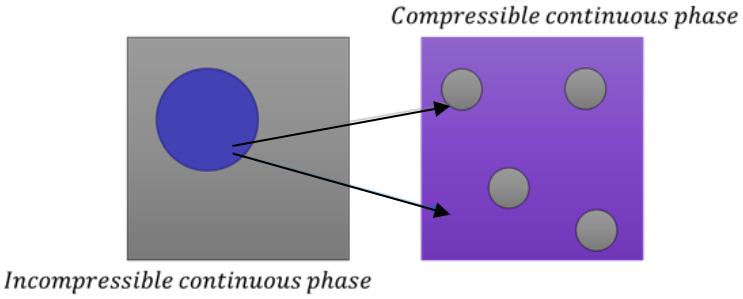

Figure 32 – Convective transport; example of compressible phase merging due to restriction on formation of compressible-compressible dispersions.

In the example of the merging phase behaviour (Figure 32), a (grey) incompressible phase is continuous in the left-hand compartment with the (blue) compressible phase dispersed within it. This material is transported to the second compartment of (purple) compressible phase as its continuum, with the (grey) incompressible phase dispersed within it. The compressible phase transported cannot join its own phase in the second compartment as it cannot form a surface to exist independent of the compressible continuum, thus results in the merging of the compressible phases (blue & purple). Unlike phase transport, reversed flow through a second convective transport definition is possible in this scenario as the compressible continuum phase can be transported to its own dispersed phase in the adjacent compartment.

3.5.1.6 The molar transport rates

The molar flowrate of a chemical species (Equation 69), $\dot{n}$, is the product of the molar chemical species molar flux, $\Phi\left(\frac{mol}{m^2 s}\right)$, interfacial area of contact between the discrete volumes of the material transport A, the activation sigmoid switch, $\Theta_{O/I}$, and a second sigmoid switch for control of material transport as a function of time Θ_{t}.

$$\dot{n} = \Phi A \Theta_{O/I} \Theta_{\mathrm{t}} (\mathrm{mol.\,s^{-1}}) \qquad \text{Equation 69}$$

The area of transport can be used to model the splitting of flow from a compartment. The procedure is to set the area of all outflows, of similar nature, from a compartment to sum to unity $1m^3$. The individual areas of transport are then equivalent to the split fraction of the flow.

Timed addition of reagents and material to a system/unit are typical in industrial applications. The behaviour and response of systems to these initial scenarios are not catalogued with compartment modelling, except in the case of (Öner *et al.*, 2019) in the modelling of a filled vessel using time activated convective flows.

Here we introduce an approach to model the timed addition of material to a compartment system, which is also extended to use with all phenomena (section 4.3.1). The velocity at the time t_i is applied to the material transport,

which determines the velocity of flow at specific simulation times; this phenomenon is still subject to deactivation if a driving force is not present reducing the velocity to zero.

The timed valve sigmoid (Equation 70) Θ_{t} is a function of the simulation time t, it activates and deactivates a flow from a set of time values $[t_i, t_{i+1} \dots]$ and state values $[\emptyset_{t_i}, \emptyset_{t_{i+1}}, \dots]$ of the same length; where 0 is a deactivated flow and 1 is an activated flow. φ is the stiffness constant which determines the accuracy of activation and deactivation of flows with regards to the time domain. This is useful for the definition of pulse and stepwise flows in the study of RTD's of unit operations, a common use of compartment modelling.

$$\Theta_{\mathrm{t}}(t) = \frac{\emptyset_{t_0}}{1 + e^{-\varphi(\mathrm{t}-t_0)}} + \sum_i \frac{\emptyset_{t_i} - \emptyset_{\mathrm{t_{i-1}}}}{1 + e^{-\varphi(\mathrm{t}-\mathrm{t_i})}} \qquad \text{Equation 70}$$

The molar flux (Equation 71), molar flow rate per area of transport, of a chemical species transported via phase transport or convective transport is the product of the chemical species concentration C (Equation 72) in the flow source volume V and a rate variable κ, both are dependent on the nature of material transport.

$$\Phi = \kappa \mathrm{C}(\mathrm{mol.\,s^{-1}.\,m^{-2}}) \qquad \text{Equation 71}$$

$$C = n/V \qquad \text{Equation 72}$$

The source volume for convective transport, phase transport and mass transfer are respectively, the source compartment volume, source phase volume and source phase volume.

The material velocity, $\kappa(\frac{m}{s})$, of both phase transport and convective flow for transport of material from a source compartment, subscript k, to a termination compartment, subscript $k+1$, are given in Table 8. The main parameters of κ, for the respective 'nature of transports', are utilised by the sigmoid activation function; the activation variables ($\boldsymbol{\Delta X}$) are given alongside in Table 8. Unlike the other transport phenomena, the activation sigmoid for phase transport is equal to unity $\Theta_{O/I} = 1$. This is because there is no difference in variable

values to propagate flow and thus no back flow possible. If no material is present, no phase transportation occurs.

Table 8 – Driving force $(\Delta \mathbf{X})$ and formula for the automatic velocity $(\boldsymbol{\kappa})$ of phase transport and convective transport phenomena.

	$\Delta \mathbf{X}$	$\boldsymbol{\kappa}$
Phase transport	1	$\frac{V_j}{A\tau_j}$
Convective flow	$(P_k - P_{k+1}) + \Delta P_{pump}$	$\frac{\Delta \mathrm{X}}{\tau_{flow}}$

Phase transport is driven by the volumetric concentration of phase material in the source compartment and a phase residence time, $\tau_j(seconds)$The residence time is defined as the volume of phase divided by the rate of removal of phase volume.

Convective transport is driven by the pressure difference between adjacently connected compartments with a special pressure delta introduced $\Delta P_{pump} = 0(default)$. This parameter generalises the flow to allow the modelling of mechanically driven flow and known system pressure drops, e.g., respectively, mechanically induced convection of material and pressure drops due to friction in a system. A time constant $\tau_{flow}\left(\frac{m.seconds}{Pa}\right)$ determines the response time of the system to pressure differences and is required as no momentum balances are solved in compartment modelling.

Both tau constants are deemed stiffness constants of the model.

The velocity of material can be set, as opposed to deriving the value through the equations in Table 8; where this approach is taken, the values are typically derived from CFD or experiment. If it is desired to set the volumetric flow rate, (m^3/s) of a material transport, the area of transport must be taken into consideration as it is the product of velocity and area that gives the volumetric flow of a transport.

The molar flux of mass transfer (Equation 73) differs to that of phase transport/convective transport. It is instead a function of the overall mass transfer constant κ and the difference in chemical species concentration of the two connected volumes, ΔC. The definitions for $\boldsymbol{\Delta C}$ and $\boldsymbol{\kappa}$ of Equation 73 are given in Table 9; the subscript So refers to the source volume, and the subscript T refers to the termination volume. The first row presents the definitions for transfer of chemical species from the source phase to the termination phase volume.

$$\Phi = \kappa \Delta \mathrm{C}(\mathrm{mol.\,s^{-1}.\,m^{-2}}) \qquad \text{Equation 73}$$

Table 9 – Concentration gradient $(\boldsymbol{\Delta C_i})$ and formula for the overall mass transfer coefficient $(\boldsymbol{\kappa})$ of the mass transfer phenomenon based on the liquid and gas side mass transfer coefficients.

Mass transfer basis	Mass Transfer concentration gradient, $\boldsymbol{\Delta C}$	Material velocity as the overall mass transfer coefficient, $\boldsymbol{\kappa}$
Transfer from source phase to target phase, $\Phi_{So \to T}$	$C_{i,So} - C_{i,T}S$	$\kappa = \dfrac{1}{\dfrac{S}{k_T} + \dfrac{1}{k_{So}}}$

The partition coefficient (S) typically used when referring to gas-liquid mass transfer is the Henrys coefficient which requires conversion to a dimensionless partition coefficient pre-use with the concentration-based mass transfer theory of this work. E.g., for a Henrys constant relating pressure to concentration at the interface $P = HC$, the dimensionless coefficient used within this theory is calculated as the Henrys constant divided by the ideal gas constant and temperature of operation – this is to be calculated prior to use, see example in Equation 74.

$$S = \frac{H\left(\frac{m^3 Pa}{mol}\right)}{RT}$$ Equation 74

The Henrys coefficient may be a function of temperature in a system with developing range of temperatures, however the change in value is typically not large over the operating range of a system modelled using the compartment modelling approach.

The activation of a mass transfer flow is a function of the transfer concentration gradient of the flow; $\boldsymbol{\Delta X = \Delta C_i}$, as given in Table 9, with the concentration volume based upon the phase volume. k_{So} and k_T are respectively the source and termination phase mass transfer coefficients.

The change in molar quantity of a chemical species in both the source and termination volume of a material transport is equal, conserving mass e.g., as given by Equation 75 for mass transfer.

$$\frac{dn_{i,So}}{dt} = \Phi_{So \to T}; \quad \frac{dn_{i,T}}{dt} = -\frac{dn_{i,So}}{dt}$$ Equation 75

3.5.2 Heat Transport

3.5.2.1 Convective

Two enthalpy changes are associated with a transport, (i) the enthalpy transported with the mass which is at the temperature of the source volume – affecting both compartment volume enthalpies equally in quantity and opposite in sign $\Delta Q_k = -\Delta Q_{k+1}$ and, (ii) the enthalpy of transport which is the associated loss/gain of enthalpy due to solution change, affecting only the source compartment enthalpy, Q_k. Any change in source temperature due to enthalpy change of transport is then reflected in the enthalpy transported with the mass (point (i)). In an ideal solution the enthalpy associated with the dissolution of a solute, ΔH_{trp}, within a solvent is null.

The total transport enthalpy change due to material transport is then the sum of enthalpy of transport ΔH_{trp}, and enthalpy transfer associated with the mass transfer and convective transport phenomena, as given in Equation 76.

$$\frac{dQ_k}{dt} = \dot{Q}_k = -T_k \sum_j Cp_j \sum_i \dot{m}_{j,k} + \dot{n}_i(-\Delta H_{trp}) \quad \text{Equation 76}$$

$$w\because m_{j,k} = Mw_i \dot{n}_i$$

The change in enthalpy of the adjacent compartment is the negative of the above without the effect of the transport enthalpy, Equation 77.

$$\dot{Q}_{k+1} = -\dot{Q}_k - \dot{n}_i(-\Delta H_{trp}) \quad \text{Equation 77}$$

For intra-compartmental mass transfer, mass is transferred internally between the phases of a single compartment. Hence, the change in enthalpy of the compartment is a reduced function– solely accounting for enthalpy change due to the transport/change of solution.

$$\dot{Q}_k = \dot{n}_i \Delta H_{trp} \quad \text{Equation 78}$$

3.5.2.2 Conductive

Modelled like intra-compartmental mass transfer, but reduced to not include material transport, heat is transferred between two compartments of temperatures $T_k(K)$ and $T_{k+1}(K)$, through the connecting area of the compartment volumes, $A(m^2)$. The difference in temperature between compartments is the driving force and activation variable for heat transfer, with the direction of heat transfer being from the high to low temperature compartment; activation of the appropriate flow is determined by the sigmoid function $\Theta_{\mathrm{I/O}} = f(\Delta T)$ with the activation variable being the temperature of the connected phases. The overall heat transfer coefficient applied here to any compartment in contact with another exhibiting inter-compartmental heat transport, $U_o\left(\frac{J}{Km^2s}\right)$, controls the relationship of heat transfer rate to compartment temperature difference ΔT.

The heat transfer rate $\dot{Q}(J/s)$ of a one directional heat flow from compartment k to compartment $k+1$ is given by Equation 79.

$$\dot{Q} = \Theta_{\mathrm{t}} \Theta_{\mathrm{I/O}} A U_o \Delta T \quad \text{Equation 79}$$

The differential associated with the change in enthalpy of compartment k is given below for a heat transfer from compartment k+1 to k: Equation 80.

$$\frac{dQ_k}{dt} = \dot{Q}_{k+1\to k} = Ak\Delta T\Theta_{\mathrm{k+1\to k}} \quad \text{Equation 80}$$

$$where: \Delta T = T_{k+1} - T_k \quad \text{Equation 81}$$

Maintaining an energy balance in the system, the change in enthalpy of the compartment $k+1$ is given in Equation 82.

$$\frac{dQ_{k+1}}{dt} = -\frac{dQ_k}{dt} \quad \text{Equation 82}$$

In line with the definition of a surrounding, if the heat source or sink is a surrounding, the enthalpy of the surrounding would not change, $\frac{dQ}{dt} = 0$. The timed sigmoid can be used to model timed heat transfer within a compartment model; its primary use is for modelling isothermal systems.

3.5.3 Reactive Transformation

Chemical reaction is the consumption and production of chemical species, taking place within a compartment. Either (a) **Homogenous**: the reaction takes place within a single-phase volume between the reactants of said phase or, (b) **Heterogenous**: reaction of chemical species at the interfacial surface between two contacting phases (continuous and a dispersed).

3.5.3.1 Stoichiometry of reaction and molar rate

A universal reaction involving four components is given in Equation 83 of reactants A and B of stoichiometric coefficients υ_a and υ_b respectively, and products C and D of stochiometric coefficients υ_c and υ_d respectively; the rate equation is given in Equation 84.

$$\upsilon_a A + \upsilon_b B \to \upsilon_c C + \upsilon_d D \quad \text{Equation 83}$$

The stoichiometric change in moles of each chemical species per the stoichiometry of Equation 83 is given in Equation 84.

$$r_{rxn} = -\frac{1}{Z}\frac{1}{\upsilon_a}\frac{dn_A}{dt} = -\frac{1}{Z}\frac{1}{\upsilon_b}\frac{dn_B}{dt} = \frac{1}{Z}\frac{1}{\upsilon_c}\frac{dn_C}{dt} = \frac{1}{Z}\frac{1}{\upsilon_d}\frac{dn_D}{dt} \quad \text{Equation 84}$$

For a dispersion-continuum reaction the basis of the reaction is the volume of the dispersed phase, $Z = V_{dispersed}$, and for a homogenous reaction the basis of the reaction is reacting per phase volume, $Z = V_j$. Products of differing phases are teleported to their respective phases, the mass transfer associated with transport is assumed described within the reaction rate phenomena.

The change in moles of a species is then the product of the reaction basis Z, reaction rate r_{rxn} and species stoichiometry, timed activation as introduced in section 3.5.1.6 The molar transport rates and sigmoid activation as per section 3.5.1.1 The mode of transport e.g., for species B;

$$\frac{dn_B}{dt} = r_{rxn} Z \upsilon_b \Theta_{\mathrm{t}} \Theta_{\mathrm{I/O}} \quad \text{Equation 85}$$

When dealing with low concentrations of chemical species, of which are involved in the reaction rate equation r_{rxn}, encountering negative concentrations is a possibility due to numerical solver overstep of the point at which the concentrations reach 0. Especially prone to occurrence where the molar rate of reaction is much higher than the moles of reactants present. Negative concentrations cause a change in the direction of the rate when instead the reaction should no longer proceed. To address this issue a means to stop reaction proceeding where one or more reactants of the rate equation approach a value of $\rightarrow 0$, must be implemented. Investigation into approaches to address this issue is performed in section 4.6.4 Bounding solution variables to the positive domain.

The driving force of reaction is the difference between the smallest molar value of the reactants of the reaction and a stiffness constant τ_{rxn}; as given in Equation 86.

$$n_{min} = \max\left(\min\left(n_{reactants}\right), \tau_{\mathrm{rxn}}\right) \quad \text{Equation 86}$$

The stiffness constant, τ_{rxn}, represents the molar value at which any reactant falls below, the reaction rate is zero.

The reaction rate, Equation 87, is a function of the rate constant k and the concentration of reactive and non-reactive (e.g., catalysts) chemical species, C_i. The concentration of chemical species is per the phase volume they inhabit. The reaction rate, r_{rxn}, is a production term and so is always greater than zero.

$$r_{rxn} = f(k, C_i \dots) \qquad \text{Equation 87}$$

The temperature dependency of the reaction rate constant k is described through the Arrhenius equation, where $k_{T_{ref}}$ is the specific reaction rate at temperature $T_{ref} = 298K(default)$, $Ea\left(\frac{J}{mol}\right) = 0(default)$ is the activation energy for the reaction, R is the ideal gas constant detailed above and T_k is the temperature of the compartment as the reaction proceeds.

$$k = k_{T_{ref}} exp^{-\frac{Ea}{R}\left(\frac{1}{T_k}-\frac{1}{T_{ref}}\right)} \qquad \text{Equation 88}$$

The reparametrized formula of Schwaab and Pinto (2007) is implemented instead of the traditional Arrhenius equation as this form provides an improved approach to frequency factor (k_0) and activation energy (Ea) parameter estimations.

3.5.3.2 Reaction enthalpy change

The change in enthalpy of the reaction compartment k, due to reaction is given by the constant value enthalpy of reaction $\Delta H_{rxn}\left(\frac{J}{mole}\right)$. Negative enthalpy indicates an exothermic reaction, whereby heat is released to the compartment to increase the temperature, and a positive enthalpy is the absorption of enthalpy into product formation reducing the enthalpy of the compartment and thus temperature.

$$\frac{dQ_k}{dt} = -\Delta H_{rxn} r_{rxn} Z \Theta_{\mathrm{t}} \Theta_{\mathrm{I/O}} \qquad \text{Equation 89}$$

The reaction enthalpy ΔH_{rxn} can be calculated from the sum of sensible energy of the products and their standard formation enthalpies subtracted

those of the reactants; $\Delta H_{f,i}^{\circ}$ from S.T.P $298K$, and stoichiometry of the partaking chemical species, υ_i; as given in Equation 90.

$$\Delta H_{rxn} = \left(T_k M_{j,products} Cp_{j,products} + \sum_{Products} |\upsilon_i| \Delta H_{f,i}^{\circ}\right) - \left(T_k M_{j,reactants} Cp_{j,reactants} + \sum_{reactants} |\upsilon_i| \Delta H_{f,i}^{\circ}\right) \quad \text{Equation 90}$$

For the example reaction scheme given of Equation 83, the change in enthalpy of the reaction compartment per mole is given by Equation 91.

$$\Delta H_{rxn} = (T_k M_{j,products} Cp_{j,products} + |\upsilon_c| \Delta H_{f,c}^{\circ} + |\upsilon_d| \Delta H_{f,d}^{\circ}) - (T_k M_{j,reactants} Cp_{j,reactants} + |\upsilon_a| \Delta H_{f,a}^{\circ} + |\upsilon_b| \Delta H_{f,b}^{\circ}) \quad \text{Equation 91}$$

As the enthalpy of formation and stoichiometry are constants in the system, the enthalpy of reaction is given as a constant value. However, it is important the modeller of the model gives the correct enthalpy of reaction to account for changes in specific heats where a reaction involves more than one phase reacting or products of a different phase to that of the reactants. Alternatively, the modeller could set all specific heats to be identical in the system, the approach typically taken in multi-phasic systems for simplicity in implementation.

3.6 Chapter Summary

A universal compartment modelling approach is developed in this chapter, the compartment is conceptualised as a fixed volume filled with one or more phase(s) which have a volume related to the nature of the phase (incompressible, compressible), an alternative to the assumed *solvent* modelling typically performed in literature. The concept of a phantom phase ensures the phase volumes always sum to that of the compartment, and the

concept of a phantom species ensures no phase reaches zero volume – a key concept where nucleation of phase material or concentrations are referred to within a model as otherwise a Div!0 error would result.

The representative phasic volumes in conjunction with the fixed volume of a compartment allow for the introduction of a pressure variable. Two closure-models are developed to describe the pressure within a compartment (a novelty in the topic of chemical process compartment modelling), both functional of phasic (and in effect species, of which each phase can be formed of many) contents of the compartment. The pressure of a compartment is primarily calculated using an EOS, the free volume not occupied by incompressible (liquid, solid) material and moles of compressible species give the pressure of the compartment. With an incompressible factor, equal to 1 multiplied by this value. The factor increases beyond 1 where the compartment is overfilled with incompressible material; due to incompressible material densities being slight relaxed (hence the name relaxed-density closure model). An earlier developed closure model, the variable volume, based on a maximum set compartment pressure is described but discarded from the universal theory in place of the relaxed-density closure model as it could not be used with the container theory.

The container is introduced here to model the change in volume of compartments within a model; whilst maintain the sum of compartments to that of the vessel volume. This novel approach to dynamic volume addresses the attempts to model changing compartment volumes observed in literature (section 2.3.3), whilst also extending compartment modelling applications to systems where pressure influences the change in continuum volumes in a vessel e.g., the change in headspace and liquor volume of a vessel.

To address the need for the change in area due to density in dispersive phase in a sub volume of a process, a model for dynamic area calculation as a function of dispersed volume, assuming spherical shape, is included in the model (section 3.2.3.1 Continuum-dispersion composition of a compartment). This is integrated with the modelling of Intracompartmental mass transfer and

not considered in literature when modelling mass transfer between dispersed and continuous phases, instead assuming fixed interfacial areas.

Surroundings is another concept introduced in this chapter, a type of compartment where species and enthalpy are of fixed values throughout the simulations. Built into the theory from the constant equilibrium concentrations observed in mass transfer and continuous fixed source flows to models of infinite material.

The variable compartment pressure, a novel entry in the compartment modelling, is utilised here as a natural driving force for material transport. Addressing the tedium of setting multiple flowrates of compartment systems. Instead, the area between systems can be defined for each transport as a “splitting of the flow”. The resultant flowrates in the network are then a function of inlet outlet flowrate, if fixed, or of surrounding and sink pressures.

The most prevalent phenomena of literature are also defined within the framework; these are in order of appearance, (i) Mass Transfer, (ii) Phase transport, (iii) convective transport, (vi) heat transport and (v) reaction.

Chapter 4 Implementation of CompArt

4.1 Introduction

Following the developed theory of a universal compartment model, as outlined in Chapter 3, this chapter presents the implementation of said theory, named "CompArt" in a python environment. CompArt is developed to address the lack of universal modelling tool for the compartment modelling of unit operations as identified in literature review of Chapter 2. Python is chosen as it is a general-purpose programming language with an open-source community driven library of modules; of specific interest are the available numerical solver libraries required in the solution of compartment models. The alternative programming language MATLAB, used in ~50% of research papers conducting compartment modelling studies (Appendix A), was considered but due to being non-open-source and lacking the ability to integrate with other languages which host a larger library of numerical solvers (e.g., DiffEqPy of Julia) - python was instead chosen as the superior option. The Subsequent chapter (Chapter 5) will use the implementation of the theory, here out referred to as "CompArt", to construct and solve compartment model case studies for validation.

The CompArt process is depicted in Figure 33 from model description to solution. The language, which is Initially developed using Python syntax is upgraded to a novel text-based input language which replaces the indecipherable API of python to allow for model description in an easily communicated format. The model description is parsed and converted into (i) a python data structure with the initial variable values (y_0) and, (ii) a function $f()$ which returns the differential vector of the model (Equation 92).

$$dy(t)/_{dt} = f(y_0) \qquad \textit{Equation 92}$$

A pictorial language for design and distribution of compartment models between discipline is used throughout this work, the pictorial representations link to the high-level input language; structural terms (e.g., container,

compartment, phase) and phenomenological terms (e.g., convective transport, phase transport, mass transfer) of the language - each have a specified symbol/shape as detailed in the illustration guide of Appendix C.

Following model parsing into the data structure, any missing property values in the data structure not defined in the model description are set to their defaults, as declared in Table 12. The Data structure is then tested iteratively and extended to ensure inclusion of all species and phases in the relevant compartments (as determined by the nature of phenomena and flows in and between compartments and phases).

The solution of the ODE uses external ODE solvers, several of which are included in the python package SciPy or wrapped from external languages such as the package DiffEqPy from Julia. The solution Matrix ($y\ vs\ t$) is exported to excel, where each variable is tabled for all solution times, and a plot is automatically generated.

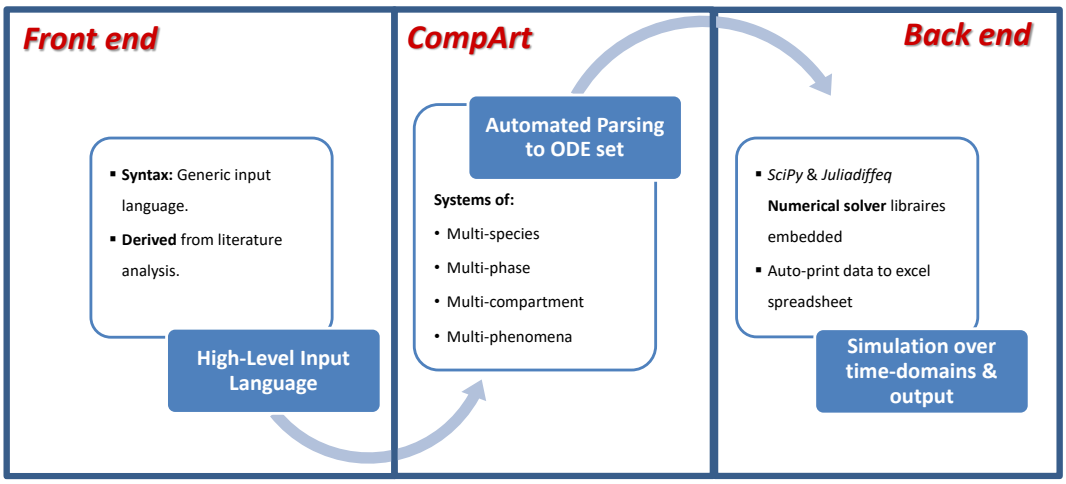

Figure 33 – CompArt stages, from model description to model solution.

The repository of *CompArt* can be requested at.

https://github.com/GrandadsJumper/UniversalCompartmentModelling.

4.2 Definition of the input syntax

The language of CompArt is designed to specify a broad range of compartment models in an efficient manner. From the work conducted in Chapter 2, it is found that a compartment model is described and defined by:

(i) Volumes of containers and compartments, and flow rates between compartments as well as conditions such as temperature and pressure.

(ii) The phase's present within each of the compartments and their nature $(incompressible/compressible)$ and the associated characteristic diameters and densities of said phases

(iii) The composition of the phases; the molar quantities of species and the species molecular weight values.

(vi) Phenomena taking place within and between the various phases.

(v) Model parameter defaults, stiffness constants and solution algorithm options.

The above points are captured in the input language of CompArt, the resultant language is developed from observed language in literature and so forms a natural intuitive approach for the definition of compartment models. The form of the input is literary, sentence-wise per structural or phenomenological input to make description an ease for new users of the implementation – whilst maintaining the necessary complexity to describe a universal range of compartment models.

In the early-stage development of CompArt, the syntax was in essence a python command file, accessing the base classes of the code (API) to generate model objects (Table 10). As an example, to describe a volume of water "H2O" of phase "aqueous" within a tank named "tank 1", one would require the generation of the compartment object $Compartment\_1$, a phase object $Phase\_1$ and a species object $Chemicalspecies$. As well as the specification of relevant object properties, e.g., the volume of tank, moles of a specie, and the location of the species within the phase, and the phase within the compartment through reference to the object reference ID's.

Table 10 – Direct python Syntax model description of a Water filled Tank.

```
Compartment_1 = Compartment()

Compartment_1.id = “tank_1”

Compartment_1.volume = 10

Compartment_1.temperature = 500

Compartment_1.continous_phase = Phase_1

Phase_1 = IncompressiblePhase()

Phase_1.id = “aqueous”

Phase_1. density = 1000

Phase_1.compartment_id = Compartment_1

Chemicalspecies = ChemicalSpecies()

Chemicalspecies.id = “H2O”

Chemicalspecies.mw = 0.018

Chemicalspecies.n = 400

Chemicalspecies.phase_id = Phase_1

Chemicalspecies.compartment_id = Compartment_1
```

The description of a compartment model through the base classes of python is cumbersome. Setting object references as other object properties quickly lead to a web of references – even in this simple one compartment, of no phenomena, the python syntax is indecipherable (Table 10).

For greater clarity and ease when forming and reviewing model descriptions, an intuitive higher-level language is developed. The input syntax terms used are mapped from the language used to describe the model structure (Species, phases, compartments, containers) and phenomena (Mass transfer, reaction, heat transfer, phase transport) in the theory chapter (Chapter 3). The improved syntax allows complete definition of a compartment model in a natural way. The python syntax description example of Table 10 is repeated in Table 11, using this high-level input language.

N.B. Text following a vertical bar "|" is treated as a comment, providing further information on units of the properties and description of the code in the line.

Table 11 – High-level input language description of a Water filled Tank.

```
DefineComponents
   H2O : 0.018 | species id : molecular weight (kg/mole)

Compartment tank_1 of continuous phase phase_1
   volume : 10 |m^3
   temperature : 500 |Kelvin
   IncompressiblePhase phase_1 to tank_1
      H2O : 400 | species id : moles
      density : 1000 |kg/m^3
```

Model terms are defined in a single line sentence of a set format. The line contains the nature of the item to be defined, its name (reference ID) and associated items (e.g., for Compartment the continuous phase name, Table 11). Additional properties of the model term are set in an indented block below the main statement in the form of $property : value$ pairs (e.g., volume: 10, property definition for compartment of Table 11).

As can be seen by comparing Table 10 to Table 11, the improved syntax is more concise and easier to read. It also removes unnecessary redundancy such as calling a class with a temporary variable as required in the python syntax, example from Table 10: Phase_1 = *IncompressiblePhase*().

There is clear advantage of an elevated domain language which permits modellers focus upon the conception of the compartment model, as opposed to drawing attention away and towards tackling the difficulties associated with implementation.

4.3 CompArt High-level input language

An integral part of this chapter is, for greater clarity and ease when describing models, the development of an intuitive higher-level language (Table 12) built upon the python syntax-based interface of CompArt (Table 13).

The input language defines model terms using sentences with keywords and values. For instance, referring to Table 11,

Compartment *tank_1* **of continuous phase** *phase_1*

Defines *tank_1* as a compartment which contains a continuous phase of name, *phase_1*.

Subsequent statements, of the $property : value$ pair form, set the compartment's **Volume** and **Temperature.**

Behind the scenes, CompArt converts each keyword sentence in to objects in the model data structure, or sets the value of an objects property. The API underpinning this is described in more detail in section 4.4 CompArt API.

A full description of the high-level language is presented in Table 12. The following notation is used to describe the statements of Table 12:

Input **language statements** are printed in Bold. The language statements (bold keywords) are unique and cannot be used in other property or statement values/names. Obligatory properties embedded in the model term line are given in normal text. e.g., **Compartment** tank_1.

Input language *Property names* are given in italics and user provided values are given in normal text, e.g., *property* : default. Optional statements are enclosed in square brackets e.g., [*property* : default].

Property values must be of one of the five data types, with each property accepting only one of these data types as its value.

1. A string consisting of a combination of any uppercase and lowercase letters (A-Z, a-z), digits (0-9), and underscore characters (_): “$MeOH$”

2. A float or integer: $10.002\ or\ 98$

3. A Boolean: $True\ or\ False$

4. A list of strings: [“$MeOH$”,“$N2$”]

5. A list of integers, floats, or mixture of the two: $[2, 0.03, 124.2]$

The reference ID is a string property common to all classes. Each declared instance, aside from phases of the same nature (incompressible/compressible) and species, must be of a unique reference ID. E.g., Upon defining **IncompressiblePhase** of reference ID “Phase_1”, the reference ID could not then be used to define a **Compressible** phase of reference ID “Phase_1” but could be used to define the same phase within another compartment. As with chemical species, the same reference id can be used to specify the species within another phase in multiple phases of the same compartment and others, but only once per phase instance.

In addition to the language of Table 12 & Table 13, the properties related to time activated phenomena are discussed in more detail separately in section (section 4.3.1), as the properties of timed activation apply to all phenomena (convective transport, phase transport, heat transfer, reaction & mass transfer) and is more convenient to discuss separately.

In addition to model definition, the input language also allows the specification of the solver type and properties of the solver, and the associated stiffness constants. Further discussion upon the solution of the models within CompArt is given in section 4.6 Solution methods & data output.

Table 12 - CompArt Higher level input language statements and descriptive examples

Class object(s)	Statement	Description
Solver	**Solver** numerical_solver *[t_start : 0]* *[t_final : 100]* *[max_step_size : 10**3]* *[atol : 10**-6]* *[rtol : 10**-6]* **Example:** **Solver** BDF *t_final* : 600 *atol* : 10**-10	The numerical solver, here BDF (other options, not limited to, include LSODA and RADAU) – see https://docs.scipy.org/doc/scipy/reference/generated/scipy.integrate.solve_ivp.html. With a start time of 0 seconds to an end time of 600 seconds. Modification to the absolute tolerance of the solver, *atol*, to a value of 10^{-10}. More details are given in the solution section of this chapter.
Chemical Species	**DefineComponents** *[chemical_species_reference_id : value]* ***Example:***	The molecular weight of chemical species in the model can be defined here for each occurring species in the system. Without this

Class object(s)	Statement	Description
	DefineComponents *H2O : 0.018 |kg/mole* *CO2 : 0.044 |kg/mole*	class object, the molecular weight would need to be given every time a species is added to the system. The example shows the definition of the molecular weight of species H2O and CO2 as 0.018 and 0.044 kg/mole respectively.
GlobalDefaults	**Defaults** *[model_name : “”]* *[container_tau : 0.000001]* *[epsilon : 2]* *[flow_tau : 0.01]* *[Mw_p :0.001]* **Example:** **Defaults** *model_name* : model_2 *flow_tau* : 10**3	properties and values set in the default class are set globally if the property is not defined locally with the model component call. container_tau is defined in the Container row; epsilon is defined in the compartment row and flow_tau is defined in the convective transport row.

Class object(s)	Statement	Description
IncompressiblePhase **&** **ChemicalSpecies**	**IncompressiblePhase** id **to** compartment_id [*char_diameter* : 0.001]|metres [*heat_capacity* : 4200]|J/kg.K [*density* : 900]|kg/m3 [*Chemical_species_id* : n]|moles …[*Chemical_species_id* : n]|moles **Example:** **IncompressiblePhase** aqueous **to** tank_1 *density* : 900 | kg/m3 *A* : 2000 |moles *B* : 80.9 |moles	Adds an in-compressible phase of ID aqueous, to compartment of ID tank_1. The chemical species object is called within phases; here 2000 moles of species ID A and 80.9 moles of species ID B are added to the aqueous phase. A phase generated within a system which propagates phase material between compartments (e.., convective flow) will be automatically generated in the data structure as present in those compartments (see section 4.5 Linkage & population of model components in the python data-structure) Multiple **chemicalspecies** can be added under a phase declaration, as shown in the example for the addition of both species A and B.
CompressiblePhase & **ChemicalSpecies**	**CompressiblePhase** id **to** compartment_id *[char_diameter : 0.001]* |*metres* *[heat_capacity : 1000]* |*J/kgK*	Adds a compressible phase of ID gas_1, of heat capacity 1300J/kgK to compartment of ID tank_1. The chemical species class object is called within phases; here 200moles of species ID

Class object(s)	Statement	Description
	[Chemical_species_id : n] |*moles* …[*Chemical_species_id* : n] **Example:** **CompressiblePhase** gas_1 **to** tank_1 *Heat_capacity* : 1300 |J/kg.K *H2O* : 200 |moles *Ethanol* : 10 |moles	H2O and 10 moles of species ID Ethanol are added to the gas_1 phase. A phase generated within a system which propagates phase material between compartments (e.., convective flow) will be automatically generated in the data structure as present in those compartments (see section 4.5 Linkage & population of model components in the python data-structure) Multiple **chemicalspecies** can be added under a phase declaration, as shown in the example for the addition of both species' H2O and Ethanol.
Compartment	**Compartment** compartment_id **of continuous phase** continuous_phase *[volume :* 1] |m3 *[temperature* : 298]|Kelvin *[epsilon : 2]*	Generates a compartment of ID tank_1 with continuous phase of ID aqueous; and phantom compressible phase with phantom species moles (section 3.2.2.2 Phantom phase).The compartments default minimum and maximum compressible pressures are respectively 1Pa and 101325Pa; this refers to the operating range of the compartments pressure, beyond the P_max value indicates the relaxation of incompressible phase material.

Class object(s)	Statement	Description
	[p_min : 1] |Pascals *[p_max :* 101325*]* |Pascals **Example:** **Compartment** tank_1 **of continuous phase** aqueous	Epsilon is the stiffness constant relating the impact of incompressible phase density relaxation upon the compartment pressure. The value ranges from $1 \rightarrow$, it is multiplied by the compressible pressure of the compartment determined to be of a maximum value P_max.
Surrounding	**Surrounding** surrounding_id **of continuous** **phase** continuous_phase *[volume : 1]* *[pressure : f(contents)]* *[temperature : 298]* *[epsilon : 2]* **Example:** **Surrounding** source_1 **of continuous phase** aqueous	Same procedure as Compartment above. e.g., Generates a reservoir named source_1 with continuous phase of ID aqueous, and phantom compressible phase with phantom species moles. In addition to the procedure of a compartment, in a surrounding definition the pressure of a surroundings can be set, inducing automatic modifies the phantom material to set the pressure of the surroundings.

Class object(s)	Statement	Description
Container	**Container** id **encapsulating compartments** [t1][t2]… *[volume : 10] |m3* *[container_tau : 0.01]* **Example:** **Container** cont_1 **encapsulating compartments** tank_1 tank_2 tank_3	Generates a container of ID cont_1, which contains the volumes of compartments tank_1, tank_2 and tank_3 to the container volume, which is default = $10m^3$. Any number of compartments can be added to a container, the reference ids of the encapsulated compartments must be listed separated by a space. $V_l = V_1 + V_2 + V_3$
ConvectiveTransport	**ConvectiveTransport** id **from** source_compartment **to** termination_compartment *[pump_pressure* : 0] |Pascals *[flow_tau* : 0.01] *[transport_enthalpy* : 0] |Joules/mole *[area* : 1] |m2 *[velocity* : f(ΔP)] |m/s	Generates a convective transport, id of trans_1, from compartment tank_1 to compartment tank_2. If velocity is set, the transport is set at a constant velocity; otherwise, it is a function of the pressure difference of tank_1 and tank_2. $\frac{dn_A}{dt} = velocity \times area \times C_{A_{phase}}$ Or: $\frac{dn_A}{dt} = \frac{\Delta P}{\tau_{flow}} \times area \times C_{A_{phase}}$

Class object(s)	Statement	Description
	[fixed_flow : False] *[sigmoid_error : 2]* *[activation_times*: None] |seconds *[activation_response* : None] **Example:** **ConvectiveTransport** trans_1 **from** tank_1 **to** tank_2 *velocity* : 23.99 | m3/s	Fixed flow, when set to a value of True, removes the requirement of a positive pressure gradient for the activation of a convective flow. Used in conjunction with a set value for the phenomena velocity, a fixed constant flow rate can be set between two compartments independent of driving forces. A common approach to flow modelling in literature.
Reaction	**Reaction** id reaction_mechanism *phase :* *contacting_phase :* *rate_equation :* *[k : 1] |f(rate equation)* *[rxn_enthalpy : 0] |Joules/mole* *[Ea : 5∗ 10^{-4}] |Joules/mole*	Reaction of species A of the aqueous phase with species B of the gas_1 phase to produce species X in the aqueous phase and species Y in the gas_1 phase; at stoichiometric quantities as defined in the *reaction_mechanism* and at a rate equivalent to the rate equation. Where the conditions for the reaction to take place are met within a compartment, the phenomena are applied to the respective compartment and species.

Class object(s)	Statement	Description
	[t_ref : 298]|Kelvin *[activation_times: None]* *[activation_response : None]* *[reaction_tau: 10^{-7}]* *[sigmoid_error: 2]* **Example:** **Reaction** react_1 2A **+** 3[B] **->** 2X **+** 3[Y] *phase* : aqueous *contacting_phase* : gas_1 *k* : 0.01 *rate_equation* : k*A*[B]/ A)	The mechanism species and stoichiometry are captured in one property; the *reaction_mechanism,* which must follow the example format $specie_{id} + \cdots \rightarrow specie_{id} + \cdots$. The number of species is limitless; in the string defining the rate mechanism, brackets must be used to represent species inhabiting the *contacting phase*, and no use of brackets for species within the *phase.* E.g., [A] + 2B -> [C], A in the *contacting phase* reacts with B in the *phase* to produce C in the *contacting phase*. The rate equation follows the same bracket notation for species; except full mathematical symbols can be used in the rate equation [(,), *, /, ^, +. -]. Any properties defined for the reaction, in this example the rate constant *k*, can be referenced in the rate equation. $$\frac{dN_A}{V_j dt} = k\frac{C_A C_B}{C_A}$$

Class object(s)	Statement	Description
Mass transfer **Intra-compartmental**	**MassTransfer** id **of species** species **from** source **to** termination *ks :* *kt:* *[area : 1] |m2* *[transfer_enthalpy : 0] |Joules/mole* *[S : 1]* *[sigmoid_error : 2]* *[activation_times: None]* *[activation_response : None]* **Example:** **MassTransfer** MTR_**1 of species** O2 **from** Aqueous **to** Gaseous *ks* : 0.001 |m/s	Like with reaction, this is a global mechanism where the system is searched for compartments with the Aqueous and Gaseous ID phases in contact. If the source phase, in this example the Aqueous phase has an oxygen species present, the mass transfer of said species to the Gaseous phase is generated. The symbols ks and kt are the mass transfer coefficients of the source and termination phases respectively, S is the partition coefficient which defines the equilibrium concentration ratio of species A at the interface between the two phases: $$S = \frac{[A]_{Aqueous}}{[A]_{Gaseous}}$$ The enthalpy change of the compartment is the product of molar transfer rate, calculated within the tool per time step and fed to the solver as a differential, and transfer enthalpy. $$\frac{dN_{A_{Aqueous}}}{dt} = -K \times \frac{6V_j}{d_{p,j}}([A]_{aqueous,k} - S[A]_{gaseous,k})$$ With $d_{p,j}$ the characteristic size of the dispersed phase, defining the spherical interfacial area of the dispersed phase over which

Class object(s)	Statement	Description
	kt: 0.003 |m/s *area* : 0.045 *transfer_enthalpy* : -200 |Joules/mole S : 2.5	mass transfer takes place, and K the overall mass transfer coefficient based upon the two individual coefficients. $$K = \frac{1}{\frac{S}{k_t} + \frac{1}{k_s}}$$ *sigmoid_error, activation_times, and activation_response are explained in more detail in section* ***Error! Reference source not found.***.
Mass transfer **Inter-compartmental**	**Example:** **MassTransfer** MTR_2 **of species** O2 **from** compartment_1 **to** compartment_2 *ks* : 0.001|m/s *kt:* 0.003 |m/s *area* : 0.045 |m2 *transfer_enthalpy* : -200 |Joules/mole *S* : 2.5	Inter-compartmental mas transfer is not a globally define mechanism, instead it is specific to the two compartments within the definition. This example transfers species O_2 from the continuous phase of compartment_1 to the continuous phase of compartment_2; transfer reaches equilibrium when the $\frac{concentration\ of\ O2\ in\ the\ terminationphase}{concentration\ of\ O2\ in\ the\ source\ phase} = 2.5$ as per the partition coefficient S. With K is given in the example of Intra compartmental mass transfer.

Class object(s)	Statement	Description
		$\frac{dn_{A,j,k}}{dt} = -K \times area \times \left([A]_{aqueous,k} - S[A]_{gaseous,k+1}\right)$ The area of an Inter-compartmental mass transfer is a fixed value set by the user, in the example of value $= \frac{6*0.045}{d_{p,j}}$.
Heat Transfer	**HeatTransfer** id **from** source_compartment **to** termination_compartment *[U :1000] |Joules/s.K.m2* *[area : 1] | m2* *[sigmoid_error : 2]* *[activation_times: None]* *[activation_response : None]* **Example:** **HeatTransfer** HTR_1 **from** Shell **to** tube	Transfer of enthalpy from compartment_1 to compartment_2 at a rate equivalent to the product of temperature gradient $\Delta T = T_{compartment\_2} - T_{compartment\_1}$, heat transmittance U and area of transfer $area$. $\frac{dQ_{shell}}{dt} = U_o \times A \times (T_{Tube} - T_{shell})$

Class object(s)	Statement	Description
Phase Transport	**PhaseTransport** id **of phase** phase_id **from** source_compartment **to** termination_compartment *[transport_tau : 0.01]* *[transport_enthalpy : 0]* |*Joules/mole* *[area : 1]* |*m2* *[velocity : 1]* */m/s* *[sigmoid_error : 2]* *[activation_times: None]* *[activation_response : None]* **Example:** **PhaseTransport** PT_1 of **phase** Aqueous **from** tank1 to tank2	Phase transport, the transport of all species of the following phase at rates relative to their phase concentration, of Aqueous phase from compartment_1 to compartment_2. $$\frac{dn_{A,j}}{dt} = \frac{V_j}{\tau_{transport}} \times [A]_j$$ Where the velocity is given for a phase transport phenomenon, the term $\frac{V_j}{\tau_{transport}}$ is instead replaced with the constant value of the property.

Further high-level input not declared in Table 12 is the language related to timed activation of phenomena, presented here. Transportation and transformation of material throughout a compartment system is controlled by the prevalent phenomenological models. The concept of timed activation was introduced in the theory chapter (section 3.5.1.6 The molar transport rates) whereby the transport and transformation of mass and enthalpy through a system can be halted or allowed to proceed at given time spans within the simulation time. Introduced as a useful mechanism for modelling the behaviour of valve-controlled inlets and outlets. The timed phenomena mechanism is extended to all phenomena of compartment modelling, the language associated with the mechanism is described herein.

A code snippet demonstrating the timed activation in the modelling of a flow filling compartment_2 with species material from compartment_1 is given in Figure 34.

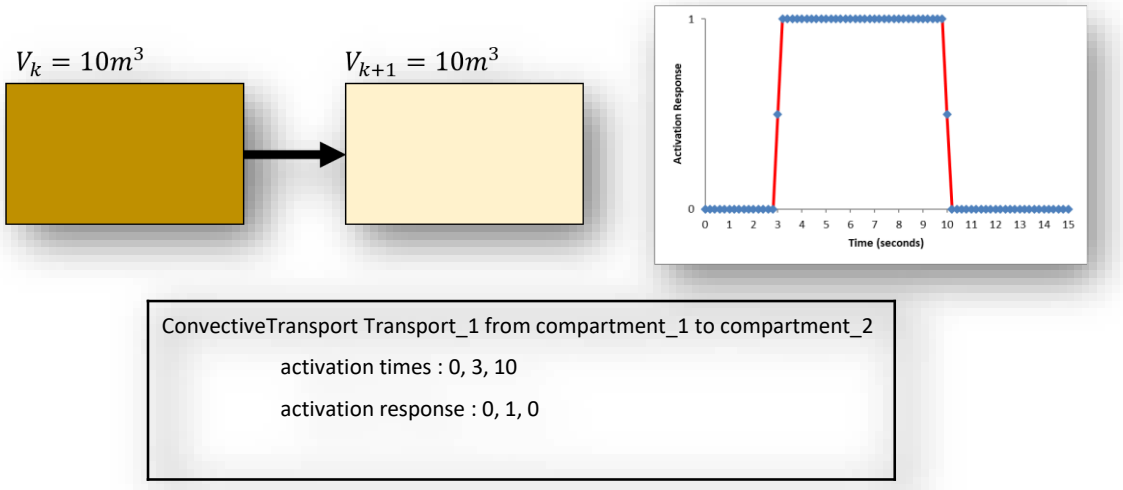

Figure 34 – Timed convective transport of material from comaprtment_1 to compartment _2, illustration, input file and result of timed activation response showing activation two spans of deactivation and a central span of time activated.

In the example of Figure 34 the flow from compartment_1 to compartment_2 is initially deactivated, then activated between the times of $t = 3 \rightarrow 10$ beyond which for the remainder of the simulation the flow is deactivated. Although the timed flow dictates the flow can be active, it still may not result if the driving

force is insufficient, e.g., if the receiver compartment pressure is above that of the source compartment. This can however be overcome by forcing flow without a driving forced, e.g., synonymous with fixed flows of literature, by setting the property $fixed\_flow$ to the Boolean value True.

Three properties define the timed activation of a phenomena, these are

(1) the *activation times,* a lists of n numeric value, separated by commas *e.g., activation times* $t_1, t_2 \ldots, t_n$.If the first declared time is not the initial time of the simulation, for all time before this declared time value t_1, the phenomena is deactivated.

(2) The *activation response***,** a lists of n values separated by commas $(\Theta_1, \Theta_2 \ldots, \Theta_n)$. The rate of the phenomena is multiplied by the activation response, ranging between $0 \leq \Theta_t \leq 1$.

(3) The *timed sigmoid* φ represents the time scale over which the activation response is of a value between 1 (activated) and 0 (deactivated).

The timed activation utilises a sum of sigmoid equations, as given in section 3.5.1.6 The molar transport rates:

$$\Theta_{\mathrm{t}}(t) = \frac{\Theta_{t_0}}{1 + e^{-\varphi(\mathrm{t}-t_0)}} + \sum_i \frac{\Theta_{t_i} - \Theta_{t_{i-1}}}{1 + e^{-\varphi(\mathrm{t}-\mathrm{t_i})}} \qquad \textit{Equation 93}$$

The sharpness of the response to time is determined by the property $timed\_sigmoid$ of default value $\varphi = 50$. This value is set as the default as it is high enough to ensure timed phenomena activate and deactivate over a small enough period around the activation time, and low enough to ensure the system does not become too stiff for the solvers to solve correctly. Lowering φ value may reduce stiffness, or if increased will increase the accuracy of the timed activation.

4.4 CompArt API

The python syntax-based API of CompArt, the basis of the CompArt high-level input language (section 4.3 CompArt High-level input language), is a set of class objects, each class object is a template representing either a structural

(e.g., container, compartment, phase, species) or phenomenological (e.g., reaction, mass transfer, phase transport, convective transport) term of the universal compartment modelling theory.

The theory model terms (e.g., compartment, convective transport, phase, species) are directly mapped to the API, e.g., a compartment and its behaviour, as described in the theory chapter, is completely encapsulated within the Compartment object, along with the properties of a compartment (e.g., compartment volume, compartment pressure…) and its methods (e.g., pressure calculation, enthalpy…).

In the python environment an instance is a copy of a class object, its properties, and methods – the data of each instance is different, but the methods are the same. A model data structure is formed of multiple instances, derived from one or more of the API class objects; resulting in a collection of class instances. The number of each class instance depends upon the model encoded.

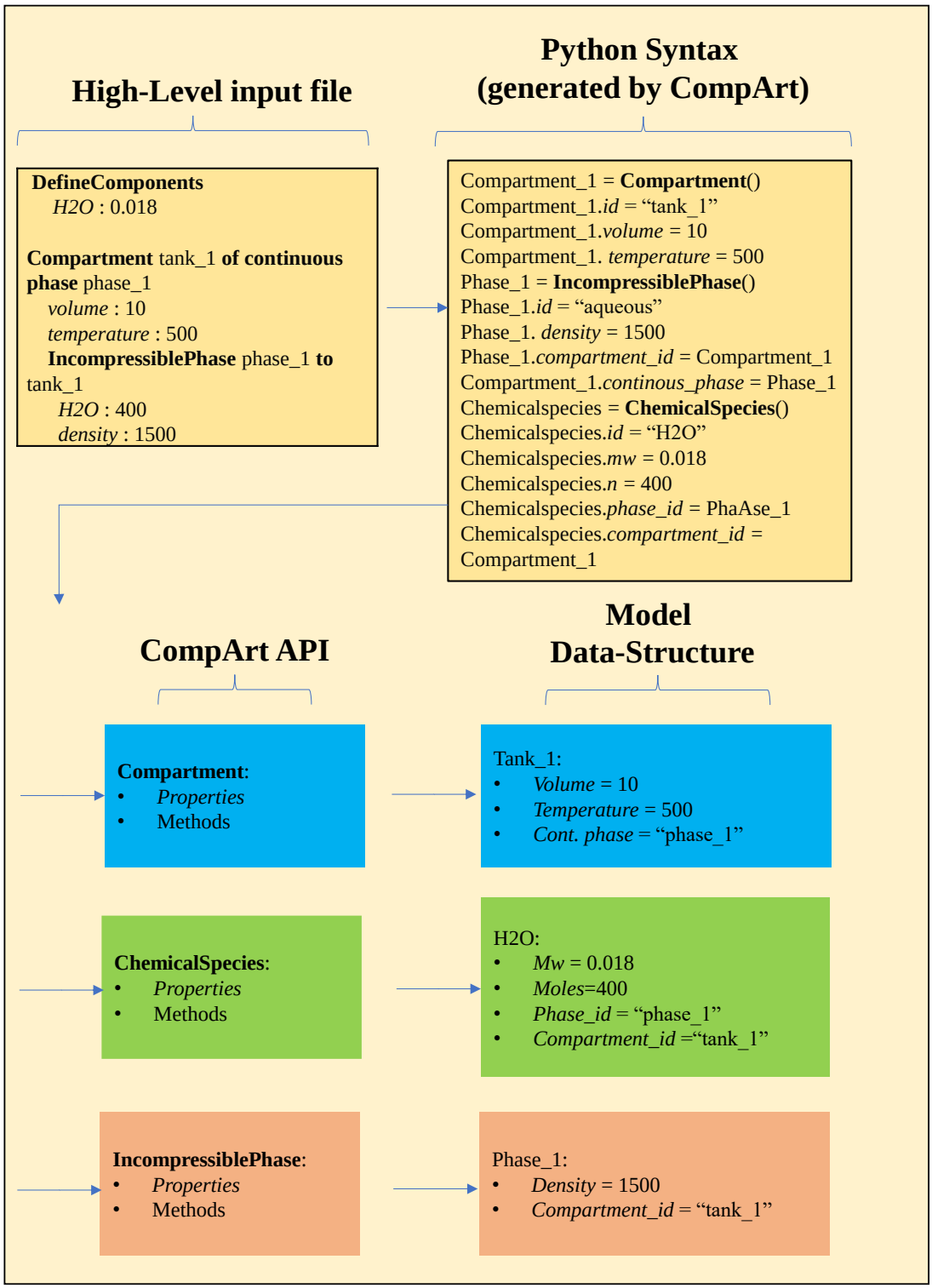

Figure 35 – CompArt model input file parsing flow chart, example of auto-parsing of high-level input language into model data structure.

Figure 35 illustrates the automatic procedure of model input file translation into python data structure. The model input file is parsed into the API by

CompArt. Python reads this API directly, forming an instance of each; the **Compartment** object, **IncompressiblePhase** object and **ChemicalSpecies** object, in this example. The properties of each instance are modified to reflect the values set in the input file, if not set then default values are assigned as declared in Table 12.

The resultant data structure is stored in lists, one list for each class of the API. Instances are appended to the list of the respective class they're formed from, e.g., see Equation 94 for example of Figure 35 data structure. The list structure is important for interconnecting instances, e.g., connecting species to the phase instance they inhabit (section 4.5 Linkage & population of model components in the python data-structure).

$$compartments = [Tank_1] \qquad \textit{Equation 94}$$

$$phases = [Phase_1]$$

$$species = [H2O]$$

Class objects, operation of each class objects and associated properties are given within Table 13 for each class of the Python syntax-based API of CompArt.

Table 13 – CompArt API Classes and properties, with reference section in Chapter 3.

Class	Definition	Units	Comment/example
Species	Section 3.2.1 Chemical species		Adds n moles of species id of phase $phase\_id$ of compartment $compartment\_id$ to the model space.
ID	Species reference		*id = "MeOH"*
Phase ID	Phase reference		$phase\_id = "aqueous"$
Compartment ID	Compartment reference		$compartment\_id = "Tank\_1"$
Mw	Molecular Weight	$kg/mole$	$mw = 0.002$
N	Moles of species	$Moles$	$n = 12$
IncompressiblePhase	Section 3.2.2 Phase		Adds an incompressible phase $phase\_id\ of$ compartment $compartment\_id$ with a characteristic diameter $char\_diameter$, heat capacity c and density $density$ to the model space. *

Class	Definition	Units	Comment/example
ID	Phase reference		*id* = "*aqueous*"
Compartment ID	Compartment reference		$compartment\_id = "Tank\_1"$
Char Diameter	Characteristic diameter	$metres$	$char\_diameter = 0.001$
Heat Capacity	Sensible heat capacity	J/kgK	$c\_j = 4200$
Density	Density of the phase	kg/m^3	$density = 900$
CompressiblePhase	Section 3.2.2 Phase		Adds a compressible phase $phase\_id\ of$ compartment $compartment\_id$ with a characteristic diameter $char\_diameter$ and heat capacity c to the model space. *
ID	Phase reference		*id* = "*gaseous*"
Compartment ID	Compartment reference		$compartment\_id = "Tank\_1"$
Char Diameter	Characteristic diameter	$metres$	$char\_diameter = 0.001$
Heat Capacity	Sensible heat capacity	J/kgK	$heat\_capacity = 1000$

Class	Definition	Units	Comment/example
Compartment	Section 3.2.3 The Compartment		Adds a compartment id of continuous phase $phase\_id$ and volume $volume$, temperature $temperature$ and stiffness values epsilon $epsilon$ & alpha $alpha$ to the model space. **
ID	Compartment reference		$id = "Tank\_1"$
Continuous phase	Continuous phase reference		$continuous\_phase = "aqueous"$
Volume	Compartment volume	m^3	$volume = 0.1$
Temperature	Initial temperature	$Kelvin$	$temperature = 298$
Epsilon	Relaxed density, pressure response		$epsilon = 2$
Compressible min P	Minimum compressible pressure Pa		$p\_min = 1$

Class	Definition	Units	Comment/example
Compressible max P	Maximum compressible pressure Pa		$p\_max = 101325$
Surrounding	Section 3.2.4 Surrounding		Adds a surrounding id of continuous phase $phase\_id$ and volume $volume$ and temperature $temperature$ to the model space. **
ID	Surrounding reference		$id = "Tank\_1"$
Continuous phase	Continuous phase reference		$continuous\_phase = "aqueous"$
Volume	surrounding volume	m^3	$volume = 0.1$
Temperature	Initial temperature	$Kelvin$	$temperature = 298$
Pressure	Pressure, set via automatic phantom moles adjustment	$Pascals$	$Pressure = 101325$

Class	Definition	Units	Comment/example
Epsilon	Relaxed density, pressure response		$epsilon = 2$
Alpha	Minimum compressible volume factor		$alpha = 10^{-3}$
Container	Section 3.4 The Container Theory		Adds a container id of volume $volume$ and tau value $container\_tau$ containing the following compartments: $contents$, to the model space.
ID	Container reference		$id = "container\_1"$
Contents	A list of Contained compartments		$contents = ["tank\_1", " tank\_2"]$
Volume	Container volume	m^3	$volume = 10$
Container Tau	Resistance to compartment volume change		$container\_tau = 0.01$

Class	Definition	Units	Comment/example
ConvectiveTransport	Section 3.5.1.5 Convective Transport		Adds convective transport phenomena id from $source\_compartment$ to $termination\_compartment$ over the transport area $area$; either at a set velocity $velocity$ or driven by the pressure difference between the compartments, the pump induced pressure $pump\_pressure$ and resistance to flow set by the $activation\_pressure$ value. The molar flux of each species is relative to the species volumetric fraction within the source compartment.
ID	Transport reference		$id = "flow\_1"$
Source Compartment	Source compartment reference		$source\_compartment = "tank\_1"$
Termination Compartment	Termination compartment reference		$termination\_compartment = "tank\_2"$

Class	Definition	Units	Comment/example
Pump Pressure	Induced flow pressure	$Pascals$	$pump\_pressure = 0$
Flow Tau	Resistance to flow		$flow\_tau = 0.01$
Enthalpy Transport	Transport enthalpy	$Joules/moles$	$transport\_enthalpy = 0$
Area	Area of transport	m^2	$area = 1$
Velocity	Set flow rate	m/s	$velocity = 1$
Sigmoid error	Error associated with the smoothing of the transport activation		$sigmoid\_error = 2$

Class	Definition	Units	Comment/example
Reaction	Section 3.5.3 Reactive Transformation		Adds reaction of chemical species $mechanism\_species$ at stoichiometry defined by $stoichiometry$ at a depletion/formation rate equivalent to the evaluation of the $rate\_equation$ (with the rate constant k defined separately) and the stoichiometry of reactants/products. The reaction either occurs within a single-phase $phase$ or at the interface of two phases in contact (of the same compartment) $phase$ and $contacting\_phase$.***
ID	Reaction ID		$id =$ "$react\_1$"
Phase	Single-phase or dispersed/continuous Phase reference		$dispersed\_phase =$ "$gaseous$"

Class	Definition	Units	Comment/example
Contacting Phase	Continuous/dispersed Phase reference		$contacting\_phase = "aqueous"$
Rate Equation	The conversion rate of reactants to products	mol/sV_j	$rate\_equation = "k(A * [B])/2"$
Mechanism species	Mechanism species concerning stoichiometry		$Mechanism_{species} = [A, B, C]$
Stoichiometry	Stochiometric quantities of the reactants and products		$stoichiometry = [-1, -2, 1]$
krxn	Reaction rate constant		$krxn = 0.001$
Rxn Enthalpy	Enthalpy of reaction	$Joules/mole$	$rxn\_enthalpy = -400000$
Ea	Activation energy	$Joules/mole$	$ea = 5 * 10^{-4}$
T Ref	Arrhenius equation reference temperature	$Kelvin$	$t\_ref = 298$

Class	Definition	Units	Comment/example
Reaction tau	Minimum moles required per reactant for reaction to proceed		$reaction\_tau = 10^{-7}$
Sigmoid error	Error associated with the smoothing of the transport activation		$sigmoid\_error = 2$
MassTransfer	Section 3.5.1.3 Mass transfer		Adds mass transfer mechanism id, transferring species $species$ from compartment/phase $source$ to compartment/phase $termination$ over a contact area $area$; with transfer coefficients ks, kt and s.***
ID	Mass Transfer reference		$id =$ "MTR_1"
Species	Species reference		$species =$ "$MeOH$"

Class	Definition	Units	Comment/example
Source	Source compartment/phase of species		$source = "aqueous"$ or $= "compartment\_1"$
Termination	Termination compartment/phase of species		$termination = "gaseous"$ or $= "compartment\_2"$
Area	Area of transport	m^2	$area = 1$
Transfer Enthalpy	Enthalpy of Transfer	$Joules/mole$	$transfer\_enthalpy = -12000$
Ks	Source phase MTR coefficient	m/s	$ks = 0.001$
Kt	Termination phase MTR coefficient	m/s	$kt = 0.01$
S	Partition coefficient		$s = 1$

Class	Definition	Units	Comment/example
Sigmoid error	Error associated with the smoothing of the transport activation		$sigmoid\_error = 2$
HeatTransfer	Section 3.5.2 Heat Transport		Adds enthalpy transfer from $source\_compartment$ to $termination\_compartment$ over the contact area $area$ at a rate dependent on the temperature difference of compartments and heat transmittance u.
ID	Heat transfer reference		$id = "heat\_flow"$
Source Compartment	Source compartment of species		$source\_compartment = "tank\_1"$
Termination Compartment	Termination compartment of species		$termination\_compartment = "tank\_2"$

Class	Definition	Units	Comment/example
Area	Area of transport	m^2	$area = 1$
U	Overall heat transmittance	J/sm^2K	$u = 1000$
Sigmoid error	Error associated with the smoothing of the transport activation		$sigmoid\_error = 2$
PhaseTransport	Section 3.5.1.4 Phase transport		Adds transport of the species of phase $phase\_id$ from $source\_compartment$ to $termination\_compartment$ over a contact area $area$.
ID	Transport reference		$id = "phase\_transport\_1"$
Phase ID	Transported phase		$phase\_id = "gaseous"$
Source Compartment	Source compartment of phase		$source\_compartment = "tank\_1"$

Class	Definition	Units	Comment/example
Termination Compartment	Termination compartment of phase		$termination\_compartment = "tank\_2"$
Enthalpy Transport	Transport enthalpy	$Joules/moles$	$transport\_enthalpy = 0$
Area	Area of transport	m^2	$area = 1$
Transport Tau	Mean Residence time of phase in source compartment		$transport\_tau = 0.01$
Sigmoid error	Error associated with the smoothing of the transport activation		$sigmoid\_error = 2$

* Initialising also creates a (phantom) species and adds it to the phase.

Phantom species is a derivation class of Species, with a small number of moles and no interaction with other species or phenomena, defined in section 3.2.1.1 Phantom Chemical species.

****** Initialising object also adds a compressible (phantom) phase to itself (compartment/surrounding) and adds a (phantom) species to the compressible phase.

Phantom phase is a derivation of **CompressiblePhase**; no transport occurs between compartments, as defined in section 3.2.2.2 Phantom phase.

******* For intra compartmental MTR and reaction the mechanism needs only to be defined once; where the source species/phases are present in the model space and in contact (dispersion/continuum phases) the mechanism of species transfer is applied.

Further detail into the auto-addition of phenomena to locations of the model is given section 4.5 Linkage & population of model components in the python data-structure**.**

The format for describing a compartment model directly from the API class objects utilises the syntax of Python. The base syntax knowledge required to call and alter instance properties is as follows (summarised in Table 14); (i) A temporary reference variable is required to initialise an object instance and reference its property values for modification. e.g., In the first line of Table 14, the object *"ModelTerm"* is initialised and linked to the reference variable *"referencevariable"* using the equality sign. (ii) A property *"property"* of the instance is then accessed and equated to a new value *"value"*; which must be of the correct DataType (see section 4.3 CompArt High-level input language).

Table 14 - Python Syntax basics when declaring terms through the low-level CompArt API.

ReferenceVariable = **ModelTerm**()
ReferenceVariable.*property* = Value

A deconstruction of the example given of Table 10, a $10m^3$ compartment of temperature $500K$ with an incompressible continuum phase of ideal density $1500kg/m^3$, composed of 400moles of species H2O of molecular weight $0.018kg/mole$ is decomposed in this section using the CompArt API to illustrate the automated procedure of CompArt's parsing algorithm (High level input language → low-level language readable by python) .

First, the syntax creating a compartment and altering its attributes is shown with obligatory properties is defined as so.

```
Compartment_1=Compartment()
Compartment_1.id = "tank_1"
```

Altering the properties utilises the temporary reference variable to access the compartment instance.

```
Compartment_1.volume=10
Compartment_1.temperature = 500
```

The reference ID of the compartment (“Compartment_1”) is passed to other instances as a property, it is used to identify and link model objects together by CompArt’s interpretation algorithm which sits between CompArt’s API and the python data structure (section 4.4 CompArt API, Figure 35). An example is given in the below example for the creation of an **IncompressiblePhase**. The compartment property “Continuous phase” is set to the reference id string of the newly created phase “Phase_1”. Similarly, the newly created phase’s Compartment property is set to the compartments reference id.

Phase_1 = **IncompressiblePhase**()

Phase_1.*id* = “Phase_1”

Phase_1.*density* = 1000

Phase_1.*compartment_id* = “tank_1”

Compartment_1.*continous_Phase* = “Phase_1”

Addition of a chemical species requires initiation through the class object and the definition of the chemical species properties. Again, we see the *compartment_id* and *phase_id*, which combined represent the spatial location of the species, are values equal to the reference id’s of, respectively, pre-defined compartment and phase instances.

Chemicalspecies = **ChemicalSpecies**()

Chemicalspecies.*id* = “H2O”

Chemicalspecies.*mw* = 0.018

Chemicalspecies.*n* = 400

Chemicalspecies.*phase_id* = “aqueous”

Chemicalspecies.*compartment_id* = “tank_1”

The key benefit to the user of the CompArt high level language is the removal of python language syntax tedium’s e.g.,

(Dot notation: Phase_1.*id)*,

(Bracketed class calls: **ChemicalSpecies**()),

($referencevairables$: Compartment, Phase_1, Chemicalspecies);

which would otherwise prove impenetrable to a non-programming user of the tool. This example illustrates the difference between the low- and high-level languages, the higher-level language enabling modellers without programming knowledge to implement compartment models with ease.

4.5 Linkage & population of model components in the python data-structure

The construction of a compartment model in CompArt is the conversion of the input file into the python data structure, this section is the next stage of the model development within the python data structure, entailing (i) user input error detection , (ii) the conversion of string type property values to instances within the data structure (e.g., in Figure 36, *phase_reference_id* = “phase_1” → *phase_reference_id* = **phase_1**) and, (iii) automated population of the data structure with instances of phases & species and phenomena otherwise not given in the input file but generated due to phenomena action and phases/species presence respectively.

Object instances are constructed initially with values assigned to each property (either the default or user supplied value), as depicted in the “Resultant model Data-structure” part of Figure 36.

(i) Once all objects are generated, all *reference_id* properties are compared for each instance of the same class (e.g., Compartments, containers, reactions …) to ensure no user input error associated duplicate use of a unique *reference_id* for two separate instances. As multiple phases can exist of the same *reference_id* (e.g., aqueous phase in multiple compartments) we instead check those phases of the same *reference_id* value have unique *compartment_reference_id* values. Similarly, for chemical species, the *phase_reference_id* property is compared between same *reference_id* species to ensure no duplicates.

(ii) Properties of an instance which refer to another instance’s *reference_id* within the data structure are converted from their string format into a direct reference to the instance; the converted properties are illustrated in Figure 36,

highlighted in grey – arrows between instance blocks indicate the accessible relationships between instances through the converted property values.

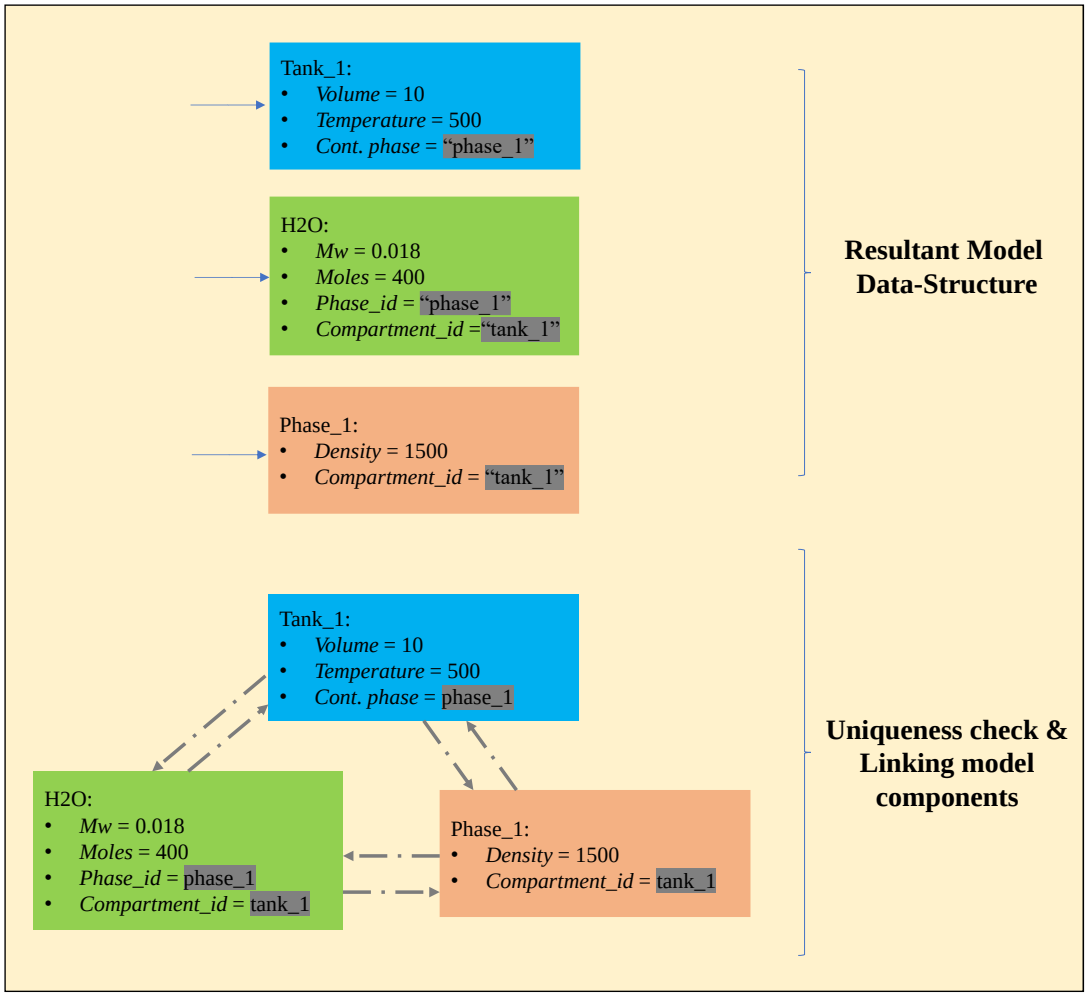

Figure 36 – CompArt reference properties conversion and user input error check

An example of the auto-population of the python data structure is given in Table 15 for the simple model of a compartment being filled from a source surrounding. In the input file the phase and species of the target compartment need not be defined (see red text in Table 15) – the **IncompressiblePhase** phase_1 and species *A* of value 0 moles are auto-populated in the model data structure post input file read in by CompArt.

Table 15 – Species A Fed compartment from source surroundings, a CompArt Input file. The red text is not submitted with the input file, but rather appended by the auto-population algorithm of CompArt.

```
DefineComponents
   A : 0.002
Surroundings surroundings_1 of continuous phase Liquid
   volume : 10
   pressure : 101325
   IncompressiblePhase Liquid to surroundings_1
      A : 400
Compartment comp_1 of continuous phase phase_1
   volume : 10
   CompressiblePhase phase_1 to comp_1

   IncompressiblePhase Liquid to surroundings_1
      A : 0
ConvectiveTransport transport_1 from surroundings_1 to comp_1
```

The benefit of the automated system generation becomes more impacting when a phenomenon is applied to a model, as phenomenon typically affects multiple locations of the model e.g., Single phase reaction in a multi-compartment model with each composed of the same phase and species continuum, see Figure 37. Simplifying the term count in the input file focuses the attention of the input file towards describing key information about the model being simulated.

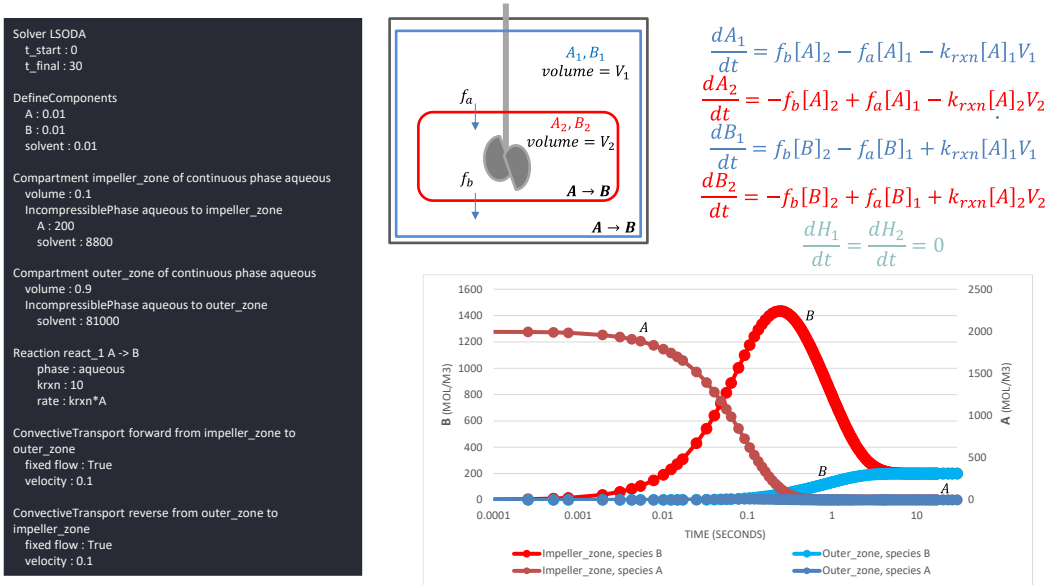

Figure 37 - Two compartment model of an impeller stirred reactor, A->B, from left to right [*input file, illustration, results, respective differential system*]

Instead of defining the reaction N times in the input file, it is defined once pre-simulation and through an iterative run through the python data structure of

the model – the species variables and phenomena terms are added to the data structure respective object lists and for species transformation due to reaction are added to the respective ODE's.

In the example of Figure 37 the reaction is defined once; the reactant A is present in the central impeller compartment initially and not present in the outer compartment. Through the population of the instances in the data structure, discussed next in section 4.5 Linkage & population of model components in the python data-structure, an instance of A with 0 moles is generated in the outer compartment. The existence of A in both compartments of the phase stated, aqueous, in the reaction definition induces the phenomena to be generated for both compartments from the single statement in the input file.

The same methodology is applied to intra-compartmental mass transfer where the contact of two phases of the transfer, with the source phase embodying the transferred species is identified as a candidate for mass transfer and results in generation of the phenomena in the data structure and species of the termination phase if not already present.

4.6 Solution methods & data output

With the data structure fully populated, the variables extracted from the data structure are **one variable**, each representing the **moles present, per species** for each phase/compartment location if it is present. This includes phantom species, of which one exists per phase, and **a variable for the enthalpy of each compartment** in the data structure. An **additional volume variable** for each compartment encapsulated in a container. And **one variable for each** of the following: (i) total system mass, (ii) total surroundings mass, (iii) total system enthalpy, and finally (iv) total surroundings enthalpy. System & surrounding mass/enthalpy is the summed total of mass/enthalpy in the system & surroundings of the system; the initial values are automatically calculated within the tool. The purpose of these variables is as a comparative measure of the mass and enthalpy balance within the system.

The total number of variables, y'_{total}, in a compartment model is thus given by Equation 95, where y'_x is the number of variables associated with the **bold** points above.

$$y'_{total} = y'_i + y'_{ii} + y'_{iii} + y'_{iv} \qquad \textit{Equation 95}$$

For each species variable, an initial value is set by the user. Or when CompArt adds species to the tool through the auto-population procedure the species values are set to $0\ moles$. Compartment volume is a property obligated to be given with a compartment statement, compartment enthalpy is a function of the compartment temperature which is either given or default of $298K$. The array of initial values which compliment y_{total} is symbolized as y_0.

The vector of differential values, y'_t, represents the instantaneous change in variable values at a time t. Each variable differential is the sum of the phenomena rates issuing a change in the value of the variable. The phenomena rate values are accessed by the solver through a differential function which is dependent on the current variable values, $f(y_t)$, which iteratively cycles through all phenomena in the data structure and sums the term differential values together for each variable to form an array of differential values of the same length as the number of variables, symbolized as y'_t. The resultant differential equations are used to find the values of the variables at an appropriately selected time point ahead of the time point at which the variables values were of value y_0; this is determined within the numerical solver algorithms convergence routine. The new values are denoted y_t, where the subscript t is the time point at which the values of the variable are equal to y_t. This process repeats with the initial values, y_{t-1}, fed to the differential function updated at each iteration to the newly calculated values y_t until the evolution of the variable values over the time domain are collected.

Thus, the variable instances of the data structure (y), initial values (y_0), and differential terms (y') (summed from affecting phenomena in the data structure) form the ordinary differential equation initial value problem (ODE IVP) problem of the compartment model.

4.6.1 The numerical Solution of a compartment model

The solution of a compartment model requires an ODE initial value problem numerical solver to solve the ODE system (numerically; $y'(t)dt$) over the time domain $[t\_start \rightarrow t\_final]$.

The solver and its properties are defined in the input file as given in Table 16.

Table 16 – High level input term for the description of numerical solver and associated properties, exert from Table 13

Solver *numerical_solver* *[t_start : 0]* *[t_final : 100]* *[max_step_size : 10**3]* *[atol : 10**-6]* *[rtol : 10**-6]*

SciPy is one of the numerical solver libraries utilised in CompArt, formed of several ODE solvers, the *numerical_solver* options within this library capable of stiff problem solutions are: **Radau, BDF** and **LSODA** – the former two are stiff system implicit solvers, the latter is both BDF and Adams method with a switching mechanism to determines the active solver per the presence of stiffness (BDF) or none (Adams).

The SciPy module is the primary source of numerical solvers to the tool. A second module “diffeqpy” in python has a more recently developed library of solvers wrapped from the Julia language. Although the solvers are more advanced, the module is a secondary option to SciPy when solving compartment model as it is less integrated with python; requiring an external Julia installation on the path of the system running CompArt. And using diffeqpy includes an up to 60 second overhead for initialisation of the Julia environment upon each model run. To accept the set of computed variable values at a given time step, the solver performs a convergence test, the local

estimated error is the difference between the calculated value (y) and next best calculated value(y^*).If this difference is less than the relative tolerance constant $(rtol)$ multiplied by the respective variable quantity plus the absolute tolerance $(atol)$ quantity then the convergence test has passed and the solution at the time step is accepted.

$$|y - y^*| < rtol * y + rtol \qquad \textit{Equation 96}$$

The relative tolerance, $rtol$, controls the number of correct digits and the absolute tolerance, $atol$, is a safety net for when the calculated value $\boldsymbol{y}$ approaches zero.

Here, the same $rtol$ and $atol$ values are applied to each variable and thus if one variable test fails, the solution is not converged, and the solver must reduce its time step size to improve the accuracy of solution in aid of passing the convergence test. The numerical solver options from diffeqpy are given in the Table 17 with recommendations as per the solver tolerances set.

Table 17 – Numerical sovlers recommended based on desired solver tolerance*

Tolerance Magnitude $min(atol, rtol)$	*numerical_solver*
$> 10^{-2}$	**Rosenbrock23** **TRBDF2** **ABDF2**
$> 10^{-8}$	**Rodas5** **Rodas4P** **Kvaerno5** **KenCarp4**
$< 10^{-9}$	**radau**

*Property values are case sensitive.

For a problem with unknown stiffness, the **LSODA** solver of SciPy or **lsoda** solver of diffeqpy are good solver options for the solution of the model.

Non-stiff solvers have been excluded from discussion as typical a compartment model with multi-phenomena and phases is of a stiff nature; information on the solvers of Table 17 and further library of non-stiff solvers available to the tool are available for diffeqpy (*ODE Solvers*, 2021) and SciPy (*scipy.integrate.solve_ivp*, 2021).

4.6.2 Improving the resolution of a solution

The final property of the solver discussed is the *max_step_size.* This property sets the maximum time step a solver can make when solving a system. For systems with timed activations, such as a pulsed influx of an RTD, setting the max step size to below that of the pulse length ensures the resolution of the solution captures the event. This does however induce a heavier load upon the solver as more steps are taken over both the periods with and without pulses or events, resulting in a longer time to solution.

4.6.3 Balancing model stiffness with attainment of solution

Stiffness is the induced numerical instability of a solution due to significant changes in y' between two near time points. The significant change in differential value causes an overshoot in predicted variable values at the next time point, resulting in a non-converged solution. The solver must reduce the step size between the current and next time point to overcome the induced stiffness. An excessive reduction of the step size without increased solution accuracy indicates instability due to problem stiffness.

Not considering the effects of stiffness can result in a continually decreasing step-size within the solver which ultimately results in either a long wait to solution beyond reasonably time, or infinitely resolving step size and solution incompletion.

To reduce the likelihood of instabilities, we can purposefully design the model with reduced stiffness through modification of stiffness constants associated with the phenomena and structural components (e.g., containers) pre-simulation. Model stiffness constants have a direct affect upon the magnitude of the variable differentials of a compartment model.

As a general approach the stiffness constants given in the theory chapter detail are coalesced into Table 18, with the direction of constant change which results in a reduction in stiffness induced by the phenomena; although care should be taken as typically with decreased stiffness, comes decreased accuracy.

Table 18 – CompArt stiffness properties description and direction of value change to reduce stiffness induced by property upon model solution.

Stiffness property	**Description of property**	**Modification to decrease stiffness, maintain above zero.**
ε	Observed in equation of incompressible relaxation factor. $f_{i\mathbb{C}} = (1 + \rho - \rho_0)^{\varepsilon}$	**Decrease**
p_min	Sets the value of α_k, the minimum compressible volume in a compartment.	**Increase**, relative to p_max.
p_max	Sets the concentration of phantom phases species in a compartment	**Increase**
$container\_tau$	Response rate determining constant of compartment volume change to pressure difference to container and/or container volume overflow.	**Increase**
$tau\_reaction$	Molar value at which any reactant is below, the reaction does not proceed.	**Increase**

Stiffness property	Description of property	Modification to decrease stiffness, maintain above zero.
$flow\_tau$	Constant which forms a linear relationship between pressure difference and volumetric flow rate of a convective transport mechanism.	**Increase**
$transport\_tau$	Constant which forms a linear relationship between an individual phase velocity and its volume size in the source compartment.	**Increase**
$sigmoid\_error$	Error associated with the smoothing of the phenomena activation.	**Increase**
$timed\_sigmoid$	A rudimentary application of the sigmoid activation for timed activation of phenomena.	**Decrease**

4.6.4 Bounding solution variables to the positive domain

The molar, enthalpic and volumetric quantities solved for throughout the time domain are not to fall below a value of zero. As this would indicate a negative mass, enthalpy or volume which are not physically realistic. Furthermore, negative moles form negative concentrations which directly interfere with the correct operation of all concentration dependent phenomena – making the model unstable. The solver property absolute tolerance was initially employed to ensure such occurrence did not occur. The property determines the accepted error tolerance when variable values approach a value of zero. If the error tolerance is not met, the step size is reduced until so. The absolute

tolerance however is not a perfect comparative approach to assess the error of a solution, sometimes faulting and allowing the solution to be accepted when a negative value for a variable is calculated by the solver. Another source of small negative values arises through truncation and roundoff errors.

An option to address this issue is to unpack and edit each numerical solver, adapt the use of the absolute tolerance and other components of the solver to bound the model solution to positive values. This would be highly involved, requiring in depth understanding of every numerical solver algorithm and the solution may not be applicable across all solvers, potential work of a future researcher. Instead, here the problem of negative value occurrences is approached from outside of the numerical solver. This is favourable, as the variation in numerical solvers that could be used to solve this model are numerous in number and variance.

A modification of the ODE system by Shampine *et al.* (2005) is to redefine the differential equations outside the feasible region. Specifically, if a component that is required to be non-negative is within the bounds of zero and a tolerance value tol, the differential passed to the solver can only be positive and thus the variable value can only ever increase when situated in this bound range of the positive domain – summarised in Equation 97.

$$y_i < tol\ ; y_i' = \max(0, y_i')\ \ y_i \geq tol\ ; y_i' = y_i' \qquad \textit{Equation 97}$$

This approach however is not applicable to solvers which assume the use of an analytical Jacobian, such as ode23 of Matlab solver suite, excluding the use of stiff solvers within the SciPy module (Radau, BDF and LSODA) with this approach to negative domain control.

An example of this in application is in in the tool COMSOL (*Avoiding negative concentrations*, 2021); developers observed a similar issue with regards to the convection-diffusion-reaction equation, r_{rxn}. The numerical solvers would overshoot the root, and a negative concentration would result, giving incorrect rates. In their solution, they conditioned the summed rate to be greater than

zero, 10^{-15}, when concentrations approach zero, through a maximum function; Equation 98.

$$\max(r_{rxn}, 10^{-15}) \qquad \textit{Equation 98}$$

This approach is effectively nullifying the change in variable values due to active phenomena if the components value is approaching zero. The approach would have to be applied to each phenomenon individually to ensure the mass and heat differentials are both nulled, and the balances are maintained. The appearance of a max function does induce discontinuity in differential values if a rate is large approaching the bound range for a variable and then immediately switched to the lower set rate of y'. A transition from the actual to set rate utilising the sigmoid response could assist in smoothing the transition.

Another approach of Shampine *et al.* (2005) is to project a value of 0 to the system variables where the system variable is less than tolerance value, $y_i < tol$. Where the tolerance is greater than zero but small enough to which it is safe in the context of compartment modelling applications to project $1 \gg tol > 0$, Equation 48 .

$$y_i < tol; y_i = 0 \; y_i \geq tol; y_i = y_i \qquad \textit{Equation 99}$$

The condition of this approach is applied post solver convergence, where on each call the equity is tested, and variable modified to zero if decidedly so through the equality check. The tol value must be small enough to not affect the model values, or inhibit model progress, yet large enough to provide a buffer zone before zero, for the variable to be controlled before negative domain entrance of the value by the solver. An issue foreseen is the solver is not aware of variable projections, the simulation proceeds on different knowledge of variable values than those projected post solver convergence; for multi-step methods and implicit methods the change in variable values is unexpected, variable values mismatching those previously calculated and utilised for next step convergence, and so the solver is in essence fed discontinuity and is likely to fail due to this.

The solutions discussed provide insight into the issue of non-negative ODE's and approach to the avoidance of the negative domain, implementation of the solutions would be futile as they do not apply to the solvers required to solve the complexity of compartment modelling. General purpose numerical solvers are not fit for the application and solution of compartment models, but at present are the only course of solution, leaving the discussion open. The advanced solvers of diffeqpy, the Julia language module implemented in python, may posses' solvers with greater reliance in solving such models within the positive domain; shown in the subsequent validation chapter of the thesis.

4.7 post-simulation data capture

Throughout the simulation of the model in CompArt, variable values for each solved time point are saved by the solver, (i) the moles of chemical species, (ii) volumes and (iii) enthalpies of compartments. The model data structure defines the spatial location of each chemical species, regarding phase and compartment; the interlinkage of variables through phenomenon interaction and the equations which define the resultant physical behaviour of the system and changing properties, e.g., change in contained compartment volumes, phase volumes, compartment temperatures.

As the changing system properties are a function of the captured ODE variable data, they are not stored during simulation. This is to save random access memory (RAM) during simulation and so the simulation time for a run is indicative of solution attainment time only. Instead, CompArt extracts model property and variables information not captured as ODE variables at each time step through construction of the model at each time point with the timed variable data output from the solver.

Values at each time point are collected for each structural (container, compartment, phase, species) and phenomenological (convective transport, phase transport, mass transfer, heat transfer, reaction) model component. Table 19 gives the values collected for each of the model components with definition if the property is a function of system properties; otherwise see Table

15. The properties to extract were chosen based on the common output of compartment modelling observed in literature.

Table 19 – CompArt extracted property values post-simulation.

Model component	Property
Container	
	$volume(m^3)$
	$Pressure(Pa)$
	$Temperature(K)$
Compartment/ surrounding	
	$volume(m^3)$
	$Pressure(Pa)$
	$Temperature(K)$
	$Enthalpy(J)$
	f_{ic}
Incompressible phase/ Compressible Phase/ Phantom Phase	
	$volume(m^3)$
	$Moles$
	$Density\left(\frac{kg}{m^3}\right)$
Chemical Species/ Phantom Chemical Species	
	$Moles$
	$Phase\ concentration\ \left(\frac{mol}{m^3}\right)$
	$Compartment\ concentration\ \left(\frac{mol}{m^3}\right)$
Phase Transport	
	$Velocity\ \left(\frac{m}{s}\right)$
	$Timed\ activation$
Mass Transfer	
	$dC\ \left(\frac{mol}{m^3}\right)$

Model component	Property
	$Area\ of\ Transfer\ (m2)$
	$Timed\ activation$
	$Activation\ response$
Convective Transport	
	$Velocity\ \left(\frac{m}{s}\right)$
	$True\ Velocity\ \left(\frac{m}{s}\right)$
	$Timed\ activation$
	$Activation\ response$
Heat Transfer	
	$Heat\ Transfer\ rate\ \left(\frac{J}{s}\right)$
	$Timed\ activation$
Reaction	
	$Reaction\ rate\ \left(\frac{mol}{s}\right)$
	$Enthalpy\ rate\ \left(\frac{J}{s}\right)$
	$Timed\ activation$
	$Activation\ response$

The properties of Table 19 form the raw data extracted from a model, these values over the simulation time domain are automatically printed to an .xlsx file where plots are atomically produced for fast evaluation of a model run. Figure 38 shows the output for the species A of the aqueous phase within the impeller zone compartment as printed in the excel document generated by CompArt; the model illustration, input file and ODE system are given in Figure 37.

Time	Moles	Phase concentration (mol/m3)	Compartment concentration (mol/m3)
0	200	2000.019739	2000
5E-06	199.9989	2000.008739	1999.989
1E-05	199.9978	1999.997739	1999.978
0.002401084	199.4725221	1994.744907	1994.725221
0.004792168	198.9487504	1989.507139	1989.487504
0.007183252	198.4264806	1984.284389	1984.264806
0.018025222	196.0770676	1960.790028	1960.770676
0.028867191	193.7580401	1937.599523	1937.580401
0.039709161	191.4690054	1914.708951	1914.690054
0.050551131	189.2095728	1892.114401	1892.095728
0.07223507	184.7779744	1847.79798	1847.779744
0.09391901	180.4602178	1804.619989	1804.602178
0.115602949	176.2533557	1762.550952	1762.533557
0.137286889	172.1545153	1721.562143	1721.545153
0.158970828	168.1608989	1681.625585	1681.608989
0.232686203	155.3352154	1553.367485	1553.352154
0.306401577	143.5936774	1435.950946	1435.936774
0.380116952	132.8437562	1328.450673	1328.437562
0.453832326	123.0008455	1230.020594	1230.008455
0.527547701	113.9875619	1139.886868	1139.875619
0.601263076	105.7331291	1057.341726	1057.331291
0.732061953	92.75736594	927.5828139	927.5736594
0.862860831	81.64987458	816.5068041	816.4987458
0.993659709	72.13741167	721.3812362	721.3741167
1.124458587	63.98672235	639.8735386	639.8672235
1.255257465	56.99870572	569.9926826	569.9870572
1.386056342	51.00344107	510.0394444	510.0344107
1.51685522	45.85588912	458.5634169	458.5588912
1.684992276	40.28711398	402.8751159	402.8711398
1.853129332	35.69631109	356.9666339	356.9631109
2.021266387	31.90409723	319.044121	319.0409723

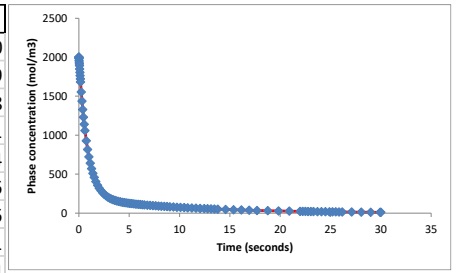

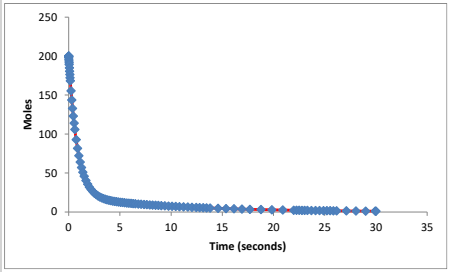

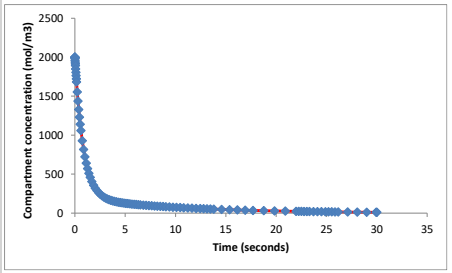

Object Trace: impeller zone, aqueous, A

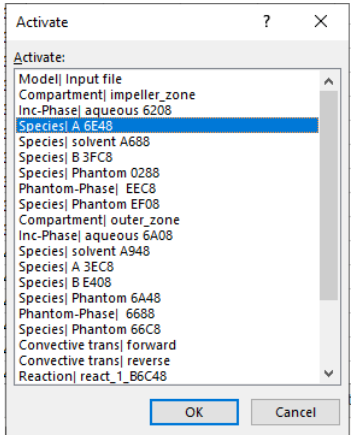

Model| Input file | Compartment| impeller_zone | Inc-Phase| aqueous 6208 | Species| A 6E48 | Species| solvent A688 | Species| B 3FC8 | Species| Pha ...

Figure 38 - CompArt Excel output, generated from the stirred tank reactor model of Figure 37; tabs indicate various ODE variables and for each variable tabulated data is presented per time, for species specifically the phase and compartment concentrations are plotted as well as molar.

4.8 Chapter Summary

A high-level language is presented which captures a broad range of compartment models and the phenomena occurring therein. The language automates the creation of python-based API. Both approaches, high-level language and API of CompArt, can be used to form a description of compartment models with greater ease compared to the direct ordinary differential equations typically passed as input in literature, being less prone to input error, more readable, scalable, and mutable.

Direct use of the API facilitates the description of the model; however, we see the high-level input language syntax is advantageous compared to the direct use of CompArt API, making redundant the need for parentheses to identify strings, temporary reference variables, or dot notation for declaring standard variables in the base python API of CompArt; allowing extension of the modelling approach to larger, more complex systems.

The auto-population algorithm of the tool is required to determine species and phases required to be generated within a compartment and phenomena between/within a compartment. This is one of the most complex sections of the tool. This algorithm propagates material through the system, adding phase and chemical species and phenomenological instances to the python data structure where they should be present but have not been declared in the input file. The complexity of this algorithm comes with the variance of phenomena which propagate material. Each phenomenon must have its own imitation function, and each of the imitation functions must be iterated over one another until no change in system size occurs, measured as the number of model variables. The imitation function was added to reduce the overhead on the user when declaring the model input file. If every chemical species and phase was required to be defined the input file length would reach obscene size for even the smallest of models.

The implemented numerical solver packages, DiffEqPy and SciPy is introduced and explored in terms of applicability to compartment problems

based on the accepted tolerances of a model. The investigation into negative domain of a solution, a failure point of the numerical solvers, was also explored with no solution found to address the occurrence of negative concentrations/variable values. Instead, reduction in model stiffness is suggested until more problem-specific numerical solvers are tested and/or developed.

CompArt is a full stack tool for the description, implementation, and solution of chemical process compartment models. The universal applicability of CompArt to chemical process compartment models is demonstrated in the following validation chapter.

Chapter 5 Validation of CompArt

5.1 Introduction

The theory developed in Chapter 3 is implemented in Python, forming the tool - CompArt; the work of Chapter 4. The tool is built in a Python 3.7 environment with the modules of Table 20 are imported into the Integrated development environment (IDE) PyCharm; on a Windows system, with an Intel i5 8250U processor (integrated graphics) and 8 GB of RAM, the equivalent specs of a current office PC.

Table 20 - Required Python Modules & operation within CompArt

Python Module (version)	Operation in CompArt
scipy (1.6.3)	Provides the numerical solver algorithms of section 4.6.1 The numerical Solution of a compartment model, for solution of the model.
pandas (1.2.4)	Translates the model solution arrays to tabulated and plotted data in a generated excel document, see section **Error! Reference source not found.**.

The objective of this chapter is to validate the implementation of the phenomenological models of CompArt through the simulation of a matrix of benchmarking models, given in Table 21. The novel container theory is prior validated in section 3.4.5 Application to a filling vessel, with an example of a batch fed vessel. Demonstration of the species, phase, and compartment meta-structure is apparent in all models of the matrix.

Quantitative validation is the process of determining the degree to which a model and its associated data are an accurate representation of the real world from the perspective of the intended uses of the model. For a single unit-operation model this is reasonably achievable, however for a universal

framework this is an extensive task, requiring the development, construction, solution, and analysis of a vast array of unit operations covered by the scope universal framework. A more appropriate validation approach, sensitive to both the scope of the universal model and project constraints, is implemented here. A piece wise validation/verification of the framework's implementation is taken, isolating the building blocks of the universal model for validation, the phenomenological models and structural behaviour of the models.

Validation refers to the accuracy of the model translation from high-level input language to model data structure within python, the realization of the structural and phenomenological model terms into the modelling space, and the accuracy of the model solutions compared to analytical and expected results. The models are purposefully simplistic to isolate phenomena where expected results can be reasonably predicted.

5.2 Phenomena validation

Table 21 is a matrix of 20 models designed to validate CompArt's phenomena. The table has one row for each of the six phenomenon types most prevalent in compartment modelling: (i) single-phase convective flow, (ii) multiphase convective flow (inc. phase transport), (iii) reaction, (vi) inter-compartmental mass transfer, (v) intra-compartmental mass transfer, and (vi) heat transfer. The complexity, measured as the number of phenomenological models per compartment, is kept low as to isolate the phenomena in each case for validation.

To validate the structural elements of the compartment modelling framework (Species-Phase-Compartment-Surroundings), the models developed are formed of both single (column 1) and multiple compartment (column 2) numbers; column 1 models utilise the surroundings as well as the single compartment in some cases, where an outside source or sink is required to demonstrate the structural/phenomenological components of the model.

Each cell of Table 21 contains one or more models, the key to identify each model is by the "*the row number – column number – the model number in the*

cell – lower case roman numerical”, e.g., the identifying key for the single-phase filling of a closed compartment with an incompressible phase is $1 - 1 - 1 - i$. A cell with the term “N/A” refers to the phenomena not being applicable; (i) in column 1 due to the phenomenon requiring multiple compartments to proceed, or (ii) column 2 as the phenomena only occurs within a compartment.

The model input files for the respective models Table 21 are given in appendix A, along with an illustration guide for the pictorial representations of the models given in this chapter, respectively in the Appendix B and Appendix C.

Table 21 - Phenomenological validation models

Phenomenon Investigated	Singular compartment (+ Surroundings)	Linear series of compartments
Single-phase convective flow	(1) The filling of a closed (no outlet) empty compartment from a source surrounding with a pressure driven feed of phase nature, (i) Incompressible (ii) Compressible (2) Model 1-1-ii with pressure-driven flow overflow to a sink surrounding.	(1) A series of 10 pressure flow connected empty compartments, with a fixed-flow feed from a source surrounding to the first compartment of phase nature, (i) Incompressible (ii) Compressible (2) Model 1-2-1 with a pressure driven flow from the final compartment in the series to a surrounding. (i) Incompressible (ii) Compressible

Phenomenon Investigated	Singular compartment (+ Surroundings)	Linear series of compartments
Multiphase convective flow *And* *Phase Transport*	(1) Filling an empty compartment with a mix of Incompressible and compressible phase flow from a source surrounding. (2) Model 2-1-1 with a pressure driven overflow to a surrounding.	(1) Single Pulse RTD; pulse and solvent of two immiscible incompressible phases. (2) A single compressible phase, phase transported from a source surrounding through a series of three compartments filled with stationary incompressible material, rising bubbles exiting to a sink surrounding.

Phenomenon Investigated	Singular compartment (+ Surroundings)	Linear series of compartments
Reaction	(1) Homogenous elementary reaction's (i) Parallel (ii) In-Series (2) Reaction between the continuous-dispersed, compressible species with incompressible species of a single compartment. (Interfacial reaction) (3) An elementary first order reaction utilising the Arrhenius equation to determine k_{rxn} as a function of compartment temperature. Taking place in two separate compartments, within one, $\Delta H_{rxn} = -5 \frac{MJ}{mole}$, and the other $\Delta H_{rxn} = 0 \frac{MJ}{mole}$.	N/A

Phenomenon Investigated	Singular compartment (+ Surroundings)	Linear series of compartments
Inter- compartmental mass transfer	N/A	(1) Diffusive mass transfer between two compartments of the same continuum phase due to initial imbalance from equilibrium. (2) Multiphase Mass transfer of material between two compartment continuums of differing phase nature (Compressible-Incompressible).

Phenomenon Investigated	Singular compartment (+ Surroundings)	Linear series of compartments
Intra- compartmental mass transfer	(1) Mass transfer between the compressible continuum and incompressible dispersed phase of a single compartment.	N/A
Heat transfer	(1) A compartment filled with multiphase material of $T = 298K$, heated from a higher temperature surrounding's; $T = 1000K$.	(1) A series of 10 compartments filled with compressible material, connected by unidirectional heat transfer phenomena (no convective flow present). The first compartment in the series is of a greater temperature than the following $1000K\ vs\ 298K$.

5.2.1 Cell 1-1 – One compartment, Single Phase Convective flow

Pressure driven flowrates, which are functional of pressure difference between connected compartments, are demonstrated within the models of this cell for both incompressible (Figure 39) and compressible (Figure 40) phase systems. Both models are initiated with an empty compartment - connected to a surrounding source of material of greater, fixed, pressure by a convective transport in the direction of source to compartment.

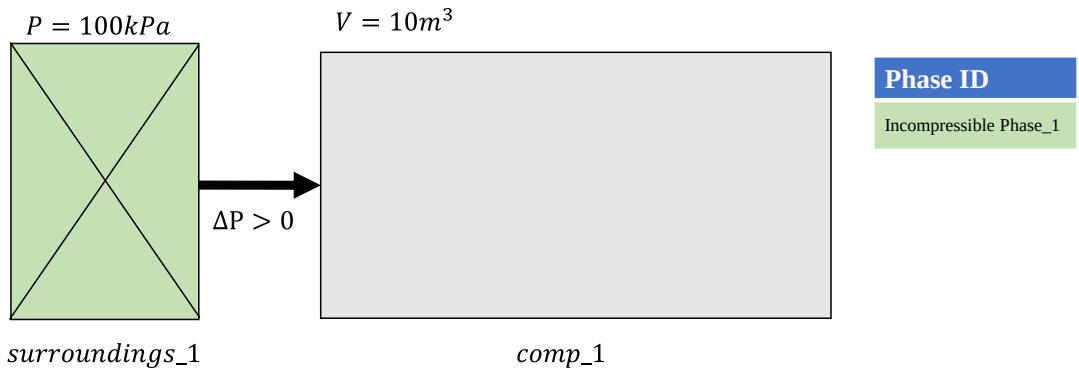

Figure 39 - Model 1-1-1-i

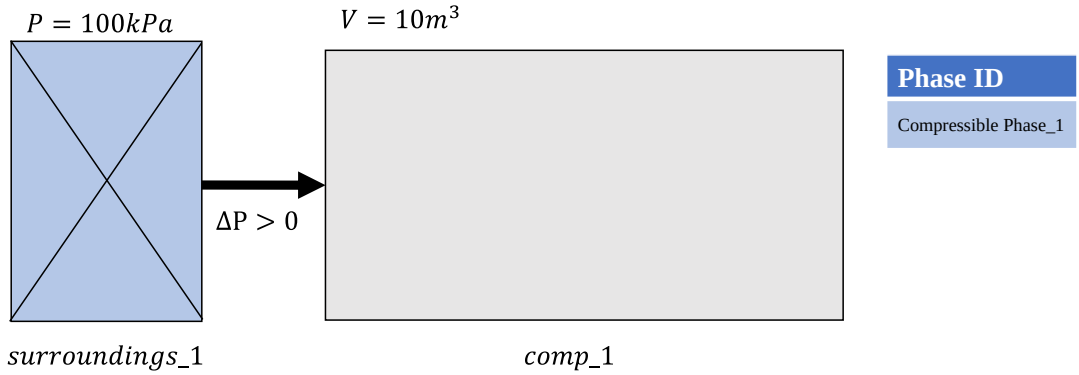

Figure 40 - Model 1-1-1-ii

The results of model 1-1-1i and ii are given in Figure 41. Comparing the increase in moles of A between both models, we see the compressible moles take a gradual curved pathway to an equilibrium quantity of 400 moles whereas the incompressible moles increase linearly with time until an abrupt plateau at 400,000 moles; the plateau in moles of A aligns with the pressure of the compartment reaching 101kPa in both models as the pressure driven

flow no longer has a driving force to feed material into the compartment, it has a pressure equal to the feeding surrounding pressure.

The pressure follows a similar path to the moles of A for the compressible model (1-1-1i). As compressible moles are added the pressure increases, reducing the driving force for the filling flow. Compressible moles have an immediate impact on the compartment pressure, as expected, whereas incompressible moles only influence the pressure of the where the incompressible volume reaches near to its limit, $(1-\alpha)V_k$; prior to this maximum volume, the pressure is calculated from the ideal gas law with the number of compressible moles of phantom phase nature only, which are of an extremely low quantity.

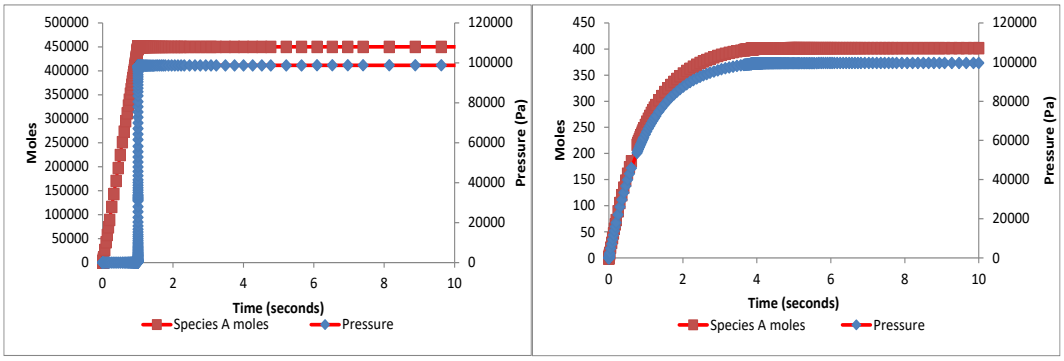

Figure 41 – Molar and pressure results of model 1-1-1-i (LHS) & model 1-1-1-ii (RHS)

Model 1-1-2 (Figure 42) is the model 1-1-1-ii with a flow from the compartment to a sink surroundings, forming a continuous flow system.

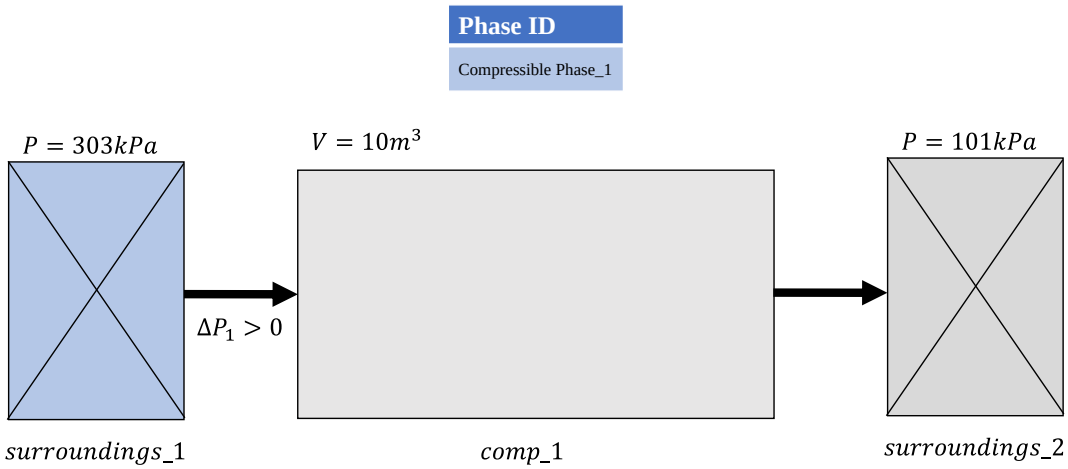

Figure 42 - Model 1-1-2

The feed surrounding of model 1-1-2 is artificially pressurised to 3 Bar (304 kPa), and the sink surrounding to 1 Bar (101kPa), as shown in Figure 43 (RHS). As expected, the surroundings pressures are constant throughout the simulation, whereas the compartment pressure rises to an equilibrium of 218kPa; from an initial value $\cong 0kPa$. The volumetric rate leaving the compartment to the sink surrounding is slightly higher than the flow rate entering from the source, resulting in a difference in volumetric flow rates Figure 43 (LHS), due to the pressure difference between source and compartment being greater than compartment and sink. However, the compartment volume is unchanged, as the equilibrium point is determined not by the volumetric flow but rather the molar balance, which is automatically determined by CompArt through the transience of the model.

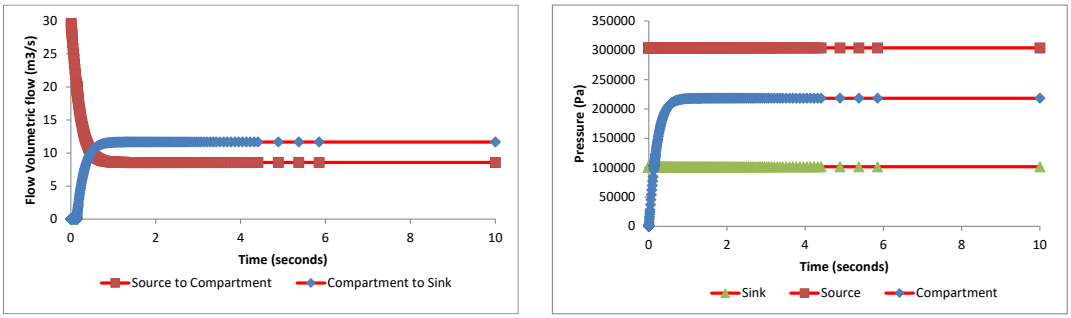

Figure 43 - Surroundings and Compartment and corresponding flow volumetric rates (LHS) and pressure (RHS), during simulation time for model 1-1-2.

5.2.2 Cell 1-2 – Linear series of compartments with Single Phase Convective flow

Within this cell of models, the models of the previous section 5.2.1 Cell 1-1 – One compartment, Single Phase Convective flow are taken and extended in size with an increased number of compartments, connected in unidirectional series with convective transport phenomena. The first model of the cell, Model 1-2-1-I is shown in Figure 44.

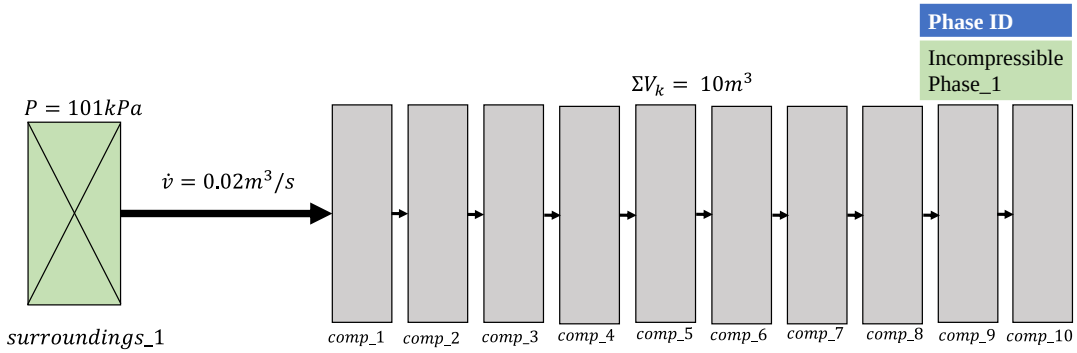

Figure 44 - Model 1-2-1-i

The results of model 1-2-1-i are shown in Figure 45, the legend refers to the number compartment in the series of model 1-2-1-i, with “1”, the first compartment connected to the source and “10” the last of which forms the end compartment of the series. This key will be used throughout the models of the chapter.

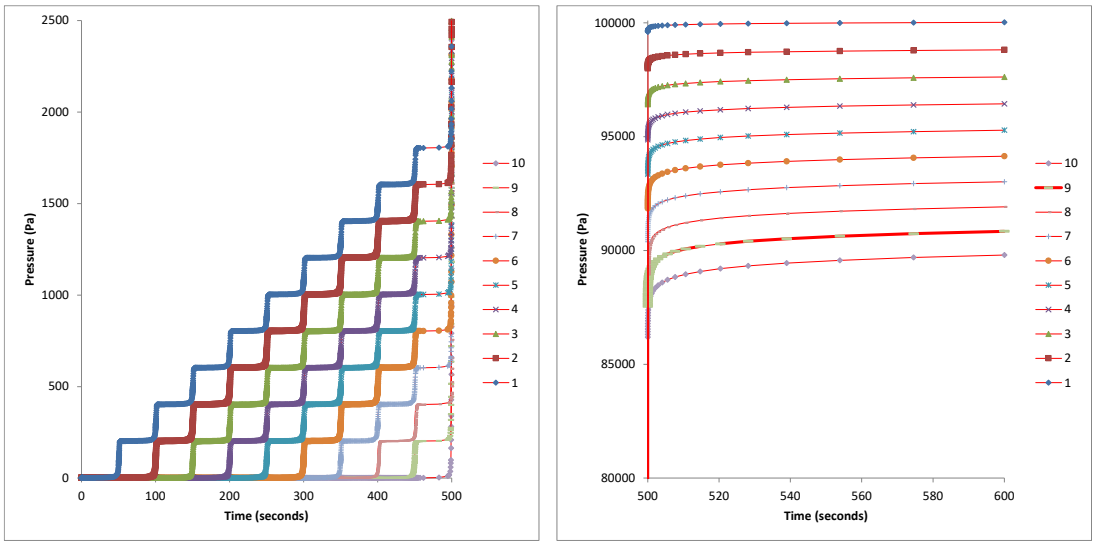

Figure 45 – Pressure of the consecutive compartments $(\mathbf{1 \rightarrow 10})$ of model 1-2-1-i.

The pressure of each compartment follows a step wise increase over the simulation time, a step occurring at each instance of a compartment reaching fill limit of incompressible material $V_k(t) = (1 - \alpha_k)V_k$; in order of compartment 1 to 10, until all compartments reach equilibrium pressures time of 600 seconds. Equilibrium pressure of a compartment is reached where the difference in compartment pressures connected by a flow is equal to 2% of the source compartment/surrounding pressure – the sigmoid activation rule; therefore, the pressures of compartments are not equal at the end of the simulation time (600s).

The stepwise pattern observed in Figure 45, between $0 \leq t \leq 500$, each step is due to the addition of anew compartment in the series causing the compartment pressures prior to plateau – the net molar change in the prior compartments equal to zero while the newly added compartment fills.

The equilibrium point of the simulation is reached when all compartments are filled with incompressible material, at which point the feed flow of connecting flows shut off due to a lack of a pressure driving force (each pair of compartments have less than the sigmoid activation percentage of 2%); see Figure 46.

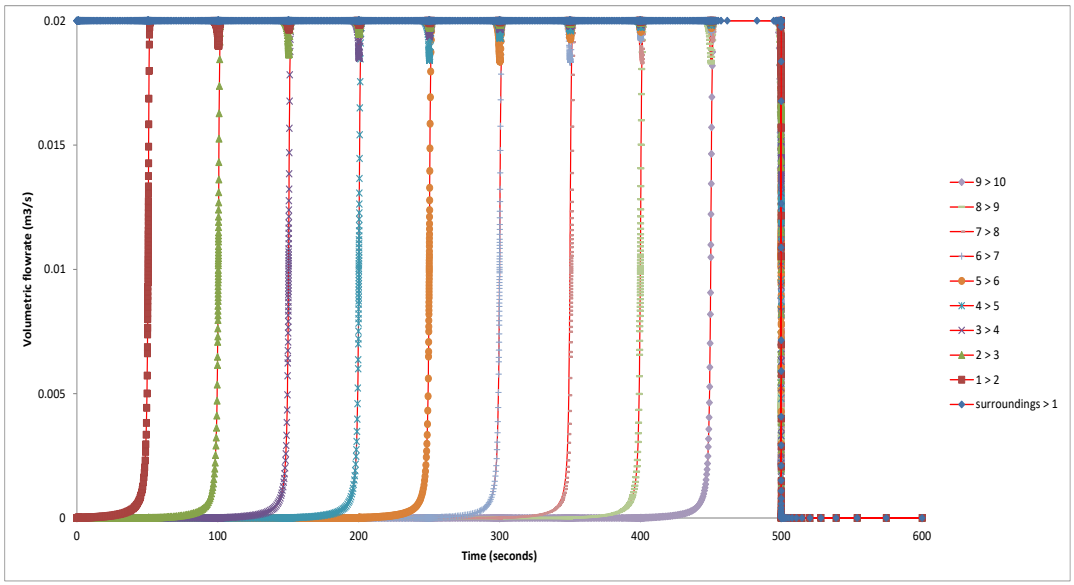

Figure 46 - Model 1-2-1-i flowrates connecting compartments in series

Model 1-2-1-ii is given in Figure 47, of the same structure as model 1-2-1-i but with a feed of compressible material as opposed to incompressible material.

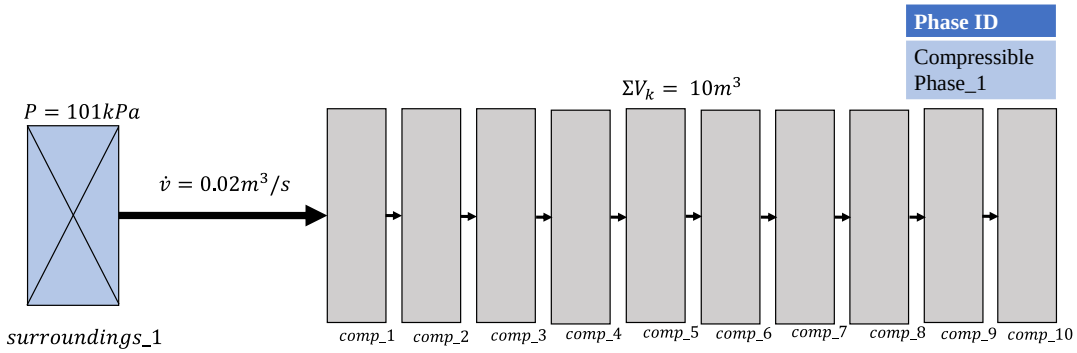

Figure 47 - Model 1-2-1-ii

From Figure 48 we see the immediate impact of compressible material upon the pressure of a compartment.

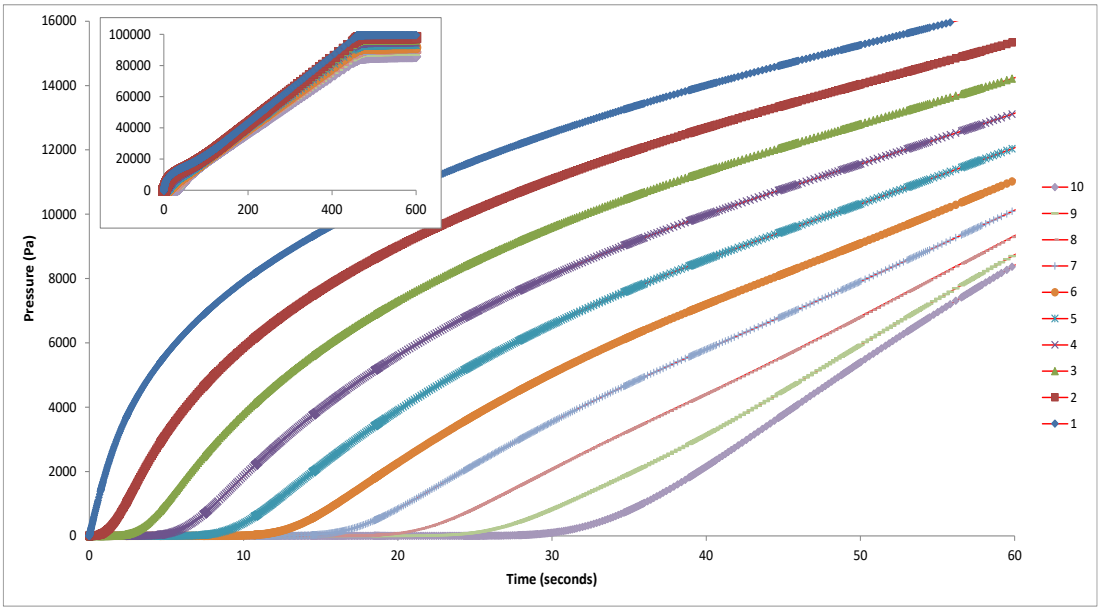

Figure 48 - Pressure evolution of series compartment, model 1-2-1-ii.

Like the incompressible model 1-2-1-i, the pressure driven flows are only activated when the pressure is 2% greater in the source compartment than the receiving compartment, see Figure 49 for velocity of flow during simulation time (as per section 3.5.1.1 The mode of transport). A unique concave bowing of pressure for the first three compartments is observed at the beginning of the run. The pressure curve is of a convex shape is observed for later compartments due to the decreasing pressure drop between compartments beyond the third, due to an increased number of compartments involved in the series sharing the total pressure drop.

As shown in the sub-plot of Figure 48, beyond $t = 50s$, the pressure of each compartment increases linearly with time until all compartments equal that of the feed surrounding.

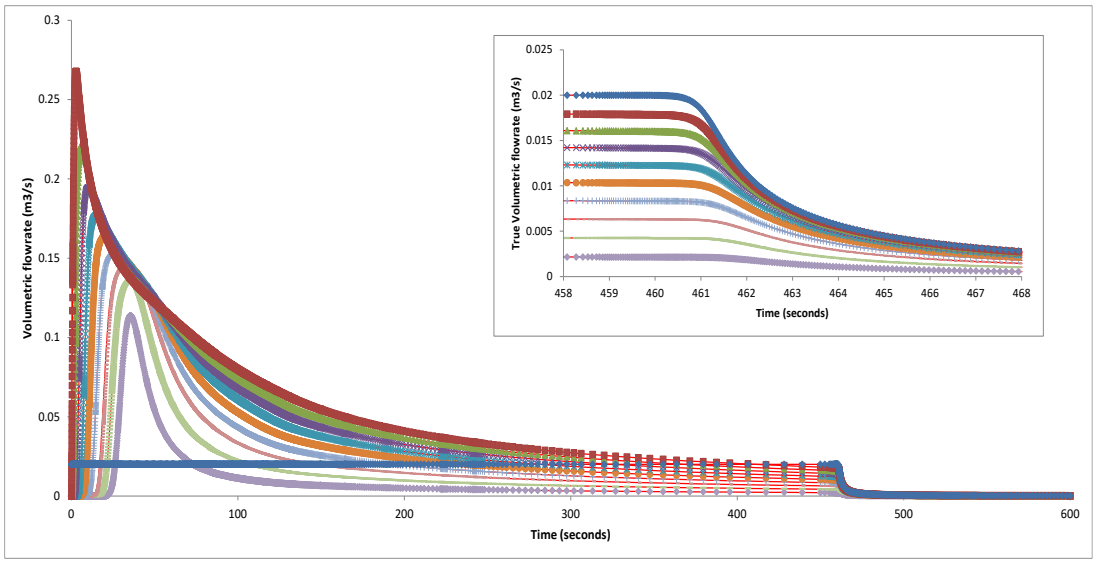

Figure 49 - Flowrates of convective transports (model 1-2-1-ii), showing decreasing rate for initiated flows with increasing compartment number.

At approximately 460 seconds, the flowrates of model 1-2-1-ii are switched off as all compartments reach a pressure equal to the source surroundings (101kPa), as indicated in Figure 49; and as expected.

The sub-plot of Figure 49 illustrates the gradual switch of flows from on to off, through the smoothing of the sigmoid activation function.

Model 1-2-2-i (Figure 50) is equivalent in structure to model 1-2-1-i, with an additional surrounding at the end of the series acting as a material sink.

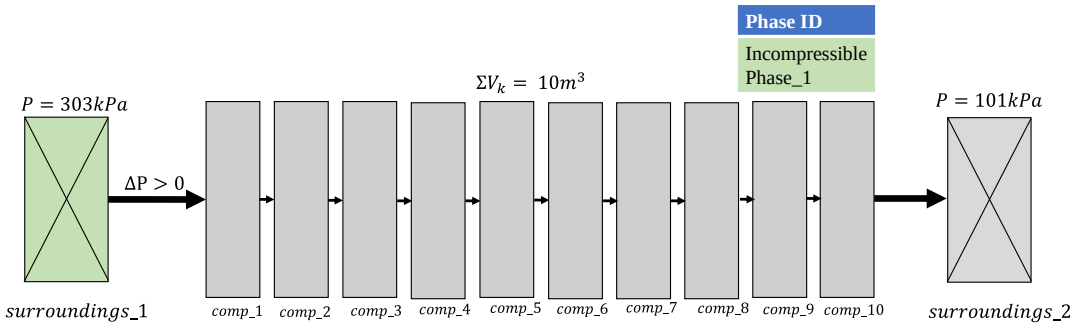

Figure 50 - Model 1-2-2-i

The pressure of each compartment in the series over the simulation time is given in Figure 51. The shape of both model 1-2-1-i and 1-2-2-i pressure plots (Figure 45 and Figure 51) are comparably the same prior to equilibrium. At equilibrium the shape deviates as the compartments of model 1-2-2-i remain

at a positive pressure gradient, within decreasing magnitude down the flow path of compartments in the series. Whereas the compartments of 1-2-1-i coalesce to the same pressure value. This is because the model 1-2-2-i is open and thus flow of material persists through the system at equilibrium. The equilibrium is reached faster in model 1-2-2-i due to the source surrounding being of 3x the pressure and thus 3x the flowrate feeding to the compartment series.

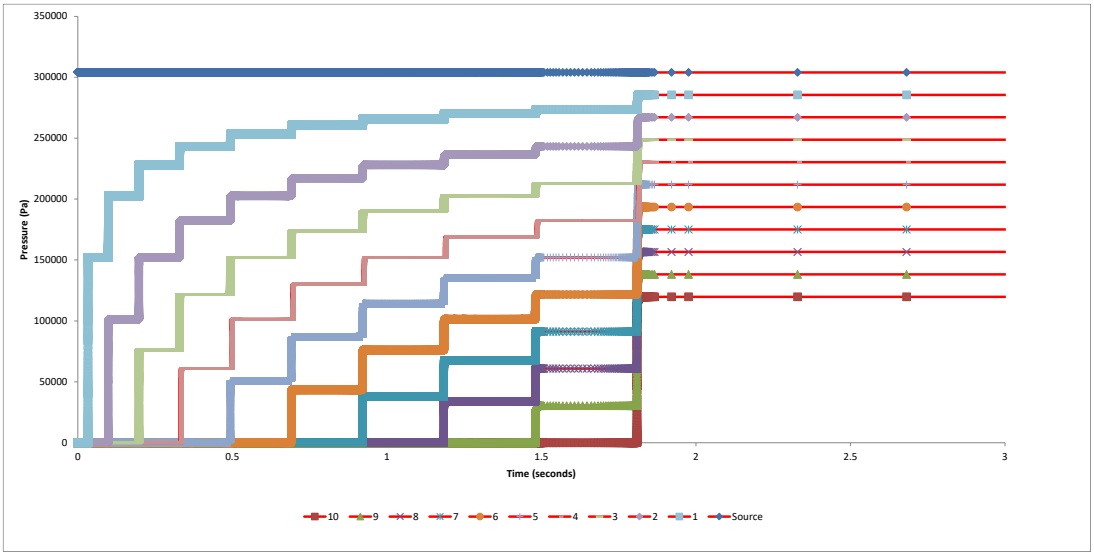

Figure 51 - Model 1-2-2-i compartment and source pressures; shows a stepwise increase in pressure then a fixed difference between compartments to propagate material through the series from the source to sink (303kPa & 101kPa respectively).

Similar behavioural changes observed between the models 1-2-1-i & 1-2-2-i are observed between the models 1-2-1-ii & 1-2-2-ii; illustration of Model 1-2-2-ii is given in Figure 52.

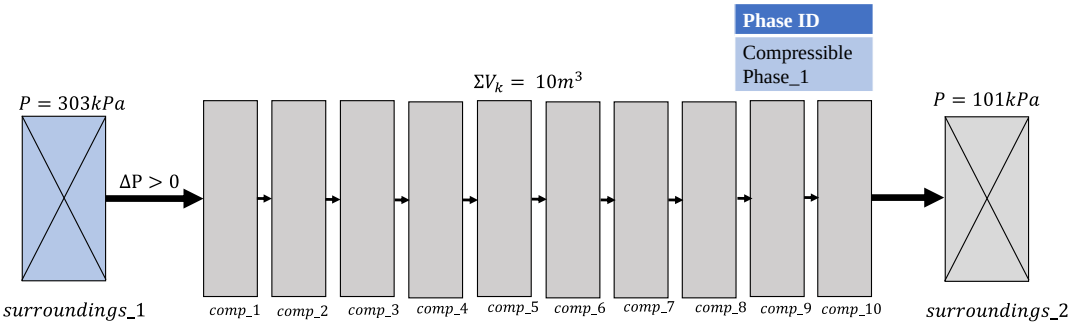

Figure 52 - Model 1-2-2-ii

The same shape of the pressure changes in Figure 48 is present within the results of 1-2-2-ii (Figure 53). The equilibrium pressure of each compartment decreases in magnitude down the length of the series. The equilibrium of model 1-2-2-ii differs to model 1-2-1-ii, plateauing with differences in pressure value between compartments instead of coalescing to a single equal pressure; present to propagate material through the open system.

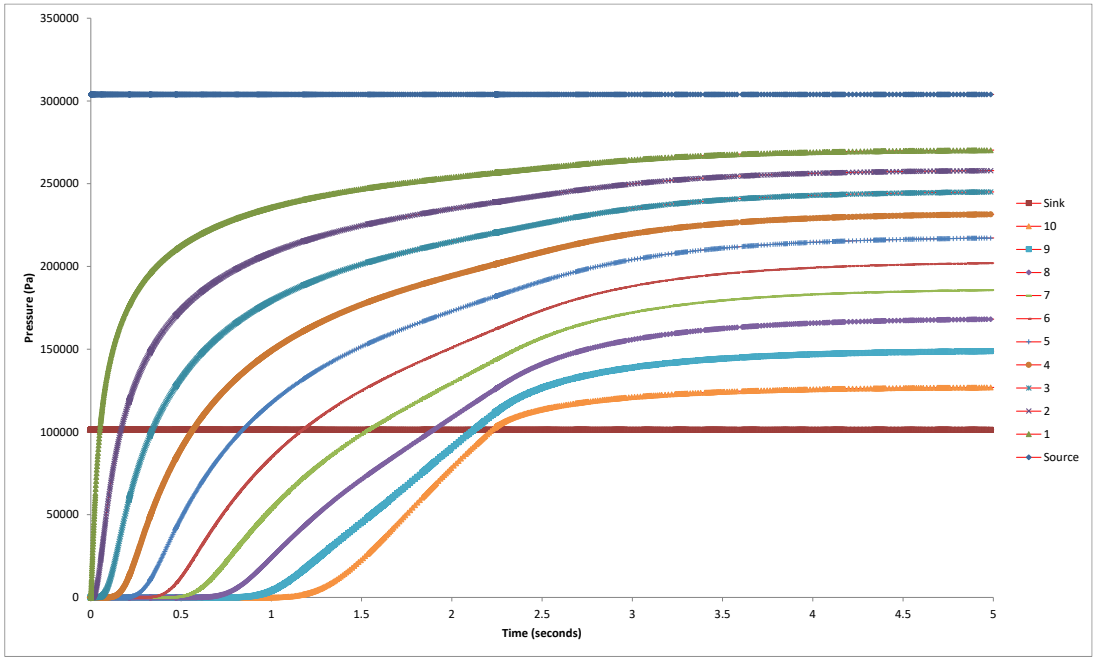

Figure 53 - Model 1-2-2-ii compartment pressures; follows the pressure dynamics of Figure 48, with an equilibrium pressure of each compartment sitting between that of the source and sink surroundings.

Open-systems with continuous flow driven by pressure difference between multiple-compartments can be formed with CompArt as demonstrated in the modelling of this cell. Compressible and incompressible systems behave in a similar manner when open or closed-systems, until equilibrium at which closed-systems halt in convective transport of material, and open-systems reach a pressure-difference equilibrium between compartments at which all convective transports balance. This equilibrium point of these systems is automatically located within the transience of the simulation.

5.2.3 Cell 2-1 - One compartment, Multi- Phase Convective flow

The models of cell 2-1 demonstrate the pressure driven convective transport of multi-phase flow. The multiphase flow fed to compartment 1 of model 2-1-1 (Figure 54) is of a phase molar ratio (compressible/incompressible) equal to 3.25.

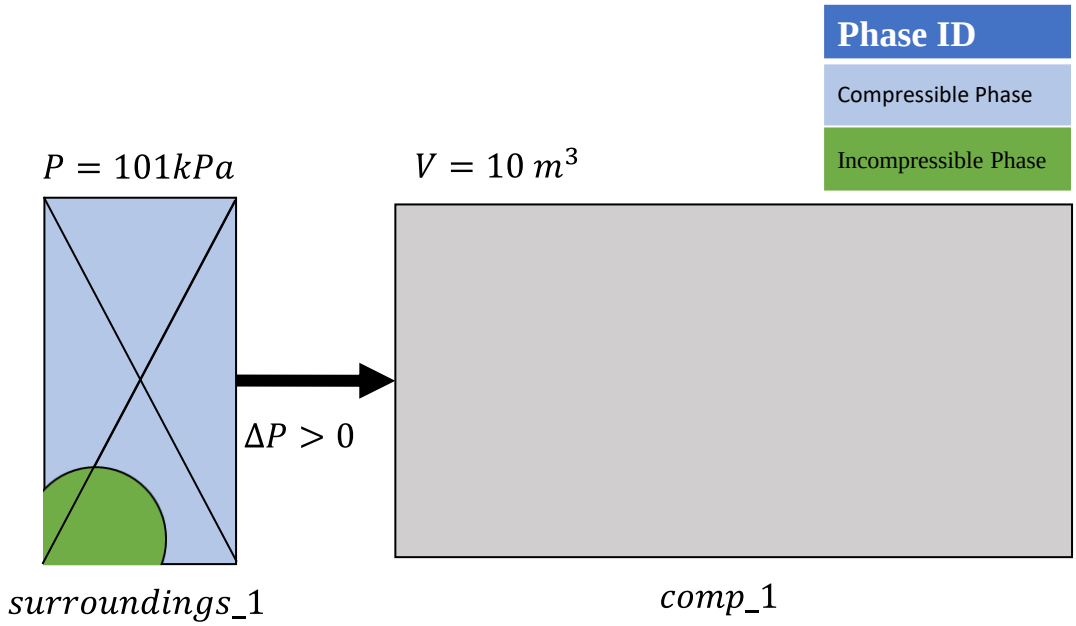

Figure 54 - Model 2-1-1

The molar quantities of the multiphase material in compartment_1 are given in Figure 55, along with the molar ratio, confirming the correct implementation of the multiphase flow phenomena.

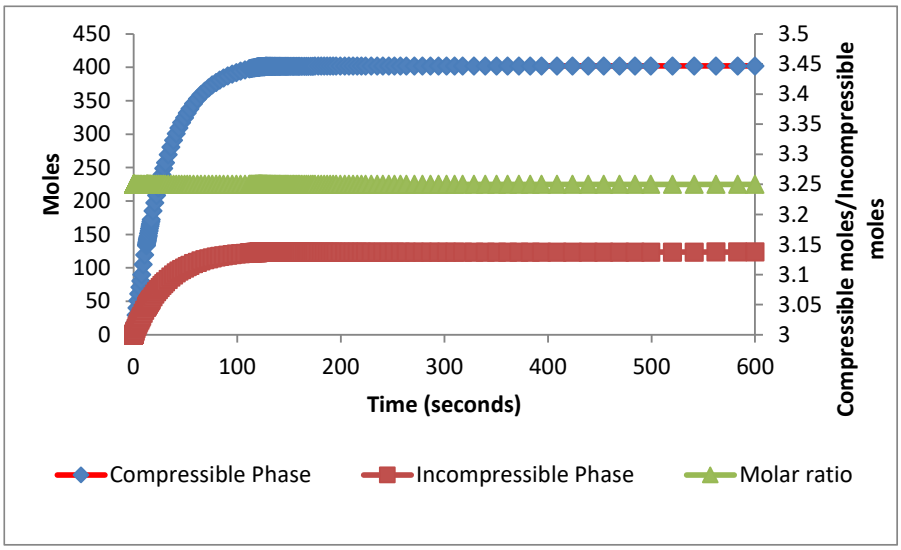

Figure 55 - Model 2-1-1; illustrating the correct ratio of compressible to incompressible moles within compartment_1 throughout simulation, equal to 3.25.

Model 2-1-2 is model 2-1-1 repeated with the material of the compartment discarded to a sink surrounding of low pressure, an open flow multi-phase model; illustrated in Figure 56.

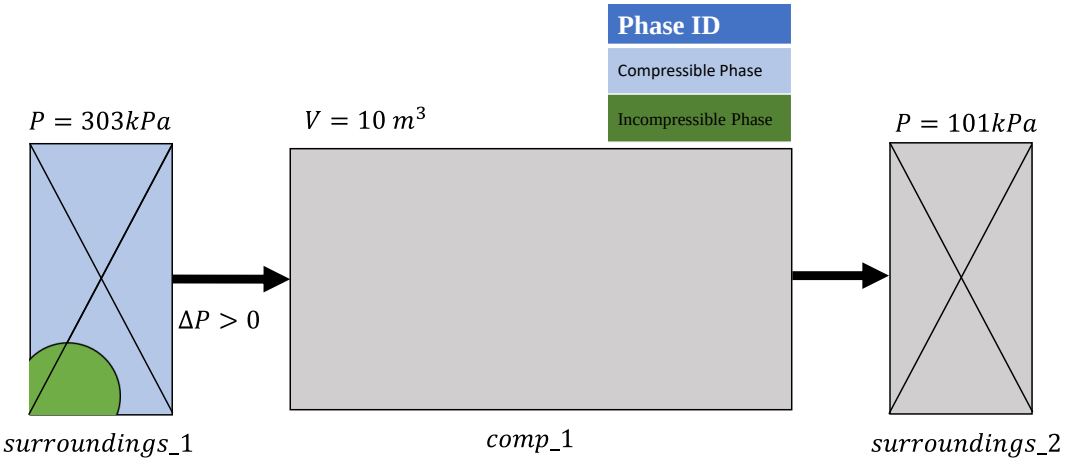

Figure 56 - Model 2-1-2

The pressure of the compartment is slightly higher in model 2-1-2 compared to model 2-1-1, as shown in (Figure 57), due to the requirement of the pressure difference between compartment and sink to be 2% of the compartment of greater to propel material through the open system, whereas model 2-1-1 was a closed system with fixed pressure source at 101kPa.

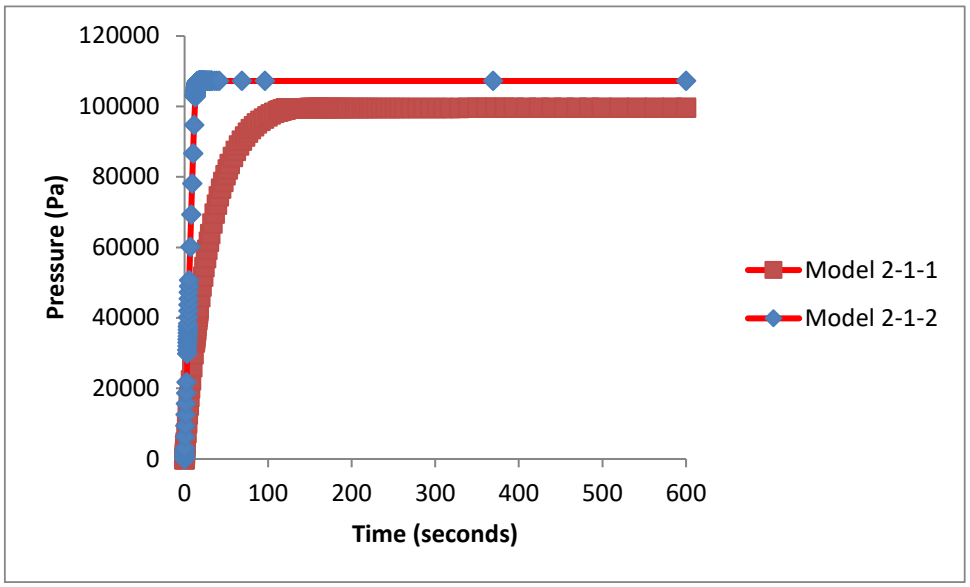

Figure 57 - Model 2-1-2 vs model 2-1-1 compartment pressures; illustrating the increase in pressure due to increased surrounding pressure of model 2-1-2.

The multiphase flow into and out of a compartment is proven accurate with the ratio of molar species in the compartment (equal to 3.25) equivalent to that in the feed surroundings; see Figure 58.

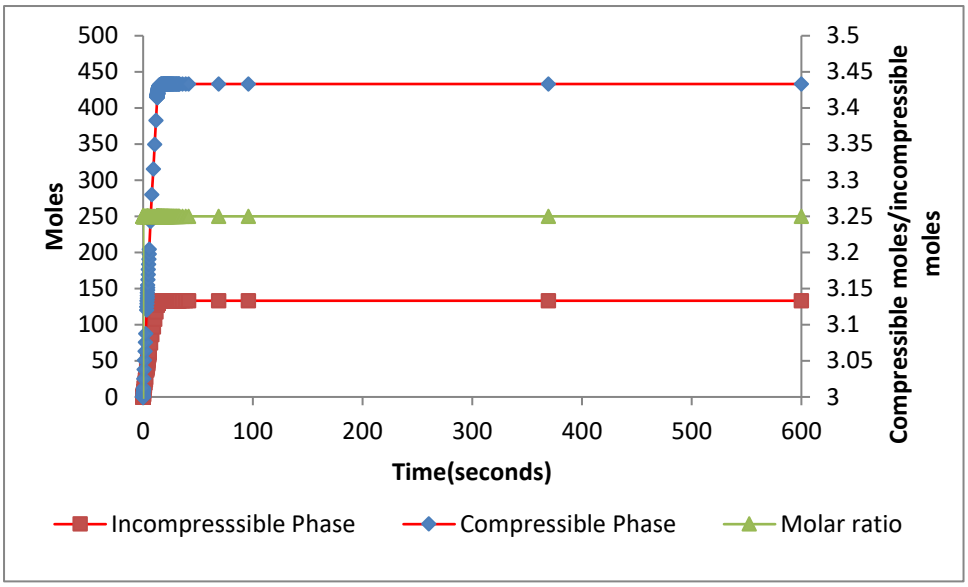

Figure 58 - Model 2-1-2; illustrating the correct ratio of compressible to incompressible moles within compartment_1 throughout simulation, equal to 3.25.

5.2.4 Cell 2-2 - Linear series of compartments with multi-phase Convective flow, and Phase Transport

Model 2-2-1 is a residence time distribution model, modelled as a chain of 10 compartments connected in series (Tanks-in-series model) with a sink surrounding – as illustrated in Figure 59.

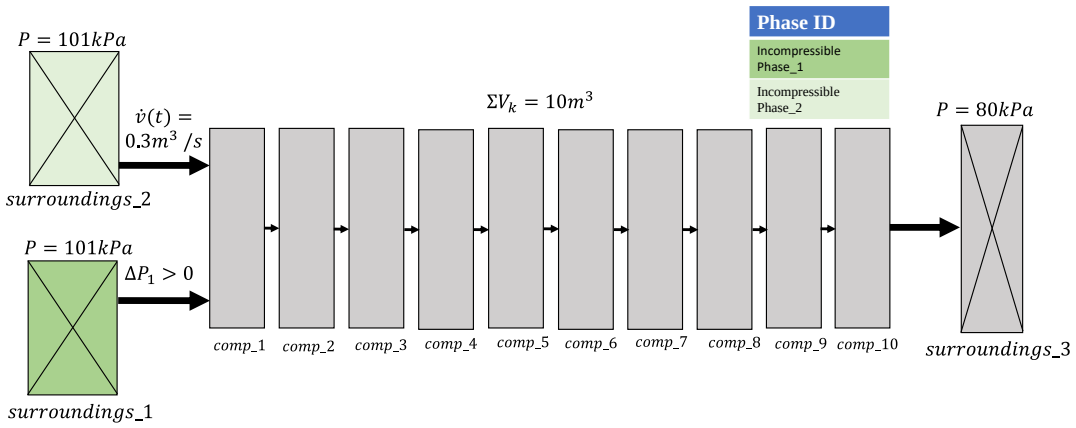

Figure 59 - Model 2-2-1

A feed of “phase_1” is passed through the series until the system is filled with phase_1, at which time ($t_{pulse} = 200s$) a small amount of immiscible incompressible phase “pulse_phase” (of species B) is injected into the first compartment of the system, referred to as ‘tracer’. The *max_step_size* property of the solver introduced in 4.6.2 Improving the resolution of a solution is utilised here to ensure the solver captures the pulse input to the model, of which spans only 1 second of the simulation time. The molar quantity of species B within each compartment of the system over the simulation time is given in Figure 60.

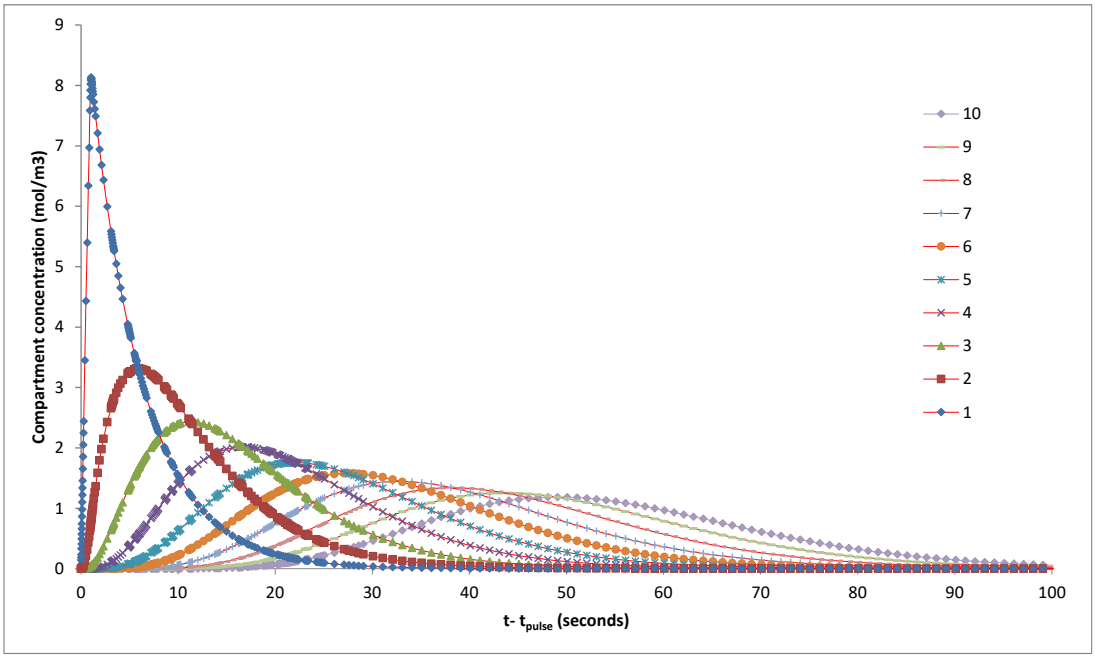

Figure 60 – Model 2-2-1. RTD of species B (of *pulse_phase*) through series of compartments of continuous phase (*phase_1*).

The concentration of tracer in the source surroundings is $300mol/m^3$, the pulse injection is of a volumetric flowrate of $0.3m^3/s$ and activated for 1 second. The expected maximum moles in compartment one is 90moles,

$$\left(\frac{300mol}{m^3} * \frac{0.3m^3}{s} * 1second = 90moles\right)$$

However, as shown in Figure 60, the maximum moles in compartment one is underestimated at $82moles$. This is likely due to a combination of the numerical solver identifying the initiation of the injection later than declared in the input file; the accuracy of the identification can be increased by decreasing the *max_step_size* property of the solver. And secondly due to pulse early injection pulse material passing through to the second compartment in the chain before the full 1 second has passed – reducing the maximum moles in compartment 1. And due to moles exiting compartment one whilst the pulse is fed.

Figure 60 shows the species B molar contents in each compartment, with a depletion in maximum quantity of material and increase in spread of the curve

as the material is propagated through the series of compartments – the dispersion of tracer material.

The exit age of B, Equation 100, is a function of concentration of [B] in the final compartment $[B]_{10}$, and the residence time of material of the system τ_{res}; τ_{res} is calculated from the E(t) curve per Equation 101, t_{pulse} is the time at which the pulse material is injected into the system in this example at 200 seconds.

$$E(t) = \frac{[B]_{10}(t)}{\int_{t-t_{pulse}}^{\infty} [B]_{10}(t)dt} \qquad \textit{Equation 100}$$

$$\tau_{res} = \int_{t-t_{pulse}}^{\infty} tE(t)\,dt \qquad \textit{Equation 101}$$

The number of tanks-in-series N is then analytically calculated as the square of the residence time of material in the system τ_{res} and variance of the $E(t)$ curve, σ^2; given in Equation 102 and Equation 103 respectively.

$$N = \frac{\tau^2}{\sigma^2} \qquad \textit{Equation 102}$$

$$\sigma^2 = \int_{t-t_{pulse}}^{\infty} (t-\tau_{res})^2 E(t)\,dt \qquad \textit{Equation 103}$$

A parallel is drawn between the tanks of the tanks-in-series model and compartments of this model, both acting as well-mixed CSTR's. Based on the procedure of Wiley, Hepburn and Levenspiel (1999), the value for number of tanks is calculated to be $N = 10.18$, an acceptable numerical error of 1.8%, the value near equal to the number of compartments utilised in the model (10) and hence validating the RTD. The residence time of material in the system is calculated from the known volumetric flow ($\dot{V} = 0.18m^3/s$) and total volume of the system ($V = 10m^3$) as $55.54s^{-1}$; the calculated residence time (Equation 101) based upon the simulation concentration of B is $55.4s^{-1}$.

Model 2-2-2 (Figure 61) tests the operation of the phase transport phenomena, the model is composed of a fixed series of three compartments with compressible phase (bubbles) transported through the series.

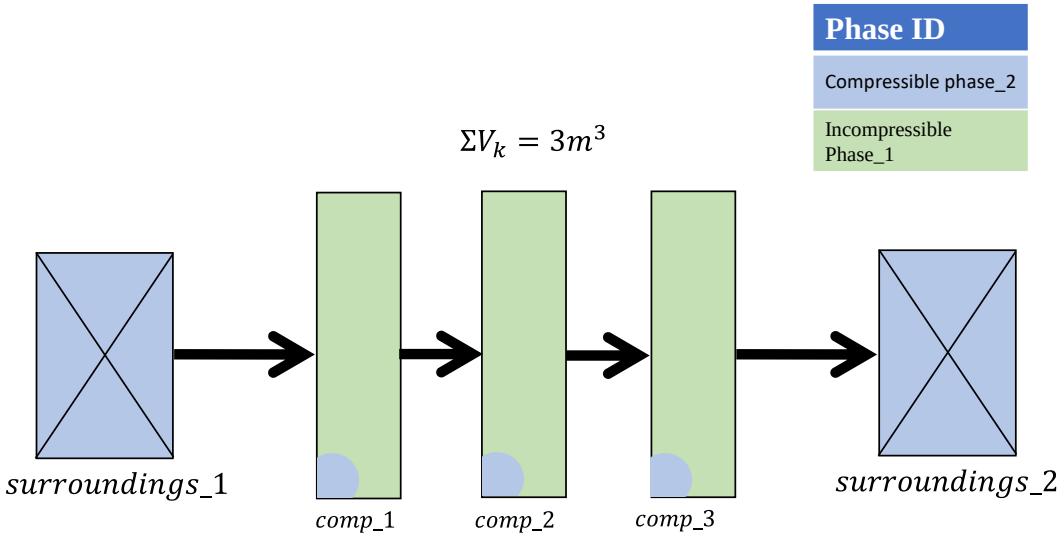

Figure 61 - Model 2-2-2

The flow of bubble phase is driven by the volumetric size of the bubble phase in the source compartment of each transport. The feed rate of compressible phase is fixed at $1000 m^3/s$ from the source surroundings. The compressible phase is propagated through the system at a volumetric rate of 33 m^3/s; a ratio of 30:1; see Figure 62.

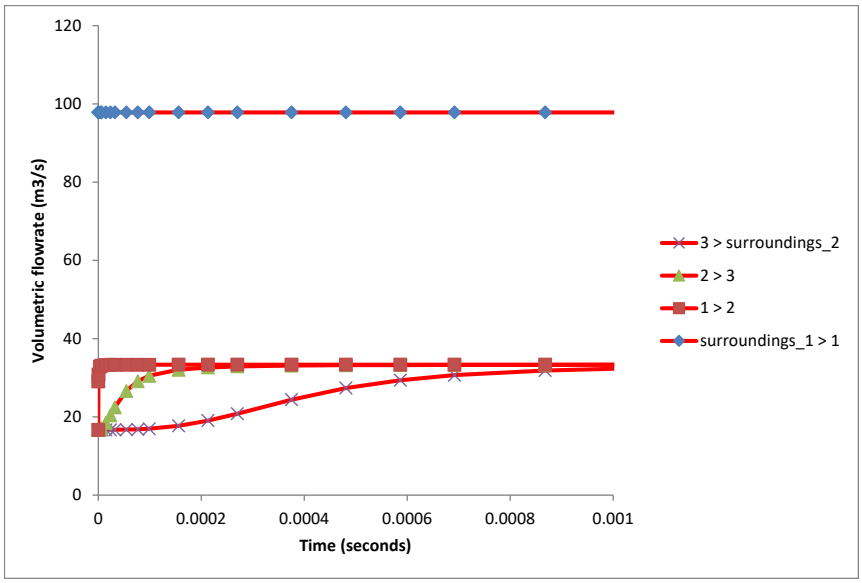

Figure 62 - Model 2-2-2 volumetric compressible phase transport rates

The imbalance in volumetric flows is expected due to a difference in compartment pressures and thus compressible phase volumes, the resultant concentrations of species A (bubbles) in the compartments, due to this difference in pressure, is much higher than the surroundings, at an equivalent and opposite ratio to the volumetric rate 1:30 (Figure 63).

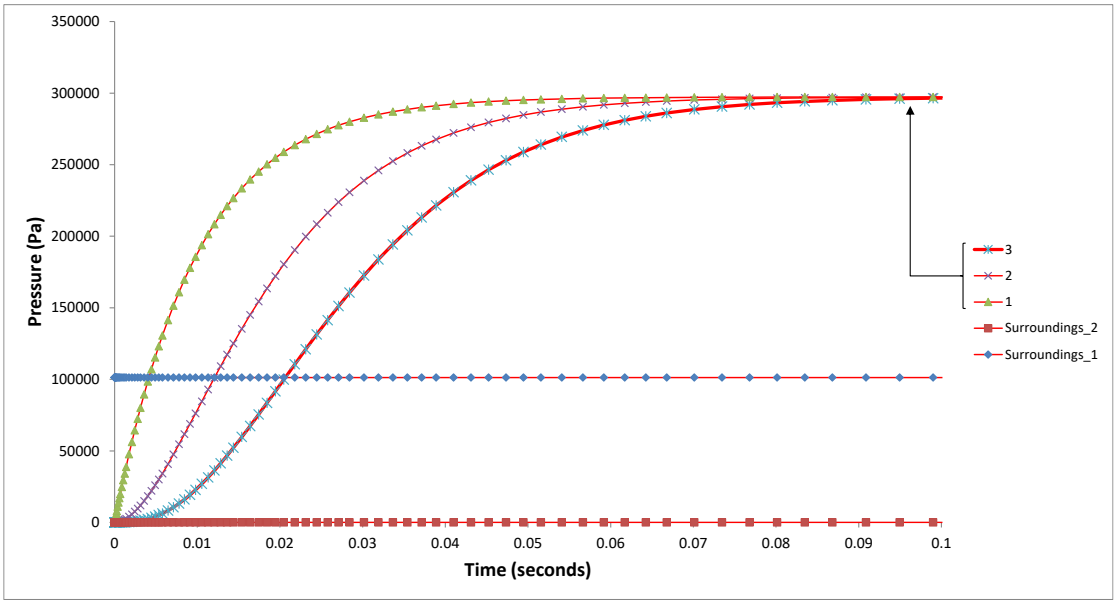

Figure 63 - Model 2-2-2 Compartment and surrounding pressures

5.2.5 Cell 3-1 – Single & interfacial Reaction

Model 3-1-1-i describes a pair of elementary competing parallel reactions, as illustrated in Figure 64.

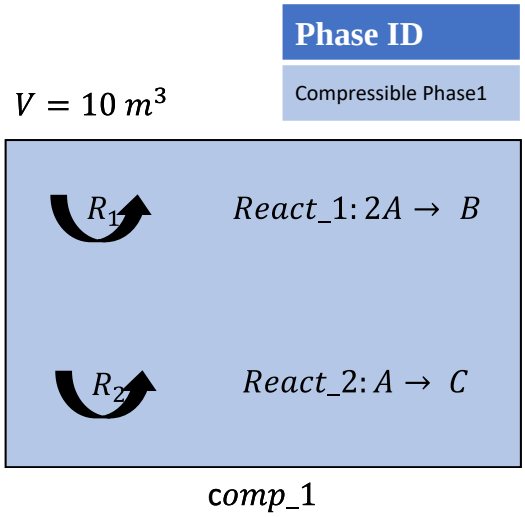

Figure 64 - Model 3-1-1-i

The concentration results of the simulation are given in Figure 65. To validate the reaction, the ratio of final species (B & C) at equilibrium are compared with the ratio of reaction constants associated with the product species. The concentration ratio at t=10s is $66: 27\ mol/m^3$ (Figure 65); this is equal to the ratio of reaction constants $0.6: 0.25$, validating the model.

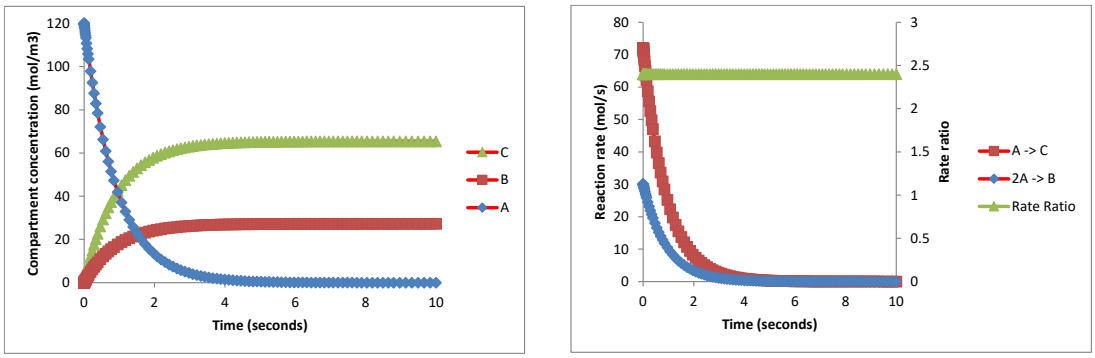

Figure 65 - Reaction rates (LHS) and species concentrations (RHS), model 3-1-1-i.

The rate of reaction of (A->C) is faster than (2A->B) as dictated by the larger reaction constant. Throughout the reaction time, the ratio of rates is constant, equal to the ratio of kinetic constants, further validation to the correct simulation of the competing parallel reaction.

Model 3-1-1-ii is a pair of series reactions, (A->B->C), taking place within the same compressible phase of compartment “comp_1” – illustrated in Figure 66.

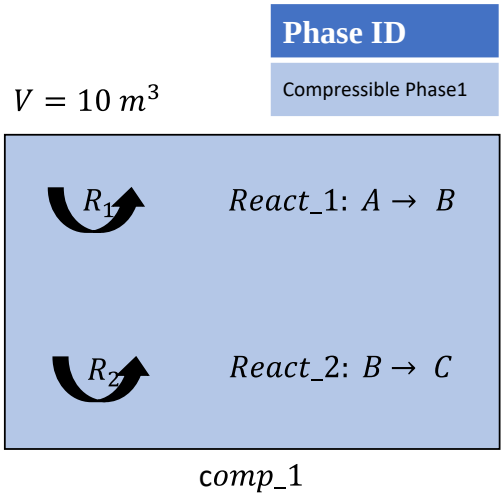

Figure 66 - Model 3-1-1-ii

Equation 104 is the analytical equation to determine the time at which the intermediate product is at its maximum value.

$$t_{max,[B]} = \frac{\ln\left(\frac{k_2}{k_1}\right)}{k_2 - k_1} \qquad \textit{Equation 104}$$

From the simulation, the time at which the concentration of B is at its maxima is $t = 2.56$s; the maxima data point is labelled in Figure 67. Inputting the kinetic constants of the reaction's series $(k_1 = 0.25, k_2 = 0.6)$, $t_{max,[B]} = \frac{\ln\left(\frac{0.6}{0.25}\right)}{0.6-0.25} = 2.5$.

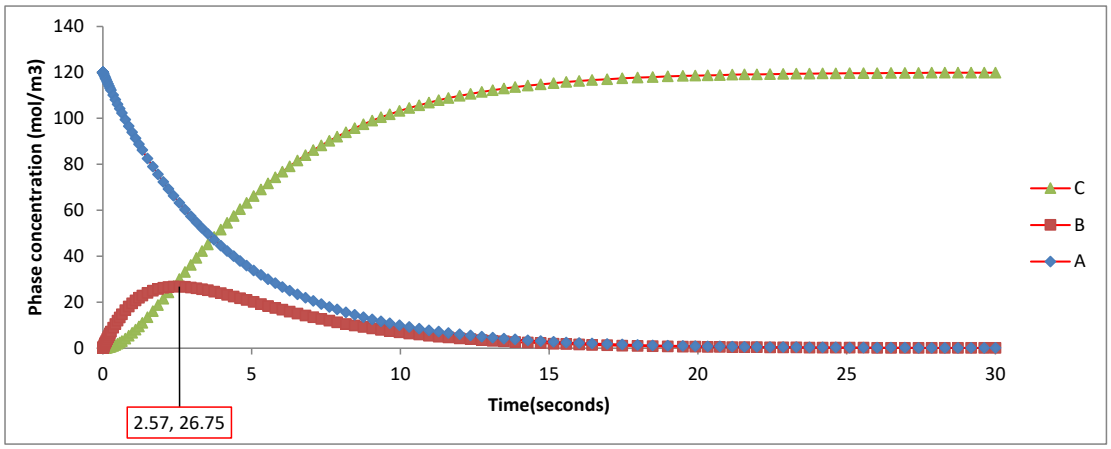

Figure 67 - Model 3-1-1-ii concentration plot of A->B->C.

Model 3-1-2 (Figure 68) demonstrates the multi-phase reaction modelling capability of CompArt. In this case reactants from two differing phase combine to form a product of a single phase.

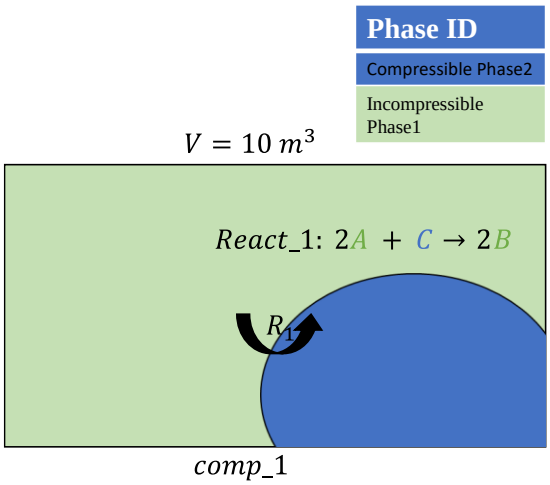

Figure 68 - Model 3-1-2

The reaction (2A+C->B) is 1st order, the resultant concentration and mole quantities for each of the species are given in Figure 69.

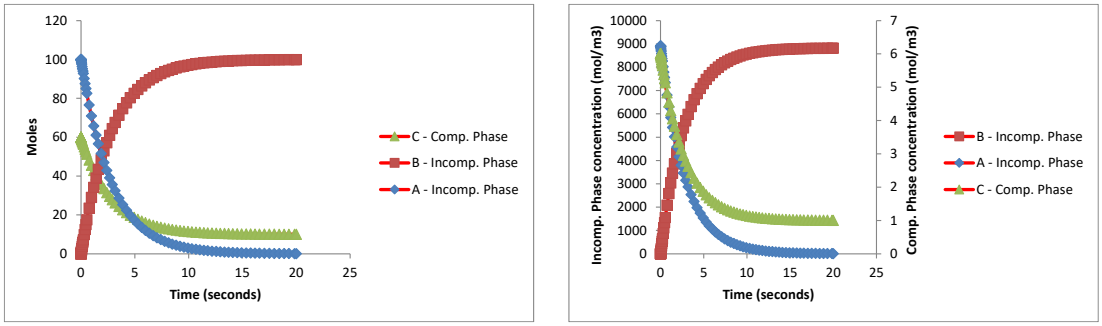

Figure 69 - Model 3-1-2 Molar (LHS) and concentration (RHS), quantities through the simulation.

The concentration profiles of Figure 69(RHS) show an increase in concentration of product B and decrease in concentration of reactants A and C. The compressible reactant concentration of C is plotted on the secondary y-axis as it is 10^{-3} the magnitude of the incompressible species A and B. This is because the compressible material inhabits 99% of the compartment volume, as the moles of the incompressible are extremely low throughout simulation, see Figure 69(LHS); and so are diluted. The reactant moles remaining, post-reaction, are 10 moles of C and 0 moles of A; this aligns with

the stoichiometry of the reaction e.g., 100 moles of A are consumed, 50moles of B are consumed and 100 moles of C are produced.

This model demonstrates the multi-phasic reaction phenomena, and the automatic population of species from the input file description. The component B was not specified in the input file but appended to the correct phase by CompArt pre-simulation.

Model 3-1-3 (Figure 70) is a simple first order reaction, utilising the Arrhenius equation to determine the kinetic constant as a function of compartment temperature; the model has two compartments.

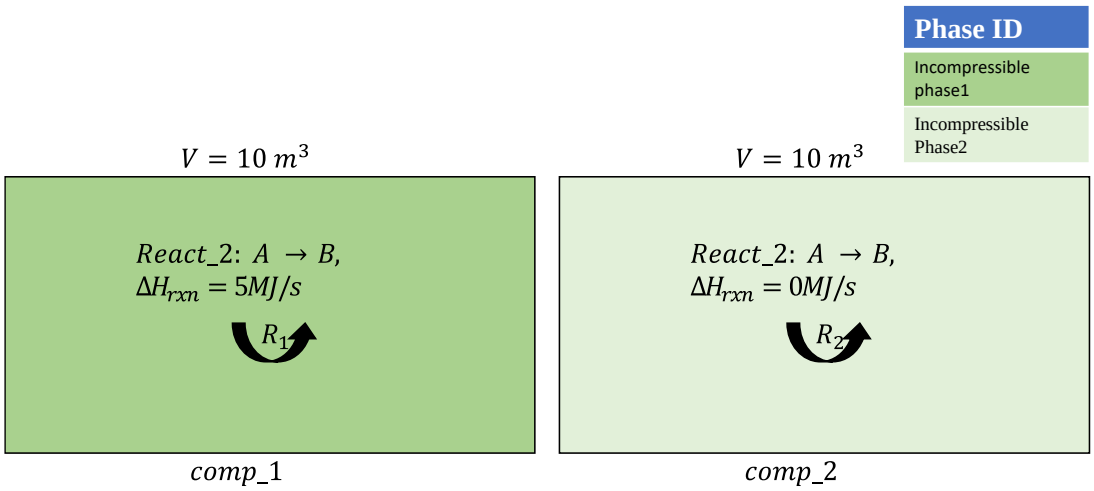

Figure 70 - Model 3-1-3

Both compartments are identical except the enthalpy of reaction phenomenon is set to $\Delta H_{rxn} = 5MJ/mole$ in the first compartment and $\Delta H_{rxn} = 0MJ/mole$ in the second compartment. The reaction rate of the second compartment ($\Delta H_{rxn} = 0MJ/mole$)is exclusively a function of species A concentration, with a decreasing rate following the depleting concentration as shown in Figure 71.

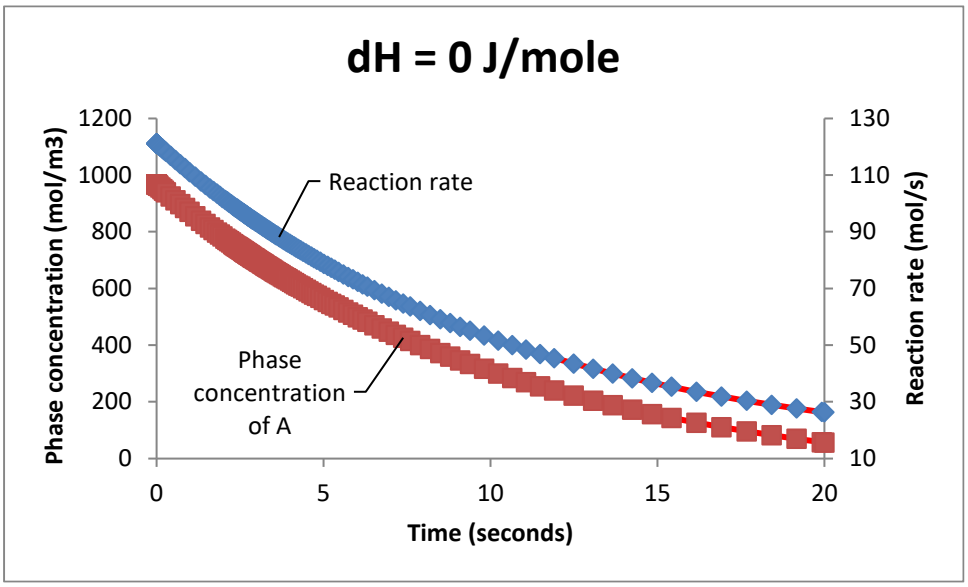

Figure 71 - Model 3-1-3, $\Delta H_{rxn} = 0 MJ/mole$

The endothermic reaction of the first compartment reduces the sensible enthalpy of the compartment over time, decreasing the temperature of the compartment as it proceeds. The reducing temperature over the course of the reaction contributes to a decrease in reaction rate as shown in Figure 72.

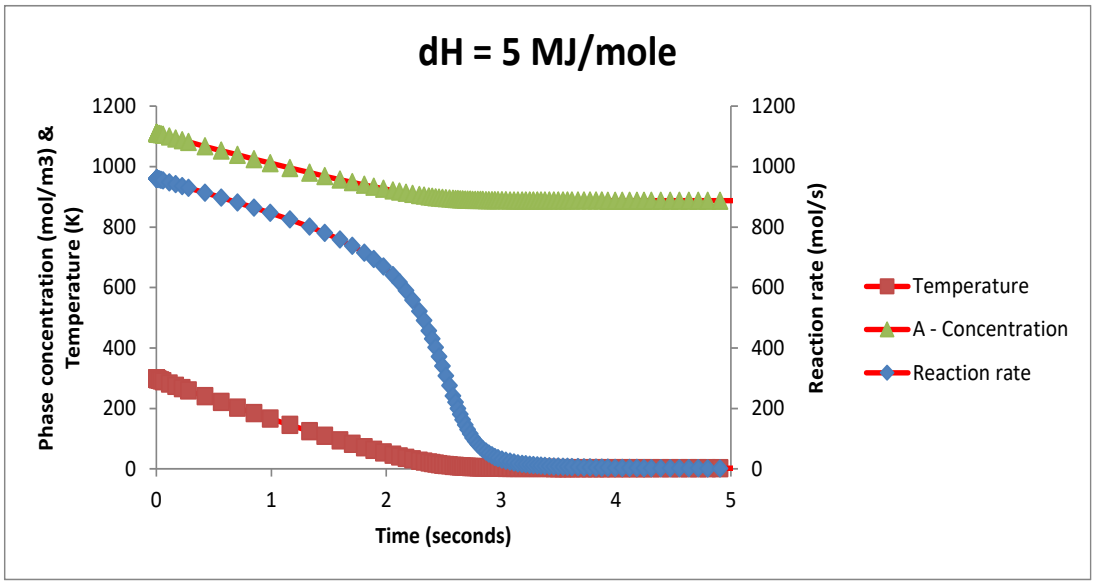

Figure 72 - Model 3-1-3; endothermic reaction with Arrhenius equation control. $\Delta H_{rxn} = 5 MJ/mole$

For the reaction with $\Delta H_{rxn} = 5 MJ/mole$, the rate progresses linearly with concentration until $t = 2s$, where the temperature of the compartment nears $75\ Kelvin$; as indicated in Figure 72. From $t = 2 \rightarrow 3s$, an exponential

decrease in reaction rate occurs, with the temperature of the compartment slowing in descend; the equilibrium point is reached with the temperature of the compartment $T = 0K$ and reaction ceased. The exponential decrease in reaction rate between the times $t = 2 \rightarrow 3s$ is instigated by the Arrhenius equation's exponential decrease during this period, functional of the temperature (see Figure 73).

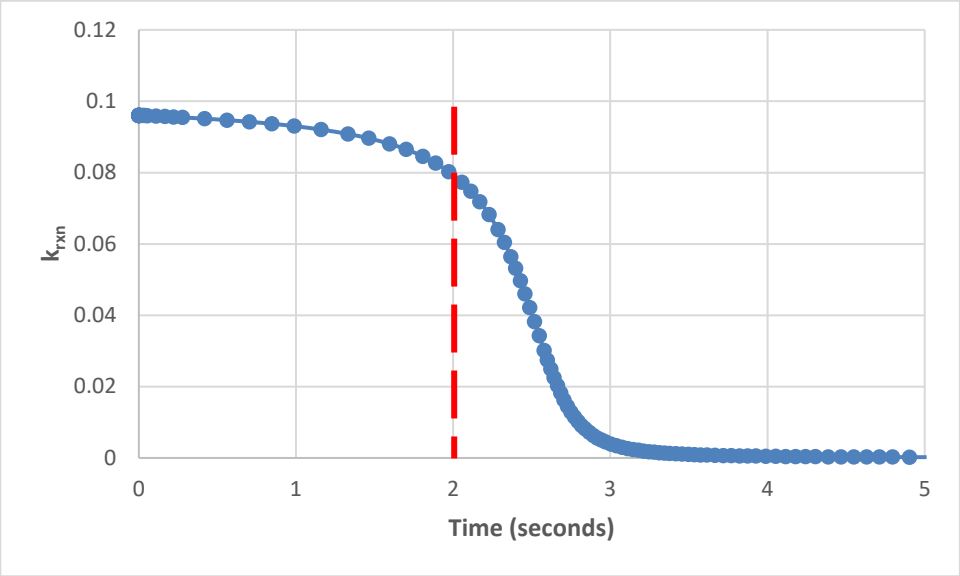

Figure 73 - Model 3-1-3; Exponential decay of reaction kinetic constant via Arrhenius equation, due to decrease in compartment temperature.

Although at $t = 3s$ the concentration of species A is at $800\,mol/m^3$ (abundant), the reaction cannot proceed as the temperature dictates a zero-value kinetic constant of reaction. From experiment it is observed that without the Arrhenius equation to limit reaction based on temperature, a situation may arise where an endothermic reaction depletes the system enthalpy to a point where a negative temperature results, breaking the simulation space.

Within this cell of validation, multiple reactions within a single phase and between phases has been demonstrated to operate as expected. The enthalpy of reaction and temperature dependence of the Arrhenius equation have been validated. The Arrhenius equation limits the operation of reactions to operate within the bounds of temperature activation, without the implementation of the Arrhenius equation a highly endothermic reaction with

sufficient reactant material could result in thermodynamically unachievable temperatures.

5.2.6 Cell 4-2 – Inter-compartmental Mass Transfer

Model 4-2-1 (Figure 74) illustrates the diffusive mass transfer of species A between two compartments (inter-compartmental).

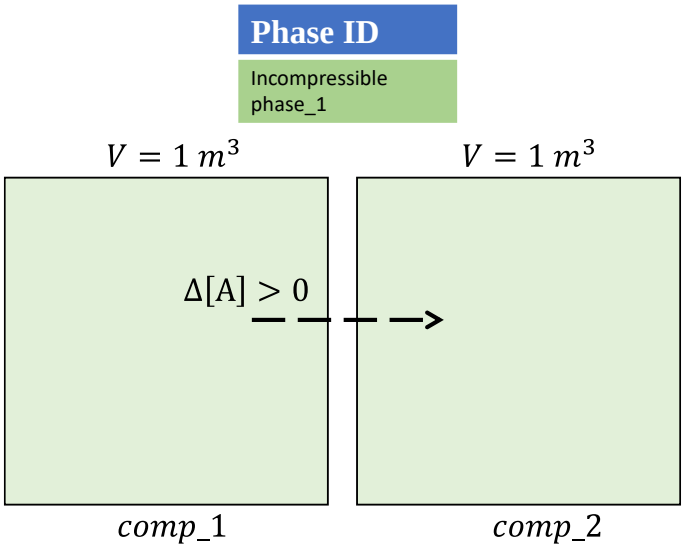

Figure 74 - Model 4-2-1

The rate of mass transfer is linearly related to the driving force, the difference in phase concentration of species A between the continuous phases of the connected compartments. This linear relationship is confirmed in Figure 75, the rate of mass transfer continues to decrease with decreasing driving force, $\Delta[A]$.

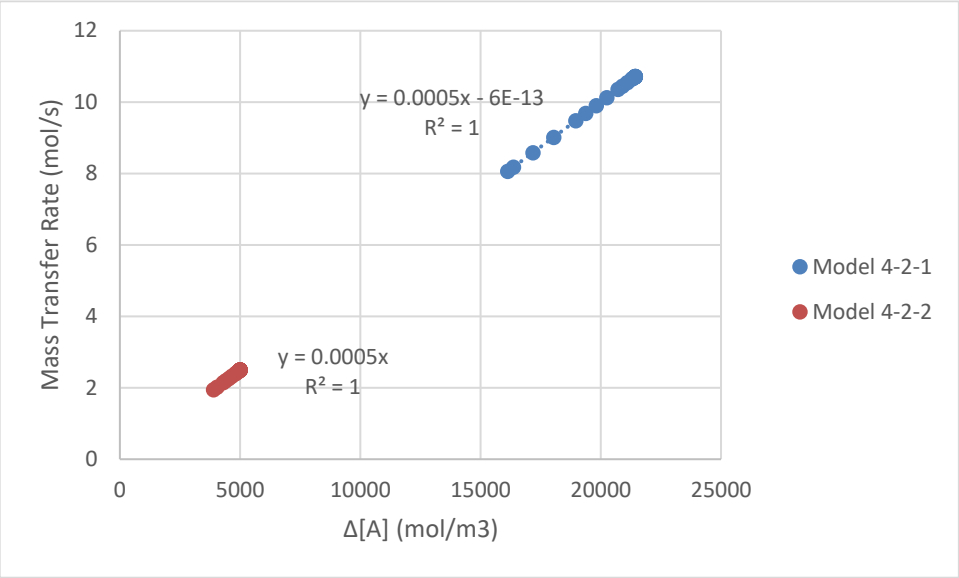

Figure 75 - Linear relation of MTR rate to $\Delta[A]$ of transfer connected continuous phases.; Model 4-2-1 & Model 4-2-2.

The same plot of concentration driving force and MTR rate is given in Figure 75 for model 4-2-2 (Figure 76), this model differs in that mass transfer of species A is from a compressible continuous phase to the incompressible continuous phase (differing phase nature MTR).

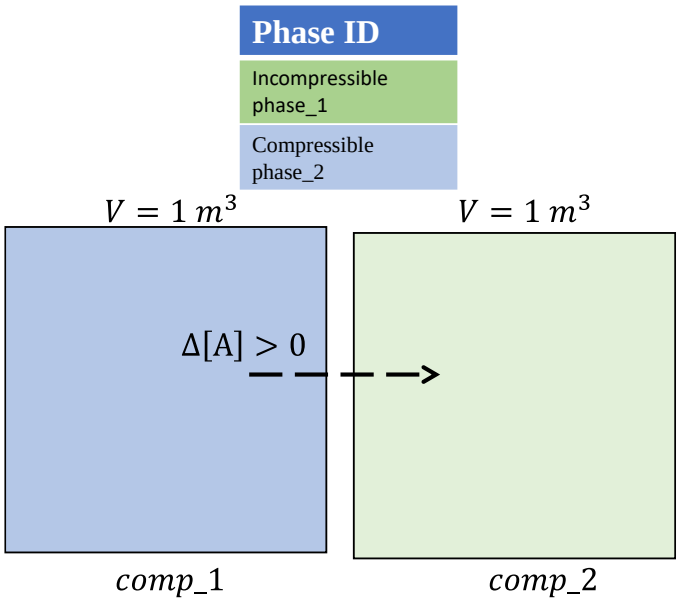

Figure 76 - Model 4-2-2

The linear relationship is as observed in 4-2-1 is present in model 4-2-2. However, the concentration difference and MTR ranges are comparably

smaller than model 4-2-1. The reduced concentration difference is due to the source of the same molar amount of species A (of model 4-2-2) being within a compressible phase which inhabits the entirety of the compartment volume – as opposed to a small fraction of the compartment volume in the case of the incompressible model (model 4-2-1). And thus, in model 4-2-2, the species is distributed amongst the entire compartment volume, whereas in model 4-2-1, the incompressible species is within a phase volume of approximately 20% of the compartment volume; based upon the density of the phase and molar quantity of solvent and species A.

5.2.7 Cell 5-1 – Intra-compartmental Mass Transfer

The mass transfer of species A from the compressible continuous phase to incompressible dispersed phase of the same compartment is presented in model 5-1-1; illustrated in Figure 77.

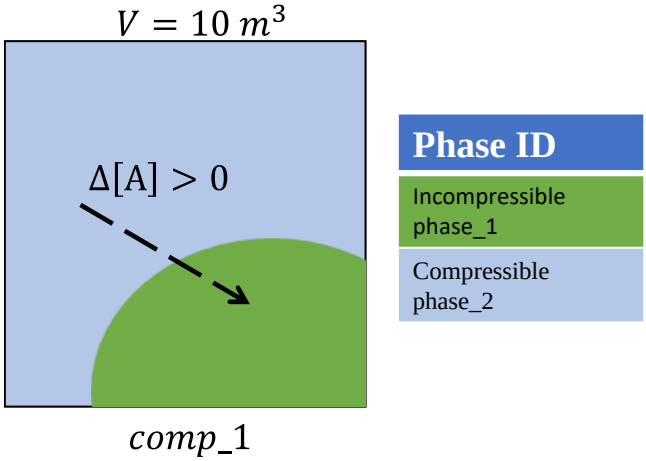

Figure 77 - Model 5-1-1

The partition coefficient of the transfer is $S = 10$. To validate this phenomenon, we expect the ratio of species phase concentrations to be equal to this value at equilibrium; at which point the driving force of the mass transfer is null. As the mass transfer is reducing the molar number of compressible species in the compartment, a decrease in the pressure is also expected with a halt in pressure change where no driving force is present. The results of the simulation are presented in Figure 78; the molar concentration ratio of

compressible to incompressible species A converges to 10 and the pressure of the system decreases as the mass transfer proceeds in line with reduction in compressible phase moles and the partition constant $S = 10$.

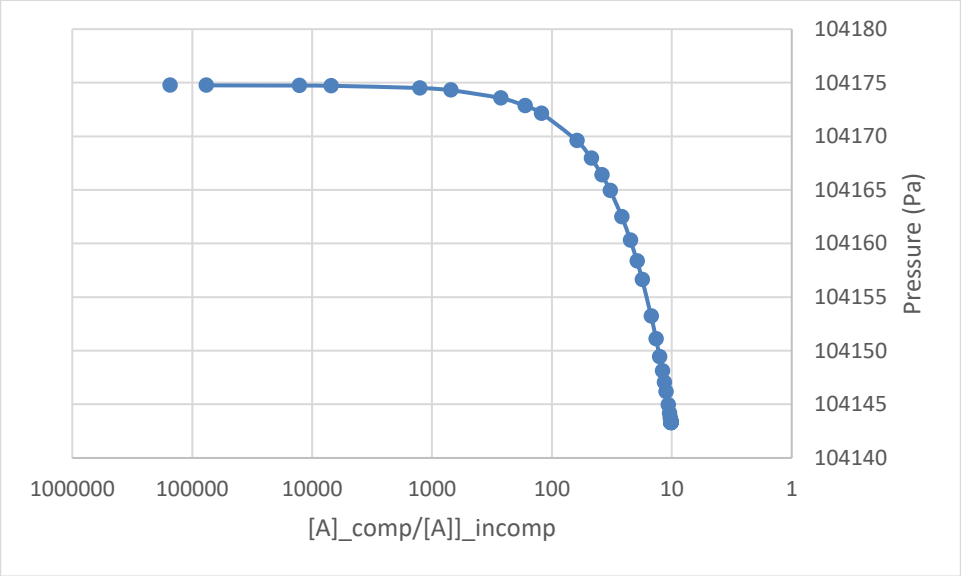

Figure 78 - Model 5-1-1; the ratio of species A phase concentration decreases to a value of 10, equal to that of the partition coefficient of the phenomenon. The compartment pressure decreases as the molar concentration of A in the compressible phase decreases.

The area of mass transfer (A) is a function of dispersed phase volume (V) and dispersed phase characteristic area ($D_{p,j}$), Equation 105 repeated from section 3.2.2 Phase.

$$A = \frac{6V}{D_{p,j}} \qquad \textit{Equation 105}$$

In Figure 79 the plot of mass transfer area vs dispersed phase volume produces a linear fit of equation $y = \left(\frac{1}{6}\right)x$; where x is the dispersed phase mass transfer area and y is the dispersed phase volume. As $D_{p,j} = 1$, the relationship between the plotted data is identical to Equation 105, validating the area calculation within CompArt. The volume of the dispersed phase increases as specie material is passed to it increasing its molar quantity and thus volume.

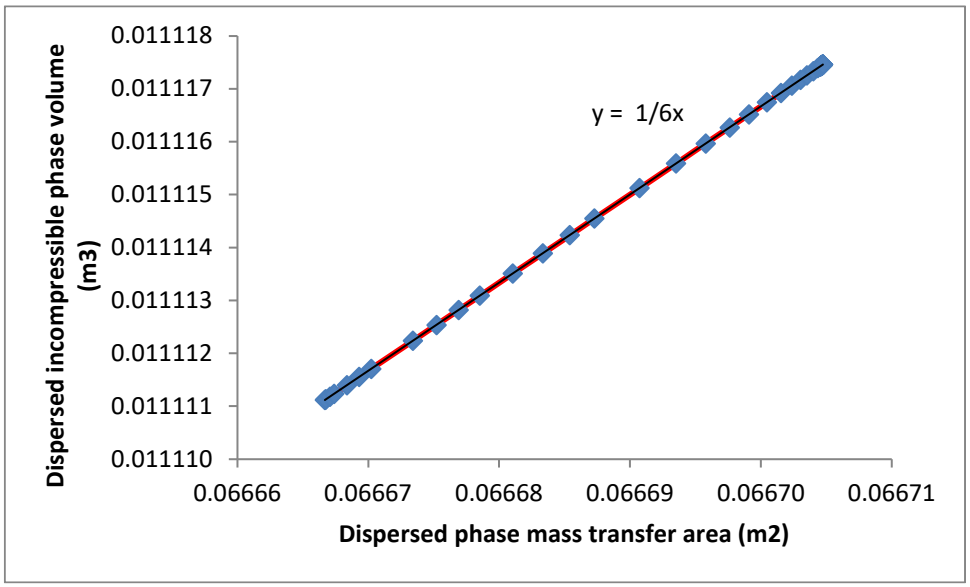

Figure 79 - Model 5-1-1; Automatic area calculation, functional of dispersed phase volume.

5.2.8 Cell 6-1 – One Compartment Heat Transfer

The heating of a compartment from a fixed temperature surrounding is the simulated in model 6-1-1 – see Figure 80 for the illustration of the model.

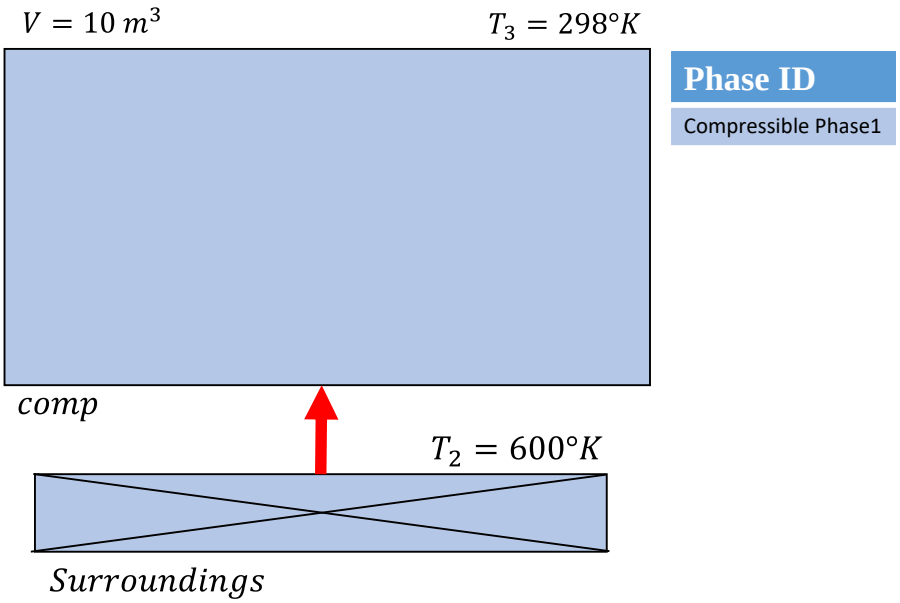

Figure 80 - Model 6-1-1

Initially the temperature difference between the surrounding and compartment is positive in the direction of transfer towards the compartment. A transfer of

heat ensues at a rate equivalent to the dynamically changing temperature difference and heat transfer coefficient $U = 1000W/m^2K$; until the driving force is no longer present.

The temperature and heat transfer rate results of model 6-1-1 are given in Figure 81.

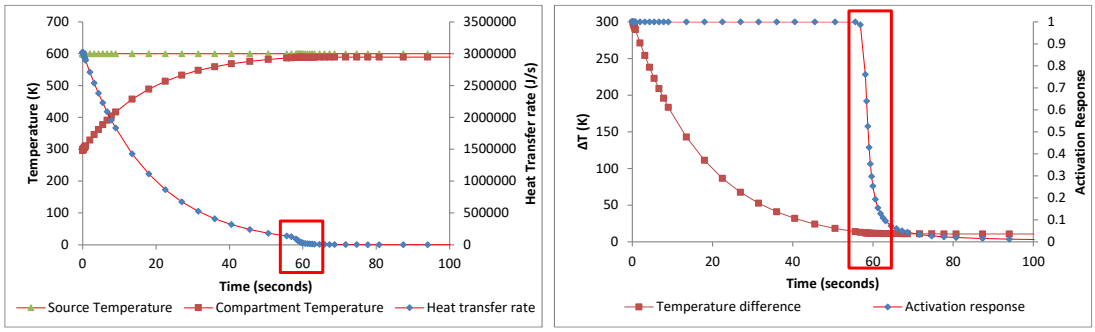

Figure 81 - Model 6-1-1; temperature increase of compartment 1 towards the source temperature, with depleting heat transfer rate as ΔT driving force decreases.

The expected trend of increasing compartment temperature towards the temperature of the source, is observed. The rate of heat transferred, decreases with time due to a decreased temperature driving force between the source surrounding and compartment. The tail of the heat transfer rate plot ($t \approx 60s$) shows a sudden drop in value, highlighted in Figure 81 within the red box. This drop is due to the heat transfer turning off, being deactivated by the sigmoid control (section 3.5.1.1 The mode of transport). The sigmoid which controls the heat transfer activation is plotted in Figure 81 for confirmation; deactivating when the temperature difference reaches $9.96K$. This is a large temperature difference to be accepted at equilibrium, however correct as the error of the sigmoid is set to 2% of the source temperature of approx. $10K$. Reduction of this error is easily controlled by setting a lower accepted error percentage for the phenomenon sigmoid – however, as this chapter is validation not optimisation of results – this will not be demonstrated.

5.2.9 Cell 6-2 – Linear series of compartments with Heat Transfer

Model 6-2-1 explores the transfer of heat through a chain of air-filled compartments, each at 298K initially except for the first compartment in the chain at a temperature of 1000K – as illustrated in Figure 82.

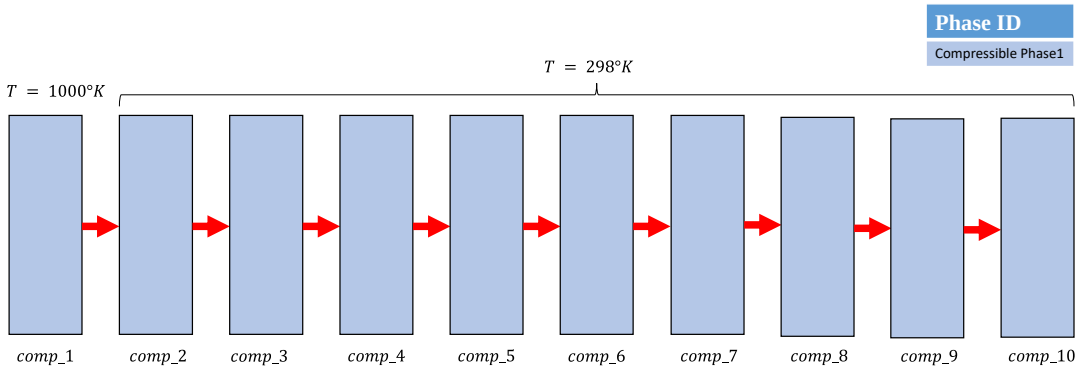

Figure 82 - Model 6-2-1

The initial total enthalpy in the system is equal to $4712kJ$; calculated from the specific heat of air $C_p = 1000\,J/kgK$. The purpose of the heat transfer is to distribute the enthalpy of the system amongst the volumes equally. The resultant temperature expected is $368K$, as per the formula $Q = MC_p\mathrm{T}$, considering all compartment material and enthalpy as a single mass M. The temperature of the compartments in the chain are given in Figure 83.

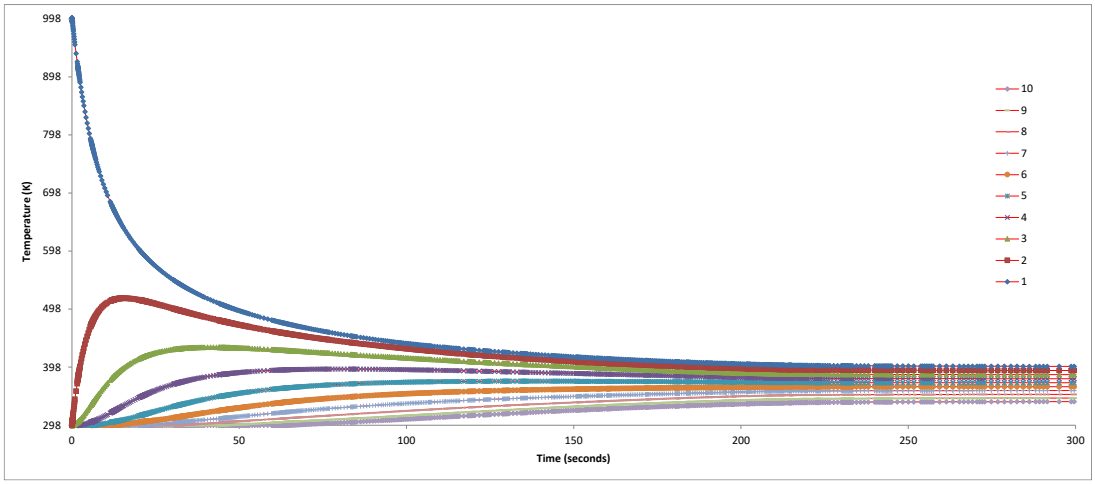

Figure 83 - Model 6-2-1; Evolution in temperature of compartments in series with $T_1 = 1000K$ initially and $T_{2\to10} = 298K$ initially.

The results (Figure 83) show the temperatures of the compartments climbing towards equilibrium of range $340 - 397K$. The range is due to the deactivation (through the activation sigmoid) of the heat transfer where the temperature difference is less than 2% of the source temperature. The midpoint between the temperature range is $368K$, equal to the expected equilibrium temperature of the system without the sigmoid error. To reduce the spread of compartment temperatures, the *sigmoid_error* property of the heat transfer can be reduced, this does however incur greater numerical costs due to increased difficulty in on/off switch of heat transfer by the numerical solver (due to discontinuity) – see Table 18 for direction of stiffness constant adjustment for increased accuracy and the effect upon the time to solution.

5.2.10 Time to solution

The time to solution is the time taken for a simulation to complete, for each model given in Table 22. The time to report the data and plot the table and figures in an excel document is not included in this time value.

Table 22 – Validation models time to solution

Model Number	Time to solution (seconds)
$1-1-1-i$	0.09
$1-1-1-ii$	0.08
$1-1-2$	0.09
$1-2-1-i$	48.00
$1-2-1-ii$	4.97
$1-2-2-i$	129.00
$1-2-2-ii$	2.17
$2-1-1$	0.11
$2-1-2$	0.21
$2-2-1$	189.00
$2-2-2$	0.14
$3-1-1-i$	0.08
$3-1-1-ii$	0.06
$3-1-2$	0.05
$3-1-3$	0.05
$4-2-1$	0.02
$4-2-2$	0.02
$5-1-1$	0.05
$6-1-1$	0.02
$6-2-1$	0.50

Absolute solution times cannot be compared directly as many parameters of the models were changed, including the amount of time simulated ($t_{final} - t_{start}$), the numerical solver employed (BDF, radau, LSODA) and solver tolerances (atol, rtol); parameter modification was made to ensure solution

was reached, however a sensitivity analysis of the parameters upon the solution ascertainment was not performed. The relative solution times do however give an indication of the most difficult phenomena of CompArt to solve.

75% of the models completed in under 1 second, whereas models 1-2-1-i, 1-2-1-ii, 1-2-2-i and 1-2-2-ii ranged from 2.17 to 129 seconds to solve. The common factor amongst these larger time to solution models is that they involve the propagation of material through a series of compartments via pressure-driven convective transport. The larger of these model solution times corresponds to those models where incompressible material (1-2-1-i, 1-2-2-i) is transported, with models of compressible material transport showing a comparatively lower solution time (1-2-1-ii and 1-2-2-ii); of the four larger time to solution models mentioned, the compressible flow models solve 25x faster than the incompressible flow models.

Model 2-2-1 took the longest time to solve, of 189 seconds. This model involved both compressible and incompressible phase material propagated through a series of compartments via convective transport. The increased solution time compared to the similar model of 1-2-2-i is due to two changes (i) the enforced *maximum_time_step* property of the solver, limiting the internal numerical solver step to 1 second which in effect reduces the efficiency of the solver but is a necessary property to ensure the pulse input is identified by the solver, and (ii) the inclusion of a timed pulse of material into the system via timed convective transport.

Model solution times in literature are not explicitly given, but instead are described as between seconds and minutes when comparing them to CFD/DEM modelling

Chapter 6 Conclusion

6.1 Thesis Summary & Insights

Within this work, a universal framework for the compartment modelling of unit operations in the field of chemical engineering is developed. The framework is based on a systematic review of compartment modelling of literature (Chapter 2), the framework focuses on the implementation of phenomena most prevalent (reaction, Mass-transfer, heat transfer, material flow and phase transport) and the required topology to universally construct unit operation compartment models; reaction is the most prevalent phenomenon applied in the surveyed models of literature (50%).

The approach to compartmentalisation of a system is $> 50\%$ through the aggregation of CFD cells to form compartments, with the extraction of the volumetric flow rates between compartments from the velocity field of the CFD map. The compartments are formed by aggregating cells which show a change in particular process-influencing properties within a given tolerance range.

The number of flow phenomena is related to the number of compartments via $No_Q = 1.25No_k^{1.6}$. Flows have a lesser impact on the solution difficulty as the rates remain consistent, with any change in rate typically smooth, occurring slowly over time. Whereas other phenomena are either/both discontinuous and of a faster rate; traits of a model leading to greater, if at all, time to solution.

The complexity of a model within this work is attributed to the number of non-flow phenomena applied to the model. Complex models, those with greatest non-flow phenomena, are of compartment number 163 or less. Models of greater than 163 compartments are either strictly flow based or include simple elementary reaction with a detailed flow network between compartments.

The approach to model construction and solution is bespoke, direct programming of ODE's and numerical solvers using a general-purpose programming language (Python, Matlab).

A gap in the knowledge is a combined universal approach to both implementation and solution; no tool exists for compartment models of unit operations. Although the models investigate a variety of systems (reactors, separators, waste wate treatment, polymer systems) the phenomena and structure and construction of compartment models is common between them.

In Chapter 3 advanced structural concepts of compartment modelling are developed. A novel shift in modelling technique is made where phase volumes are no longer assumed to fill the fixed compartment volumes, but their volumes are calculated as a product of density and material quantity (dynamic volume), bringing greater accuracy and representation to that of the real system.

The pressure evolution of compartments is tightly intertwined with the volume of phase material in a compartment, this relationship permits the inclusion of an automatically calculated pressure-driven convective transport of material between compartments, isolating the user from the tedium of flowrate setting within a compartment system.

A further novelty of the framework is the use of the compartment pressure to drive the functional change in the, previously fixed, compartment volume. This is driven by the goal of equilibration of the compartment pressures; synonymous with the equilibration of continuum volumes of a system (e.g., headspace and liquor).

The prevalent phenomena of literature (Reaction, Mass-transfer, reaction, heat transfer, material flow and phase transport) are embedded within the novel framework structure.

Phenomena are modelled as unidirectional mechanisms, utilising the mathematical sigmoid equation as an on/off switch, where the driving force of a phenomenon crosses between a positive/negative value. This switch controls the severity of the discontinuity, creating a gradual change in rate, reducing the difficulty for the numerical solver to identify and correctly solve the changing phenomenon rate. Without the sigmoid the solution smoothing the activation transition of phenomena, the problem would be discontinuous,

and phenomena could be stepped over by the solver and not considered in the converged solution. The sigmoid equation trades discontinuity for stiffness, a difficulty of ODE problems more readily handled by general purpose numerical solvers; resulting problems, although relived of discontinuity, can be incredibly stiff.

The universal framework is implemented in Python 3.7 and described in Chapter 4. Prior to this work a universal compartment modelling framework was not present in the field, neither was a universal implementation (tool). Typically, in literature, models were described as a set of ODE's. Based on the compartment structure and phenomena observed in literature, a high-level language is developed to allow modelling of a wide range of compartment models; for the specification of the phenomena and compartments they are within. CompArt interprets the language and formulates a set of ODE equations, solvable by a universal set of numerical solvers.

The language of CompArt isolates the modeller from the coding of differential equations of the model. Further, an algorithm of CompArt automatically populates the model data-structure with variables omitted from the input file by the user (species, phases) but created through phenomenological mechanisms. The result, clear input files, more readily decipherable by those of different disciplines.

Two Issues related to the application of general-purpose numerical solvers to compartment model problems are explored in Chapter 4, (i) how to restrict variable values to the positive domain and, (ii) how to control the stiffness of a model. At present, the solution to both issues is a combination of modifying the stiffness parameter values, which alleviates strain on the solver, and setting a maximum step size the solver algorithm can take between converged points; the latter applied in model 2-2-1.

To resolve the solutions more robustly a numerical solver specific to the solution of unit operation compartment models is required; the attributes of such solver would include the ability to identify and address stiffness and discontinuity, maintain solution values within the positive domain and identify

events such as the activation & deactivation of phenomena on small timescales.

The purpose of the validation was to confirm the correct operation of the framework implemented in CompArt, mass and energy, although not explored in detail showed a minor cumulative error of 10^{-14} in both mass and energy balances; attributed to the computational rounding error.

The implementation of phenomenological models and structural elements of the framework are validated against analytical, and numerical solutions in Chapter 5. 20 models are successfully described using the universal language, built - parsed automatically into the differential format, and solved by CompArt. Most of the models are solved near instantly (0.01 seconds) with 5 cases of models solving between 48 & 189 seconds. The longer solution times is the result of solution of two or more pressure-driven convective transport phenomena, specifically the transmission of incompressible material through the system. The solution time for these models could be improved with the optimisation of the stiffness constants associated with the convective transport and incompressible phase relaxation phenomena, however performance evaluation was not a goal of this work but would be a good next stage of research in the development of CompArt.

A minor error in equilibrium values of models compared to expected/analytical results (~2%) was observed for models involving the use of the sigmoid activation; an expected and necessary result of reducing the discontinuity of the model solution though the sigmoid activation function. The error associated with the discontinuity sigmoid function can be reduced at the expense of increased solution time.

In summary, the key innovation of this work is the theoretical specification of a universal compartment modelling framework, based on comparison of phenomena and networks occurring in literature. Implementation of the framework in python. Design of an accompanying language, based on the broad application of compartment models to unit operations observed in literature; together forming the tool CompArt. The language, utilised to

describe compartment models, is interpreted automatically by CompArt to generate the associated ODEs of a model within the python data structure. This data-structure, the ODE's, variables, and associated equations of the model are solved by a numerical solver wrapped into the tool. The compartment modelling framework and implementation of the framework (CompArt) has been validated.

6.2 Future work Recommendations

6.2.1 Demonstration of CompArt

Proven as a tool capable of modelling the prevalent phenomena of unit operations accurately, CompArt is successfully deployed in the work (Hydrogenation and Pulsed column systems) of multiple MEng and PhD students at the university of Leeds, the application of CompArt to real-world systems would further demonstrate the tools capability.

6.2.2 CompArt developments

The language developed to describe models in CompArt is sufficient for models of the target size, as captured from literature, of compartment number 163 and less. Although vast improvement upon the ODE definition of compartment models in literature has been made with the development of the CompArt language, the input method for description of larger networks of compartments could be tedious to describe. One such conception is the generation of a large compartment network based upon specification of a continuum shape (same-phase material spanning a large volume of a unit), e.g., a conical cylinder of a pipe, or spiralled vortex within a vessel due to impeller action. The shape is filled with compartments, the flow rates between compartments functional of the area of contact between them. These shapes may be described through an extension of the current language of CompArt or potentially a graphical illustration, which is then converted to the language or directly to the data structure.

Population balance modelling is a modelling approach combined with 16% of the surveyed compartment models in Chapter 2. Integration of the approach

with CompArt, as an optional phenomenon, would extend the modelling approach to application of biomass, crystal, and polymer population density modelling.

At present, a property can be defined as a set value in CompArt's language, the inclusion of a UDF to define each property as a function of the system variable and parameter values would improve the generality of the tool. For example, flowrates could be set to be functional of material viscosity, specific heat of phase material set to be functional of temperature and pressure, and density of a phase functional of species composition. This increased level of complexity does however come with an increased level of difficulty in solution, as with more equations to define there are more equations to solve and parameters interlinked.

An even greater level of complexity would be introduced through the ability to define system parameters as variables; and apply custom phenomena to the variables. An example being the kinetic turbulence within a vessel, a variable typically extracted from CFD simulations, used to identify homogenous zones, and compartmentalise a system. The kinetic energy could be functional of impeller rotation speed, and the flow rates between compartments functional of kinetic energy. Although such complexity does stray the modelling approach further from generality.

6.2.3 Solution of Compartment model's

The presence of discontinuity associated with phenomena switching on/off is addressed with a sigmoid equation, trading discontinuity with stiffness. An alternative approach to handling discontinuous functions of a model, could be to inform a numerical solver of the discontinuous points in the model; for instance, defining event functions or passing times of events known to the model onto the solver. Or more ideally, the development of a bespoke solver based on the structure of the ODE which can extract such time and event information automatically.

The stiffness coefficients of a model are currently set based on achieving a solution of a model. Sensitivity analysis of the different stiffness constants on

the stiffness of the model, measured as time to solution, could give a better understanding of the greatest contributing phenomena or equations to model stiffness.

Beyond the core methods of SciPy, the more recently developed library of Julia Diffeqpy, already wrapped into the CompArt tool, could be tested to evaluate the most appropriate solvers for the types of problems a compartment model delivers.

Bibliography

Alvarado, A. *et al.* (2012) ‘A compartmental model to describe hydraulics in a full-scale waste stabilization pond’, *Water Research*. Elsevier Ltd, 46(2), pp. 521–530. doi: 10.1016/j.watres.2011.11.038.

Alves, S. S., Vasconcelos, J. M. T. and Barata, J. (1997) ‘Alternative compartment models of mixing in tall tanks agitated by multi-rushton turbines’, *Chemical Engineering Research and Design*, 75(3), pp. 334–338. doi: 10.1205/026387697523642.

Arizmendi-Sánchez, J. A. and Sharratt, P. N. (2008) ‘Phenomena-based modularisation of chemical process models to approach intensive options’, *Chemical Engineering Journal*, 135(1–2), pp. 83–94. doi: 10.1016/j.cej.2007.02.017.

Avoiding negative concentrations (2021). Available at: https://uk.comsol.com/support/knowledgebase/952 (Accessed: 25 November 2021).

Barrett, P. H. R. *et al.* (1998) ‘SAAM II: Simulation, analysis, and modeling software for tracer and pharmacokinetic studies’, *Metabolism: Clinical and Experimental*, 47(4), pp. 484–492. doi: 10.1016/S0026-0495(98)90064-6.

Bashiri, H. *et al.* (2014) ‘Compartmental modelling of turbulent fluid flow for the scale-up of stirred tanks’, *Canadian Journal of Chemical Engineering*, 92(6), pp. 1070–1081. doi: 10.1002/cjce.21955.

Beck, J. *et al.* (2020) ‘Compartment model of mixing in a bubble trap and its impact on chromatographic separations’, *Processes*, 8(7), pp. 1–9. doi: 10.3390/pr8070780.

Bermingham, S. K., Kramer, H. J. M. and Van Rosmalen, G. M. (1998) ‘Towards on-scale crystalliser design using compartmental models’, *Computers and Chemical Engineering*, 22(SUPPL.1). doi: 10.1016/s0098-1354(98)00075-1.

Bezzo, F. and Macchietto, S. (2004) ‘A general methodology for hybrid multizonal/CFD models: Part II. Automatic zoning’, *Computers and Chemical Engineering*, 28(4), pp. 513–525. doi: 10.1016/j.compchemeng.2003.08.010.

Bezzo, F., Macchietto, S. and Pantelides, C. C. (2003) ‘General hybrid multizonal/CFD approach for bioreactor modeling’, *AIChE Journal*, 49(8), pp. 2133–2148. doi: 10.1002/aic.690490821.

Bezzo, F., Macchietto, S. and Pantelides, C. C. (2004) ‘A general methodology for hybrid multizonal/CFD models: Part I. Theoretical framework’, *Computers and Chemical Engineering*, 28(4), pp. 501–511. doi: 10.1016/j.compchemeng.2003.08.004.

Bian, S. *et al.* (2005) ‘Compartmental modeling of high purity air separation columns’, *Computers and Chemical Engineering*, 29(10), pp. 2096–2109. doi: 10.1016/j.compchemeng.2005.06.002.

Bisgaard, J. *et al.* (2021) ‘Automated compartment model development based on data from flow-following sensor devices’, *Processes*, 9(9). doi: 10.3390/pr9091651.

Bohbot, J. *et al.* (2009) ‘Simulations multi-échelles de moteur à combustion interne par couplage de modèle 0D/1D avec un code de combustion 3D’, *Oil and Gas Science and Technology*, 64(3), pp. 337–359. doi: 10.2516/ogst/2009007.

Chaudhury, A., Armenante, M. E. and Ramachandran, R. (2015) ‘Compartment based population balance modeling of a high shear wet granulation process using data analytics’, *Chemical Engineering Research and Design*. Institution of Chemical Engineers, 95, pp. 211–228. doi: 10.1016/j.cherd.2014.10.024.

Delafosse, A. *et al.* (2010) ‘Development of a compartment model based on CFD simulations for description of mixing in bioreactors’, *Biotechnology, Agronomy and Society and Environment*, 14(SPEC. ISSUE 2), pp. 517–522.

Delafosse, A. *et al.* (2014) ‘CFD-based compartment model for description of mixing in bioreactors’, *Chemical Engineering Science*. Elsevier, 106, pp. 76–

85. doi: 10.1016/j.ces.2013.11.033.

Delafosse, A. *et al.* (2015) ‘Euler-Lagrange approach to model heterogeneities in stirred tank bioreactors - Comparison to experimental flow characterization and particle tracking’, *Chemical Engineering Science*. Elsevier, 134, pp. 457–466. doi: 10.1016/j.ces.2015.05.045.

Dompazis, G., Kanellopoulos, V. and Kiparissides, C. (2006) ‘Development of a multi-compartment dynamic model for the prediction of particle size distribution and particle segregation in a catalytic olefin polymerization FBR’, *Computer Aided Chemical Engineering*, 21(C), pp. 345–350. doi: 10.1016/S1570-7946(06)80070-2.

Du, Y. *et al.* (2015) ‘Equivalent Reactor Network Model for the Modeling of Fluid Catalytic Cracking Riser Reactor’, *Industrial and Engineering Chemistry Research*, 54(35), pp. 8732–8742. doi: 10.1021/acs.iecr.5b02109.

Dueñas Díez, M. *et al.* (2006) ‘Validation of a compartmental population balance model of an industrial leaching process: The Silgrain ® process’, *Chemical Engineering Science*, 61(1), pp. 229–245. doi: 10.1016/j.ces.2005.01.047.

Egedy, A. *et al.* (2018) ‘Kinetic-compartmental modelling of potassium-containing cellulose feedstock gasification’, *Frontiers of Chemical Science and Engineering*, 12(4), pp. 708–717. doi: 10.1007/s11705-018-1767-y.

Eriksson, E. (1971) ‘Compartment Models and Reservoir Theory’, *Annual Review of Ecology and Systematics*, 2(1), pp. 67–84. doi: 10.1146/annurev.es.02.110171.000435.

Farzan, P. and Ierapetritou, M. G. (2018) ‘A framework for the development of integrated and computationally feasible models of large-scale mammalian cell bioreactors’, *Processes*, 6(7). doi: 10.3390/pr6070082.

Fenila, F. and Shastri, Y. (2018) *Optimization of Cellulose Hydrolysis in a Non-ideally Mixed Batch reactor*, *Computer Aided Chemical Engineering*. Elsevier Masson SAS. doi: 10.1016/B978-0-444-64235-6.50274-6.

Fenila, F. and Shastri, Y. (2019) ‘Optimization of cellulose hydrolysis in a non-

ideally mixed reactors', *Computers and Chemical Engineering*. Elsevier Ltd, 128, pp. 340–351. doi: 10.1016/j.compchemeng.2019.06.014.

Golberg, A. and Rubinsky, B. (2013) *Mass Transfer Phenomena in Electroporation*, *Transport in Biological Media*. Elsevier Inc. doi: 10.1016/B978-0-12-415824-5.00012-6.

Gresch, M. *et al.* (2009) 'Compartmental models for continuous flow reactors derived from CFD simulations', *Environmental Science and Technology*, 43(7), pp. 2381–2387. doi: 10.1021/es801651j.

Guha, D. *et al.* (2006) 'CFD-based compartmental modeling of single phase stirred-tank reactors', *AIChE Journal*, 52(5), pp. 1836–1846. doi: 10.1002/aic.10772.

Haag, J. *et al.* (2018) 'Modelling of Chemical Reactors: From Systemic Approach to Compartmental Modelling', *International Journal of Chemical Reactor Engineering*, 16(8), pp. 1–22. doi: 10.1515/ijcre-2017-0172.

Horton, R. R., Bequette, B. W. and Edgar, T. F. (1991) 'Improvements in dynamic compartmental modeling for distillation', *Computers & Chemical Engineering*, 15(3), pp. 197–201. doi: 10.1016/0098-1354(91)85006-G.

Huang, P., Niokal, S. and Chance, B. (2002) 'A four compartment model of oxygen delivery to muscle tissue from capillary', *Proceedings of the IEEE Annual Northeast Bioengineering Conference, NEBEC*, 2002-Janua, pp. 259–260. doi: 10.1109/NEBC.2002.999564.

Jourdan, N. *et al.* (2019) 'Compartmental Modelling in chemical engineering: A critical review', *Chemical Engineering Science*. Elsevier Ltd, 210, p. 115196. doi: 10.1016/j.ces.2019.115196.

Kim, M. *et al.* (2020) 'Modeling long-time behaviors of industrial multiphase reactors for CO2 capture using CFD-based compartmental model', *Chemical Engineering Journal*. Elsevier, 395(April), p. 125034. doi: 10.1016/j.cej.2020.125034.

Kim, Y., Kim, A. and Chung, J. (2021) 'Population pharmacokinetic / pharmacodynamic modeling of delayed effect of escitalopram-induced QT

prolongation', *Journal of Affective Disorders*. Elsevier B.V., 285(February), pp. 120–126. doi: 10.1016/j.jad.2021.02.048.

Knysh, P. and Mann, R. (1984) *Utility of Networks of Interconnected Backmixed Zones To Represent Mixing in a Closed Stirred Vessel.*, *Institution of Chemical Engineers Symposium Series*. The Institution of Chemical Engineers. doi: 10.1016/b978-0-85295-171-2.50012-8.

Komninos, N. P., Hountalas, D. T. and Kouremenos, D. A. (2004) 'Development of a new multi-zone model for the description of physical processes in HCCI engines', *SAE Technical Papers*, 2004(724). doi: 10.4271/2004-01-0562.

Komninos, N. P. and Rakopoulos, C. D. (2016) 'Heat transfer in hcci phenomenological simulation models: A review', *Applied Energy*. Elsevier Ltd, 181, pp. 179–209. doi: 10.1016/j.apenergy.2016.08.061.

Kougoulos, E., Jones, A. G. and Wood-Kaczmar, M. W. (2006) 'A hybrid CFD compartmentalization modeling framework for the scaleup of batch cooling crystallization processes', *Chemical Engineering Communications*, 193(8), pp. 1008–1023. doi: 10.1080/00986440500352022.

Kozarac, D., Lulic, Z. and Sagi, G. (2010) 'A six-zone simulation model for HCCI engines with a non-segregated solver of zone state', *Combustion Theory and Modelling*, 14(3), pp. 425–451. doi: 10.1080/13647830.2010.489959.

Krychowska, A. *et al.* (2020) 'Mathematical Modeling of Hydrodynamics in Bioreactor by Means of CFD-Based Compartment Model', *Processes*, 8(10), p. 1301. doi: 10.3390/pr8101301.

Laakkonen, M. (2006) *Development and Validation of Mass Transfer Models for the Design of Agitated Gas-Liquid Reactors*.

Laakkonen, M. *et al.* (2006) 'Dynamic modeling of local reaction conditions in an agitated aerobic fermenter', *AIChE Journal*, 52(5), pp. 1673–1689. doi: 10.1002/aic.10782.

Laakkonen, M. *et al.* (2007) 'Modelling local bubble size distributions in

agitated vessels', *Chemical Engineering Science*, 62(3), pp. 721–740. doi: 10.1016/j.ces.2006.10.006.

Laínez-Aguirre, J. M., Blau, G. E. and Reklaitis, G. V. (2014) 'Postulating compartmental models using a flexible approach', *Computer Aided Chemical Engineering*. Elsevier, 33(2011), pp. 1171–1176. doi: 10.1016/B978-0-444-63455-9.50030-1.

Leaning, M. S. and Boroujerdi, M. A. (1991) 'A system for compartmental modelling and simulation', *Computer Methods and Programs in Biomedicine*, 35(2), pp. 71–92. doi: 10.1016/0169-2607(91)90068-5.

Lee, Y. *et al.* (2019) 'Multicompartment Model of an Ethylene-Vinyl Acetate Autoclave Reactor: A Combined Computational Fluid Dynamics and Polymerization Kinetics Model', *Industrial and Engineering Chemistry Research*, 58(36), pp. 16459–16471. doi: 10.1021/acs.iecr.9b03044.

Li, T. S. *et al.* (2003) 'Dynamic compartmental models of uniformly-mixed and inhomogeneously-mixed Gibbsite crystallizers', *Chemical Engineering and Technology*, 26(3), pp. 369–376. doi: 10.1002/ceat.200390057.

Morsi, B. I. and Basha, O. M. (2015) 'Mass Transfer in Multiphase Systems', in *Mass Transfer - Advancement in Process Modelling*. InTech, pp. 267–322. doi: 10.5772/60516.

Le Moullec, Y. *et al.* (2010) 'Comparison of systemic, compartmental and CFD modelling approaches: Application to the simulation of a biological reactor of wastewater treatment', *Chemical Engineering Science*. Elsevier, 65(1), pp. 343–350. doi: 10.1016/j.ces.2009.06.035.

Moxon, T. E. and Bakalis, S. (2016) *Simulation-Based Food Process Design*, *Computer Aided Chemical Engineering*. Elsevier. doi: 10.1016/B978-0-444-63683-6.00014-9.

Muthuramalingam, a, Himavathi, S. and Srinivasan, E. (2008) 'Neural Network Implementation Using FPGA : Issues and Application', *Journal of Information Technology*, 4(2), pp. 86–92. Available at: http://citeseerx.ist.psu.edu/viewdoc/download?doi=10.1.1.131.9059&re

p=rep1&type=pdf.

Nadal-Rey, G. *et al.* (2021) ‘Development of dynamic compartment models for industrial aerobic fed-batch fermentation processes’, *Chemical Engineering Journal*. Elsevier B.V., 420(P3), p. 130402. doi: 10.1016/j.cej.2021.130402.

Nauha, E. K. *et al.* (2018) ‘Compartmental modeling of large stirred tank bioreactors with high gas volume fractions’, *Chemical Engineering Journal*, 334(June 2017), pp. 2319–2334. doi: 10.1016/j.cej.2017.11.182.

Nauha, E. K. and Alopaeus, V. (2013) ‘Modeling method for combining fluid dynamics and algal growth in a bubble column photobioreactor’, *Chemical Engineering Journal*. Elsevier B.V., 229, pp. 559–568. doi: 10.1016/j.cej.2013.06.065.

Nauha, E. K. and Alopaeus, V. (2015) ‘Modeling outdoors algal cultivation with compartmental approach’, *Chemical Engineering Journal*. Elsevier B.V., 259, pp. 945–960. doi: 10.1016/j.cej.2014.08.073.

Nørregaard, A. *et al.* (2019) ‘Hypothesis-driven compartment model for stirred bioreactors utilizing computational fluid dynamics and multiple pH sensors’, *Chemical Engineering Journal*. Elsevier, 356(July 2018), pp. 161–169. doi: 10.1016/j.cej.2018.08.191.

ODE Solvers (2021). Available at: https://diffeq.sciml.ai/dev/solvers/ode_solve/ (Accessed: 25 November 2021).

Öner, M. *et al.* (2018) *Scale-up Modeling of a Pharmaceutical Crystallization Process via Compartmentalization Approach*, *Computer Aided Chemical Engineering*. Elsevier Masson SAS. doi: 10.1016/B978-0-444-64241-7.50025-2.

Öner, M. *et al.* (2019) *Scale-up Modeling of a Pharmaceutical Antisolvent Crystallization via a Hybrid Method of Computational Fluid Dynamics and Compartmental Modeling*, *Computer Aided Chemical Engineering*. Elsevier Masson SAS. doi: 10.1016/B978-0-12-818634-3.50119-3.

Piemonte, V. *et al.* (2017) ‘A Novel Three-Compartmental Model for Artificial

Pancreas: Development and Validation', *Artificial Organs*, 41(12), pp. E326–E336. doi: 10.1111/aor.12980.

Pladis, P. *et al.* (2011) 'Dynamic Modeling and Optimization of Flash Separators for Highly-Viscous Polymerization Processes', *Computer Aided Chemical Engineering*. Elsevier B.V., 29, pp. 723–727. doi: 10.1016/B978-0-444-53711-9.50145-0.

Portillo, P. M., Muzzio, F. J. and Ierapetritou, M. G. (2006) 'Modeling and designing powder mixing processes utilizing compartment modeling', *Computer Aided Chemical Engineering*, 21(C), pp. 1039–1044. doi: 10.1016/S1570-7946(06)80183-5.

Rahimi, M. and Mann, R. (2001) 'Macro-mixing, partial segregation and 3-D selectivity fields inside a semi-batch stirred reactor', *Chemical Engineering Science*, 56(3), pp. 763–769. doi: 10.1016/S0009-2509(00)00287-6.

Rico-Ramirez, V. *et al.* (2020) 'Modeling, simulation and optimization of combined fractional-ordinary dynamic systems', *Computers and Chemical Engineering*. Elsevier Ltd, 133, p. 106651. doi: 10.1016/j.compchemeng.2019.106651.

Rigopoulos, S. and Jones, A. (2003) 'A hybrid CFD-reaction engineering framework for multiphase reactor modelling: Basic concept and application to bubble column reactors', *Chemical Engineering Science*, 58(14), pp. 3077–3089. doi: 10.1016/S0009-2509(03)00179-9.

Roy, S., Duduković, M. P. and Mills, P. L. (2000) 'Two-phase compartments model for the selective oxidation of n-butane in a circulating fluidized bed reactor', *Catalysis Today*, 61(1), pp. 73–85. doi: 10.1016/S0920-5861(00)00352-7.

Schramski, J. R., Kazanci, C. and Tollner, E. W. (2011) 'Network environ theory, simulation, and EcoNet® 2.0', *Environmental Modelling and Software*. Elsevier Ltd, 26(4), pp. 419–428. doi: 10.1016/j.envsoft.2010.10.003.

Schwaab, M. and Pinto, J. C. (2007) 'Optimum reference temperature for reparameterization of the Arrhenius equation. Part 1: Problems involving one

kinetic constant', *Chemical Engineering Science*, 62(10), pp. 2750–2764. doi: 10.1016/j.ces.2007.02.020.

scipy.integrate.solve_ivp (2021). Available at: https://docs.scipy.org/doc/scipy/reference/generated/scipy.integrate.solve_ivp.html (Accessed: 25 November 2021).

Shampine, L. F. *et al.* (2005) 'Non-negative solutions of ODEs', *Applied Mathematics and Computation*, 170(1), pp. 556–569. doi: 10.1016/j.amc.2004.12.011.

Skupin, P. *et al.* (2017) *Modelling of the imperfect mixing in a hybrid exothermic chemical reactor with simulated heat of reaction*, *Computer Aided Chemical Engineering*. Elsevier Masson SAS. doi: 10.1016/B978-0-444-63965-3.50476-1.

Stanley, S. J. *et al.* (2008) 'Reconciling Electrical Resistance Tomography (ERT) Measurements with a Fluid Mixing Model for Semi-Batch Operation of a Stirred Vessel', *The Canadian Journal of Chemical Engineering*, 83(1), pp. 48–54. doi: 10.1002/cjce.5450830109.

Stoller, M., Bravi, M. and Chianese, A. (2005) 'The effect of scaling on the performances of a DTB crystallizer by means of a compartmental simulation model', *Chemical Engineering Research and Design*, 83(2 A), pp. 126–132. doi: 10.1205/cherd.03384.

Švantner, M., Študent, J. and Veselý, Z. (2020) 'Continuous walking-beam furnace 3D zonal model and direct thermal-box barrier based temperature measurement', *Case Studies in Thermal Engineering*, 18(November 2019). doi: 10ac.1016/j.csite.2020.100608.

Tajsoleiman, T. *et al.* (2019) 'A CFD based automatic method for compartment model development', *Computers and Chemical Engineering*. Elsevier Ltd, 123, pp. 236–245. doi: 10.1016/j.compchemeng.2018.12.015.

Uno, Y. *et al.* (2019) 'A three-compartment pharmacokinetic model to predict the interstitial concentration of talaporfin sodium in the myocardium for photodynamic therapy: A method combining measured fluorescence and

analysis of the compartmental origin of the fluorescence', *Bioengineering*, 6(1), pp. 1–11. doi: 10.3390/bioengineering6010001.

Vrábel, P. *et al.* (2000) 'Mixing in large-scale vessels stirred with multiple radial or radial and axial up-pumping impellers: Modelling and measurements', *Chemical Engineering Science*, 55(23), pp. 5881–5896. doi: 10.1016/S0009-2509(00)00175-5.

Wang, J. and Langemann, H. (1994) 'Unsteady two-film model for mass transfer accompanied by chemical reaction', *Chemical Engineering Science*, 49(20), pp. 3457–3463. doi: 10.1016/0009-2509(94)00160-X.

Weber, M. (1949) 'Methodology of social sciences', *Methodology of Social Sciences*, pp. 1–210. doi: 10.4324/9781315124445.

Wells, G. J. and Ray, W. H. (2005a) 'Methodology for modeling detailed imperfect mixing effects in complex reactors', *AIChE Journal*, 51(5), pp. 1508–1520. doi: 10.1002/aic.10407.

Wells, G. J. and Ray, W. H. (2005b) 'Mixing effects on performance and stability of low-density polyethylene reactors', *AIChE Journal*, 51(12), pp. 3205–3218. doi: 10.1002/aic.10544.

Wiley, J., Hepburn, K. and Levenspiel, O. (1999) *Chemical Reaction Engineering - third edition*, *Chemical Engineering Science*. doi: 10.1016/0009-2509(64)85017-X.

Yang, S. *et al.* (2019) 'Optimization of reaction selectivity using CFD-based compartmental modeling and surrogate-based optimization', *Processes*, 7(1). doi: 10.3390/pr7010009.

Zhao, W. *et al.* (2017) 'Application of the compartmental model to the gas-liquid precipitation of CO 2 -Ca(OH) 2 aqueous system in a stirred tank', *AIChE Journal*, 63(1), pp. 378–386. doi: 10.1002/aic.15567.

Zheng, X., Smith, R. and Theodoropoulos, C. (2005) 'Modelling and optimisation of distributed-parameter batch and semi-batch reactor systems', in *Computer Aided Chemical Engineering*, pp. 1087–1092. doi: 10.1016/S1570-7946(05)80023-9.

Appendix A

Surveyed literature data from 48 Chemical process unit operation compartment modelling papers; (-) indicates insufficient information to extract quantitative information.

Reference	Unit Operation	Differential Variables per compartment	Phases	Number of compartments	Phenomena Number per compartment	Compartmentalisation	Tool	Solver
(Alvarado *et al.*, 2012)	Water stabilization pond	Mass concentration (2)	Liquid	25	Mass flow (4.7) Reactions (8)	CFD	-	-
(Alves, Vasconcelos and Barata, 1997)	Tall tank with multiple Rushton turbines	Mass concentration (1.8)	Liquid	12	Mass flow (1.8)	Heuristic	-	-

Reference	Unit Operation	Differential Variables per compartment	Phases	Number of compartments	Phenomena Number per compartment	Compartment alisation	Tool	Solver
(Arizmendi-Sánchez and Sharratt, 2008)	Cooled reactor vessel	Mass (2) Compartment volume (1)	Liquid	2	Reaction (2) Convective heat transfer (2) Conductive heat transfer (0.5) Volumetric flow (5)	Heuristic	-	-
(Bashiri *et al.*, 2014)	Stirred tank	-	-	2	Mass flow (1)	CFD	-	-
(Beck *et al.*, 2020)	Chronographic bubble trap	Molar Concentration (1)	Liquid	3	Volumetric flow (2)	Heuristic	CADET	-

Reference	Unit Operation	Differential Variables per compartment	Phases	Number of compartments	Phenomena Number per compartment	Compartmentalisation	Tool	Solver
(Bermingham, Kramer and Van Rosmalen, 1998)	Suspension crystallization unit	Median Crystal size (1)	Solid Liquid	7	Volumetric flow (1)	Heuristic	gProms	DAE solver Speed-Up
(Bezzo and Macchietto, 2004)	Mixing Tank	Mass fraction (2)	Liquid	100	Mass flow (3.6)	CFD	-	-
(Bezzo, Macchietto and Pantelides, 2003)	Batch Bioreactor	Mass Concentration (4)	Liquid Gas	20	Reactions (3) Mass transfer (1) Mass flow (-)	CFD	gProms	DAE solver

Reference	Unit Operation	Differential Variables per compartment	Phases	Number of compartments	Phenomena Number per compartment	Compartmentalisation	Tool	Solver
(Bezzo, Macchietto and Pantelides, 2004)	Crystallisation unit	Mass (2)	Solid Liquid	4	Mass flow (2) PBM (1)	CFD	gProms	-
(Bian *et al.*, 2005)	High purity air separation column	Mass (3) Enthalpy (1)	Liquid Gas	15	Molar flow (2.2)	Heuristic	Matlab	ode15s
(Bisgaard *et al.*, 2021)	Stirred Tank	Mass Concentration (1)	Liquid	24	Exchange volumetric flow (0.8)	Heuristic	Python	LSODA

Reference	Unit Operation	Differential Variables per compartment	Phases	Number of compartments	Phenomena Number per compartment	Compartment alisation	Tool	Solver
(Delafosse *et al.*, 2010)	Bioreactor	-	Liquid	1800 -> 4300	Exchange volumetric flowrate (-) Volumetric flow (-)	CFD	-	-
(Delafosse *et al.*, 2014)	Bioreactor	Molar Concentration (1)	Liquid	12960	Volumetric flow (8)	CFD + NoZ	-	-
(Delafosse *et al.*, 2015)	Stirred Bioreactor	Mass Concentration (1)	Solid Liquid	9000 & 28000 & 35000	Exchange volumetric flow (8)	CFD + NoZ	-	-

Reference	Unit Operation	Differential Variables per compartment	Phases	Number of compartments	Phenomena Number per compartment	Compartmentalisation	Tool	Solver
(Egedy *et al.*, 2018)	Two-step pyrolysis-gasification reactor	-	Solid Liquid Gas	32	Reaction (8) Volumetric flow (1.1)	Heuristic	Matlab	ode23tb
(Farzan and Ierapetritou, 2018)	Mammalian cell bioreactor	Scalar concentration (1) Molar Concentration (5)	Liquid	16	Mass flow (-) Mass transfer (1) Sedimentation [PT] (1) Reaction (4)	CFD	-	"Step size 10^-9, stiff solver"

Reference	Unit Operation	Differential Variables per compartment	Phases	Number of compartments	Phenomena Number per compartment	Compartmentalisation	Tool	Solver
(Fenila and Shastri, 2019)	Fed-batch Cellulose hydrolysis reactor	Mass Concentration (5) Scalar concentration (2) Temperature (1)	Liquid	18	Reaction (3) Volumetric flow (0.3) Exchange volumetric flow (0.8) Conductive heat transfer (0.4) Convective heat transfer (1.2)	Heuristic	Matlab	-
(Gresch *et al.*, 2009)	Wastewater ozonation reactor	-	Liquid	100 & 200 & 400	Reaction (-) Exchange Volumetric flow (-)	CFD	In house software	-

Reference	Unit Operation	Differential Variables per compartment	Phases	Number of compartments	Phenomena Number per compartment	Compartment alisation	Tool	Solver
(Guha *et al.*, 2006)	Stirred-tank reactor	Molar concentration (3)	Liquid	120->720	Volumetric flow (6) Exchange volumetric flow (6) Reaction (2)	CFD + NoZ	-	-
(Horton, Bequette and Edgar, 1991)	Distillation column	Mass (1)	Liquid Gas	6	Mass flow (2.3)	Heuristic	-	-

Reference	Unit Operation	Differential Variables per compartment	Phases	Number of compartments	Phenomena Number per compartment	Compartmentalisation	Tool	Solver
(Kim *et al.*, 2020)	Multiphase CO2 capture reactor	Mass (1) Molar concentration (7) Temperature (1)	Liquid Gas	163	Bubble slip mass flow [PT] (6.1) Reactions (8) Mass transfer (1) System temperature balance (1)	CFD	Matlab	IDAS (Sundials)
(Kougoulos, Jones and Wood-Kaczmar, 2006)	Batch crystallisation	Temperature (1) Volumetric concentration (1)	Solid Liquid	4	PBM (1) Volumetric flow (1.5) Convective heat transfer (1.5)	CFD	gProms	-

Reference	Unit Operation	Differential Variables per compartment	Phases	Number of compartments	Phenomena Number per compartment	Compartment alisation	Tool	Solver
(Krychowska *et al.*, 2020)	Bioreactor (Bio Flo® 415)	Weight percent (1)	Liquid	5	Mass flow (2.6)	CFD	Simulink (Matlab)	RK45
(Laakkonen *et al.*, 2006)	Agitated aerobic fermenter	Moles (2) Population balance (1)	Liquid Gas	42	Bubble slip velocity [PT] (2.6) Volumetric flow (2.6) PBM (-) Reaction (6)	CFD	-	Gill's modification of RK45
(Le Moullec *et al.*, 2010)	Biological wastewater treatment	Molar concentration (12)	Liquid Gas	20	Reaction (8) Volumetric flow (5)	CFD	FORTRAN	DASSL

Reference	Unit Operation	Differential Variables per compartment	Phases	Number of compartments	Phenomena Number per compartment	Compartmentalisation	Tool	Solver
(Lee *et al.*, 2019)	Ethylene-vinyl acetate autoclave reactor	Mass (2) Compartment Temperature (1)	Liquid	214	Mass flow (~1.4) Reaction (3) Convective heat transfer (~1.4)	CFD	-	ODE (Sundials)
(Li *et al.*, 2003)	Gibbsite crystalliser	Molar Concentration (1) Number of crystals (1)	Liquid Solid	2	Volumetric flow (2) PBM (-)	CFD	-	-
(Nadal-Rey *et al.*, 2021)	Fed Batch Fermenter	Mass (5)	Solid Liquid gas	14->27	Mass flow (-) Reaction (3) Mass transfer (1)	CFD	Matlab	Ode15s

Reference	Unit Operation	Differential Variables per compartment	Phases	Number of compartments	Phenomena Number per compartment	Compartment alisation	Tool	Solver
(Nauha and Alopaeus, 2013)	Bubble column photobioreactor	Molar concentration (6) PBM (1)	Solid Liquid Gas	53	PBM (-) Reactions (5) Mass transfer (1) Volumetric flow (-) Bubble slip velocity [PT] (-) Light incidence model (1)	CFD	-	-

Reference	Unit Operation	Differential Variables per compartment	Phases	Number of compartments	Phenomena Number per compartment	Compartment alisation	Tool	Solver
(Nauha and Alopaeus, 2015)	Bubble column photobioreactor	Molar concentration (6) PBM (1)	Solid Liquid Gas	82	PBM (-) Reactions (5) Mass transfer (1) Volumetric flow (-) Bubble slip velocity [PT] (-) Light incidence model (1)	CFD	-	-

Reference	Unit Operation	Differential Variables per compartment	Phases	Number of compartments	Phenomena Number per compartment	Compartment alisation	Tool	Solver
(Nauha *et al.*, 2018)	Large, stirred tank bioreactors	Bubble size (1) Mass (2)	Liquid gas	89	PBM (1) Bubble slip velocity [PT] (~1.7) Volumetric flow (~1.7) Reaction (1)	CFD	-	-
(Nørregaard *et al.*, 2019)	Three Rushton disc turbine pilot scale bioreactor	Molar Concentration (1)	Liquid	4	Volumetric flow (1.3)	CFD	Matlab	ode15s

Reference	Unit Operation	Differential Variables per compartment	Phases	Number of compartments	Phenomena Number per compartment	Compartment alisation	Tool	Solver
(Nørregaard *et al.*, 2019)	Three Rushton disc turbine pilot scale bioreactor	Molar Concentration (1)	Liquid	56	Mass flow (1.1)	CFD	Matlab	ode15s
(Öner *et al.*, 2019)	Anti-solvent crystallisation	Compartment Volume (1) Mass (1)	Liquid	6	Volumetric flow (0.5) Timed Volumetric flow (0.7)	CFD	Simulink (Matlab)	-
(Pladis *et al.*, 2011)	High pressure flash separator	Mass (1.5) Enthalpy (0.5)	Liquid Gas	4	Mass Flow (4) Mass Transfer (1) Reaction (1)	Heuristic	-	-

Reference	Unit Operation	Differential Variables per compartment	Phases	Number of compartments	Phenomena Number per compartment	Compartmentalisation	Tool	Solver
(Portillo, Muzzio and Ierapetritou, 2006)	Powder mixing process	Scalar number of particles (1)	Solid	5	Particle flux (0.8)	Heuristic	-	-
(Rahimi and Mann, 2001)	Semi-batch stirred vessel	Molar concentration (4)	Liquid	32768	Volumetric flow (2) Exchange volumetric flow (4) Reaction (2)	NoZ	-	-
(Rigopoulos and Jones, 2003)	Bubble column reactor	Molar concentration (2)	Liquid Gas	30	Volumetric flow (1.1) Mass transfer (1) Reaction (2)	CFD	FORTRAN90	LSODE

Reference	Unit Operation	Differential Variables per compartment	Phases	Number of compartments	Phenomena Number per compartment	Compartment alisation	Tool	Solver
(Roy, Duduković and Mills, 2000)	circulating fluidized bed reactor	Molar Concentration (1)	Solid Gas	2 -> 12	Exchange volumetric flow (0.5) Reaction (3) Volumetric flow (1.2)	CFD	-	RK45
(Skupin *et al.*, 2017)	Hybrid reactor	Temperature (1) Molar Concentration (0.6)	Liquid	3	Convective heat transfer (2) Volumetric flow (2) Reaction (1) Conductive heat transfer (0.3)	Heuristic	-	-

Reference	Unit Operation	Differential Variables per compartment	Phases	Number of compartments	Phenomena Number per compartment	Compartment alisation	Tool	Solver
(Stanley *et al.*, 2008)	Semi-batch stirred vessel	Molar concentration (1)	Liquid	12000	Volumetric flow (2) Exchange volumetric flow (4)	NoZ	-	-
(Švantner, Študent and Veselý, 2020)	Walking beam furnace	Temperature (1)	Solid	11	Conductive Heat transfer (8)	Heuristic	In house software	Merson's modification of RK45
(Vrábel *et al.*, 2000)	Multiple Rushton Fermenter ($12m^3$)	-	Liquid	75	Exchange volumetric flow (0.8) Volumetric flow (1)	NoZ	-	-

Reference	Unit Operation	Differential Variables per compartment	Phases	Number of compartments	Phenomena Number per compartment	Compartment alisation	Tool	Solver
(Vrábel *et al.*, 2000)	Multiple Rushton Fermenter $(30m^3)$	-	Liquid	100	Exchange volumetric flow (0.8) Volumetric flow (1)	NoZ	-	-
(Wells and Ray, 2005a)	Agitated autoclave reactor	Temperature (1) Mass concentration (1) weight fraction (2)	Liquid	100	Reaction (6) Mass flow (-)	CFD	-	DASSL

Reference	Unit Operation	Differential Variables per compartment	Phases	Number of compartments	Phenomena Number per compartment	Compartment alisation	Tool	Solver
(Yang *et al.*, 2019)	Dual impeller stirred tank reactor	Mass concentration (1)	Liquid	1920	Mass flow (-) Reaction (2)	CFD	-	-
(Zhao *et al.*, 2017)	Gas-liquid reaction vessel	Mass (6) Population density (1)	Solid Liquid Gas	58	Reaction (1) Volumetric flow (-) PBM (1)	CFD	-	-
(Zheng, Smith and Theodoropoulos, 2005)	Semi-batch reactor	Molar Concentration (4) compartment volume (1)	Liquid	8000	Reaction (2) Volumetric flow (7)	NoZ	-	DASPK

Appendix B

B.1 Model 1-1-1-i

```
Solver LSODA
    t_start : 0
    t_final : 100
    atol : 10**-10
    rtol : 10**-10

Defaults
    flow_tau : 10**4

DefineComponents | name : molecular weight (kg/mole)
    A : 0.02

Surroundings surroundings_1 of continuous phase phase_1
    volume : 10
    pressure: 100000
    IncompressiblePhase phase_1 to surroundings_1| name : moles
        A : 449000

Compartment comp_1 of continuous phase phase_1
    volume : 10
    epsilon : 1
    IncompressiblePhase phase_1 to comp_1

ConvectiveTransport transport_1 from surroundings_1 to comp_1

end
```

B.2 Model 1-1-1-ii

```
Solver LSODA
    t_start : 0
    t_final : 10
    atol : 10**-10
    rtol : 10**-10

Defaults
    flow_tau : 10**4

DefineComponents
    A : 0.02

Surroundings surroundings_1 of continuous phase phase_1
    volume : 10
    pressure : 101325
    CompressiblePhase phase_1 to surroundings_1
        A : 400

Compartment comp_1 of continuous phase phase_1
    volume : 10
    CompressiblePhase phase_1 to comp_1| name : moles

ConvectiveTransport transport_1 from surroundings_1 to comp_1

end
```

B.3 Model 1-1-2

```
Solver LSODA
    t_start : 0
    t_final : 10
    atol : 10**-10
    rtol : 10**-10

Defaults
    flow_tau: 10**4

DefineComponents | name : molecular weight (kg/mole)
    A : 0.002

Surroundings surroundings_1 of continuous phase phase_1
    volume : 10
    pressure : 303975
    CompressiblePhase phase_1 to surroundings_1 | name : moles
        A : 1200

Compartment comp_1 of continuous phase phase_1
    volume : 10
    CompressiblePhase phase_1 to comp_1| name : moles

Surroundings surroundings_2 of continuous phase phase_1
    volume : 10
    pressure : 101325
ConvectiveTransport transport_1 from surroundings_1 to comp_1

ConvectiveTransport transport_2 from comp_1 to surroundings_2

end
```

B.4 Model 1-2-1-i

```
Solver Radau
    t_start : 0
    t_final : 600

Defaults
    flow_tau : 10**4

DefineComponents | name : molecular weight (kg/mole)
    A : 0.018

Surroundings surroundings_1 of continuous phase phase_1
    volume : 10
    pressure : 101325
    IncompressiblePhase phase_1 to surroundings_1| name : moles
        A : 500000

Compartment comp_1 of continuous phase phase_1
    volume : 1
    IncompressiblePhase phase_1 to comp_1

Compartment comp_2 of continuous phase phase_1
    volume : 1
    IncompressiblePhase phase_1 to comp_2

Compartment comp_3 of continuous phase phase_1
    volume : 1
    IncompressiblePhase phase_1 to comp_3

Compartment comp_4 of continuous phase phase_1
    volume : 1
    IncompressiblePhase phase_1 to comp_4

Compartment comp_5 of continuous phase phase_1
    volume : 1
    IncompressiblePhase phase_1 to comp_5

Compartment comp_6 of continuous phase phase_1
    volume : 1
    IncompressiblePhase phase_1 to comp_6

Compartment comp_7 of continuous phase phase_1
    volume : 1
    IncompressiblePhase phase_1 to comp_7

Compartment comp_8 of continuous phase phase_1
    volume : 1
    IncompressiblePhase phase_1 to comp_8

Compartment comp_9 of continuous phase phase_1
    volume : 1
    IncompressiblePhase phase_1 to comp_9

Compartment comp_10 of continuous phase phase_1
    volume : 1
    IncompressiblePhase phase_1 to comp_10

ConvectiveTransport transport_1 from surroundings_1 to comp_1
    velocity : 0.02
```

```
ConvectiveTransport transport_2 from comp_1 to comp_2

ConvectiveTransport transport_3 from comp_2 to comp_3

ConvectiveTransport transport_4 from comp_3 to comp_4

ConvectiveTransport transport_5 from comp_4 to comp_5

ConvectiveTransport transport_6 from comp_5 to comp_6

ConvectiveTransport transport_7 from comp_6 to comp_7

ConvectiveTransport transport_8 from comp_7 to comp_8

ConvectiveTransport transport_9 from comp_8 to comp_9

ConvectiveTransport transport_10 from comp_9 to comp_10

end
```

B.5 Model 1-2-1-ii

```
Solver LSODA
    t_start : 0
    t_final : 600
    atol : 10**-10
    rtol : 10**-10
Defaults
    flow_tau : 10**4

DefineComponents | name : molecular weight (kg/mole)
    A : 0.018

Surroundings surroundings_1 of continuous phase phase_1
    volume : 10
    pressure : 101325
    CompressiblePhase phase_1 to surroundings_1| name : moles
        A : 400

Compartment comp_1 of continuous phase phase_1
    volume : 1
    CompressiblePhase phase_1 to comp_1

Compartment comp_2 of continuous phase phase_1
    volume : 1
    CompressiblePhase phase_1 to comp_2

Compartment comp_3 of continuous phase phase_1
    volume : 1
    CompressiblePhase phase_1 to comp_3

Compartment comp_4 of continuous phase phase_1
    volume : 1
    CompressiblePhase phase_1 to comp_4

Compartment comp_5 of continuous phase phase_1
    volume : 1
    CompressiblePhase phase_1 to comp_5

Compartment comp_6 of continuous phase phase_1
    volume : 1
    CompressiblePhase phase_1 to comp_6

Compartment comp_7 of continuous phase phase_1
    volume : 1
    CompressiblePhase phase_1 to comp_7

Compartment comp_8 of continuous phase phase_1
    volume : 1
    CompressiblePhase phase_1 to comp_8

Compartment comp_9 of continuous phase phase_1
    volume : 1
    CompressiblePhase phase_1 to comp_9

Compartment comp_10 of continuous phase phase_1
    volume : 1
    CompressiblePhase phase_1 to comp_10

ConvectiveTransport transport_1 from surroundings_1 to comp_1
    velocity : 0.02
```

```
ConvectiveTransport transport_2 from comp_1 to comp_2

ConvectiveTransport transport_3 from comp_2 to comp_3

ConvectiveTransport transport_4 from comp_3 to comp_4

ConvectiveTransport transport_5 from comp_4 to comp_5

ConvectiveTransport transport_6 from comp_5 to comp_6

ConvectiveTransport transport_7 from comp_6 to comp_7

ConvectiveTransport transport_8 from comp_7 to comp_8

ConvectiveTransport transport_9 from comp_8 to comp_9

ConvectiveTransport transport_10 from comp_9 to comp_10

end
```

B.6 Model 1-2-2-i

```
Solver LSODA
    t_start : 0
    t_final : 600
    atol : 10**-10
    rtol : 10**-10

Defaults
    flow_tau : 10**4

DefineComponents | name : molecular weight (kg/mole)
    A : 0.018

Surroundings surroundings_1 of continuous phase phase_1
    volume : 10
    pressure : 303975
    IncompressiblePhase phase_1 to surroundings_1| name : moles
        A : 500000

Compartment comp_1 of continuous phase phase_1
    volume : 1
    IncompressiblePhase phase_1 to comp_1

Compartment comp_2 of continuous phase phase_1
    volume : 1
    IncompressiblePhase phase_1 to comp_2

Compartment comp_3 of continuous phase phase_1
    volume : 1
    IncompressiblePhase phase_1 to comp_3

Compartment comp_4 of continuous phase phase_1
    volume : 1
    IncompressiblePhase phase_1 to comp_4

Compartment comp_5 of continuous phase phase_1
    volume : 1
    IncompressiblePhase phase_1 to comp_5

Compartment comp_6 of continuous phase phase_1
    volume : 1
    IncompressiblePhase phase_1 to comp_6

Compartment comp_7 of continuous phase phase_1
    volume : 1
    IncompressiblePhase phase_1 to comp_7

Compartment comp_8 of continuous phase phase_1
    volume : 1
    IncompressiblePhase phase_1 to comp_8

Compartment comp_9 of continuous phase phase_1
    volume : 1
    IncompressiblePhase phase_1 to comp_9

Compartment comp_10 of continuous phase phase_1
    volume : 1
    IncompressiblePhase phase_1 to comp_10

ConvectiveTransport transport_1 from surroundings_1 to comp_1
```

```
ConvectiveTransport transport_2 from comp_1 to comp_2

ConvectiveTransport transport_3 from comp_2 to comp_3

ConvectiveTransport transport_4 from comp_3 to comp_4

ConvectiveTransport transport_5 from comp_4 to comp_5

ConvectiveTransport transport_6 from comp_5 to comp_6

ConvectiveTransport transport_7 from comp_6 to comp_7

ConvectiveTransport transport_8 from comp_7 to comp_8

ConvectiveTransport transport_9 from comp_8 to comp_9

ConvectiveTransport transport_10 from comp_9 to comp_10

ConvectiveTransport transport_out from comp_10 to surroundings_2

Surroundings surroundings_2 of continuous phase phase_1
    volume : 10
    pressure : 101325
    IncompressiblePhase phase_1 to surroundings_2

end
```

B.7 Model 1-2-2-ii

```
Solver LSODA
    t_start : 0
    t_final : 600
    atol : 10**-10
    rtol : 10**-10
Defaults
    flow_tau : 10**4

DefineComponents | name : molecular weight (kg/mole)
    A : 0.018

Surroundings surroundings_1 of continuous phase phase_1
    volume : 10
    pressure : 303975
    CompressiblePhase phase_1 to surroundings_1| name : moles
        A : 400

Compartment comp_1 of continuous phase phase_1
    volume : 1
    CompressiblePhase phase_1 to comp_1

Compartment comp_2 of continuous phase phase_1
    volume : 1
    CompressiblePhase phase_1 to comp_2

Compartment comp_3 of continuous phase phase_1
    volume : 1
    CompressiblePhase phase_1 to comp_3

Compartment comp_4 of continuous phase phase_1
    volume : 1
    CompressiblePhase phase_1 to comp_4

Compartment comp_5 of continuous phase phase_1
    volume : 1
    CompressiblePhase phase_1 to comp_5

Compartment comp_6 of continuous phase phase_1
    volume : 1
    CompressiblePhase phase_1 to comp_6

Compartment comp_7 of continuous phase phase_1
    volume : 1
    CompressiblePhase phase_1 to comp_7

Compartment comp_8 of continuous phase phase_1
    volume : 1
    CompressiblePhase phase_1 to comp_8

Compartment comp_9 of continuous phase phase_1
    volume : 1
    CompressiblePhase phase_1 to comp_9

Compartment comp_10 of continuous phase phase_1
    volume : 1
    CompressiblePhase phase_1 to comp_10

ConvectiveTransport transport_1 from surroundings_1 to comp_1
```

```
ConvectiveTransport transport_2 from comp_1 to comp_2

ConvectiveTransport transport_3 from comp_2 to comp_3

ConvectiveTransport transport_4 from comp_3 to comp_4

ConvectiveTransport transport_5 from comp_4 to comp_5

ConvectiveTransport transport_6 from comp_5 to comp_6

ConvectiveTransport transport_7 from comp_6 to comp_7

ConvectiveTransport transport_8 from comp_7 to comp_8

ConvectiveTransport transport_9 from comp_8 to comp_9

ConvectiveTransport transport_10 from comp_9 to comp_10

ConvectiveTransport transport_out from comp_10 to surroundings_2

Surroundings surroundings_2 of continuous phase phase_1
    volume : 10
    pressure : 101325
    CompressiblePhase phase_1 to surroundings_2


end
```

B.8 Model 2-1-1

```
Solver LSODA
    t_start : 0
    t_final : 600
    atol : 10**-10
    rtol : 10**-10

Defaults
    flow_tau : 10**4

DefineComponents | name : molecular weight (kg/mole)
    A : 0.002

Surroundings surroundings_1 of continuous phase phase_1
    volume : 100
    pressure : 101325
    IncompressiblePhase phase_2 to surroundings_1| name : moles
        A : 40
    CompressiblePhase phase_1 to surroundings_1 | name : moles
        A : 130

Compartment comp_1 of continuous phase phase_1
    volume : 10

ConvectiveTransport trans_1 from surroundings_1 to comp_1

end
```

B.9 Model 2-1-2

```
Solver LSODA
    t_start : 0
    t_final : 600
    atol : 10**-10
    rtol : 10**-10

Defaults
    flow_tau : 10**4

DefineComponents | name : molecular weight (kg/mole)
    A : 0.002

Surroundings surroundings_1 of continuous phase phase_1
    volume : 100
    pressure : 303975
    IncompressiblePhase phase_2 to surroundings_1| name : moles
        A : 40
    CompressiblePhase phase_1 to surroundings_1 | name : moles
        A : 130

Compartment comp_1 of continuous phase phase_1
    volume : 10

Surroundings surroundings_2 of continuous phase phase_1
    volume : 10
    pressure : 101325

ConvectiveTransport trans_1 from surroundings_1 to comp_1

ConvectiveTransport trans_2 from comp_1 to surroundings_2


end
```

B.10 Model 2-2-1

```
Solver BDF
    t_start : 0
    t_final : 600
    atol : 10**-5
    rtol : 10**-5
    max step size : 1


Defaults
    flow_tau : 10**4

DefineComponents | name : molecular weight (kg/mole)
    A : 0.018
    B : 0.012

Surroundings surroundings_1 of continuous phase phase_1
    volume : 10
    pressure : 101325
    IncompressiblePhase phase_1 to surroundings_1| name : moles
        A : 500000

Surroundings surroundings_2 of continuous phase phase_2
    volume : 1
    pressure : 101325
    IncompressiblePhase pulse_phase to surroundings_2| name : moles
        B : 300

Compartment comp_1 of continuous phase phase_1
    volume : 1
    IncompressiblePhase phase_1 to comp_1

Compartment comp_2 of continuous phase phase_1
    volume : 1
    IncompressiblePhase phase_1 to comp_2

Compartment comp_3 of continuous phase phase_1
    volume : 1
    IncompressiblePhase phase_1 to comp_3

Compartment comp_4 of continuous phase phase_1
    volume : 1
    IncompressiblePhase phase_1 to comp_4

Compartment comp_5 of continuous phase phase_1
    volume : 1
    IncompressiblePhase phase_1 to comp_5

Compartment comp_6 of continuous phase phase_1
    volume : 1
    IncompressiblePhase phase_1 to comp_6

Compartment comp_7 of continuous phase phase_1
    volume : 1
    IncompressiblePhase phase_1 to comp_7

Compartment comp_8 of continuous phase phase_1
    volume : 1
    IncompressiblePhase phase_1 to comp_8

Compartment comp_9 of continuous phase phase_1
```

```
    volume : 1
    IncompressiblePhase phase_1 to comp_9

Compartment comp_10 of continuous phase phase_1
    volume : 1
    IncompressiblePhase phase_1 to comp_10

Surroundings surroundings_3 of continuous phase phase_1
    volume : 1
    pressure : 80000
    IncompressiblePhase phase_1 to surroundings_3

ConvectiveTransport transport_1 from surroundings_1 to comp_1

ConvectiveTransport transport_exit from comp_10 to surroundings_3

ConvectiveTransport transport_12 from surroundings_2 to comp_1
    activation_times : 0, 200, 201
    activation_response : 0, 1, 0
    velocity : 0.03
    activation sigmoid : True

ConvectiveTransport transport_2 from comp_1 to comp_2

ConvectiveTransport transport_3 from comp_2 to comp_3

ConvectiveTransport transport_4 from comp_3 to comp_4

ConvectiveTransport transport_5 from comp_4 to comp_5

ConvectiveTransport transport_6 from comp_5 to comp_6

ConvectiveTransport transport_7 from comp_6 to comp_7

ConvectiveTransport transport_8 from comp_7 to comp_8

ConvectiveTransport transport_9 from comp_8 to comp_9

ConvectiveTransport transport_10 from comp_9 to comp_10

end
```

B.11 Model 2-2-2

```
Solver BDF
    t_start : 0
    t_final : 60
    atol : 10**-6
    rtol : 10**-6

Defaults
    flow_tau : 10**4

DefineComponents | name : molecular weight (kg/mole)
    A : 0.018
    B : 0.012

Surroundings surroundings_1 of continuous phase phase_2
    volume : 10
    pressure : 101325
    CompressiblePhase phase_2 to surroundings_1
        A : 40

Surroundings surroundings_2 of continuous phase liquid
    volume : 1
    IncompressiblePhase liquid to surroundings_2


PhaseTransport PT0 of phase phase_2 from surroundings_1 to comp_1
    tau flow : 0.8

PhaseTransport PT1 of phase phase_2 from comp_1 to comp_2
    tau flow : 0.8

PhaseTransport PT2 of phase phase_2 from comp_2 to comp_3
    flow_tau: 0.8

PhaseTransport PT3 of phase phase_2 from comp_3 to surroundings_2
    flow_tau: 0.8

Compartment comp_1 of continuous phase phase_1
    volume : 1
    IncompressiblePhase phase_1 to comp_1
       B : 50000

Compartment comp_2 of continuous phase phase_1
    volume : 1
    IncompressiblePhase phase_1 to comp_2
       B : 50000
Compartment comp_3 of continuous phase phase_1
    volume : 1
    IncompressiblePhase phase_1 to comp_3
       B : 50000


end
```

B.12 Model 3-1-1-i

```
Solver BDF
    t_start : 0
    t_final : 10
    atol : 10**-6
    rtol : 10**-6

DefineComponents |name: molecular weight(kg/mole)
    A : 0.001
    B : 0.002
    C : 0.001

Compartment comp_1 of continuous phase phase1
    volume : 10
    CompressiblePhase phase1 to comp_1
        A : 1200

Reaction react_1 2A -> B
        phase : phase1
        krxn : 0.25
        rate equation: krxn*A

Reaction react_2 A -> C
        phase : phase1
        krxn : 0.6
        rate equation : krxn*A
end
```

B.13 Model 3-1-1-ii

```
Solver BDF
    t_start : 0
    t_final : 30
    atol : 10**-6
    rtol : 10**-6

DefineComponents |name: molecular weight(kg/mole)
    A : 0.002
    B : 0.002
    C : 0.002

Compartment comp_1 of continuous phase phase1
    volume : 10
    CompressiblePhase phase1 to comp_1| name:moles
        A : 1200

Reaction react_1 A->B
        phase : phase1
        krxn : 0.25
        rate equation : krxn*A

Reaction react_2 B -> C
        phase : phase1
        krxn : 0.6
        rate equation : krxn*B
end
```

B.14 Model 3-1-2

```
Solver BDF
    t_start : 0
    t_final : 20
    atol : 10**-6
    rtol : 10**-6


DefineComponents |name: molecular weight(kg/mole)
    A : 0.001
    B : 0.002
    C : 0.002
    Solvent : 0.001

Compartment comp_1 of continuous phase phase1
    volume : 10
    IncompressiblePhase phase1 to comp_1| name:moles
        A : 100
        Solvent : 10000
    CompressiblePhase phase2 to comp_1
        C : 60

Reaction react_1 2 [A] + C-> 2 [B]
        phase : phase2
        contacting_phase : phase1
        krxn : 0.0002
        rate equation : krxn*[A]

end
```

B.15 Model 3-1-3

```
Solver BDF
    t_start : 0
    t_final : 20
    atol : 10**-6
    rtol : 10**-6
DefineComponents |name: molecular weight(kg/mole)
    A : 0.01
    B : 0.01
    solvent : 0.01
Compartment comp_1 of continuous phase phase1
    volume : 10
    IncompressiblePhase phase1 to comp_1
        A : 10000
        solvent : 800000
Reaction react_1 A -> B
        phase : phase1
        dH : 5000000
        A : 0.1
        Ea : 100
        Rate equation : A
Compartment comp_2 of continuous phase phase2
    volume : 10
    IncompressiblePhase phase2 to comp_2
        A : 10000
        solvent : 800000
Reaction react_2 A -> B
        phase : phase2
        A : 0.1
        Ea : 100
        rate equation : A
        dH : 0
end
```

B.16 Model 4-2-1

```
Solver BDF
    t_start : 0
    t_final : 60
    atol : 10**-5
    rtol : 10**-5


DefineComponents | name : molecular weight (kg/mole)
    A : 0.018
    solvent : 0.012

Compartment comp_1 of continuous phase phase_1
    volume : 1
    IncompressiblePhase phase_1 to comp_1
        solvent : 10000
        A : 5000

Compartment comp_2 of continuous phase phase_1
    volume : 1
    IncompressiblePhase phase_1 to comp_2
        solvent : 10000

MassTransfer MTR_1 of species A from comp_1 to comp_2


end
```

B.17 Model 4-2-2

```
Solver BDF
    t_start : 0
    t_final : 60
    atol : 10**-5
    rtol : 10**-5


DefineComponents | name : molecular weight (kg/mole)
    A : 0.018
    solvent : 0.012

Compartment comp_1 of continuous phase phase_2
    volume : 1
    CompressiblePhase phase_2 to comp_1
        solvent : 10000
        A : 5000

Compartment comp_2 of continuous phase phase_1
    volume : 1
    IncompressiblePhase phase_1 to comp_2
        solvent : 10000

MassTransfer MTR_1 of species A from comp_1 to comp_2


end
```

B.18 Model 5-1-1

```
Solver BDF
    t_start : 0
    t_final : 1000
    atol : 10**-6
    rtol : 10**-6

DefineComponents
    A : 0.124
    solvent : 0.001

Compartment comp_1 of continuous phase phase1
    volume : 10
    CompressiblePhase phase1 to comp_1
        A : 420
    IncompressiblePhase phase2 to comp_1
        solvent : 10000

MassTransfer mtr_1 of species A from phase1 to phase2
    S : 10
    ks : 0.1
    k : 0.2

end
```

B.19 Model 6-1-1

```
Solver LSODA
    t_start : 0
    t_final : 600
    atol : 10**-4
    rtol : 10**-5

DefineComponents |name: molecular weight(kg/mole)
    H2O : 0.018

Compartment comp of continuous phase phase1
    volume : 10
    CompressiblePhase phase1 to comp
       H2O : 10000


Surroundings surroundings of continuous phase phase1
    volume : 10
    temperature : 600
    CompressiblePhase phase1 to surroundings

HeatTransfer HT1 from surroundings to comp
    U : 1000 | W/m^2K (Convective heat transfer coefficient of water)
    area : 10
end
```

B.20 Model 6-2-1

```
Solver LSODA
    t_start : 0
    t_final : 1000
    atol : 10**-6
    rtol : 10**-8

DefineComponents |name: molecular weight(kg/mole)
    A : 0.032

Compartment comp_1 of continuous phase phase1
    volume : 1
    temperature : 1000
    CompressiblePhase phase1 to comp_1
        A : 40

Compartment comp_2 of continuous phase phase1
    volume : 1
    CompressiblePhase phase1 to comp_2
        A : 40

Compartment comp_3 of continuous phase phase1
    volume : 1
    CompressiblePhase phase1 to comp_3
        A : 40

Compartment comp_4 of continuous phase phase1
    volume : 1
    CompressiblePhase phase1 to comp_4
        A : 40

Compartment comp_5 of continuous phase phase1
    volume : 1
    CompressiblePhase phase1 to comp_5
        A : 40

Compartment comp_6 of continuous phase phase1
    volume : 1
    CompressiblePhase phase1 to comp_6
        A : 40

Compartment comp_7 of continuous phase phase1
    volume : 1
    CompressiblePhase phase1 to comp_7
        A : 40

Compartment comp_8 of continuous phase phase1
    volume : 1
    CompressiblePhase phase1 to comp_8
        A : 40

Compartment comp_9 of continuous phase phase1
    volume : 1
    CompressiblePhase phase1 to comp_9
        A : 40

Compartment comp_10 of continuous phase phase1
    volume : 1
    CompressiblePhase phase1 to comp_10
        A : 40
```

```
HeatTransfer HT1 from comp_1 to comp_2
    U : 100 | Gases
    area : 1

HeatTransfer HT2 from comp_2 to comp_3
    U : 100 | Gases
    area : 1

HeatTransfer HT3 from comp_3 to comp_4
    U : 100 | Gases
    area : 1

HeatTransfer HT4 from comp_4 to comp_5
    U : 100 | Gases
    area : 1

HeatTransfer HT5 from comp_5 to comp_6
    U : 100 | Gases
    area : 1

HeatTransfer HT6 from comp_6 tom comp_7
    U : 100 | Gases
    area : 1

HeatTransfer HT7 from comp_7 to comp_8
    U : 100 | Gases
    area : 1

HeatTransfer HT8 from comp_8 to comp_9
    U : 100 | Gases
    area : 1

HeatTransfer HT9 from comp_9 to comp_10
    U : 100 | Gases
    area : 1

end
```

Appendix C

Model Illustrations guide

Model illustrations are drawn in 2-dimensions; basic shapes represent the structure of the models. Arrows of varying colours and dash types indicate the movement direction and conversion (reaction phenomena) of mass and energy between phases within compartments and between compartments. Relevant information, such as compartment temperatures and pressures, chemical species quantities, are appended to the illustrations where necessary to the model specificities. A supporting key for phase colour to phase id is also added to the illustration where phase number exceeds reasonable interpretation without a key.

Containers are represented as a thick-walled quadrilateral shape.

Compartments are represented as thin-walled quadrilaterals; when present in a model with a container, they are distinguished by their walls and their contents. Containers contain compartments, whereas compartments contain phases.

Surroundings are similar in appearance to the compartments, except with a cross-connected to the corners of the quadrilateral shape to indicate the locked nature of the surroundings mole and energies quantities.

Each **phase** material within a system is represented by a colour key. Dispersed phase material is represented as a circle within the corner of a compartment – their size equivalent to the relative characteristic diameter of the phase to the others within the system. The continuous phase fills the volume of the compartment surrounding the dispersed phases. A final phase, the phantom phase, is assumed dispersed within the continuum and fills any void material within the compartment. Phase material undergoing phenomenological interaction can be positioned in the corner of the compartment, gaseous at the top and liquid/solid at the base of the compartment.

Light pastel colours are used to represent continuous mediums, and vivid colours for dispersed phase material; Where a phase is both dispersed and a continuous phase within the same model, the pastel-vivid colour type does not apply – instead one is chosen to represent the phase throughout the model.

Gaseous phase material being a shade of blue (although compressible (gas) the phantom phase being a shade of grey to separate it from other compressible phases of a model – assumed present in non-empty compartments), liquids a shade of green and solids either black or brown shades. Both solid and liquid phases are of the same phase nature (Incompressible Phase).

Where a compartment is initially empty, the continuous/dispersed phase can be identified from the corresponding model input file.

Three **material transports** exist within the framework; the transfer direction, source, and termination volumes of the transfer are indicated by a single black arrow. The make-up of the arrow, weight, and dashes differ between each of the transports. Small, rich pictures containing the phases and their distribution are connected to the flow arrows to indicate the transferred material.

(i) *Inter/ Intra-compartmental* **Mass Transfer** & (ii) **Phase Transport**: A (i) dotted / (ii) solid lined empty head arrow between the two phasic volumes involved in the transfer, pointing from source to termination volume. The mass transfer arrow is accompanied by the id of the transported chemical species.

Convective Transport is represented as a solid lined, full headed arrow from the wall of one compartment to the wall of the termination compartment.

The above illustrative guidance applies to **one-directional** and **reversible** flows; however, **exchange** flow illustration differs. Instead, a double-headed arrow is used to represent the continuous exchange of material.

The **reaction** of material either occurs based on the surface (catalyst) or in the volume of a phase. The former is represented as a circular arrow encasing the letter “*R*” with a subscript number for reaction number taking place, indicating a reaction takes place, situated upon the border of the phases

involved in the reaction. The same symbol within the bulk of a phase indicates a reaction within the phase volume.

Heat transfer is represented in the diagrams as a red, solid lined, full headed arrow. The direction of heat transfer is indicated by the direction of the arrow.

An example illustration including all the illustrative structural and phenomenological components is given in Figure 84.

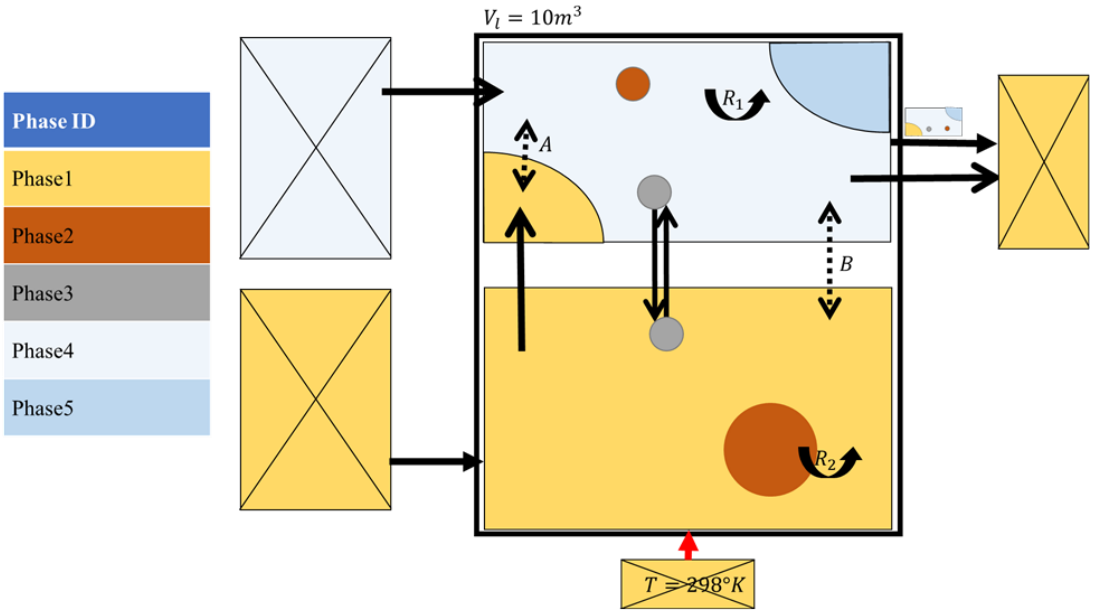

Figure 84 - Universal illustration guide, full phenomenological and structural illustration.